The impact of changing intestinal amino acid transporter expression and luminal nutrient content on healthy ageing

ABIGAIL AMANDA MORNEMENT

Department of Biosciences

The impact of changing intestinal amino acid transporter expression and luminal nutrient content on healthy ageing

Abigail Amanda Mornement

Thesis submitted for the degree of Doctor of Philosophy

December 2022

Declaration

The work described herein was carried out in the department of Biosciences (Formally the School of Biological and Biomedical Sciences), University of Durham between October 2018 and December 2022. All the work is my own, except where specifically stated otherwise. No part has previously been submitted for a degree at this or any other university.

Statement of Copyright

Abstract

Thanks to improved sanitation and advances in healthcare, humans are living for longer than ever before, however, the number of years an individual remains healthy has not improved, putting a strain on health services. Improving the health of this elderly population is therefore of great importance.

Unintentional weight loss, along with metabolic and body-composition changes, are common characteristics of ageing and frailty, associated with significant adverse health outcomes, increased mortality and progressive disability. While these changes may be partially explained by dietary changes and the metabolic cost of immune activation and inflammation that occur with age, other factors must contribute.

The intestine has been shown to be a key organ in the progression of ageing, undergoing many changes which directly impact mortality and morbidity. Nutrient absorption is a key role of the intestine which has not been studied in the context of ageing. Given the age-related intestinal changes which may impact its function, from an increased bacterial load to dysplasia and loss of intestinal barrier integrity, it is likely that nutrient absorption is a contributing factor to this unintentional weight loss.

This thesis aims to uncover whether changes to intestinal nutrient dynamics impact ageing phenotypes, using *Drosophila* as a model. Here I developed an assay to understand changes in the intestinal nutrient profile with age, showing increased luminal/faecal concentrations of amino acids upon advancing age and microbial association. This assay has the potential to be more widely applied to answer other biological questions. My data also links changes in the expression of intestinal amino acid transporters to age-related decline, through interaction with several key age-related pathways. Knockdown of the cationic amino acid transporter *Slimfast*, which has been shown to act as a nutrient sensor through interaction with mTORC1, extended lifespan and was unexpectedly found to link the JNK and JAK-STAT pathways. Modulation of the glutamate transporter, Eaat1, was also shown to impact lifespan, and stem-cell expression of Eaat1 was found to be important for their division. This opens a new avenue for ageing research, to understand the biology of ageing, and gain a better understanding of how targeted dietary interventions may improve the outcomes of ageing.

Acknowledgements

I acknowledge the BBSRC for funding this project.

To my supervisor, Rebecca Clark, thank you for your support and guidance throughout this PhD. Thank you for helping to grow my confidence and independence as a researcher. To Jeanette, my fellow Clark lab student, thank you for welcoming me so warmly. Sharing this journey with you has been special, and I would not have wanted anyone else by my side through all the ups and downs.

I would also like to give a special thank you to David Doupé, for stepping in to provide support and supervision when Rebecca was unable. I cannot adequately express how grateful I am. My thanks extends to the Doupé group for accepting me as one of their own, and to everyone in Lab20 for creating such a positive and cooperative working environment.

Thank you to the Bioanalytics department, particularly the late Ian Cummins with whom I began the mass-spectromentry work, and Rachael Dack who stepped in and carried out all of the mass spectrometry work within this thesis. Much of this work would not have been possible without their expertise.

To my family, thank you for your unwavering love and support throughout the years. This would not be possible without you, and I would not have made it through the ups and downs of the last four years without you. A special mention goes to my sister Alex for proving the most tranquil environment to write up this thesis, which made the process far more enjoyable.

Finally, thank you to the guinea pigs three; Daphne, Lucy and Popcorn, who's company and constant entertainment saved my mental health through the pandemic and beyond.

Table of Contents

Table of figures

List of tables:

List of Abbreviations

4E-BP1	Eukaryotic translation initiation factor 4e binding protein 1
AAT	Amino acid transporter
AD	Alzheimer's disease
AMP	Antimicrobial peptides
AMPA	α-amino-3-hydroxy-5-methyl-4-isoxazolepropionic
ARD	Age-related disease
ASCT	Alanine serine cysteine threonine transporter
BCAA	Branched-chain amino acid
bsk	Basket
C. elegans	Caenorhabditis elegans
cafe	Capillary feeding
CAT	Cationic amino acid transporter
dALS	*Drosophila* acid-labile subunit
Dif	Dorsal-related immunity factor
Dilp	*Drosophila* insulin-like peptides
dmGlut	Dietary and metabolic glutamate transporter
Dome	Domeless
DPT	Diptericin
DR	Dietary restriction
DRS	Drosomycin
DUMP	*Drosophila* undigested metabolite profiling
DUOX	Dual oxidase
E. coli	Escherichia coli
Eaat	Excitatory amino acid
EB	Enteroblast
EC	Enterocyte
EE	Enteroendocrine
ER	Endoplasmic reticulum
FOXO	Forkhead box O
GC	Glutamate carrier
gpaAT	Glycoprotein-associated amino acid transporter
HAT	Hetero(di)meric amino acid transporter

HG	HindgutFI
IGF-1	Insulin/insulin-like growth factor 1
IGF-BP	Insulin growth factor binding partner
iGluR	Ionotropic glutamate transporter
IIS	Insulin/insulin-like growth factor 1 signalling
IMD	Immune deficiency
InR	Insulin receptor
ISC	Intestinal stem cell
JAK-STAT	Janus kinase signal transducer and activator of transcription
JNK	c-Jun N-terminal kinase
kcc	Kazachoc
LC-MS/MS	Liquid Chromatography with tandem mass spectrometry
MAPK	Mitogen activated protein kinase
mGluR	Metabotropic glutamate receptor
mnd	Minidiscs
mTOR	Mechanistic target of rapamycin
NAAT1	Nutrient amino acid transporter 1
NCX	Sodium-calcium exchanger
NF-kB	Nuclear factor kappa-B
NMDA	N-methyl-D-aspartate
Path	Pathetic
PAU/mass	Percent abundance/mass
PBS	Phosphate buffered saline
pH3	Phosphorylated histone H3
PI3K	Phosphatidylinositol 3-kinase
PIP2	Phosphatidylinositol 4,5-biphosphate
PIP3	Phosphatidylinositol 3,4,5-biphosphate
PKA	Protein kinase A
PMCA	Plasma membrance calcium APTase
PTEN	Phosphatase and tensin homolog
puc	Puckered
ROS	Reactive oxygen species
RSD	Relative standard deviation
RU	Mifepristone

RU-486	Mifepristone
S6K1	S6 kinase 1
SAH	s-adenosyl homocysteine
SAM	s-adenosyl methionine
SASP	Senescence associated secretory pathway
sbm	Sobremesa
SCFA	Short-chain fatty acid
SERCA	Sarco-endoplasmic reticulum ATPase
SLC	Solute carrier
Slif	Slimfast
Slif-anti	Slimfast antisense line
SNP	Single nucleotide polumorphism
SOCE	Store-operated calcium entry
STIM	Stromal interaction molecule
TAG	Triacylglyceride
TSC	Tuberous sclerosis complex
UAS	Upstream activating sequence
upd3	Unpaired 3
VGLUT	Vesicular glutamate transporter
WG	Whole gut

1 Introduction

1.1 Ageing

Humans have made staggering advances in lifespan, with life expectancy at birth rising from 47 to 73 years of age since 1950[1]. This is due to improved sanitation and advances in healthcare, and it is estimated that by the middle of the 21st century, a quarter of the European population will be older than 65[2]. Unfortunately, parallel increases in healthspan, i.e. the number of years an individual remains in good health, have not been achieved. Indeed it is estimated that individuals will live with at least one morbidity for one-fifth of their life[3], putting a lot of strain on healthcare services, and decreasing quality of life.

Despite this, there are large variations in the consequences of ageing, with some elderly people remaining in relatively good health until end-of-life, avoiding the debilitating effects of many age-related diseases (ARDs), while others undergo progressive decline and loss of functions (mobility, cognition, bodily functions). There is a lot of interest in understanding the cause of these differences, in an effort to bridge the gap between lifespan and healthspan. Indeed, certain molecular pathways, and environmental changes are known to be important in health and longevity (discussed below), however ageing is complex and multifaceted and much remains to be uncovered.

1.2 *Drosophila melanogaster* as a model organism

Drosophila melanogaster (hereby referred to simply as *Drosophila*) have been used as a model organism since the start of the 20th century, and have greatly contributed to our understanding of genetics, neuroscience and development. They are one of the cheapest laboratory animals to culture as they do not require much space or starting equipment.

Despite the obvious differences, there is a surprising degree of genetic conservation between *Drosophila* and humans, indeed 75 % of disease-related genes in humans have functional orthologs in the fly[4].

1.2.1 Life cycle

The *Drosophila* life cycle is a multi-stage process (Figure 1.1). This life cycle is temperature dependent but takes approximately 10 days from egg to adult fly at 25°C. Adult *Drosophila* can live around 70 days at 25°C, although this is dependent on genotype.

Adult females become sexually mature 8-12 hours after eclosion, and each female can lay around 300 eggs. The embryos hatch 16 hours after deposition, eating the chorion in which they are enclosed and the bacteria on the surface. It is in this way that sterile embryos first gain gut microbiota[5]. The hatched larvae proceed to eat for the next 5 days, undergoing 2 moulting stages through to second and third instar larvae. In the wandering phase, the mature third instar larvae leave the food and wander to find a dry place to pupate. After pupariation, during metamorphosis, some larval tissues are completely remodelled as the adult fly develops. Adult flies consist almost entirely of post-mitotic cells, with the exception of cells in their reproductive organs, and some cells in the gut which continue to divide[6].

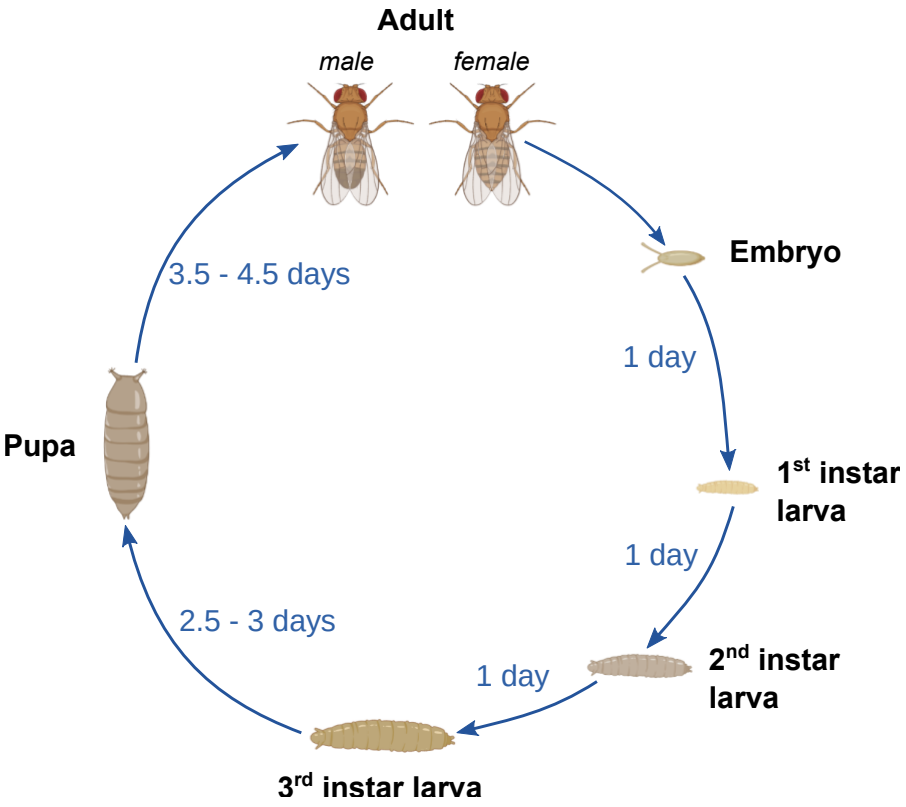

Figure 1.1 | *Drosophila* Life Cycle at 25°C. Figure made using BioRender

1.2.2 Genetics and husbandry

One of the advantages of *Drosophila* as a genetic tool is that they are sexually dimorphic. Additionally, it is possible to distinguish sexually immature, virgin females due to a delay in pigmentation, and the presence of a dark spot on their abdomen[7]. This spot is the meconium; the remains of their last meal before pupariation. The selection of virgin females ensures that they can be crossed with a male of a chosen genetic background.

The *Drosophila* genome contains just 4 chromosomes, the X (1st), 2nd, 3rd and 4th chromosomes, which are divided by the centromeres into left and right arms and contain around 15,000 genes[8]. Many powerful tools for genetic manipulation have been developed. Traditionally, mutagenic agents and transposable *P*-elements were used to isolate new mutants and thereby discover new genes required for the development of *Drosophila*[8]. In the early 1990's, two more tools were added to the *Drosophila* tool kit. The Gal4/UAS[9] and the FLP-FRT[10–12] systems which allow for more sophisticated genetic manipulation.

The Gal4/UAS system is comprised of Gal4, a yeast transcriptional activator, which binds to an upstream activating sequence (UAS) that contains Gal4 binding sites, and is inserted into the promotor region of a gene of interest. Once bound to the UAS, Gal4 recruits transcriptional machinery, resulting in expression of the downstream gene. It is a binary system where the Gal4 and the UAS target gene are expressed by different transgenic flies which must be combined through mating to drive expression[9]. Using this system, it is possible to express any cloned gene that has a UAS within its promotor region[9]. This system was further enhanced to become the drug-inducible GeneSwitch system which enabled spatial and temporal control of transgene expression[13,14]. Here the gal4 is fused to a partial progesterone receptor ligand-binding domain which is activated in the presence of a steroid drug, mifepristone (RU-486, hereafter referred to as RU)[13,14]. In this system, the chimeric Gal4 cannot bind to the UAS and activate gene expression, unless bound to RU.

Further systems for the modification of *Drosophila* gene expression have been developed[15,16], but, as they were not used in this thesis, they will not be mentioned here.

1.2.3 *Drosophila* and Ageing

Due to their short lifespans, tractable genome and high conservation between genes and pathways, *Drosophila* have become a useful model in ageing research with several important markers of ageing being characterised thus far which will be further discussed below. These include systemic immune activation, loss of intestinal barrier integrity, and dysbiosis – a disruption to the balance of microbes within the intestine, characterised by an expansion of total bacteria, and changes in the composition of the bacterial community.

One of the greatest advantages of using *Drosophila* to study ageing, is the large populations that can be used to track lifespans and measure the rate of mortality. Tracking the lifespan of large populations gives a more robust measure, particularly when the median lifespan, or the age at which 50% of the population remains alive, is used as it is less likely to be affected by outliers (than maximal lifespan).

While the median survival provides a good measure to observe, at a population level, whether interventions influence ageing and lifespan, it does not give much insight into how such changes occur. This is where it is important to look at other biological markers of ageing which will be discussed below.

1.3 Ageing and the intestine

There is a significant body of evidence to show the importance of the intestine in healthy ageing. The intestinal epithelium of all organisms acts as a barrier to the environment, separating the external environment including intestinal content and the microbiota, from the surrounding tissues[17]. Ageing is associated with myriad intestinal changes, from decreased intestinal motility[18] and increased intestinal permeability[19–22], to chronic inflammation (known as 'inflamm-ageing')[23–25] and changes to the composition and abundance of the intestinal microbiota[26–30]. Indeed, as many as 40 % of people will suffer gastrointestinal decline with age[31,32].

1.3.1 *Drosophila* intestine as a model

The *Drosophila* intestine has emerged as a good model system to study intestinal epithelial homeostasis and host-microbial interactions, as well as their role in age-related decline. It is a dynamic organ, and an important epithelial barrier protecting the organism against ingested biotic and abiotic hazards. It is also an important immune epithelial barrier, mediating the relationship between host and its intestinal microbiota.

The *Drosophila* gut is structurally and functionally analogous to the human intestine. Whilst it can be subdivided along the anteroposterior axis into the foregut, midgut and hindgut (Figure 1.2), the midgut can be further subdivided based on morphological and functional differences. It is typically split into six regions[33], however as many as 14 subregions have been identified based upon morphological, histological and genetic properties[34]. The posterior midgut (R4-R5) is analogous to the human small intestine, with high metabolic and immune responsiveness.

The *Drosophila* intestine is simpler than its mammalian counterparts, made up of only four cell types (Figure 1.2); the intestinal stem cells (ISCs) which can divide symmetrically into two daughter ISCs or two enteroblasts (EBs)[35], or asymmetrically to generate one ISC and one EB, a progenitor daughter cell. The EB can then differentiate into an absorptive enterocyte (EC), or a secretory enteroendocrine (EE) cell. *Drosophila* ECs and EEs perform antimicrobial functions that are fulfilled by specialised cells in mammalian intestines e.g. goblet and Paneth cells[36,37].

Importantly, the *Drosophila* intestine undergoes comparable changes with age, to mammalian intestines. It associates with a microbiota, which itself is remodelled with age, as well as diet. The *Drosophila* intestine is immune active, enabling control of the microbiota, and response to pathobionts, however immune dysregulation is characteristic of ageing in *Drosophila* and other organisms[22–24]**.** Additionally, loss of intestinal homeostasis is observed, with overproliferation of ISCs and accumulation of mis-differentiated and polyploid cells. This affects intestinal barrier integrity, and likely impacts upon intestinal functions e.g. nutrient absorption. Finally, intestinal barrier integrity shares importance between species, and it has been shown that loss of intestinal barrier function in flies and mice precedes and predicts mortality.

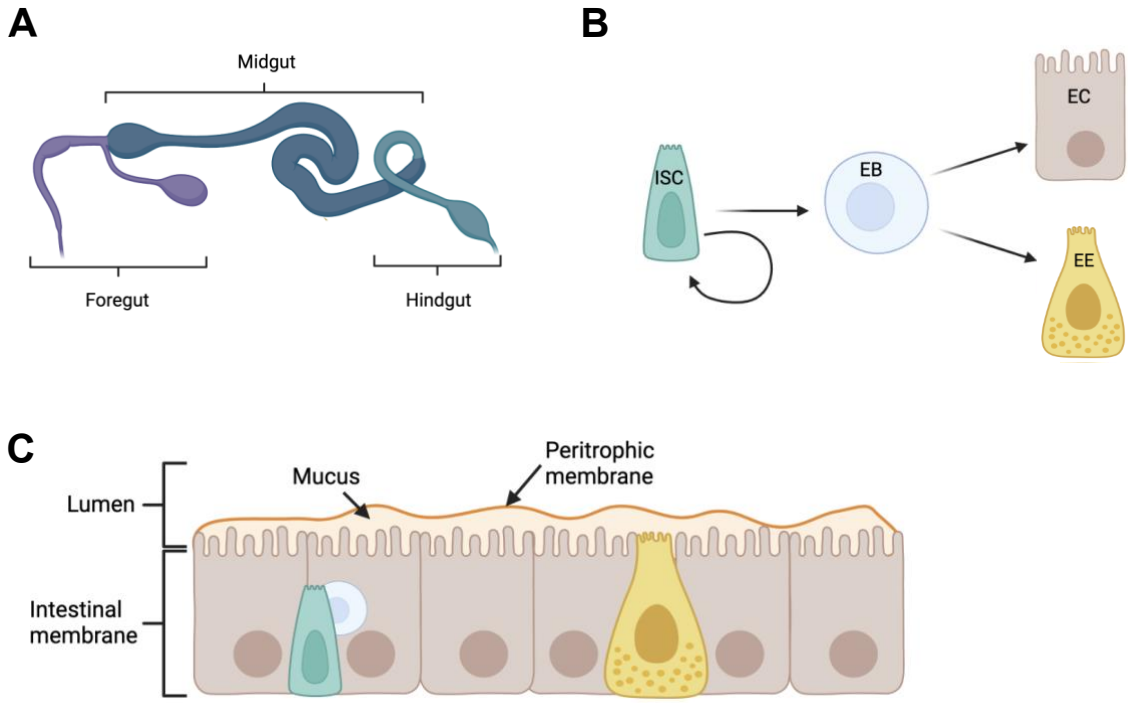

Figure 1.2 | Structure of the *Drosophila* intestine.

(A) Simplified schematic of the *Drosophila* intestine with the foregut in purple, the midgut in dark blue and the hindgut in teal. **(B)** Simplified schematic of the division of intestinal stem cells (ISC) and differentiation of daughter progenitor cells (enteroblast; EB) into absorptive enterocytes (EC) or secretory enteroendocrine cells (EE). (C) Simplified schematic of the structure of the intestinal membrane, made up of a single layer of ECs and EEs, with a stem cell niche where ISCs proliferate and differentiate to regenerate the lining. The cell layer is protected from the luminal contents by a mucus lining, and the peritrophic membrane formed of proteins, glycoproteins, and chitin microfibrils in a proteoglycan matrix. Figure made using BioRender.

1.3.2 Intestinal phenotypes of ageing

Ageing is characterized by a progressive loss of physiological integrity, leading to impaired function and increased vulnerability to death[38]. Ageing doesn't appear to affect individuals at the same rate.

There is, it seems, a difference between chronological age, that is an individual's age in years, and biological age, or how aged an individual is on a physiological level. The core reasons underlying this difference in the rate of ageing is not well understood and is difficult to study in humans.

The use of *Drosophila* in the study of ageing, however, enables us to gain important insights into these differences. Indeed, several markers of ageing including systemic immune activation, loss of intestinal barrier integrity, and dysbiosis have been characterised in this model and are shared by higher organisms. These are expanded upon below.

1.3.2.1 Loss of intestinal barrier integrity

Overproliferation of ISCs and accumulation of mis-differentiated and polyploid cells is typical of the ageing intestine This affects intestinal barrier integrity, and likely impacts upon intestinal functions e.g. nutrient absorption

Loss of intestinal barrier integrity is one biomarker of age-related decline which, importantly, can be assayed non-invasively. The addition of a non-absorbable blue food dye to the fly's food for 24 hours allows those lacking barrier integrity to be identified through blue staining of the haemolymph. Because of their blue hue, these flies are termed 'smurfs'. It has been demonstrated in *Drosophila* that age-related changes to the intestinal microbiota, which drive inflammation and mortality[22], are associated with an increase in intestinal permeability[39], and this has been corroborated in mice[40]. Importantly, this assay can be used as a marker for biological age within a chronologically age-matched population. The ability to differentiate between these populations better enables insights into the drivers of age-related decline, or the changes that occur within the biologically aged individuals.

Interestingly, although age-related loss of intestinal barrier integrity was first characterised in *Drosophila*, it has been shown to be conserved in higher organisms[40] and has even been employed within intensive care settings to monitor the health of patients, and predict sepsis[41].

In mice, the increased permeability of the intestinal lining allows microbial products to enter the bloodstream, where it further increases inflammation and a heightens their immune response[40]. A similar mechanism is thought to exist in *Drosophila*, although it has not yet been proven. It has however been shown that smurf flies exhibit lower levels of expression of septate junction and adherens junction genes[39]. Septate junctions are functionally analogous to tight junctions in mammals. Further to this, overexpressing snakeskin, a septate junction protein, delays onset of the smurf phenotype, extends lifespan and improves other age-related phenotypes including immune activation and dysbiosis[42], discussed below. Additionally, it improves flies' outcome when orally

infected with pathogenic bacteria, by preventing their translocation from the intestine[42]. This supports a model where loose connections between the cells allow movement of bacteria or bacterial products into the circulation where they stimulate the immune system. Activation of the immune system may then work in a positive feedback loop, changing the microbial communities, and causing stress to the intestinal cells, resulting in further loss of cell junctions. Another contributing factor may be that the loss of septate junctions allows tissue fluid into the intestine, stimulating expansion of specific microbial communities and further driving dysbiosis.

1.3.2.2 Age-related activation of stress signalling

The control of stress-response and proliferative pathways must be tightly controlled to maintain homeostasis. Two of these pathways are the c-Jun N-terminal kinase (JNK) pathway and the Janus kinase (JAK)-signal transducer and activator of transcription (STAT) pathway, both of which have been associated with the ageing process, and found to be chronically activated in the intestine with age.

1.3.2.2.1 JNK

The JNK pathway (Figure 1.3) is a stress-response pathway activated by both intrinsic and extrinsic stimuli[43]. It is highly conserved and a critical determinant in the control of longevity.

JNKs belong to the superfamily of mitogen activated protein kinases (MAPKs), which act in a cascade of sequential phosphorylation and activation. JNKs are involved in both cell proliferation and apoptosis, dependent on stimulus and cell type. Mammals contain 3 JNK proteins (1, 2 and 3[44]), however *Drosophila* contain a single JNK, *basket.*

In *Drosophila*, JNK signalling is initiated by stressors or inflammatory cytokines, which leads to selective activation of a JNKKK (several are known including, but not limited to MLK2, MEKK1 and TAK1), and a cascade of phosphorylation of a JNKK (Hemipterous or dMKK4), and the lone JNK *basket*[45]. Phosphorylation of *basket* leads to the activation and transcription of many genes including *puckered (puc)* which limits JNK activity in a negative feedback loop[46]. JNK activity also mediates transcription of the cytokine *unpaired 3 (upd3)* which itself activates the JAK-STAT pathway[46,47] (See below). The signalling cascade is very similar in other organisms, with additional complexity in mammals, with more JNK, JNKK and JNKKK's within the cascade[44].

Activation of the JNK pathway protects cells from stress damage, thereby promoting survival[43,46]. It also suppresses the effects of insulin/insulin-like growth factor signalling (IIS) by activating the

transcription factor Foxo[48]. Whilst this all points towards a beneficial longevity effect of JNK signalling, there is a conflicting impact of chronic JNK pathway activity, as observed in the *Drosophila* intestine with age[49].

In the *Drosophila* intestine, JNK has different functions depending on the cell type. In ISCs, JNK signalling promotes symmetric division, increasing the number of ISC[47,49]s, however in ECs, increased JNK signalling promotes apoptosis[50]. These responses work together to promote intestinal turnover to protect adult flies from stress damage, however chronic activation of the JNK pathway, as seen during the course of ageing[49], promotes intestinal dysplasia and contributes to the age-related deterioration of the intestinal epithelium through expansion of the ISC pool, mis-differentiation of progenitor cells and loss of ECs[49,51].

1.3.2.2.2 JAK-STAT

As mentioned above, *Upd3* is a cytokine, induced in the intestine upon damage to regulate the repair response through the JAK-STAT pathway[47] (Figure 1.3). Upd cytokines bind and activate the pre-dimerised JAK-STAT receptor Domeless[52–54]. This causes the receptor associated JAK tyrosine kinase Hoscotch[55] to phosphorylate itself, and STAT92E[54,56,57]. Phosphorylation of STAT92E results in its dimerization and translocation to the nucleus where it induces gene expression[57].

Another pathway implicated in ageing, JAK-STAT signalling is required for homeostasis and regeneration in the intestine. When enterocytes are subjected to apoptosis, infection, or JNK-mediated stress-signalling, they produce cytokines (upd1, upd2 and upd3) which activate JAK-STAT signalling in ISCs. This promotes their rapid division, and progenitor cell differentiation[47].

This pathway must be tightly controlled; chronic activation of JAK-STAT signalling in the gut of ageing *Drosophila* is associated with age-related metaplasia, microbial dysbiosis and functional decline of the gastrointestinal tract[58]. The JAK pathway is also more highly active in the fat tissue of aged mice[59]. Some of this chronic activation may be due to the presence of senescent cells. In mammalian systems, the JAK pathway is more active in senescent than non-senescent cells, and inhibition of JAK-STAT signalling suppresses the senescence-associated secretory phenotype and alleviates age-related dysfunction[59–61]. While there have been extensive studies of cellular senescence in mammalian systems, there is little evidence of senescence in invertebrate models, although it has been shown that activation of the RAS oncogene with mitochondrial dysfunction can induce senescence in the *Drosophila* imaginal epithelium[62–64].

The effect of increased JAK-STAT signalling with age appears to be tissue (and sex) dependent. Overexpression of *upd1* in the *Drosophila* intestine leads to a reduction in median lifespan by 54.1%

in males and 18.9% in females, whereas *upd1* overexpression in the fat body and in the nervous system increased the median lifespan of male flies, but had no effect on female longevity[65].

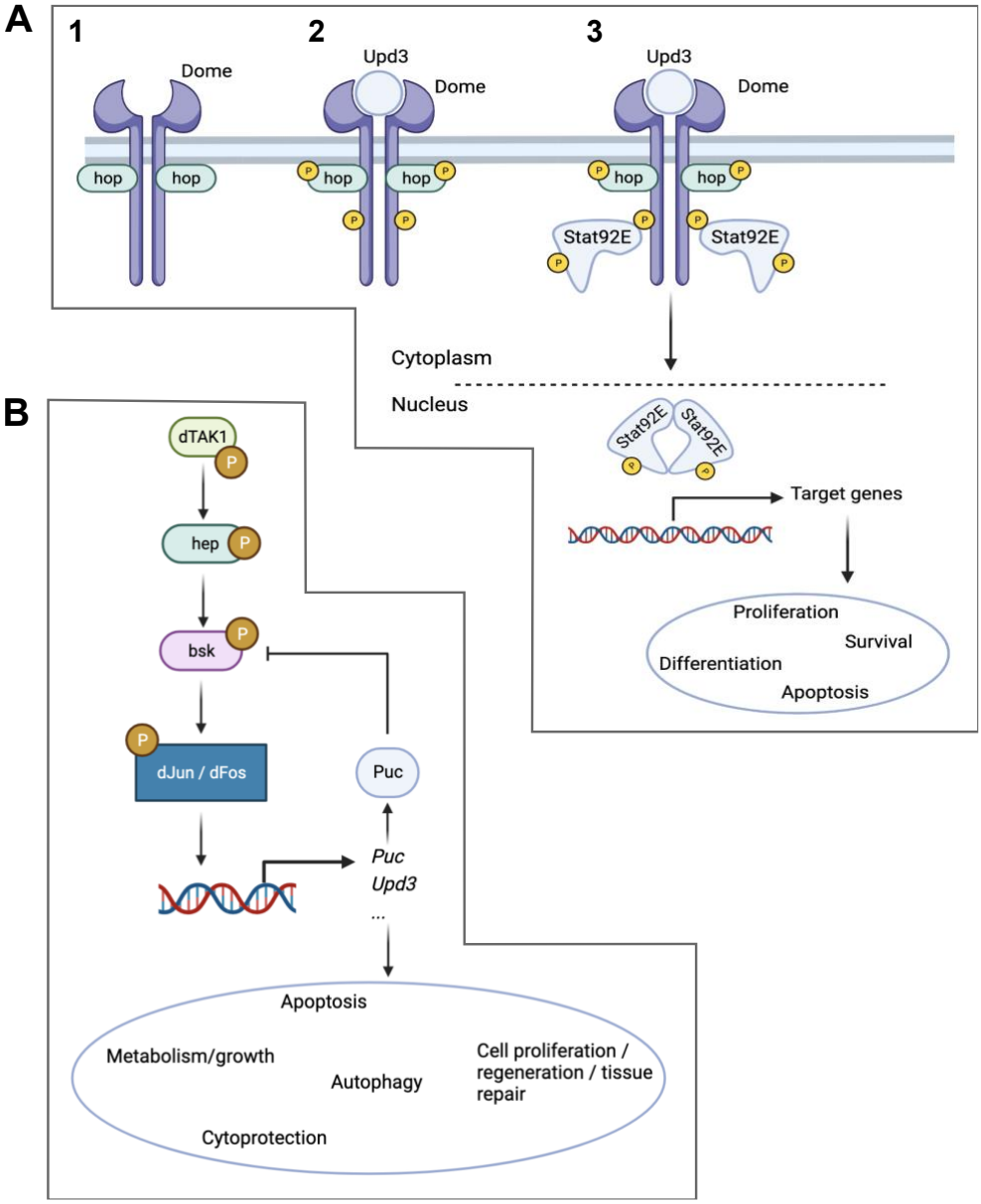

Figure 1.3 | Simplified schematics of JAK-STAT and JNK signalling pathways.

(A) Schematic of the *Drosophila* JAK-STAT pathway, where 1. Depicts the unbound/inactive receptor domeless, 2. Shows binding of the ligand, upd3, to domeless, resulting in hopscotch (hop) self-phosphorylating, and phosphorylating a tyrosine residue on domeless. 3. Shows binding of Stat92E to the phosphorylated receptor, its phosphorylation, dimerization and translocation to the nucleus where it induces expression of its target genes. **(B)** Schematic of the *Drosophila* JNK pathway. Activation of the JNK pathway by intrinsic and extrinsic signals leads to a cascade of phosphorylation and activation of kinases, resulting in phosphorylation of the *Drosophila* JNK, basket (bsk), its phosphorylation of dJun and dFos leads to transcription of several genes including the JAK-STAT ligand upd3, and negative regulator puckered (puc). Figure made with the use of BioRender.

1.3.2.3 Age-related immune activation

The ability to respond to, and defend against, infection from pathogens is essential throughout organismal life. This ability does, without a doubt, extend lifespan in the face of infection, however evidence suggests that ageing results in dysregulation and chronic activation of the immune system, thought to exacerbate age-related decline.

Immunosenescence is a conserved hallmark of ageing, characterised by the chronic activation and progressive decline of immune system function with age[66–71]. In humans, this is associated with a reduced ability to defend against infection, resulting in increased morbidity and mortality among the elderly population[72–74].

Mammalian immunity is complex, formed of two main branches; the highly conserved innate immune response, and the specialised adaptive immune response. The *Drosophila* immune system, in contrast, contains just the conserved innate immune system. This relative simplicity, alongside the aforementioned genetic tools, and high levels of conservation have led to the use of *Drosophila* as an important tool in the study of innate immunity. Additionally, it appears that age-related changes in immunity may also be conserved, with both immunosenescence and overexpression of immune genes observed in old flies.

The fat-body of the fly is generally thought to be the centre of immunity, integrating immune and metabolic pathways. Here there are two main immune pathways in *Drosophila*, which activate nuclear-factor kappa-B (NF-κB) transcription factors, resulting in the expression of anti-microbial peptides (AMPs) which are released from the fat-body into the haemolymph where they can have a systemic effect. These are the Toll and Immune Deficiency (IMD) pathways (Figure 1.4), activated by the NF-κB transcription factors *Dif* (*dorsal-related immunity*) and *relish* respectively. These pathways are complementary to one another, responding to infection from different pathogens.

Toll is activated by fungi and Gram-positive bacteria. Proteolysis of spätzle from a pro-protein to its active form is required for Toll pathway activity. Activation of Toll by spätzle, leads to the recruitment of an adaptor protein, MyD88. MyD88 then binds Tube, and this complex recruits Pelle, resulting in Pelle autophosphorylation, the subsequent phosphorylation of cactus, and transcription factor release. Depending on the context, either Dif or Dorsal is released, translocating to the nucleus to initiate the transcription of immune effector genes (Figure 1.4B).

The IMD pathway is activated by Gram-negative bacteria. Binding of peptidoglycan from the cell walls of gram-negative bacteria to peptidoglycan recognition protein (PGRP)-LC results in the

activation of a signalling cascade, culminating in nuclear translocation of the IMD NF-κB transcription factor *Relish,* and the subsequent transcription of AMPs e.g. Diptericin (Figure 1.4A)

The fly gut has also been shown to be an important immune organ. As well as providing a physical barrier between the microbiota and the internal environment of the fly, it plays an important role in controlling the community of resident microbiota. It must differentiate between neutral or beneficial microbes, and pathogenic microbes, initiating a robust immune response only upon infection from pathogens. The Toll pathway does not function in the *Drosophila* gut[75], instead gut epithelia mount two distinct responses to infection; activation of the IMD pathway and release of AMPs into the gut lumen, and activation of the dual oxidase (DUOX) pathway that controls release of microbicidal reactive oxygen species (ROS). It is important to tightly regulate the immune activity however, even in the face of the microbial diversity within the intestinal lumen, as initiation of an immune response is metabolically costly, resulting in a trade-off with fecundity[76], and loss of metabolic stores[22,77]. Additionally, while AMPs are specific to prokaryotic cells, ROS is indiscriminate about the cells it affects and is cytotoxic to eukaryotic host cells. Indeed chronic DUOX activity results in cell apoptosis and early host death[78].

Expression of several AMP genes, including *Drosomycin* and *Diptericin* (expressed through the Toll and IMD pathways respectively; Figure 1.4) have been shown to increase with age, indicating activation of these immune pathways. Interestingly, although the Toll pathway is not thought to be active in the intestine, *Drosomycin* has been found to be expressed in intestinal samples[39]. This could perhaps be explained through poor primer specificity, as the JAK/STAT pathway has been shown to contribute a subset of AMPs in the intestine, in the form of *Drosomycin*-like peptides[79].

The reasons behind increased immune activation with age are not clear-cut. One infection study noted lower levels of *Diptericin* transcripts in aged flies following inoculation with heat-killed bacteria, but higher levels of *Diptericin* transcripts were found, over a greater period of time, in aged flies than young flies following inoculation with live bacteria[76]. The authors proposed that aged flies have an impaired immune response which enables bacteria to survive longer, causing a persistent infection and prolonged, or increased, activation of NF-κB pathways and subsequent AMP production.

Increased immune activation with age is not dependent upon infection however. It has been shown that expression of transgenic tagged AMP constructs is able to partially predict the remaining lifespan in young flies, indicating that immune activation is closely linked with lifespan, even in uninfected *Drosophila*[80]. Further to this, inhibition of NF-κB pathways prolongs the lifespan of

Drosophila[81], and artificial activation of the Toll or the IMD pathway increases the proportion of Smurfs within the population, and significantly reduces lifespan in *Drosophila*[39], highlighting the deleterious effect that poor control of these pathways has with age.

This increase in immune activity is not limited to expression of AMPs. One study found that transcription of five peptidoglycan receptor proteins, which activate the Toll pathway in *Drosophila*, increase with age[82], whilst other studies have shown that key genes within the immune pathways (E.g. *Relish and Eiger*) also show increased levels of transcription with age[83–85]. Additionally, while the *Drosophila* cellular immune response, involving circulating haemocytes, is less well characterised than the humoral response, it has been found that females display a substantial decrease in the numbers of circulating haemocytes with age, although this was not observed in males[86]. Haemocytes respond to infection in several ways, for example, phagocytosis and encapsulation of invading microbes[87]**,** however it has been shown that phagocytosis of bacterial and fungal spores declines with age[86]. This demonstrates that the decline in immune function within *Drosophila* is not limited to the humoral response.

Unsurprisingly, links have been made between microbial dysbiosis and age-related immune changes. Supporting this argument, studies have shown that the presence of microbiota induces a local immune response, primarily through the IMD pathway[88], and mounting of a systemic immune response upon loss of barrier function drives mortality in aged flies[39]. Additionally, flies reared under axenic conditions exhibit decreased expression of immune genes, although age-related immune activation is observed even without microbiota[89,90]. This may be due to an increase in senescent cells and their associated 'senescence-associated inflammatory phenotype' (SASP) which has been shown to deregulated IMD signalling in the gut[91]. Although, as noted in section 1.3.2.2.2, there is uncertainty surrounding the presence of senescence in invertebrates.

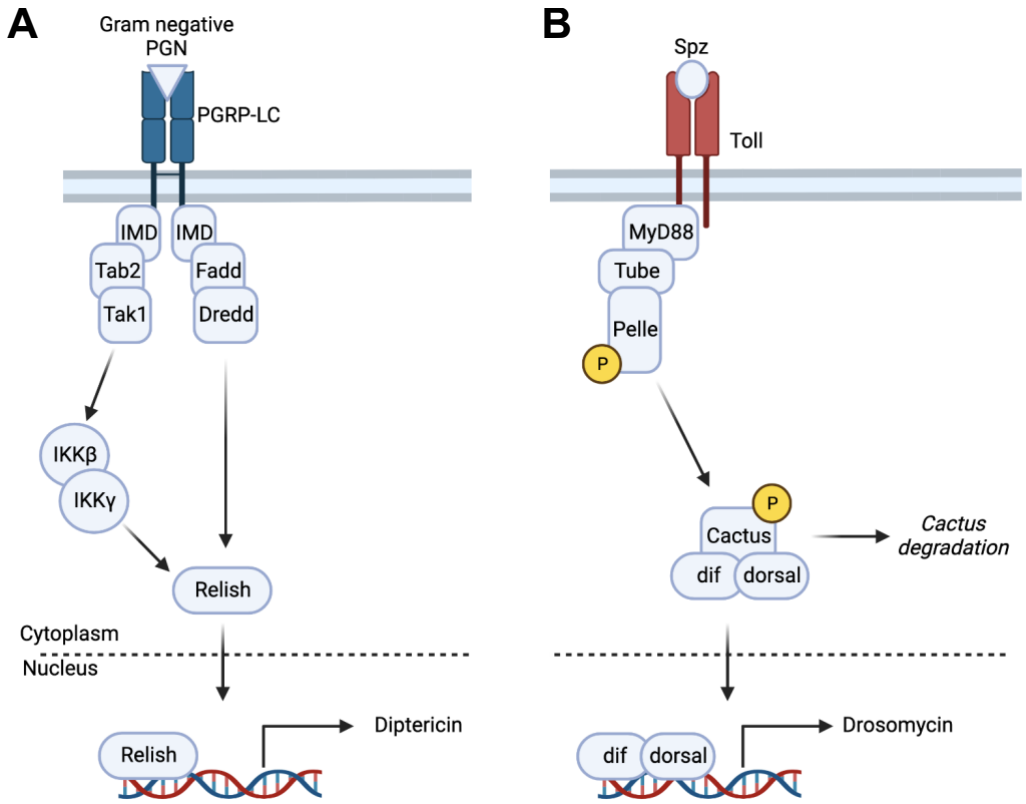

Figure 1.4 | Schematic of the *Drosophila* immune pathways.

(A) Simplified schematic of the immune deficiency (IMD) pathway. Activation of the transmembrane receptor, PGRP-LC by gram-negative peptidoglycans (PGN), results in a signalling cascade leading to nuclear translocation of the NF-kB transcription factor Relish, and transcription of AMPs including Diptericin. **(B)** Simplified schematic of The Toll pathway. Activation of Toll by spätzle (Spz) leads to recruitment of the adaptor protein MyD88. MyD88 binds Tube, which recruits Pelle resulting in its autophosphorylation. Phosphorylation of Pelle results in the phosphorylation and subsequent degradation of cactus, and the release of the transcription factor, either Dif or Dorsal depending on context. Nuclear translocation of Dif or Dorsal results in the transcription of effector genes including the AMP Drosomycin. Figure made with the use of BioRender.

1.3.2.4 Dysbiosis

Dysbiosis refers to deleterious changes in the composition and quantity of intestinal microbiota, and has been shown to occur with age in a wide range of animals, including humans, mice and *Drosophila*[27,40,92]. This is now thought to be an intrinsic factor of ageing, occurring irrespective of gender, genotype and diet. Indeed, populations of genetically homogenous mice, raised and fed in the same conditions show age-related decreases in bacteria thought to be beneficial, such as *A. Muciniphila* and short chain fatty acid (SCFA) producing members of Clostridium family, along with an increase in pro-inflammatory microbes[93]. Additionally, it has been shown that colonising middle-aged African Killifish with microbes from young fish results in longer-lived fish with significantly increased activity later in life than controls[94]. The microbiome of fish colonised with the young-fish

microbes retained diversity, and key microbes were shared with young fish, perhaps indicating an importance of these species for the improved health outcomes.

As well as age, dysbiosis has been linked to a wide variety of diseases, many of which increase in incidence with age. Examples include inflammatory bowel conditions[95–97], neurological conditions[98,99], metabolic conditions[100], as well as frailty and arthritis[101–103]. Due to the complexity of the microbial communities, and natural variation between individuals, there is large amount of variation in the changes observed with age. Certain alterations have however been identified, particularly at the phylum level, which correlate with poorer outcomes with age. Recent data from a cohort of humans aged 18 - 98 suggests that microbial communities become increasingly divergent between individuals with age, with this 'uniqueness', as well as a decrease in the abundance of *Bacteriodes* indicative of more healthy ageing[104]. Additionally, increased proportions of Proteobacteria in relation to Firmicutes have been identified as a biomarker of both ageing and inflammatory bowel disease[105,106], and increased levels of Proteobacteria and Enterobacteriaceae have been correlated with inflammation[107] and frailty[102] respectively in the elderly. Murine models of colitis have also found a correlation between increased levels of Enterobacteriaceae and inflammation[108].

In *Drosophila* an increased bacterial load is commonly observed with age[39,89,90,92,109], and an expansion of γ-proteobacteria has been associated with poor health outcomes[39]. One advantage of *Drosophila* is the ability to raise them axenically, with no microbiota. Such flies have been shown to have reductions in age-related markers including immune activation, dysplasia and loss of barrier function[39,89,92,109]. This highlights the potentially deleterious effects of the microbiota. Despite this, there is no consensus on whether sterile flies live longer, with the effects likely impacted by the nutritional environment. As an example, it has been found that the fungal microbe *Issatchenkia orientalis* can rescue lifespan in periods of undernutrition, by increasing the available pool of amino acids[110], sterile flies under these conditions live less long.

As well as the microbiota impacting host nutrition, host diet is thought to be a strong contributor to microbiome composition in humans[111–113], and likely across the animal kingdom, and may therefore modulate dysbiosis. The interaction between diet and microbiota will be discussed further below.

1.3.3 The importance of Diet

1.3.3.1 Diet and ageing

Diet has long been associated with health and longevity. One of the best known, and most widely studied methods for increasing longevity is a regime of dietary restriction. This is the reduction in

caloric consumption without malnutrition, and the benefits and mechanisms involved have been shown to be conserved throughout the animal kingdom, from single celled yeast, through to *Drosophila* and mammals[114–117]. Some studies have shown this increase in longevity to be dependent on the ratio of sugar and protein within the diet; a higher proportion of carbohydrate to protein resulting in increased longevity when calories are matched[118–121]. Indeed the abundance of single amino acids (methionine and tryptophan) have been shown to modulate lifespan[122–129].

Poor diet is also widely associated with poor health and increased morbidity. Diets high in saturated fat, sugar and salt but low in nutrient and fibre rich fruits and vegetables are well documented in the development of cardiovascular disease, type 2 diabetes, and even impaired cognition in the elderly.

High or medium protein diets have also been shown, in humans, to increase the risk of type 2 diabetes (in over 50s), and all-cause and cancer-related mortality among those aged 50-65[130]. The same study however found the reverse to be true in individuals over 66, where a high or moderate protein diet lowered the risk of all-cause mortality[130]. A higher intake of protein by elderly people, may help them to offset or prevent sarcopenia and frailty, conditions which result in unintentional weight loss, and loss of muscle mass, and which increase morbidity and mortality.

This suggests that a more nuanced approach may be required when investigating the impact of diet, on health and longevity, with an increased understanding of the nutritional requirements at each age, and how an optimum diet should be adjusted to reflect this and support continued health.

1.3.3.2 Nutrient-sensing pathways

Because of the high level of conservation of the response to dietary restriction, a large amount of research has been done to determine the mechanisms for this extension, identifying the mechanistic target of rapamycin (mTOR) and the insulin/insulin-like signalling (IIS) nutrient sensing pathways as drivers of this response.

1.3.3.2.1 IIS

The insulin/insulin-like growth factor-1 (IGF-1) signalling (IIS) pathway (Figure 1.5) was the first nutrient sensing pathway to be linked to ageing[131]. Regulating nutrient homeostasis, growth and ageing, the IIS pathway is conserved among *C. elegans*, *Drosophila*, mice and humans[132].

The IIS pathway is initiated by insulin-like peptides (*Drosophila insulin-like peptides* (*dilps*) in *Drosophila*), secreted in response to food. The Insulin-like peptides bind to insulin/IGF tyrosine kinase receptors[133] (*insulin receptor* (*InR*) in *Drosophila*) which, when activated, transduce signal to phosphatidylinositol 3-kinase (PI-3K) directly, or indirectly through the intracellular insulin-receptor

substrate (*CHICO* in *Drosophila*[134,135]). PI-3K converts phosphatidylinositol 4,5-biphosphate (PIP_2) to phosphatidylinositol 3,4,5-biphosphate (PIP_3)[136]. PIP_3 acts as a secondary messenger that activates a protein kinase cascade, eventually resulting in phosphorylation of the forkhead box O (FOXO) transcription factor, and its cytoplasmic retention[137]. This prevents unphosphorylated FOXO transport into the nucleus, and subsequent gene transcription. The action of PI-3K is regulated by antagonism from phosphatase and tensin homolog (PTEN) which catalyses the reverse reaction of PIP_3 to PIP_2[138–141].

Drosophila has 8 dilps[135,142,143], although dilp2, the homolog to insulin has been most extensively studied[144]. Inhibition of dilps and other negative regulators of FOXO (e.g. InR and CHICO) leads to lifespan extension[143,145–148]. Additionally, activation or overexpression of IIS negative regulators e.g. PTEN or dFOXO also extends *Drosophila* lifespan[149–151]. The observed lifespan extensions upon IIS pathway modulation are conserved between species[152–156]. It was thought that dietary restriction may also extend lifespan through the IIS pathway[157], however data in flies and worms suggests that these are independent mechanisms of lifespan extension[158–160].

Interestingly, other pathways linked to ageing have been shown to interact with the IIS pathway. These are the mechanistic target of rapamycin (mTOR) pathway, which is also nutrient responsive[161,162], and the JNK pathway which responds to stress levels[48,163].

1.3.3.2.2 mTOR

The mTOR pathway (Figure 1.5) has been linked to ageing in several ways, from nutrient sensing, autophagy, mitochondrial dysfunction, cellular senescence and decline in stem cell function (the role of mTOR in ageing has been well reviewed[164,165]).

mTOR is a serine/threonine kinase that plays a central role in the coordination of nutritional and hormonal signals to regulate growth and metabolism. It functions as part of two distinct multiprotein complexes; mTORC1 and mTORC2. mTORC1 comprises three key subunits, mTOR, mLST8 (Lst8 or GβL in *Drosophila*[166,167]) and Raptor[168,169], as well as PRAS40 (Lobe in *Drosophila*[167]) and DEPTOR (no known *Drosophila* homolog) – two inhibitory units. mTORC2 similarly contains mTOR and mLST8, but associates with SIN1 and Rictor, not Raptor[170,171].

When activated, mTORC1 promotes protein synthesis through phosphorylation of downstream effectors including eukaryotic translation initiation factor 4e (eIF-4E)-binding protein 1 (4E-BP1) and ribosomal protein S6 kinase 1 (S6K1). Activation of mTORC1 also blocks autophagy. Elevated levels of autophagy, in various tissues, is associated with and necessary for longevity[164,172,173]. Similarly, inhibition of mTOR activity leads to reduced mRNA biosynthesis and translation to conserve protein

levels, and autophagy recycles intracellular constituents to enhance the available intracellular amino acid pool.

Dietary amino acids activate mTORC1, with arginine and leucine being well-studied activators. Multiple amino acids have been implicated in mTORC1 activity however, with the suggestion of a 2-step process whereby certain amino acids (Ala, Arg, Asn, Gln, Glu, Gly, Pro, Thr and Ser) 'prime' or sensitise cells for mTORC1 activation, after which 'activating' amino acids (Ile, Leu, Met and Val) promote mTORC1 activation through phosphorylation[174]. The priming amino acids are necessary for mTORC signalling to be stimulated by activating amino acids, but do not themselves cause activation of mTORC1[174]. The mechanism by which amino acids activate mTORC1 is not fully established, however sestrin-2 has been implicated as a leucine sensor which interacts with GATOR2[175–177], and SLC38A9 (a lysosomal amino acid transporter) as an arginine sensor[178–180]. In addition to interaction with GATOR2, arginine activates mTORC1 by preventing the localisation of TSC2, an mTORC1 inhibitor, to the lysosome.

One of the main pharmacological interventions shown to prolong lifespan in several model organisms, including mice and *Drosophila*, is rapamycin which inhibits activation of the mTORC1 complex[181–186]. Additionally, dietary restriction, is thought to act through reduced mTORC1 signalling[187]. Indeed, deletion of specific mTOR components or specific translation initiation factors extends lifespan in yeast, *C. elegans*, *Drosophila* and mice[187–195].

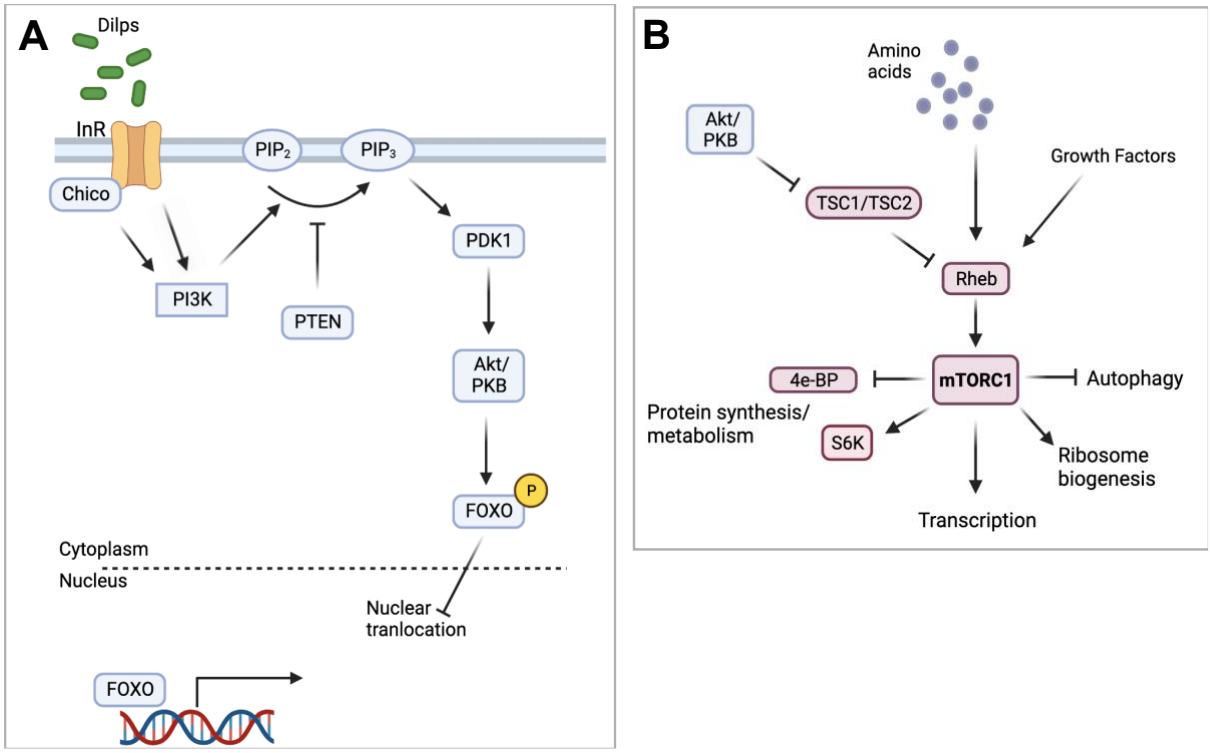

Figure 1.5 | Simplified schematics of the *Drosophila* nutrient-sensing pathways; IIS and mTOR.

(A) Simplified schematic of the *Drosophila* IIS pathway. Binding of *Drosophila* insulin-like peptides (dilps) activates the *Drosophila* insulin receptor (InR). The activated receptor phosphorylates the enzyme phosphoinositide 3-kinase (PI3K) either directly, or indirectly through the insulin receptor substrate protein Chico. Phosphorylated PI3K converts phosphatidylinositol 4,5-biphosphate (PIP2) to phosphatidylinositol 3,4,5-biphosphate (PIP3). Elevated levels of PIP3 result in activation of Akt/PKB by PDK1. Akt/PKB phosphorylated Forkhead box o (FOXO), preventing its translocation to the nucleus, and subsequent transcription of pro-aging genes. PTEN is a negative regulator of the IIS pathway. **(B)** Simplified schematic of the mTOR pathway. Activation of Rheb by amino acids or growth factors leads to the activation of the mTORC1 complex and phosphorylation of downstream effectors, resulting in programmes of enhanced translation and ribosome biogenesis, and inhibiting autophagy. Tuberous Sclerosis complex 1 and 2 (TSC1 and TSC2) are negative regulators of the mTOR pathway, and is negatively regulated by Akt/PKB linking the IIS and mTOR pathways. Figure made using BioRender.

1.3.3.3 Diet and microbiota

As well as influencing health and ageing directly, diet is the strongest determinant of microbiota composition[113,196], which further impacts healthy ageing. As mentioned above, host diet is considered one of the strongest determinants of microbiome variation in humans[111–113], with the composition rapidly changing in response to new food choices i.e. shifting between plant-based and animal-based diets[112,113], or adjusting the protein to carbohydrate ratio of ingested food[197]. This is not surprising and is likely to remain true across the animal kingdom, as host diet becomes the diet of the microbiota, and different microbial species show a preference for certain nutrients. In *Drosophila*, dietary restriction via a regime of 2 days feeding and 5 days fasting for 1 month

increases lifespan[198], likely through the mTOR pathway, however, this regime also results in lower bacterial load, which may contribute to the increased lifespan and improved gut barrier function 40 days after the treatment.

As well as being shaped by the host's diet, the microbiota provides nutrients to the host, with an impact on health and longevity. Microbes can be a source of protein for the host[199], indeed association with the yeast *Issatchenkia orientalis* has been shown to rescue the lifespan of *Drosophila* in periods of undernutrition by efficiently extracting and concentrating amino acids from food substrates, allowing increased amino acid flux to *Drosophila* upon consumption[110]. On top of this, specific members of the microbial community have also been shown to provide added benefit; it has been well established, that *lactobacillus* species support the growth of *Drosophila* larvae upon chronic undernutrition[200–203]. This benefit is not due to *Lactobacillus* as a food source, as the bacteria must be alive for the growth benefit[201]. Indeed further work has demonstrated that association with *Lactobacillus plantarum* sustains *Drosophila* peptidase activity within the midgut, promoting protein digestion and thereby increasing the pool of available amino acids[202].

Importantly, the nutritional impact of the microbiome is not limited to protein provision. *Acetobacter pomorum* provides thiamine (vitamin B1) to its host, *Drosophila*, and indeed can provide enough that flies are capable of developing on a thiamine-free diet[204]. Additionally, Consuegra *et al.* recently showed that *Acetobacter pomorum* and *Lactobacillus plantarum* species were able to compensate for the loss of nutrients including, but not limited to, vitamins (including Biotin, Folate, Riboflavin and Thiamine), Zn, Fe and Cu, as well as several amino acids[205], when each was removed individually from the diet.

The contribution of the microbiota to diet is not limited to *Drosophila*. *Lactobacillus* species have been shown to buffer the adverse effects of chronic undernutrition in juvenile mice, and support juvenile growth[206]. Additionally, bacterial conversion of free amino acids into polypeptides within the gut has been shown to be an important contributor to both amino acid metabolism and bioavailability in the mammalian gut[207]. It's more difficult to study the contribution of the microbiome to nutrition in humans, however there are some known examples of bacterially derived nutrients e.g. bacterially derived vitamin K[208–211], which has been linked to improved cognition[209] and cardiac health[212,213].

The effect of the microbiota to host health is tied to the composition of the microbial community, which in turn is dependent on diet. It is therefore important to be aware of the effect of diet on the

microbiota, and of both the diet and microbiota on ageing when designing studies, and interpreting data from published work.

1.3.3.4 Defined diet

The nutritional requirements of *Drosophila* have been studied from as far back as 1946[214], with subsequent studies optimising the amounts of various dietary components required for larval development[215] and adult fecundity[216,217]. This has resulted in a large range of 'standard' laboratory diets adopted by different *Drosophila* researchers, with significant variation between these diets.

This variation in diet is of significant impact, particularly to the ageing community, due to the known effect of diet on the microbiota, and of both the diet and microbiota on ageing, and makes interpretation and comparison of results between groups difficult. Furthermore, even within one 'standard' diet, batch-batch variation can lead to differing results, making it challenging to interpret data.

To overcome this, attempts have been made to generate chemically defined diets, with some semi-defined diets being employed for longevity studies[218–220]. Unfortunately, these diets did not overcome the problem of batch variation as they were only partially chemically defined. A new fully defined, or holidic diet was, however, published in 2014[221–223]. As this diet is entirely comprised of pure individual nutrients it does not suffer any differences between batches, which may explain the reduced (though not significantly) variance in median lifespan of this diet[222]. The authors show that the diet supports larval development (although this is delayed), adult egg-laying, and the full adult lifespan[222]. The authors also went on to further optimise this diet, by matching the amino acid ratios to estimates of the relative proportions of amino acids' present in *Drosophila's* predicted protein coding genes. They found this improved diet had no effect on lifespan but apparently removed the trade-off between fecundity and lifespan in adulthood[224].

Encouragingly, there has been good uptake of this diet by different research groups, with several now publishing with this diet[225–228]. This should essentially result in diet being controlled for across research groups, improving reproducibility between groups, and making interpretation and comparison of results between groups easier.

1.4 Thesis aims and objectives

My thesis aims to interrogate changes in intestinal nutrient dynamics with age. To understand this, I will ask what, if any, changes are occurring to the intestinal nutrient profile with age. Additionally, as the microbiota is implicated in age-related decline, I will also ask whether the presence of an intestinal microbial community affects this nutrient profile.

I will then look at whether changes to the nutrient profile directly impact lifespan, and I will assess how age-related changes in the expression of luminal nutrient transporters, specifically amino acid transporters, may impact this nutrient profile, and the ageing process.

Next, I will characterise the expression profile of two distinct *Drosophila* amino acid transporters whose intestinal expression decreased with age, and for which genetic tools were available. I will also use genetic approaches to evaluate their impact on longevity and ageing phenotypes.

1.4.1 Thesis objectives

1. Validate the use of a chemically defined media for ageing experiments
2. Develop an assay to assess the *Drosophila* luminal/faecal nutrient profile
    a. Assess changes in the *Drosophila* luminal/faecal nutrient profile with age
    b. Assess changes in the *Drosophila* luminal/faecal nutrient profile upon microbial colonisation
3. Develop a new diet to evaluate whether changes in the luminal/faecal amino acid profile drive age-related decline
4. Evaluate the expression of predicted luminal amino acid transporters
5. Take two candidates and:
    a. Characterise intestinal expression and regionalisation
    b. Assess the impact of intestinal knockdown on longevity and ageing phenotypes
    c. Assess the impact of intestinal overexpression on longevity and ageing phenotypes

2 Materials and Methods

2.1 Flies

2.1.1 Fly Husbandry

Flies were maintained in either vials or bottles in incubators with 65 % humidity and a 12-hour light/dark cycle. Stocks were maintained at 18°C and experimental flies at 25°C.

Temperature cycling was used to slow development and delay mating. To begin virgin collection, culture bottles of our desired line were cleared of any eclosed adult flies at the end of the day and placed at 18°C. Flies were allowed to eclose overnight and adult virgin females were collected the following morning based on appearance (section 1.2.2) and placed into separate vials containing 8 mL of standard cornmeal medium (section 2.1.3.1). Virgin only vials were kept at 18°C. Culture bottles were left at room temperature and virgins were collected again in the afternoon and evening. After 3 days of morning and evening collections, or once sufficient virgins were collected, virgins were allowed to mature at 25°C for 24 hours to facilitate efficient mating. Male flies were then introduced to virgin females at a ratio of 3♀: 1♂.

Where defined media (Section 2.1.3.2) is used, adult flies were sorted onto this media 48-96 hours after eclosion. Otherwise, flies were maintained on cornmeal media (section 2.1.3.1). Flies were anaesthetised using light CO_2, pushed using paintbrushes and visualised using an Olympus SZ dissection microscope.

All experiments were carried out using age-matched mated females, housed at a density of 27-32 flies per vial, and flies were flipped into fresh vials every 2-3 days. To control for bacterial growth on the food, control and experimental flies are always transferred to fresh food at the same time points, and stoppers were changed once a week. Any deviations from this will be made clear.

2.1.2 Fly Stocks

Table 2.1 | Fly stocks used in this thesis

Stock #	Designation	Source or reference	Source identifiers	Additional information	Final Genotype
1	Canton-S			Gift of Linda Partridge	
2	TIGS-2-GeneSwitch	Kabil et al., 2011[229]		Gift of David W. Walker	
4	Eaat1-TRiP	BDSC	RRID:BDSC_43287	Crossed onto a white background	W^{1118} ; P{y[+t7.7] v[+t1.8]=TRiP.HMS02659}attP40 / Cyo ; + / +
5	Eaat1 shRNAi	VDRC	RRID:VDRC_330103		W; Eaat1-shRNAi ; + / +
6	UAS-Eaat1	BDSC	RRID:BDSC_8202	Crossed onto a white background, balanced by TM6c,sb not TM6b,tb	W^{1118} ; + / +; P{w[+mC]=UAS-Eaat1.Exel}3 / TM6b, sb^1
7	Eaat1-venus	Parinejad et al. 2016[230]		Gift of Donald J. van Meyel	
8	Eaat1-gal4	BDSC	RRID:BDSC_86342	Crossed onto double balancer to rescue line, balanced by cyo not SM6a	W^{1118}; TI{GFP[3xP3.cLa]=CRIMIC.TG4.0}Eaat1[CR01303-TG4.0] / cyo; + / +
9	$Slif^{anti}$	BDSC	RRID:BDSC_52655		Y^1w^*; + / +; P{y[+t7.7]=Mae-UAS.6.11}slif[UY681]
10	UAS-Slif	BDSC	RRID:BDSC_52661	Floating cyo balancer removed	W^{1118}; + / +; P{w[+mC]=UAS-slif.C}3 / TM3, sb^1

2.1.3 Fly food

2.1.3.1 Cornmeal medium

Cornmeal medium comprised of 1 % agar (SLS, FLY1020), 3 % dried inactivated yeast (Genesee Scientific, 62-106), 1.9 % sucrose (Duchefa Biochemie, S0809), 3.8 % dextrose (Melford, G32040) and 9.1 % cornmeal (SLS, FLY1110), all given in wt/vol, and water at 90% of the final volume. Preservatives; 10 % Nipagin (SLS, FLY1136) in ethanol and an acid mixture comprised of 4.15 % phosphoric acid (VWR, 20624.262) and 41.8 % propionic acid (Sigma, P5561) in water, previously described by Lewis, 1960[231], were added following boiling.

For preparation of the medium, dry ingredients were weighed into a plastic beaker. Upon adding the water, the mixture was stirred until all the dry ingredients were suspended and no lumps remained. The mixture was then microwaved on max power and stirred regularly to prevent the formation of lumps until the food had thickened. Once thickened, the food was microwaved without stirring until it reached a rolling boil for approximately 30 seconds – care was taken to ensure it did not boil over. The medium was allowed to cool before the nipagin and acid mix was added. Once the preservatives were fully incorporated into the food, the medium was dispensed into vials or bottles using a liquid dispenser. 8 mL was aliquoted into vials designated for stock maintenance or larval development following genetic crosses, 4 mL into vials with no larval growth and 75 mL into bottles. Vials and bottles were immediately plugged to prevent loose flies from laying eggs in the food, they were left for 24 hours at room temperature to allow dispersion of condensation, then stored at 4°C. Food was kept for a maximum of 2 weeks.

2.1.3.2 Defined medium

The defined medium was prepared as in Piper et al.[222] using the suggested addition of 50 % more vitamin solution and the exome matched amino acid concentrations 'FLYAA' reported in Piper et al.[224]. Contrary to the published method, buffer A containing the metal ion solutions, low solubility amino acids, cholesterol, MilliQ water and acetate buffer was brought to a boil in the microwave, not autoclaved at 121 ° C for 15 minutes, except in the preparation of sterile medium for axenic flies. The remaining ingredients of essential and non-essential amino acid solutions, cysteine and glutamic acid solutions, vitamin solution, lipid-related metabolite solution, folate, 10 % nipagin in ethanol, and propionic acid were added once buffer A was cooled to 65 ° C, and thoroughly incorporated. Any modifications to this diet will be clearly stated.

4 mL was aliquoted into vials which were immediately plugged to prevent any loose flies from laying eggs in the food. They were left for 24 hours at room temperature to allow dispersion of condensation, then stored at 4°C. Food was kept for a maximum of 2 weeks

2.1.3.3 Mifepristone food

Mifepristone or RU-486 (Cayman chemicals, 10006317), hereafter referred to as RU, food was prepared by the addition of 250 µL RU-486 per 100 mL food. For the dose of 25 µg/mL used in this thesis, 125 µL of ethanol, and 125 µL of 20 mg/mL Ru-486 stock solution was added per 100 mL of food. Control food was prepared by the addition of 250 µL ethanol per 100 mL food. Food was mixed thoroughly to ensure a homogenous solution.

To prevent inhalation of any RU carried within the steam, all RU food was made in the fume hood and vials were immediately plugged prior to removal from the hood.

2.1.4 Generation of Axenic and Gnotobiotic Flies

To generate sterile (axenic) flies, eggs were collected on apple juice agar plates seeded with a paste of live baker's yeast and ddH_2O, then washed and treated with bleach and ethanol as described previously[5]. All steps were carried out in a laminar flow hood. Briefly, <14 hour-old embryos were dechorionated in 2 % sodium hypochlorite solution for 2.5 minutes, rinsed in 70 % ethanol for 5 minutes and then rinsed with ~200 mL sterile PBS. Embryos were then resuspended in sterile 0.01 % PBSTx (PBS + 0.01 % Triton X-100 (Sigma, X100)) and transferred to sterile autoclaved cornmeal medium.

To re-associate sterilised embryos with parental gut bacteria, 100 µL adult fly homogenate (1 fly/20 µL sterile PBS) was added to sterile cornmeal medium prior to addition of axenic embryos and allowed to dry. Flies were surface sterilised for 5 minutes in 70 % ethanol prior to homogenisation to ensure only internal microbes were present in the homogenate. Re-associated flies were used as the control for axenic flies to ensure any observed effect is due to the sterility of the flies, and not the bleach treatment of the embryos.

All medium for sterile and control flies was sterilised by autoclaving for 15 minutes at 121 °C, and all equipment used to push flies was first sterilised in Virkon for at least 20 minutes, then rinsed and stored in 80 % ethanol. Gas pads were subsequently dried by running CO_2 through them. To maintain sterility, axenic flies were sorted next to an open flame and flipped to new sterile food every 2-3 days in a laminar flow hood. Stoppers were changes at every flip

Sterile conditions were confirmed throughout lifespans by testing the sterility of soiled vials. Soiled stoppers were pressed into single wells of 12-well plates (Starlab, E2996-1610) containing 3 mL of pre-poured and set LB Miller Agar. The plates were incubated at 37 °C for 24-48 hours to check for bacterial growth.

Where conventionally reared flies were used as a further control to axenic or re-associated flies, 30 mated females were placed in vials containing sterilised cornmeal food and allowed to lay eggs for 24 hours, starting the evening prior to embryo collection.

2.2 Lifespan Analysis

To ensure the whole cohort was the same chronological age, age-matched flies were used. These flies were flipped onto new food within 24 hours of eclosing. They were then allowed at least a further 24 hours to mate before the mated females were sorted under CO_2 into vials. Flies were transferred to fresh food every 2-3 days and the number of dead flies was counted. At least 6 vials of 30 females were used per lifespan.

2.3 Smurf Analysis

The smurf assay[232] for intestinal barrier integrity was performed by flipping flies onto food containing 2.5 % FD&C blue food dye #1 for 24 hours (FastColours, 08BLU00201). This is a non-permeable dye which passes straight through the digestive tract of healthy flies. A 'smurf' phenotype is seen when the intestine becomes leaky, allowing the blue food dye across the lining of the gut where it enters the haemolymph and becomes visible in the haemolymph through the cuticle. After 24 hours, the lifespan vials are flipped back onto un-dyed food and the number of 'smurf' flies is recorded.

The proportion of Smurf flies at a given timepoint was calculated by dividing the number of smurfs in the population by the population size at that time-point. For this reason, smurf counts were performed on lifespan vials.

2.4 Gene expression Analysis

2.4.1 Reverse transcription

2.4.1.1 RNA extraction

Total RNA was extracted from 5 whole guts, 5 midguts or 3 whole flies per biological replicate. Whole guts included crop, cardia, midgut, Malpighian tubules and most of the hindgut excluding rectal papilla. Midguts included the cardia and midgut, through to the midgut-hindgut junction,

excluding the hindgut and Malpighian tubules. RNA was extracted from each condition in at least triplicate.

A standard TRIzol protocol was used to extract RNA. Briefly, flies were homogenised in 100 µL TRIzol™ (Thermofisher, 15596026) using a motorised pestle, samples were maintained on ice except for a 10 minute incubation at room temperature prior to storage at -80 °C or further processing. 20 µL chloroform (Sigma, C0549) was added, and the samples were shaken and then spun to separate the phases. 45 µL of the organic phase was extracted, and the RNA precipitated by the addition of an equal volume of RNA grade isopropanol (Sigma, I9516). 4.5 µL 3M sodium Acetate (Thermofisher, R1181) and 2 µL 20 mg/mL glycogen (Thermofisher, R0551) was added to help precipitate the RNA within gut samples prior to isopropanol precipitation. The samples were spun to pellet the RNA, then the pellets were washed in 75 % RNA grade ethanol (Sigma, 51976), resuspended in nuclease-free water (Sigma, W4502) and incubated at 55 ° C for 10 minutes to ensure the RNA is fully resolubilised.

2.4.1.2 cDNA synthesis

For a 10 µL reaction, 1 µL DNase buffer (Thermo, EN0521) and 0.5 µL DNase 1 (Thermo, EN0521) were added to 8.5 µL RNA solution (section 2.4.1.1) and incubated for 30 minutes at 37 °C, to remove any DNA contaminants. The DNase enzyme was then deactivated by the addition of 0.5 µL 50mM EDTA (Thermo, EN0521) and subsequent incubation for 10 minutes at 65 °C.

cDNA synthesis was carried out using Thermo Scientific's First Strand cDNA Synthesis kit. In short, 1 µL of random hexamers (Thermo, SO142) were added and the samples were incubated at 70 °C for 5 minutes before a 9 µL of a master mix containing 4 µL first strand buffer (Thermo, EPO442), 0.5 µL RIbolock RNase inhibitor (Thermo, EO0382), 2 µL 10mM dNTPs (Thermo, R0181), 0.2 µL RevertAid reverse transcriptase (Thermo, EPO442) and 2.3 µL molecular grade water (Sigma, W4502) per well, was added. The samples were then incubated for 10 minutes at room temperature, followed by 1 hour at 37 °C and 10 minutes at 70 °C. The samples were spun following each incubation step.

2.4.2 Bacterial DNA extraction

30 whole flies were sorted under light CO_2 anaesthesia into microcentrifuge tubes and frozen at -80 °C. Flies were then surface sterilised in 70 % ethanol for 5 minutes and rinsed twice in sterile PBS. 5 flies were sorted into sterile microcentrifuge tubes and homogenised in 200 µL lysis buffer (1 X TE, 1 % Triton X-100, 1/100 proteinase K (NEB, P8107S)) using a mechanical pestle, with a further 300 µL of lysis buffer being added after homogenisation. Lysate was incubated for 1.5 hours at 55 °C then transferred to screw cap vials containing 0.4 g sterilised low binding 100-micron silica beads (OPS Diagnostics, BLBG 100-200-11) and vortexed for 10 minutes at max speed. Lysate was then

transferred back to the original tube and incubated for a further 1.5 hours at 55 °C followed by 10 minutes at 95 °C.

2.4.3 Quantitative PCR

Bacterial DNA and *Drosophila* cDNA samples were prepared as described above. qPCR was performed with Power SYBR™ Green master mix (Fisher, 10219284) on a Bio-RAD CFX Connect Real-Time PCR detection system. Either 4.5 µL bacterial DNA or 1 µL of *Drosophila* cDNA sample, diluted to ensure values fall within the range of the standard curve, was used in a 10 µL reaction with 5 µL of Power SYBR™ Green and 0.5 µL of L + R primer mix. Any remaining volume was made up with molecular grade water.

Cycling conditions were as previously described[39]; 95°C for 10 minutes, then 40 cycles of 95°C for 15 seconds followed by 60°C for 60 seconds. All calculated gene expression values were normalised to the value of a housekeeping gene (e.g. rp49). The primer sequences used to assess gene expression in this study can be found in Table 2.2.

To distinguish between the use of genomic DNA and cDNA in the qPCR reactions, RT-qPCR is used to denote 2-step reverse transcription qPCR, where cDNA is synthesised separately and used for the qPCR reaction. qPCR will be used to denote the use of genomic DNA in the qPCR reaction.

2.4.4 Primers

All primers were obtained through Integrated DNA Technologies. Those which originate in this study were designed through the Roche Universal probe library (which was shut down in 2020) or taken from FlyPrimerBank (https://www.flyrnai.org/flyprimerbank).

Table 2.2 | Primer sequences

Target	Forward primer	Reverse primer	Reference
Actin 5C	TTGTCTGGGCAAGAGGATCAG	ACCACTCGCACTTGCACTTTC	Clark et al. 2015[39]
Bacilli	CGACCTGAGAGGGTAATCGGC	GTAGTTAGCCGTGGCTTTCTGG	Clark et al. 2015[39]
CG1698	CCAGGCGTATGTGGGTTCATT	AGAGAGCGTCTTCTTGCCATT	This study (FlyPrimerBank)
CG43693	CCGTTGGTAATCTCTCGGAAAA	AGCGATCCCTTTAGCAAGTGT	This study (FlyPrimerBank)
CG5535	TTATCCGCCTTCGATCTTACCG	CGGCATATTGCTTGGACACTT	This study (Roche)
CG7255	CGGCAGTGTCTCAAAGTCG	TGGCGAACCATTGTTCAGTAT	This study (Roche)
CG8785	AATGACTTCAACTCGAAAGCCA	GCTCGAAGGGATGGTAGGGA	This study (FlyPrimerBank)
Diptericin (DPT)	ACCGCAGTACCCACTCAATC	CCCAAGTGCTGTCCATATCC	Clark et al. 2015[39]
DmGlut	CGCCAATTAGTACCGAGATGA	CGCTGGGGTATCACGAAAT	This study (Roche)
Drosomycin (DRS)	GTACTTGTTCGCCCTCTTCG	CTTGCACACACGACGACAG	Clark et al. 2015[39]
Eaat1	ATTGTGCCGCTTTTGGTCTCA	GTAATGGCTCTGGTAGCAATCTT	This study (FlyPrimerBank)
GAPDH	CCAATGTCTCCGTTGTGGA	TCGGTGTAGCCCAGGATT	Hunter et al. 2019[233]
Kazachoc (kcc)	GCCGTGGAAATCGTATTGAC	AGCGTCCTTGGTGAAGTCC	This study (Roche)
Minidiscs (mnd)	TGTGCCCTCGCTGATATTC	CCACGTAGCTGACGTAGTTGA	This study (Roche)
Pathetic (path)	ATGTGCTCCGGTCTCATCAT	CTTGTGTCCGCATTTTACCA	This study (Roche)
Puckered (puc)	CGACTTTATCGAAGATGCACGG	CAGGGAGAGCGACTTGTACC	This study (FlyPrimerBank)
Rp49	ATCGGTTACGGATCGAACAA	GACAATCTCCTTGCGCTTCT	This study (FlyPrimerBank)
Slimfast (slif)	CACAGTGAACAGCTACACGAAGA	GGTCCAGGTTAAAGAGCATGG	This study (FlyPrimerBank)
Sobremesa	TGGGGTGGCTTTAATTGTTGG	CAGTGCGAACCAGTAAACCG	This study (FlyPrimerBank)
Unpaired 3 (Upd3)	ACTGGGAGAACACCTGCAAT	GCCCGTTTGGTTCTGTAGATT	Salazar et al. 2018[42]
16s	AGAGTTTGATCCTGGCTCAG	CTGCTGCCTYCCGTA	Claesson et al., 2010[27]
α-proteobacteria	CCAGGGCTTGAATGTAGAGGC	CCTTGCGGTTCGCTCACCGGC	Clark et al. 2015[39]
γ-proteobacteria	GGTAGCTAATACCGCATAACG	TCTCAGTTCCAGTGTGGCTGG	Clark et al. 2015[39]

2.5 Metabolic Analysis

Flies (10/vial) were sorted into agar vials (1 % agar in dH_2O) for one hour to clear their guts then transferred into microcentrifuge tubes under light CO_2 anaesthesia (5 flies/tube) and kept on ice to maintain anaesthesia. The flies were weighed with a precision scale and then decapitated before being further processed as below. Samples were normalised to the mass of the flies.

2.5.1 TAG extraction and quantification

To measure the levels of stored triglycerides (TAG) we used the assay described by Tennessen et al. 2014[234]. In short, 5 adult female flies (without heads) were homogenised in 0.05 % PBST (1 X PBS + 0.05 % Tween 20 (Sigma, P4780)). 10 µL was removed for protein quantification and stored at -80 ° C. The remaining homogenate was incubated at 70 °C for 10 minutes. 20 µL of each sample was added to each of 2 microcentrifuge tubes; 20 µL PBST was added to one to measure free glycerol and 20 µL triglyceride reagent (Sigma, T2449) was added to the other to measure free glycerol plus triglycerides. Tubes were incubated at 37 °C for 60 minutes then centrifuged at full speed for 3 minutes. 30 µL of each sample was added to a 96 well plate and 100 µL of free glycerol reagent (Sigma, F6428) was added to each well. The final absorbance at 540 nm was measured using the SPECTROstar Nano (BMG Labtech). Samples were normalised by the recorded mass. Standards were prepared by diluting the glycerol standard solution, 2.5 mg/mL triolein equivalent glycerol standard, (Sigma, G7793) 2:3 in PBST to generate a 1 mg/mL triolein standard. This was then two-fold diluted into PBST to generate the standard series. The standards were processed as the samples.

2.5.2 Glycogen extraction and quantification

Glucose and glycogen levels were measured using the assay as in section 5.1.7 of Tennessen *et al.*[234]**.** In short, 5 adult female flies (without heads) were homogenised in PBS. 10 µL was removed for protein quantification and stored at -80 ° C. The remaining homogenate was incubated at 70 °C for 10 minutes to inactivate enzymes and prevent the degradation of glycogen, then spun at maximum speed for 3 minutes. The supernatant was removed and diluted, then stored at -80 °C or immediately processed.

Glucose and glycogen standards were made by dilution of 1 mg/mL glucose (Sigma, G3285) or 20 mg/mL glycogen stock solutions (Thermofisher, R0551) to 0.16 mg/mL, then subsequent 1:2 dilutions to generate 5 standards ranging 0.16 mg/mL to 0.1 mg/mL.

30 µL of each sample 1:10 diluted, standard and PBS blank was added to two wells of the 96 well plate. 100 µL working GO reagent was added to one of the two sample, standard and blank wells to measure glucose alone. Working GO reagent was prepared by adding 20 µL o-Dianisidine (Sigma,

D2679) per mL of glucose oxidase/peroxidase reagent (Sigma, G3660) to measure free glucose. 100 µL of GO reagent + amyoglucosidase (Sigma A1602), 1 µL amyoglucosidase per mL of working GO reagent, was added to the remaining wells to measure the digestion product of glycogen plus free glucose. The plate was sealed with Parafilm™ to prevent evaporation and incubated at 37 ° C for 1 hour before 100 µL 12N sulphuric acid was added to stop the reaction. Final absorbance at 540 nm was measured using the SPECTROstar Nano (BMG Labtech). The free glucose concentration of each sample is calculated based on the glucose standard curve. The glycogen concentration of each sample is calculated based on the glycogen standard curve, by first subtracting the free glucose absorption from that of the sample digested by amyloglucosidase. Samples were all normalised to their recorded mass.

2.5.3 Protein quantification

The homogenate removed from the TAG and glycogen samples were diluted 1 in 10 in ice cold 0.05 % PBST or PBS respectively. In a clear bottom 96-well plate 5 µL of the diluted sample, PBS/PBST blank and standards were added in duplicate to 200 µL of Bradford reagent (Thermo, 1863028) and mixed thoroughly. Samples were made from a 10 mg/mL BSA solution (Fisher, BP1600). Absorbance at 595 nm was measured using the SPECTROstar Nano (BMG Labtech).

2.6 *Drosophila* Undigested Metabolite Profile (D.U.M.P) Assay

2.6.1 Preparation

This assay makes use of knowing the full content of the defined media. To prepare, defined media was cooked normally, as in section 2.1.3.2 with the addition of 2.5 % blue food dye #1 after cooking (as in the Smurf assay above, section 2.3). As well as 4 mL vials, the food was poured into petri-dishes for the assembly of collection vials.

Collection vials are open-ended glass tubes of similar dimensions to our fly vials. These were provided by the glassblowing workshop within the Durham University chemistry department. Prior to beginning the assay, collection tubes were prepared by stamping out discs of food poured into a petri-dish and securing them in place with parafilm. This plugs one end of the vial; the other end of the tube was plugged with a foam Droso-Plug (SLS, FLY1000).

24 hours prior to sample collection, flies were flipped onto experimental food (defined media containing 2.5 % FD&C blue food dye #1). This ensures that the flies' guts will be full of the assay

media containing the dye for normalisation. Additionally, this is enough time for flies losing intestinal barrier function to become clearly visible, enabling their exclusion from the assay.

2.6.2 Sample collection

To begin the assay, flies were put to sleep under light CO_2 anaesthesia, approximately 55 - 65 non-smurf, mated females were sorted into each pre-prepared collection vial. More flies do not increase the amount of faecal deposit as when overcrowded they get stuck at the bottom of the vial (own observation). 6 collection vials were used per sample to ensure that I would end up with a large enough sample for full analysis. Once the flies awoke from anaesthesia, they were incubated at 25°C for between 4 and 5 hours to eat and defecate as usual. I found that standing the vials at a 45° angle resulted in an improved sample, particularly when collecting samples from aged flies with reduced mobility (own observation).

Following incubation, the flies were anaesthetised with CO_2, the parafilm removed and the food disc along with the flies was pushed out from the bottom of the tube. The outside of the vial and the food residue was cleaned with a tissue dampened by milliQ water until the tissue comes away clean.

The collection vials were all the same weight (26.91g ± 0.41), and fit inside 50mL falcon tubes. Once within the 50 mL tube, the collection vials were thoroughly rinsed with 1.5 mL of water to collect the polar, water-soluble faecal fraction, and spun down. The same 1.5 mL of water was used to rinse all tubes. This ensured the sample could be frozen and lyophilised quickly. Two falcon tubes were used, with the collection vials each being washed, then the water sample split between the falcons, to ensure the tubes are balanced for centrifugation. Once all tubes are rinsed, the sample is then transferred to a microcentrifuge tube. The rinse is repeated a second time to ensure all faecal matter is collected, resulting in two water-wash samples of 1.5 mL.

The vials were then rinsed thoroughly with a 1:1 mixture of DCM and methanol to collect non-polar deposits. The rinses were carried out in a small glass beaker to collect sample. The volume for this wash was not limited, but approximately 5 mL was used for all the tubes. Plastic use should be avoided with the DCM:MeOH wash.

All samples were frozen at -80 ° C prior to downstream processing.

See Figure 2.1.

2.6.3 Sample processing

The two water washes were combined and 1-2 μL was removed and diluted 1/100, for the blue dye to be quantified at 628nm absorbance, on the Bio-tek Synergy H4, alongside a standard curve of known concentration. The remaining sample was split three ways to enable analyte-specific processing and quantification. The amino acid and sugar fractions were lyophilised and weighed, then resuspended in 40 μL 0.1N HCl, or 72:28 MeCN:H_2O + 0.1 % NH_4CN per mg respectively. The resuspended amino acid sample was diluted 1:100 in HILIC A for LC-MS/MS analysis, and the sugar samples were diluted between 1:10 and 1:100 in the 72:28 MeCN:H_2O + 0.1 % NH_4CN prior to LC-MS/MS analysis. The third fraction was for cholesterol analysis. An equal volume of DCM was added to the water fraction, then the sample was vortexed for 2 minutes prior to 15 minutes of centrifugation at 1000x rpm. The DCM layer was removed and added to the DCM:MeOH wash, this was dried under a stream of N_2, then resuspended in 200 μL 1:1 IPA:MeCN, and spiked with 10 μM d6-cholesterol prior to LC-MS/MS analysis.

2.6.3.1 Quantitation

2.6.3.1.1 Amino Acids

LC-MS/MS analysis was performed on a Shimadzu Nexera X2 Ultra-Fast Liquid Chromatography system consisting of binary pumps, an on-line degassing unit, an autosampler, and a column oven (Shimadzu Corporation, Kyoto, Japan), coupled with an AB Sciex 6500 QTRAP mass spectrometer consisting of an electrospray ionization (ESI) source (AB SCIEX, Framingham, MA, USA). 1 μL of sample of injected on to a BEH Amide (1.0 x 100mm, Waters, Milford, MA, USA), BEH HILIC (1.0 x 100mm, Waters, Milford, MA, USA) or Ascentis HILIC (2.1 x 150mm, Waters, Milford, MA, USA) maintained at 40 °C, at a flow rate of 0.2 mL/min or 0.3mL/min for the 1.0 and 2.1mm columns respectively. The mobile phases consisted of Solution A (85 % MeCN + 0.15 % FA + 10mM ammonium formate) and Solution B (85 % H_2) + 15 % MeCN + 0.15 % FA + 10mM ammonium formate). A gradient elution was optimized for the separation of amino acids with 1.5 min equilibration 0-6.0 min, 0 % Solution B; 6.0-10 min, 0-100 % Solution B; 10-12 min, 100 % Solution B; 12-12.1 min, 0 % Solution B; 12.1-18 min, 0 % Solution B; with a total run time of 21 min. The ion source was operated in positive mode under an optimal condition: curtain gas, 40 psi; nebulizer gas, 50 psi; auxiliary gas, 50 psi; ion spray voltage, 5500 V; and temperature, 500°C. Optimal multiple-reaction monitoring (MRM) transitions were identified for the amino acids (see Table 2.3). Data acquisition and analysis were all performed with Analyst 1.6.3 software (AB SCIEX)

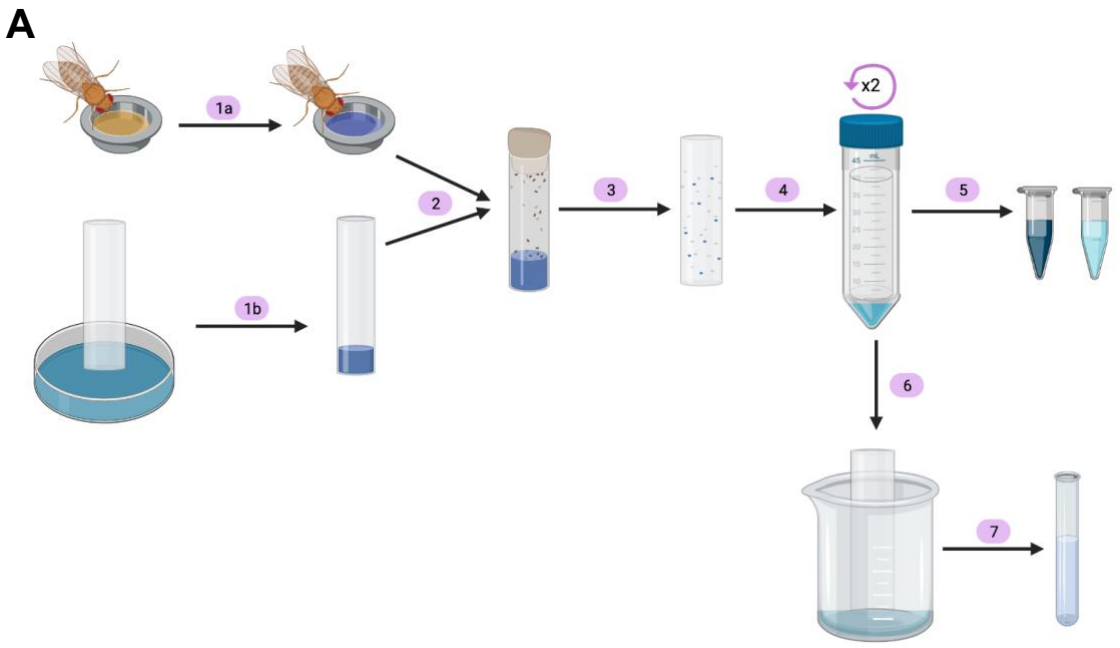
A
1a
1b
2
3
4
x2
5
6
7

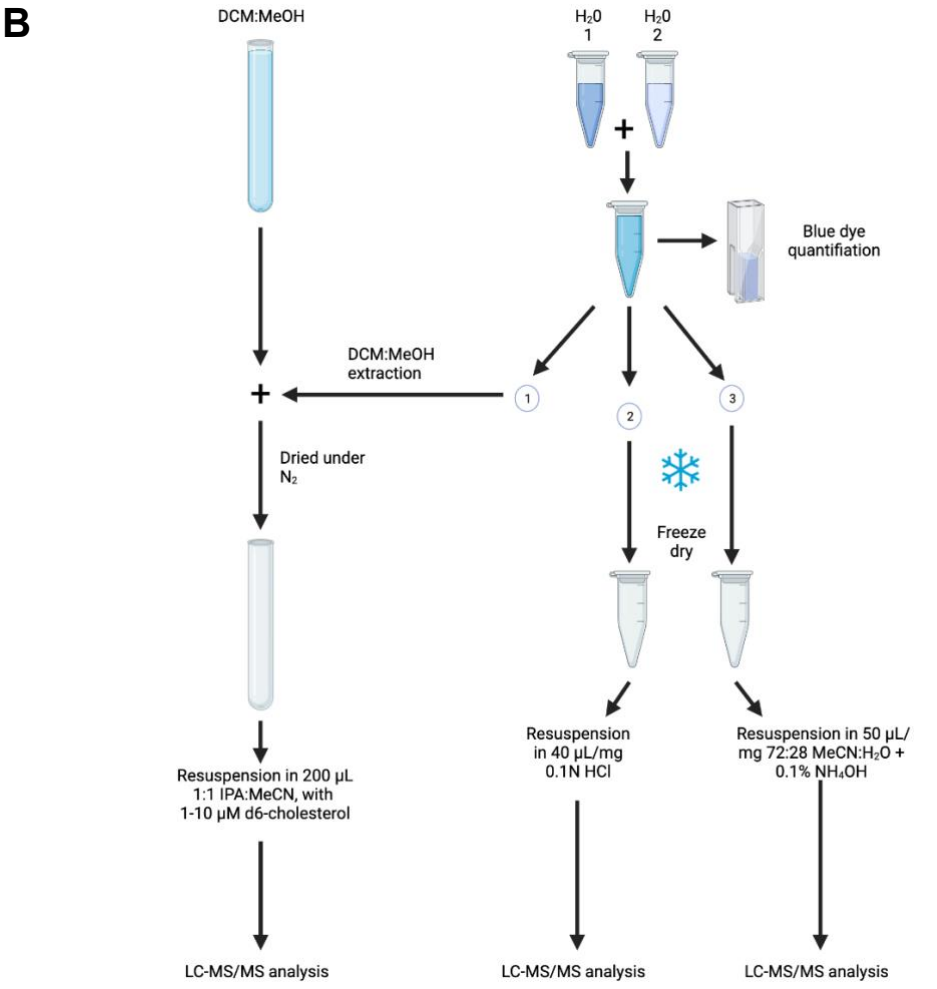
B
DCM:MeOH
H20 1
H20 2
Blue dye quantifiation
DCM:MeOH extraction
Dried under N2
Freeze dry
Resuspension in 200 µL 1:1 IPA:MeCN, with 1-10 µM d6-cholesterol
Resuspension in 40 µL/mg 0.1N HCl
Resuspension in 50 µL/mg 72:28 MeCN:H2O + 0.1% NH4OH
LC-MS/MS analysis
LC-MS/MS analysis
LC-MS/MS analysis

Figure 2.1 | Schematic of *Drosophila* Undigested Metabolite Profiling Assay

(A) Schematic of sample collection for the DUMP assay; 1a| Flies placed on blue food for 24h. 1b|collection vials prepared by stamping discs of food from petri-dish and securing in place with parafilm. 2|60 non-smurf flies transferred to collection tubes. 3| flies incubated at 25°C for up to 5 hours, then anaesthetised and removed with food from the bottom of the collection vials. Remaining food residue removed from collection vial base with damp white tissue, until no more blue dye visible on tissue. 4| All collection vials washed within falcon tubes with the same 1.5mL H_2O to produce a concentrated sample. Vials spun down to ensure all water and sample removed to base of falcon tube. Wash was repeated for all vials with a second 1.5mL H_2O. 5| water samples transferred to microfuge tubes and stored at -80°C. 6| collection vials washed in 5mL 1:1 DCM:MeOH to collect non-polar fraction. 7| DCM:MeOH sample collected in glass-storage tube to prevent reactivity with plastic vessels. Sample stored upright at -80°C. **(B)** Schematic of sample processing for the DUMP assay; the two water washes are combined and 1-2 mL removed for quantification of blue dye at 628nm. The remainder of the water washes are split three ways for 1. Cholesterol, 2. Amino acid, and 3. Sugar analysis. The non-polar fraction of the cholesterol fraction is extracted by addition of an equal volume of DCM, vortexed 2 mins and centrifuged at 1000x rpm for 15 mins. The DCM layer is collected and added to the DCM:MeOH wash sample and dried under a stream of N_2. The dried sample was resuspended in 200mL 1:1 IPA:MeCN and spiked with 1-10uM d6-cholesterol prior to LC-MS/MS analysis. The amino acid and sugar samples were lyophilised, then resuspended in 0.1N HCl or 72:28 MeCN:H_2O + 0.1% NH_4OH respectively, prior to LC-MS/MS analysis.

Table 2.3 | MRM transitions for the amino acids quantified

Q1 m/z	Q3 m/z	Time (msec)	Amino Acid	DP (V)	EP (V)	CE (V)	CXP (V)
166.1	120.1	50	Phe 1	30	10	15	12
132.1	86.1	50	Leu 1	36	10	23	14
132.1	86.1	50	Ile 1	40	7	15	8
150	104	50	Met 1	30	10	15	12
118.1	72.1	50	Val 1	30	10	15	12
116	70.1	50	Pro 1	30	10	15	12
182.1	136.1	50	Tyr 1	30	10	15	12
90.1	44.1	50	Ala 1	30	10	10	12
120	74.1	50	Thr 1	30	10	15	12
76	30.1	50	Gly 1	46	10	20	12
106	60	50	Ser 1	30	10	10	12
148	84	50	Glu 1	30	10	15	12
134	88	50	Asp 1	26	10	13	14
156	110.1	50	His 1	30	10	15	12
175.1	70.1	50	Arg 1	30	10	15	12
147.1	84.1	50	Lys 1	30	10	15	12
166	103	50	Phe 2	31	10	35	28
132.1	69	50	Leu 2	36	10	23	20
150	133	50	Met 2	21	10	13	8
118	55	50	Val 2	36	10	29	6
182.1	165	50	Tyr 2	46	10	19	6
120	56	50	Thr 2	86	10	23	6
106	42	50	Ser 2	31	10	31	4
148	102	50	Glu 2	21	10	15	4
134	70	50	Asp 2	36	10	25	6
156	93	50	His 2	41	10	31	8
175	116	50	Arg 2	46	10	19	6
147	130	50	Lys 2	16	10	13	6
122	76	50	Cys 1	30	10	10	15
205.1	146.1	50	Trp 1	36	10	10	23
147.1	84.1	50	Gln 1	30	10	10	15
133	74	50	Asn 1	30	10	25	25
133	116	50	Asn 2	31	10	13	8
205.1	188	50	Trp 2	41	7	15	9
147	102	50	Gln 2	31	10	19	12
132.1	69	50	Ile 2	40	7	24	9

2.6.3.1.2 Sucrose and glucose

LC-MS/MS analysis was performed on a Shimadzu Nexera X2 Ultra-Fast Liquid Chromatography system consisting of binary pumps, an on-line degassing unit, an autosampler, and a column oven (Shimadzu Corporation, Kyoto, Japan), coupled with an AB Sciex 6500 QTRAP mass spectrometer consisting of an electrospray ionization (ESI) source (AB SCIEX, Framingham, MA, USA). 2 μL of sample of injected on to an BEH amide column (2.1 x 50mm; Waters, Milford, MA, USA) maintained at either 75 °C or 45 °C for glucose and sucrose respectively, at a flow rate of 0.2 mL/min. The mobile phase consisted of Solution A (72:28 MeCN:H2O + 0.1 % NH4OH). A gradient elution was optimized for the separation of glucose and sucrose with 2 min equilibration 0-6.0 min, 0 % Solution B; 6.0-10 min, 0-100 % Solution B; 10-12 min, 100 % Solution B; 12-12.1 min, 0 % Solution B; 12.1-18 min, 0 % Solution B; with a total run time of 21 min. The ion source was operated in negative mode under an optimal condition: curtain gas, 20 psi; nebulizer gas, 50 psi; auxiliary gas, 50 psi; ion spray voltage, 4500 V; and temperature, 400 °C. Optimal multiple-reaction monitoring (MRM) transitions were identified for glucose and sucrose (see Table 2.4). Data acquisition and analysis were all performed with Analyst 1.6.3 software (AB SCIEX).

Table 2.4 | MRM transitions for Glucose and Sucrose

Q1 mass	Q3 mass	Time (msec)	Sugar	DP	EP	CE	CXP
179	59	600	Glucose 1	-60	-10	-22	-7
179	89	600	Glucose 2	-60	-10	-12	-9
341	59	200	Sucrose 1	-85	-10	-48	-5
341	89	200	Sucrose 2	-85	-10	-26	-15

2.6.3.1.3 Cholesterol

LC-MS/MS analysis was performed on a Shimadzu Nexera X2 Ultra-Fast Liquid Chromatography system consisting of binary pumps, an on-line degassing unit, an autosampler, and a column oven (Shimadzu Corporation, Kyoto, Japan), coupled with an AB Sciex 6500 QTRAP mass spectrometer consisting of an electrospray ionization (ESI) source (AB SCIEX, Framingham, MA, USA). 2 μL of sample of injected on to an CSH column (1.0 × 100 mm; Waters, Milford, MA, USA) maintained at 60 °C, at a flow rate of 0.14 mL/min. The mobile phases consisted of Solution A (60:40 MeCN:H2O + 10mM ammonium formate and 0.1 % formic acid) and Solution B (10:90 MeCN:IPA + 10mM ammonium formate and 0.1 % formic acid). A 3 minute equilibration was followed by a gradient as follows: 0-6.0 min, 0 % Solution B; 6.0-10 min, 0-100 % Solution B; 10-12 min, 100 % Solution B; 12-12.1 min, 0 % Solution B; 12.1-18 min, 0 % Solution B; with a total run time of 21 min. The ion source was operated in positive mode under an optimal condition: curtain gas, 40 psi; nebulizer gas, 50 psi;

auxiliary gas, 50 psi; ion spray voltage, 4500 V; and temperature, 500 °C. Optimal multiple-reaction monitoring (MRM) transitions were identified for the cholesterol and d6-cholesterol which was used as an internal standard (Table 2.5). Data acquisition and analysis were all performed with Analyst 1.6.3 software (AB SCIEX).

Table 2.5 | MRM transitions for cholesterol

Q1 mass	Q3 mass	Time (msec)	Name	DP	EP	CE	CXP
369.3	147	75	Cholesterol 1	80	10	31	20
369.3	67.2	75	Cholesterol 2	80	10	71	18
375.3	147	75	d6 Cholesterol 1	80	10	31	20
375.3	67.2	75	d6 Cholesterol 2	80	10	71	18

2.6.4 Analysis

Relative quantification was performed using the blue food dye; the mass-spec calculated concentration (μM) was adjusted for the sample dilution. This was then divided by the concentration of the blue dye (μM) for that sample.

The percentage change between young and old timepoints was calculated using the equation;

Where O is the normalised concentration at the old timepoint, and Y is the normalised concentration at the young timepoint. The young concentrations from all replicates were compared against the old concentrations from each replicate e.g. old replicate 1 was compared against young replicate 1, young replicate 2 and young replicate 3 etc.

The microbial concentration was calculated at young and old timepoints by;

Where the conventional concentrations from each replicate were compared against the axenic concentrations for each replicate and at every timepoint e.g. old replicate 1 was compared against young replicate 1, young replicate 2 and young replicate 3 etc.

2.7 Capillary feeding (Cafe) assay

Food consumption was measured using capillary feeding assay, essentially as previously described[235,236], using liquid defined media made without agar and, due to issues in solubility, without cholesterol. Variations of this will be made clear.

2.7.1 Assay preparation

Cotton wool balls were placed at the bottom of *Drosophila* vials and saturated with water. Any excess water was removed, and the vials were dried. 10 μL pipette tips were trimmed to enable capillary tubes to extend from the end with a tight fit so they wouldn't slip into the vial. *Drosophila* flugs were cut in half laterally, and three prepared tips were inserted in. The capillary tubes were prepared by loading with 2 μL of mineral oil to limit evaporation, and 10 μL of liquid food, then the interface between oil and food was marked.

2.7.2 Assay

10 mated female flies were sorted into the prepared vials. Each condition had a minimum of 10 vials. Additionally, a minimum of three evaporation control vials, containing no flies, were used for each experiment. Once the flies were awake within the vial, the capillary tubes were inserted into the tips, so the ends extended just beyond the base of the tip. The capillary tubes were changed every 24 hours, and the distance between the interface between oil and food, and the mark denoting the starting interface was recorded. The flies were allowed 24 hours to acclimate to the new feeding setup prior to measurements being recorded. Following acclimation, the assay was performed for 24-48 hours.

Food consumption was calculated in mm, by calculating the difference in the start and end interface, and subtracting the average difference in the start and end interface of the evaporation controls.

A conversion factor (X μL/mm) was calculated for each capillary tube by dividing 10 (the amount of liquid food), by the starting interface (mm). This was then used to convert food consumption in mm to μL.

2.8 Immunofluorescence of *Drosophila* tissues

2.8.1 Fixation and antibody staining

All antibodies and stains used in this thesis are listed in Table 2.6 with their dilutions.

Adult tissues were dissected in ice-cold PBS using two no5 forceps and an Olympus SZ dissection microscope and fixed for 30 minutes in 4 % paraformaldehyde (Fisher, 11490570) on a shaker. After

fixation, tissues were washed three times for 15 minutes in PBS. Samples were then blocked for 30 minutes in 5 % Natural Goat Serum (NGS) + 0.5 % Bovine Serum Albumin (BSA) in 0.5 % PBSTx (PBS + 0.5 % Triton X-100). Samples were incubated, with shaking, overnight at 4 °C with primary antibody in 0.5 % PBSTx. Samples were then washed as before and incubated for 2 hours at room temperature, protected from light, with secondary antibodies. Following incubation, the secondary antibody was removed and the tissues were incubated for 10 minutes with DAPI, washed three times then mounted on glass slides with Vectashield mounting media (Vector Labs, H-1000). The cover slip was sealed with clear nail varnish and the prepared samples were stored at 4 °C for longevity.

Where actin was stained, the guts were incubated for 1 hour with phalloidin following the secondary antibody staining, and prior to incubation with DAPI.

Table 2.6 | Antibodies and cell stains

Antibody	Description	Dilution	Source/Ref
Primary Antibodies			
anti-phospho-histone-H3 (pH3)	Monoclonal antibody against phosphorylated histone H3, raised in rabbit	1:2000	Millipore (06-570)
Anti-GFP	Polyclonal antibody against GFP, raised in chicken	1:2000	Abcam (13970)
Secondary Antibodies			
Anti-rabbit-IgG-555	Polyclonal antibody against rabbit IgG, raised in goat and conjugated to Alexa Fluor 555	1:500	Invitrogen (A21428)
Anti-chick-IgG-488	Polyclonal antibody against chicken IgG, raised in goat and conjugated to Alexa Fluor 488	1:500	Invitrogen (A11039)
Cell Stains			
DAPI (4',6-Diamidino-2-phenylindole, dihydrochloride)		1:2000	Invitrogen (D1306)
Alexa Fluor 647 Phalloidin	Alexa-fluor tagged phalloidin	1:40	Invitrogen (A22287)

2.8.2 Microscopy and Image Processing

All imaging was performed in the Durham University Microscopy and Bioimaging facility.

2.8.2.1 Light and fluorescent light microscopy

Leica StereoFluor M165 FC was used to visualise fluorescence in whole flies, and to capture whole-gut images.

The Zeiss Cell observer microscope was used to visualise pH3 staining in *Drosophila* midguts. The number of pH3 positive cells along the length of the entire midgut was quantified. At least 6 guts were quantified per condition.

2.8.2.2 Confocal microscopy

All confocal imaging was performed using the Zeiss 800 confocal microscope with airyscan processing. Raw data was stored as .czi files. Confocal stacks were processed using Fiji-2 ImageJ.

2.9 Statistics

Unless otherwise stated all experiments have been performed a minimum of two times. All Statistical analyses were performed using GraphPad Prism 9, excluding the binomial tests and principal component analyses which were performed in R (Rstudio build 372, R version 4. 0. 3).

Survival curve analysis was completed using the log-rank test in GraphPad Prism; the median survival was calculated by Graph Pad Prism 8 and is an approximation to the closest sampling time.

Gene expression data, normalised DUMP amino acid, sugar and cholesterol data, and metabolic analysis data was cleaned in GraphPad Prism, with outliers detected using the Robust regression and outlier removal (ROUT) method with Q=1. Normality or the cleaned data was tested by Shapiro-Wilk tests to determine the most appropriate statistical test.

Differences between two points were analysed by students t-test, or mann-whitney tests for normally and non-normally distributed data respectively.

Differences in bacterial load, and gene expression values between more than two time points, within one condition, were analysed by *Ordinary One-way Anova with* Holm-Sidaks *multiple comparison or Kruskal-Wallis with Dunns multiple comparison for non-normally distributed data.*

Differences in gene expression between time points, and between different conditions (e.g. drug-induced gene expression) were analysed by 2-way Anova, with Tukeys multiple comparisons.

P-values less than 0.05 were considered statistically significant. Bar-graph error bars depict ± standard error of the mean (SEM). For all box-plots shown, boxes display the 25-75th percentiles, with the horizontal bar at the median, and whiskers extending from the minimum to maximum points. Violin plots show the median (bold dashed line) and the 25-75th percentiles (dotted lines). The body of the violin extends from the minimum to maximum points, and the width corresponds with the approximate frequency of data points in each region.

3 Validation of ageing phenotypes on defined media

3.1 Introduction

As previously mentioned, diet is an important determinant of lifespan. Not only is dietary restriction and protein restriction a well-conserved method of lifespan extension, but diet is important in determining the composition of gut microbiota which is linked with health and longevity.

Due to this importance of diet in health outcomes, and the wide range of diets in use within the *Drosophila* field, experimental results can be difficult to reproduce between research groups. Additionally, batch-batch variation can also impact reproducibility within research groups, and between groups utilising the same diet. This lead to the development of a chemically defined diets, with a holidic diet published in 2014[222] which has had good uptake from the *Drosophila* community. To our knowledge, however, there has not been any data verifying the use of this defined diet when investigating the interlinking roles of diet and gut microbiota on ageing, and ageing phenotypes.

As mentioned previously (section 1.3.2) there are several ways to track ageing or the impact of lifespan interventions in *Drosophila*. One of the most common is to assess changes to the median or maximal lifespan. This provides a good measure to observe, at a population level, whether interventions influence ageing and lifespan, although does not give much insight into how such changes occur. This is where it is important to look at other biological markers of ageing, such as loss of intestinal barrier function, immune activation, changes in bacterial load or composition, or to intestinal stem cell proliferation of differentiation.

Our research group was interested to study intestinal nutrient uptake and how this changes with age. Because of this, as well as the benefits of this diet on reproducibility, we wanted to adopt the holidic media in the lab. Prior to doing so, I set out to validate the use of this diet for ageing research and to assess whether the expected phenotypes of ageing are present on this diet, and to identify any phenotypes which differ from my expectations. Additionally, as the microbiota is able to overcome deficiencies within diets, I set to confirm whether the defined media is sufficient to support sterile flies throughout their adult life, or whether the microbiota was compensating for any missing nutrients in the non-sterile flies. This will provide a baseline from which to compare future results using this diet, enabling us to understand whether observations are due to the use of this diet, or other future manipulations.

3.2 Aims and objectives

In this chapter I set out to validate the use of the defined diet for ageing research in the context of our labs specific research, as several of the assays we use to assess ageing have not been studied using this diet.

The main aim of this chapter was to set a baseline to which my future results, using the defined food, could be compared. For this, I assessed which ageing phenotypes are present in *Drosophila* within our lab fed on this media and how these compare to those fed on our laboratory's standard Cornmeal diet. Having this baseline for comparison will allow for a greater confidence that future observations stem not from the adoption of this defined diet, but from further dietary, genetic or bacterial (microbiota) manipulations.

Additionally, the possibility of maintaining sterile flies on this diet was yet to be tested. Diet is an important modulator of the gut microbiome, however the microbiota has been shown, on other diets, to overcome dietary deficiencies thereby rescuing *Drosophila* lifespans. Due to our labs interest in the gut microbiome, and the interconnection between diet, microbiota and ageing, a secondary aim of this chapter was to assess whether the defined diet was able to support the full lifespan of sterile (axenic) flies.

3.3 Results

3.3.1 Does the defined media alter the lifespan or expected ageing phenotypes of our flies?

3.3.1.1 Defined media did not alter lifespan of Canton-S

The defined media was developed to optimise adult lifespan and fecundity so it was important for me to understand whether raising adult flies on fully defined media had an effect, adverse or beneficial, on lifespan when compared to wild-type flies raised on the laboratory's standard cornmeal food. To this end, I reared wild-type Canton-S larvae on cornmeal medium and, once adults had eclosed and mated, female flies were sorted onto cornmeal food before the vials were randomly segregated to be transferred onto either cornmeal or defined media. This ensured there were no genetic differences between the two groups, or differences in their development, handling, or CO_2 exposure.

Adults were maintained on these media throughout their lifespan, and deaths were scored upon each transfer to fresh food. No difference in the lifespan of Canton-S females (Figure 3.1A) was observed; while there was a small difference of 1 day in the median lifespan of Canton-S on cornmeal (red line, 57 days) compared to defined (blue line, 56 days) media, this trend was reversed at maximal lifespan with the defined media cohort living an extra 2 days past the cornmeal cohort.

No significance was observed within individual replicates, and indeed the median lifespans were either the same or slightly increased in the defined media cohort. Together this data suggests that a diet of defined media has only a small effect on the lifespan of WT Canton-S females, although the direction of this effect, if any, is inconclusive. In either case, the lifespan of age-matched flies on this diet was very similar to those on our cornmeal food, indicating that defined media is not detrimental to Canton-S flies.

3.3.1.2 The Smurf Phenotype is present on Defined media

Intestinal barrier dysfunction is a good predictor of age-related decline and correlates closely with mortality, regardless of chronological age in *Drosophila*. This is not specific to genotype, nor to environmental conditions such as dietary restriction[22]. Loss of intestinal barrier function can be visualised in *Drosophila* by the 'smurf' phenotype of flies fed a non-absorbable blue food dye. Here, flies with normal barrier function eat and egest the dyed food with no visible phenotype, however when flies lose intestinal barrier integrity the dye leaks through the gut lining and the flies are stained blue (Figure 3.1B).

Due to the importance of this phenotype of ageing and organismal health, it was important to assess its presence in flies fed defined media. I transferred flies onto blue food for 24 hours at three distinct

timepoints, chosen to cover young (~10 days), mid-life (~25 days) and aged flies (~40 days). Importantly, smurfs were observed on the defined diet and the same, statistically significant (Binomial test, P<0.0001), trend of an increase in the proportion of smurfs (BD+) with age was seen across both diets (Figure 3.1C, D). Additionally, while the proportion of smurfs on defined media appeared lower than on cornmeal media, further tests showed this was not significant at any age (Binomial test, P>0.05).

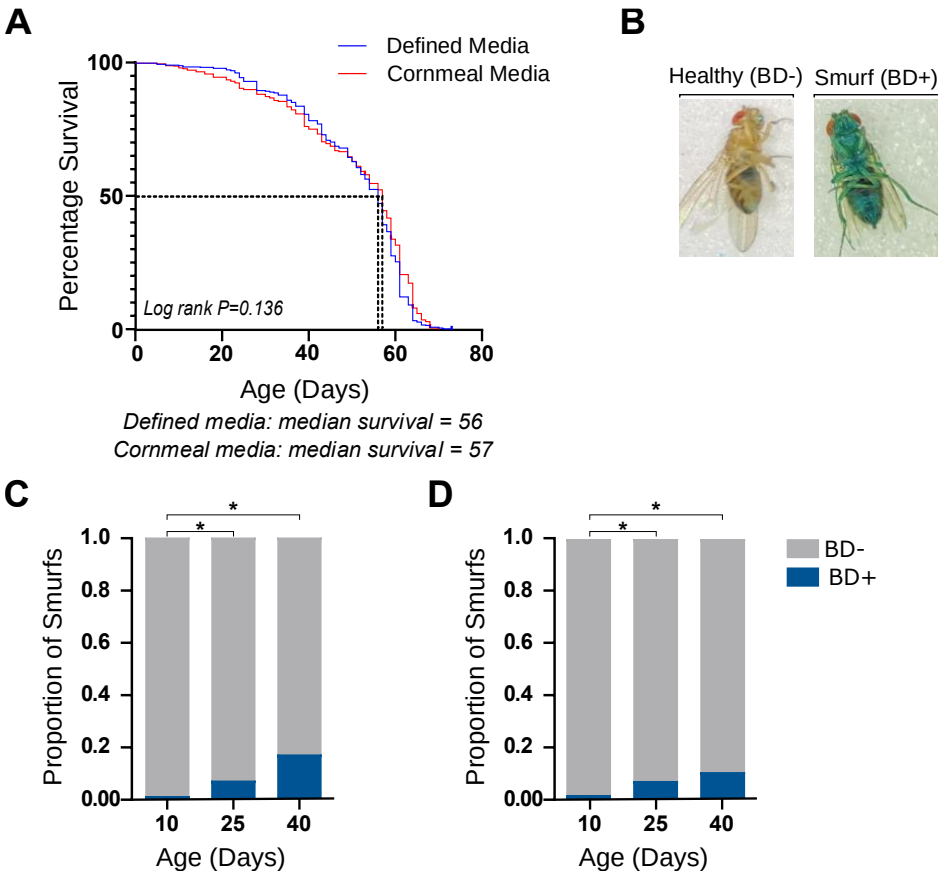

Figure 3.1 | Defined media supports adult lifespan and maintains smurf phenotype

(A) Lifespan of Canton-S female flies fed during adulthood on cornmeal or defined media. **(B)** Images displaying the characteristic smurf phenotype. Proportion of Smurf flies within the total population of Canton-S females on **(C)** cornmeal or **(D)** defined media. BD+ denotes smurf flies with barrier dysfunction. BD- denotes non-smurf flies, without evidence of barrier dysfunction. Proportions taken at 10 (10-11 days), 25 (24-25 days) and 40 (40-42) day timepoints. n > 450 flies per condition at day 1. Asterisks denote the result of binomial tests, where * P<0.05

3.3.1.3 Antimicrobial Peptide expression increases with age

Expression of antimicrobial peptides (AMPs) has been shown to increase with age, and particularly with the onset of the smurf phenotype[22,39]. To test whether the same induction of AMP expression is seen in flies on the defined media, I ran qPCRs with primers for *Drosomycin* (DRS) and *Diptericin*

(DPT); two *Drosophila* AMPs induced primarily by the Toll and IMD pathways respectively, to quantify the expression in both whole-fly, and gut-specific cDNA samples from both diets.

As expected, a significant increase in the whole-fly expression of both DRS and DPT was observed with loss of intestinal barrier function (Figure 3.2B and E) and also with chronological age (Figure 3.2C and E) in the whole-fly samples from cornmeal media.

Encouragingly, upon loss of barrier function, significant increases were observed in the expression of both DRS and DPT from whole-fly, defined media samples (Figure 3.3B and E). There was also a significant increase in the whole-fly, defined media expression of DPT with chronological age (Figure 3.3C), however while there appeared to be a trend towards increased whole-fly expression of DRS in defined media samples with chronological age (Figure 3.3E), this was not found to be significant likely due to the large amount of variation within this data.

Interestingly, an increase in the expression of DPT was observed between 10 and 40 day flies in the gut-specific samples from defined media samples (Figure 3.3), which matches previously published data[22], but not in the cornmeal samples (Figure 3.2A). There were also no significant changes in the expression of DRS in the gut-specific samples from either diet (Figure 3.2D, Figure 3.3D). This was expected as the Toll pathway is not involved in gut immunity, and this corroborates results from Clark *et al.*[39]. Overall, whilst neither cohort of flies fully showed the expected results, the increase in whole-fly AMP expression provides confidence that immune activation is still present in flies fed the defined media.

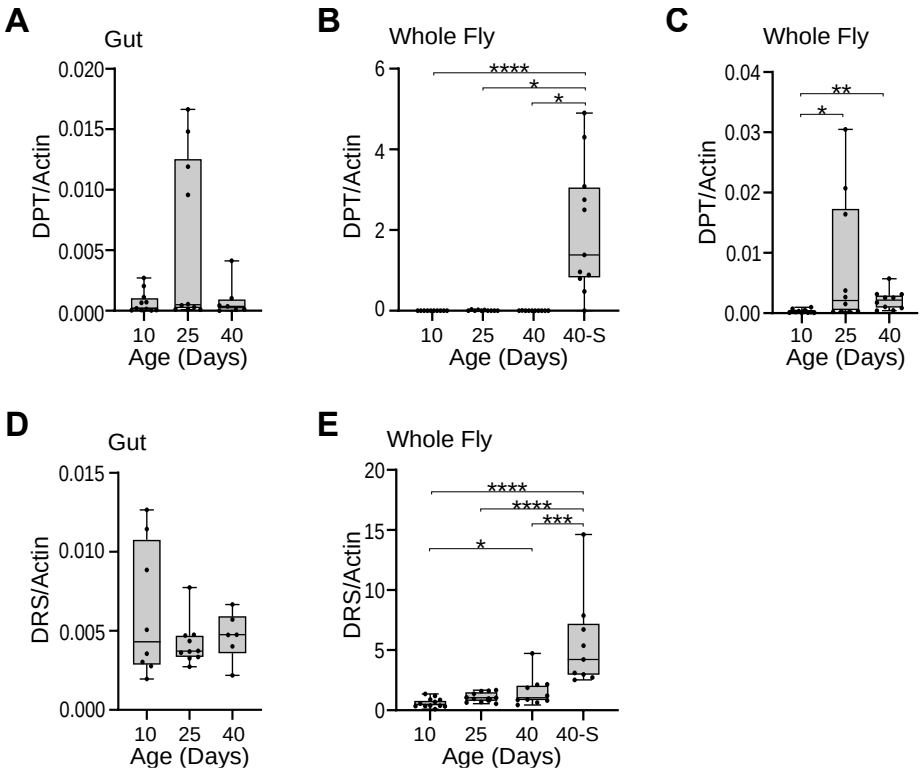

Figure 3.2 | Anti-microbial peptide expression increases with age and loss of intestinal barrier integrity on Cornmeal media

Gene expression of anti-microbial peptides in Canton-S female flies fed on cornmeal media was quantified using RT-qPCR of samples at 10 (10-11 days), 25 (24-25 days) and 40 (40-42) day timepoints. 40-S indicates old flies with the smurf phenotype. Diptericin (DPT) levels normalised to actin in **(A)** gut-specific and **(B-C)** whole-fly samples. **(C)** shows the 10-40 day data from **(B)** excluding smurf data. Drosomycin (DRS) levels normalised to actin in **(D)** gut-specific and **(E)** whole-fly samples. Box plots show the 25-75th percentiles and the median with the whiskers extending from min-max. Data from 5 guts/sample, or 3 whole-flies/sample, with a minimum of 6 samples. Asterisks denote the result of **(E)** an Ordinary One-way Anova with Holm-Sidaks multiple comparison or **(A-D)** Kruskal-Wallis with Dunns multiple comparison for normal and non-normally distributed data respectively, where * P<0.05, ** P<0.01, *** P<0.001, **** P<0.0001

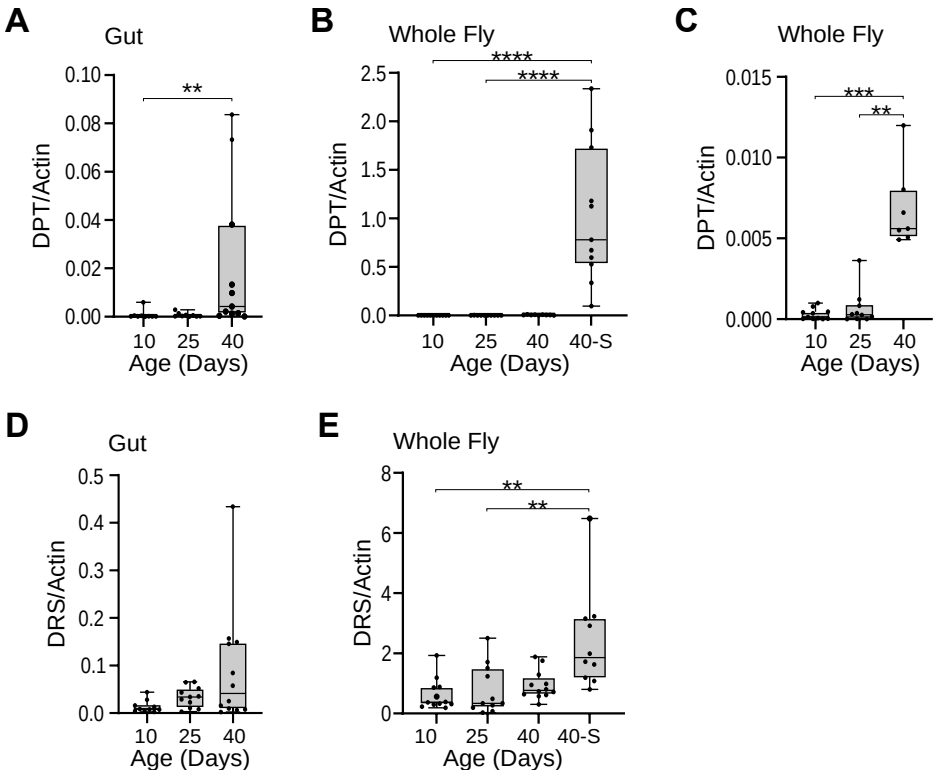

Figure 3.3 | Anti-microbial peptide expression increases with age and loss of intestinal barrier integrity on defined media

Gene expression of anti-microbial peptides in Canton-S female flies fed on defined media was quantified using RT-qPCR of samples at 10 (10-11 days), 25 (24-25 days) and 40 (40-42) day timepoints. 40-S indicates 40 day flies with the smurf phenotype. Diptericin (DPT) levels normalised to actin in **(A)** gut-specific and **(B-C)** whole-fly samples. (**C)** shows the 10-40 day data from **(B)**. Drosomycin (DRS) levels normalised to actin in **(D)** gut-specific and **(E)** whole-fly samples. Box plots show the 25-75th percentiles and the median with the whiskers extending from min-max. Data from 5 guts/sample, or 3 whole-flies/sample, with a minimum of 6 samples. Asterisks denote the result of a Kruskal-Wallis test with Dunns multiple correction, where * P<0.05, ** P<0.01, *** P<0.001, **** P<0.0001

3.3.1.4 Bacterial Load increases with loss of intestinal barrier function

Increased bacterial load is another established phenotype of ageing, shown to be closely linked to loss of intestinal barrier function and onset of the smurf phenotype, and to precede death.

As expected, there was a large significant increase in internal bacterial load upon loss of intestinal barrier integrity on cornmeal media (Figure 3.4A) and encouragingly this was also seen on defined media (Figure 3.5A). There was also a comparatively small, but significant, increase in the internal bacterial load of flies on defined media from 10 to 25 days of age, however this increase was not continued at 40 days except in smurf flies.

As the two diets have very different compositions, I wanted to investigate whether this would lead to a change in the composition of the resident gut bacteria. To test this, I used primers against different bacterial classes which have been previously shown to reside within the *Drosophila* intestine; Bacilli, α- proteobacteria and γ-proteobacteria. Importantly, as the larvae were all reared on cornmeal media, and newly emerged adults fed on cornmeal medium for at least 48 hours, all flies were exposed to the same bacteria for initial colonisation of the gut. Thus, any observed changes in the composition of the gut bacteria of flies on the defined media must happen after this point, and not be due to differences in the initial colonisation.

I was unable to quantify γ-proteobacteria from my samples on either media, indicating either an absence, or very low levels of colonisation within this class of bacteria. To validate the primer set, and ensure a non-functional primer was not the cause of the lack of signal, a qPCR using a set of standards generated from E. coli was run, and this generated a linear curve (data not shown).

Bacilli bacteria and α-proteobacteria were present in high enough quantities to quantify in both the cornmeal media and defined media flies. On both diets, the abundance of Bacilli bacteria increases significantly with chronological age and loss of intestinal barrier function (Figure 3.4D, E and Figure 3.5D, E).

The abundance of α-proteobacteria increases significantly with chronological age and onset of smurfing in cornmeal flies (Figure 3.4B, C), however while there appears to be an increase in the levels of this class of bacteria in defined flies, there was a large amount of variation and this was not found to be significant (Figure 3.5B, C).

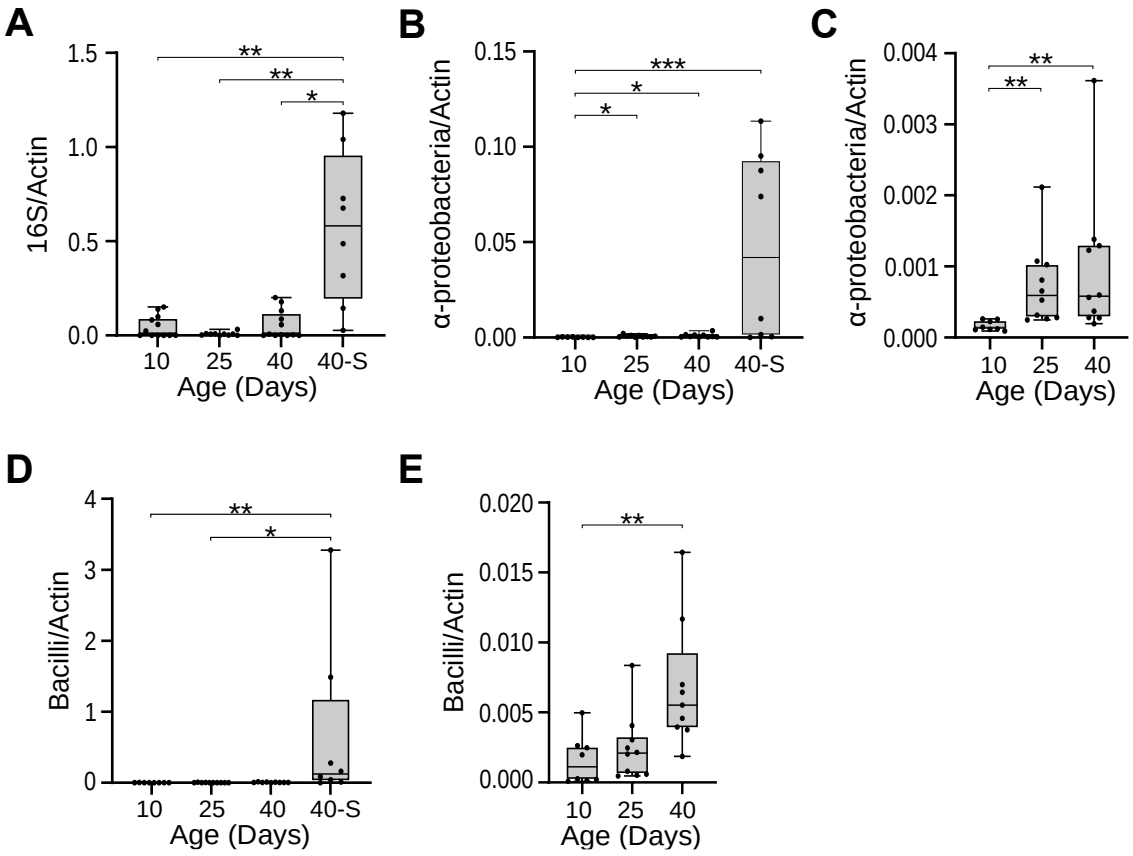

Figure 3.4 | Internal bacterial load increases with age on cornmeal media

Abundance of bacteria detected through qPCR from flies on cornmeal medium, using **(A)** universal primers for the 16S rRNA gene, and class-specific primers for **(B)** α-proteobacteria **(C)** and Bacilli bacteria, and normalised to the actin gene. Box plots show the 25-75th percentiles and the median with the whiskers extending from min-max. Data from at least 5 flies/sample, with a minimum of 6 samples. Asterisks denote the result of **(A)** an Ordinary One-way Anova with Holm-Sidaks multiple correction or **(B - E)** Kruskal-Wallis with Dunns multiple correction for normal and non-normally distributed data respectively, where * P<0.05, ** P<0.01, *** P<0.001, **** P<0.0001

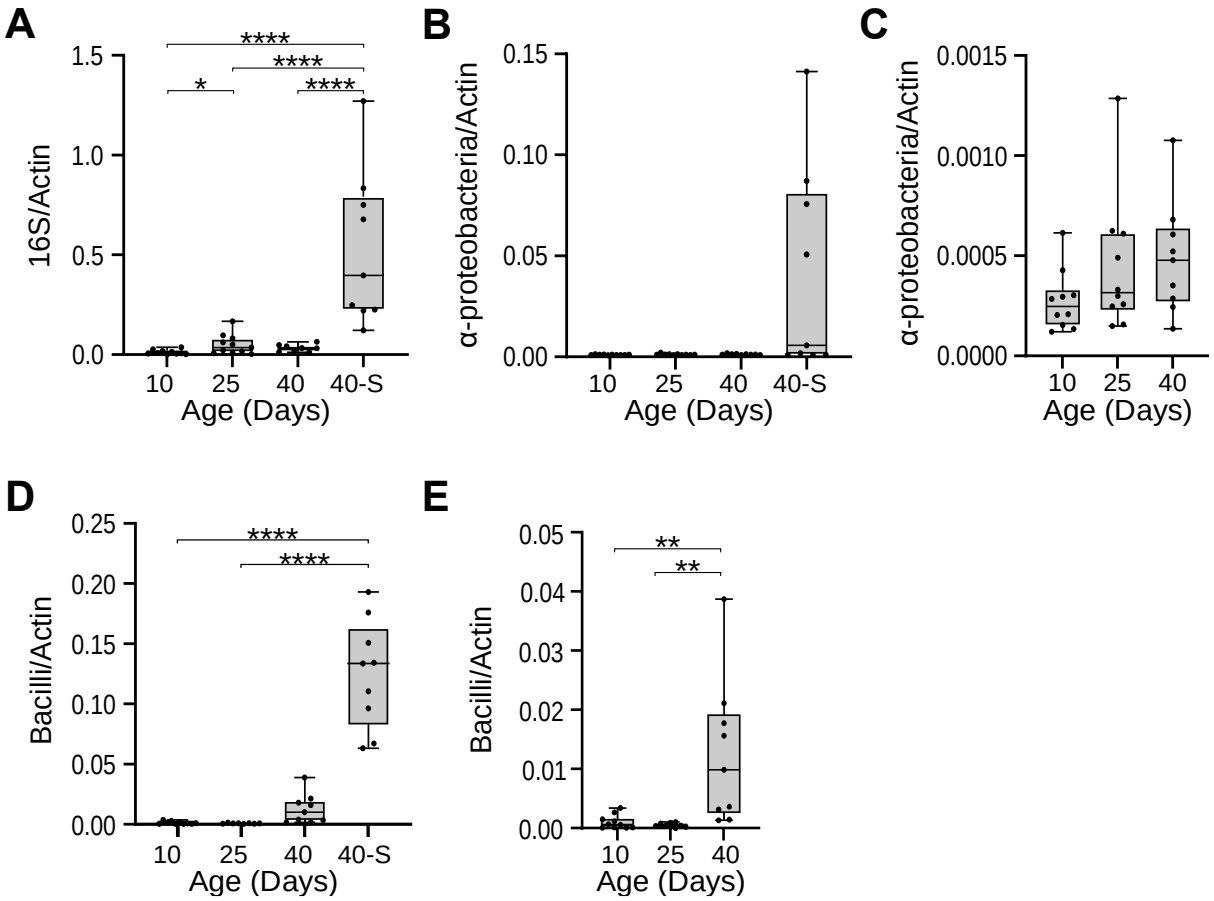

Figure 3.5. | Internal bacterial load increases with age on defined media

Abundance of total and class-specific bacteria detected through qPCR from flies on defined medium, using **(A)** non-specific bacterial 16s rDNA primer, and class-specific primers for **(B)** α-proteobacteria and **(C)** Bacilli bacteria, and normalised to the actin gene. Box plots show the 25-75th percentiles and the median with the whiskers extending from min-max. Data from at least 5 flies/sample, with a minimum of 6 samples. Asterisks denote the result of **(A)** an Ordinary One-way Anova with Holm-Sidaks multiple comparison or **(B - E)** Kruskal-Wallis with Dunns multiple comparison for normal and non-normally distributed data respectively, where * P<0.05, ** P<0.01, *** P<0.001, **** P<0.0001

3.3.1.5 Reserves of sugar, but not fat, decreases with age on defined media

Flies store nutrients for energy in the form of glycogen, for relatively short-term storage, and TAGs for longer-term storage. Due to the very different composition of the defined media compared to our standard cornmeal media, and because nutrient stores have been shown to become depleted with age[22,77], I wanted to investigate the abundance of these energy molecules in our flies with age.

The mass of defined media flies remained consistent with age, however there was a significant increase in the mass of 25 day flies on the cornmeal media compared to both the 10 and 40 day flies (Figure 3.6A, C). The protein content of flies on defined media also remained relatively consistent with age, however there was a small but significant decrease in the protein content of 40-day cornmeal media flies (Figure 3.6B, D). Interestingly, we did observe an increase in the amount of protein in defined media flies compared to cornmeal flies, with further tests showing this to be significant (Mann-Whitney, 10 day $P<0.0001$, 25 Days $P<0.001$, 40 days $P<0.001$). As the mass of the flies appeared most consistent, despite the small significant decrease at 25 days in the defined media cohort, this was the variable used to normalise the glucose, glycogen, glycerol and TAG data below. Due to the small but significant decrease in the mass of defined media flies at 25 days, more weight should be given to comparisons between 10 and 40 days, than those with the 25-day samples.

Glucose is the predominant energy source for all animals, including *Drosophila*, however it cannot be stored within cells in this form. Instead, excess glucose is converted to glycogen and stored in the adult fat body, flight muscles, halteres and gut as an accessible carbohydrate energy storage molecule which can be converted, during periods of starvation or intense activity, to glucose[237,238]. In our cornmeal flies, we observed a significant decrease in the amount of free glucose with age (Figure 3.7A), this was observed along with a significant decrease in the amount of glycogen at 25 and 40 days (Figure 3.7B). In defined media flies, there appeared to be a decrease in the amount of free glucose at 40 days, although this was not significant (Figure 3.7C). There was, however, a significant decrease in the amount of glycogen between 10 and 40 days, and 25 and 40 days, but not between 10 and 25 days (Figure 3.7D). Interestingly the levels of glycogen in defined media flies were significantly lower than cornmeal flies at all ages (Mann-Whitney, 10 days $P<0.0001$, 25 Days $P<0.01$, 40 days $P<0.001$), likely reflecting the lower sugar content within this diet. The stable levels of glucose combined with decreases in glycogen storage may indicate reduced uptake of sugar from the diet, but intact glucose regulatory mechanisms using the glycogen reserves to maintain stable levels of circulating glucose.

Triacylglycerol (TAG) is another essential energy storage molecule in animals, including *Drosophila*. It represents the most concentrated form of chemically bound energy and can be stored within specialised organelles; lipid droplets[239]. We observed a significant decrease in the levels of free glycerol in cornmeal media flies (Figure 3.8A (Kruskal-Wallis with Dunns multiple comparison, 10-25 days P<0.001, 10-40 days P<0.05)), and a significant decrease in the levels of TAG in cornmeal flies by 25 days, however no further reductions were observed at 40 days (Figure 3.8B). The levels of both free glycerol and TAG within the defined media cohort showed no significant changes with age, although there did appear to be a trend towards reduced levels of both molecules with age (Figure 3.8C, D). Interestingly the levels of TAG was lower in the defined media cohort than the cornmeal cohort, although this was not significant at 25 days of age (Unpaired t-test; 10 days P<0.0001, 25 days P>0.05. Mann-Whitney; 40 days P<0.05). This may again reflect the lower sugar content within this diet, as excess sugar, as well as fat, can be converted to TAG. It likely also indicates lower fat content within the defined diet, however, without quantifying the fat content of the cornmeal media, we cannot say for sure.

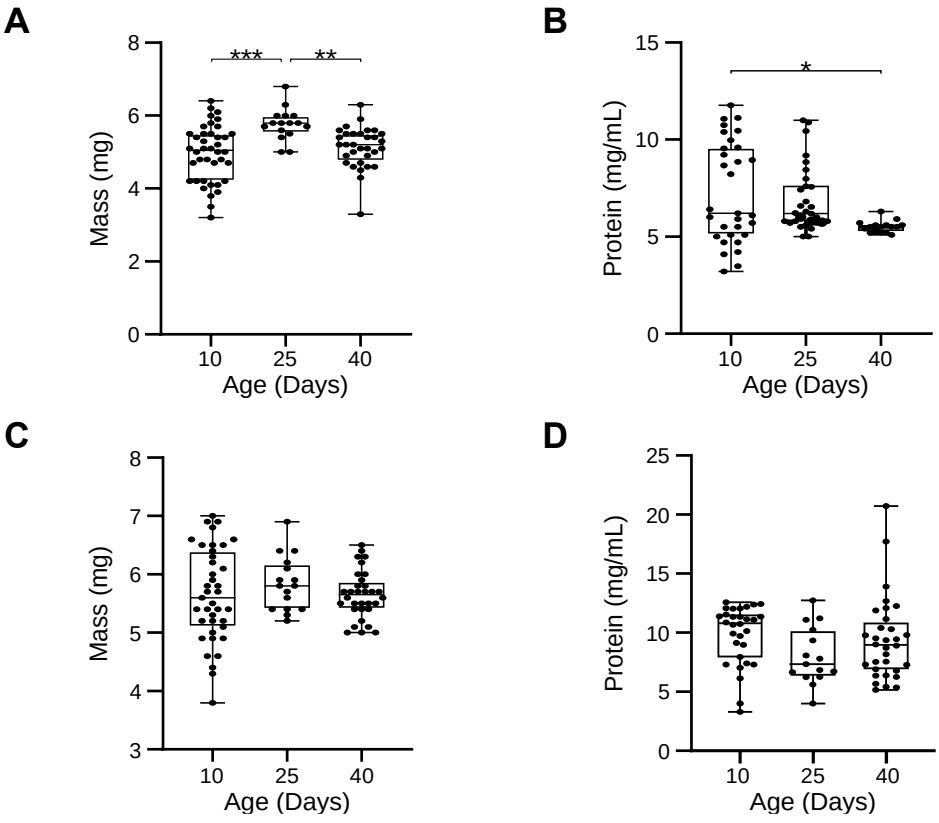

Figure 3.6 | Differences in mass and protein with age observed on the cornmeal, but not the defined diet

The mass of Canton-S female flies on **(A)** cornmeal and **(C)** defined medium, and the protein content of the same flies on **(B)** cornmeal and **(D)** defined medium was measured from 10 (10-11 days), 25 (24-25 days) and 40 (40-42) day old flies. Box plots show the 25-75th percentiles and the median with the whiskers extending from min-max. Data from 5 flies/sample, with at least 6 samples. Asterisks denote the result of **(A – C)** an

Ordinary One-way Anova with Holm-Sidaks multiple comparison or **(D)** a Kruskal-Wallis with Dunns multiple comparison for normal and non-normally distributed data respectively, where * P<0.05, ** P<0.01, *** P<0.001, **** P<0.0001

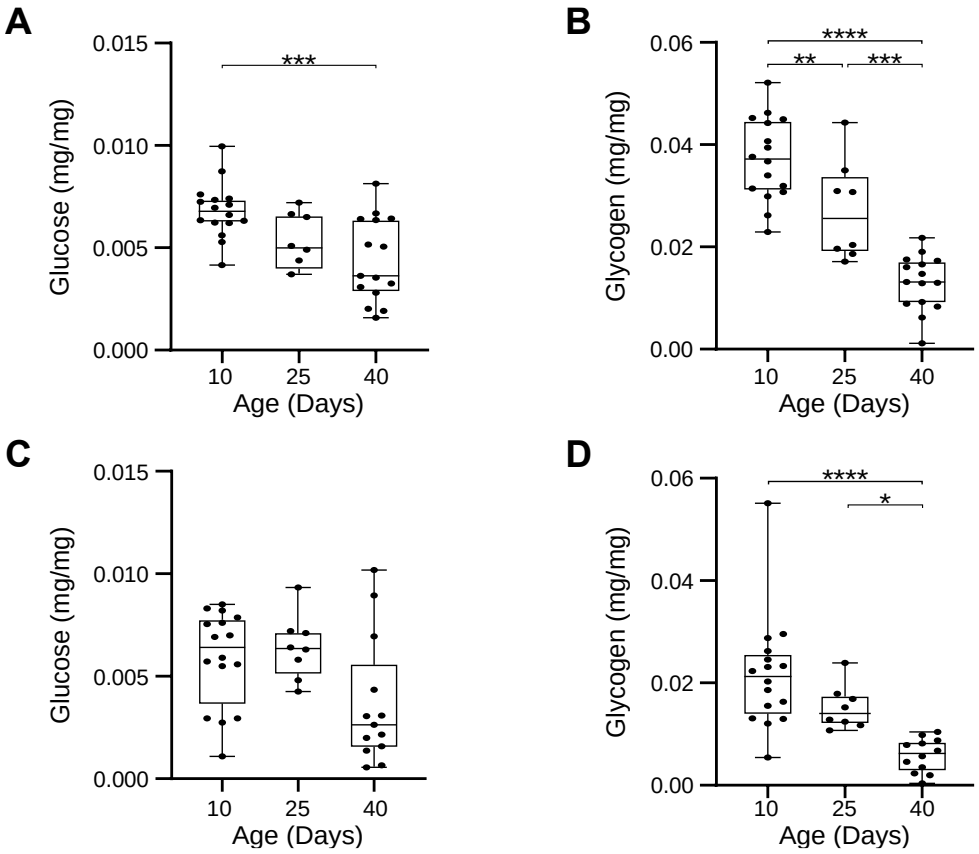

Figure 3.7 | Sugar reserves decrease with age irrespective of diet

Canton-S adult female flies were raised on **(A-B)** cornmeal or **(C-D)** defined media. **(A,C)** Total glucose and **(B,D)** glycogen, normalised to mass, were measured at 10 (10-11 days), 25 (24-25 days) and 40 (40-42) days of age. Box plots show the 25-75th percentiles and the median with the whiskers extending from min-max. Data from 5 flies/sample, with at least 6 samples. Asterisks denote the result of **(A, B)** an Ordinary One-way Anova with Holm-Sidaks multiple comparison or **(C, D)** Kruskal-Wallis with Dunns multiple comparison for normal and non-normally distributed data respectively, where * P<0.05, ** P<0.01, *** P<0.001, **** P<0.0001

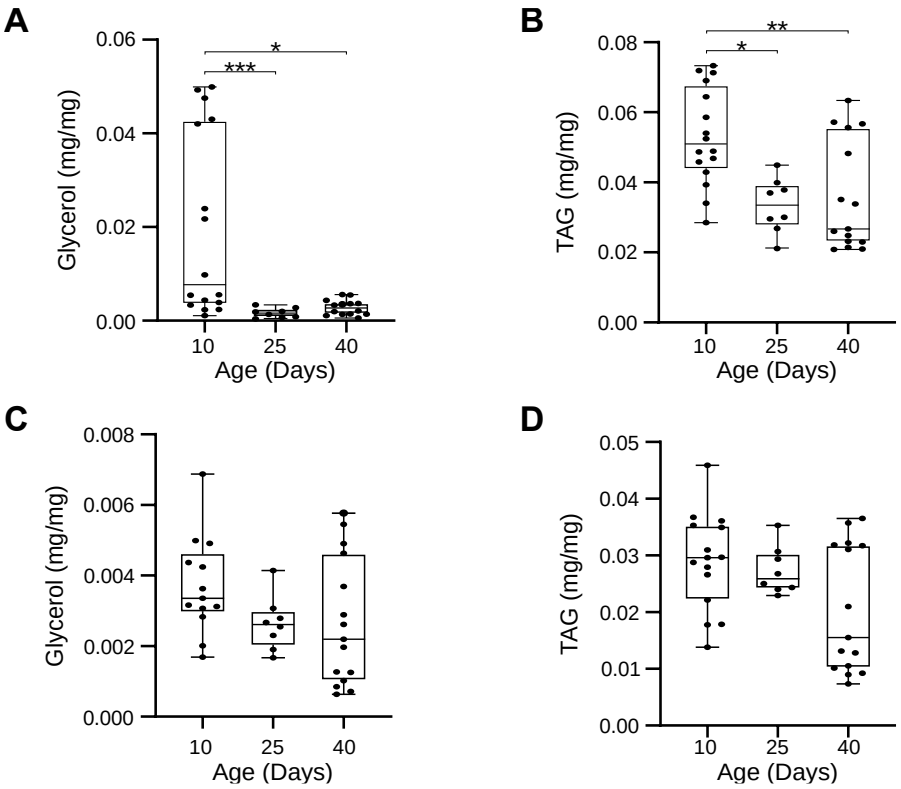

Figure 3.8 | Fat reserves decrease with age on cornmeal but not defined diet

Canton-S adult female flies were raised on **(A-B)** cornmeal or **(C-D)** defined media. **(A,C)** Total glycerol and **(B, D)** TAG normalised to mass, were measured at 10 (10-11 days), 25 (24-25 days) and 40 (40-42) days of age. Box plots show the 25-75th percentiles and the median with the whiskers extending from min-max. Data from 5 flies/sample, with at least 6 samples. Asterisks denote the result of **(A)** an Ordinary One-way Anova with Holm-Sidaks multiple comparison or **(A, B, D)** Kruskal-Wallis with Dunns multiple comparison for normal and non-normally distributed data respectively, where * P<0.05, ** P<0.01, *** P<0.001, **** P<0.0001

3.3.2 Is the defined media sufficient to support flies lacking a microbiome?

3.3.2.1 Defined media is sufficient to support flies without bacterial contribution

It is understood that bacteria can overcome some dietary deficits and enhance the survival of flies on deficient diets. It was important for me to assess whether this was occurring on defined media, particularly as larval development is reported to be delayed on this media[222], indicative of nutrient deficiencies or imbalances. I hypothesised that if the defined media was not sufficient then axenic flies, without gut microbiota, would have poor survival. To test this, I generated a cohort of axenic, re-associated and age-matched conventionally reared flies, and performed a lifespan experiment. Sterile defined media was used for all three conditions to ensure any differences observed were due to the microbiota and not differences in food composition.

We observed a significant increase in lifespan under axenic conditions, with a median lifespan of 53 days (Figure 3.9). Encouragingly, the lifespan of re-associated flies showed only a small increase

compared to conventionally reared flies (48 vs 47 days), which indicates that any effect from dechorionation is very small. The maximum lifespan followed the same trend with axenic flies longest lived at 75 days. Re-associated and conventional flies reached 73 and 71 days respectively. The increase in lifespan of axenic flies shows that defined media is sufficient to support the flies throughout adult life. Encouragingly, this data also matches previous data showing that raising Canton-S flies under sterile conditions, here on cornmeal food, increases lifespan[39].

3.3.2.2 Smurfing is reduced under axenic conditions

At select timepoints throughout the lifespan, I also transferred the flies onto blue food to assess the proportions of smurf flies. The proportion of smurfs in the axenic cohort was lower than that of the re-associated and conventional cohorts at all timepoints following 10 days (Figure 3.9, binomial tests $P<0.05$ (P values not adjusted for multiple comparisons)). The proportion of smurfs in the re-associated cohort was lower than that of the conventional cohort at 10 and 25 days, perhaps suggesting a lower starting bacterial load, however at 40 days, the proportion of smurfs in the re-associated cohort was significantly higher than that of the conventional cohort. This once again corresponds with what we expect from previously published results, although the proportions of smurfs in all cohorts here are much lower than what has previously been published. This could be due to the subjective scoring of 'smurfness', with potentially light smurfs here being missed and included in the 'healthy' cohort. The proportions shown here are, however, in line with those in Figure 3.1.

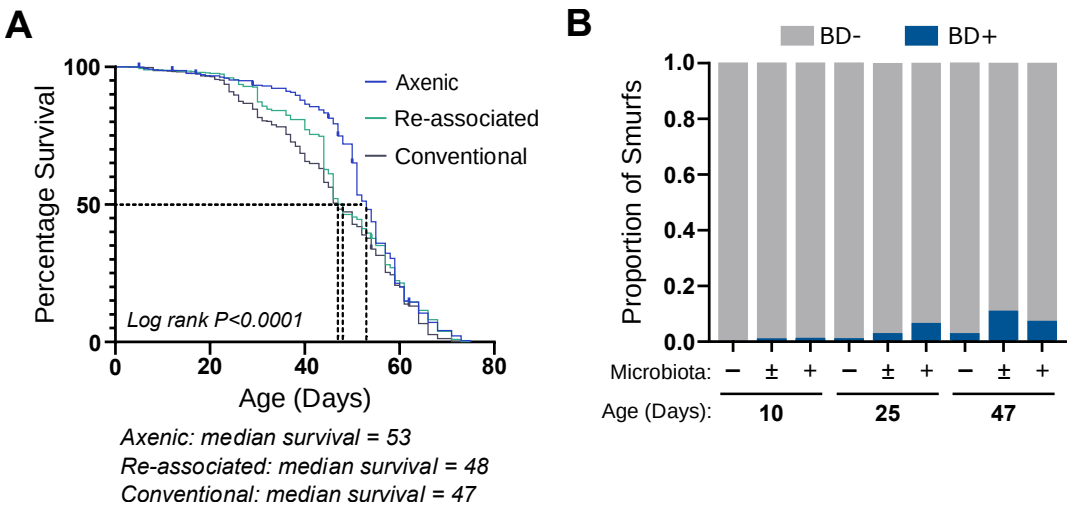

Figure 3.9 | Defined media is sufficient to support axenic flies

(A) Lifespan of axenic, re-associated and conventionally reared Canton-S female flies fed during adulthood on defined media. **(B)** Proportion of Smurf flies within the total population of axenic (-), re-associated (±) or conventionally reared (+) Canton-S females on defined media. BD+ denotes smurf flies with barrier dysfunction. BD- denotes non-smurf flies, without evidence of barrier dysfunction.

3.4 Discussion

3.4.1 *Defined media supports the full adult lifespan and maintains the smurf phenotype*

Age-related phenotypes, including lifespan, are highly sensitive to diet, with calorie consumption, the relative ratios of macronutrients, and indeed the quantities of single amino acids, all being shown to affect longevity[118,123,127,225,240–244]. As the composition of the defined diet is so different from our laboratory's standard cornmeal food, it was therefore important to identify whether flies on this diet still display the expected phenotypes of ageing that I would be interested in.

To start assessing this, I measured the lifespan and smurf proportions of the flies on both the cornmeal diet used within our laboratory group, and the defined diet[221,222,224]. Lifespan analysis is very useful in determining differences in survival between two treatment groups. Typically, the median survival, or the point at which 50% of the population remain, is the point used for comparison rather than the maximal lifespan which can be easily affected by outliers.

Unexpectedly, the flies in this study raised on cornmeal medium, had an increased median lifespan of over 15 days compared to the same genotype raised on the same food in Clark *et al.*[39]. Our Canton-S flies were sourced from the Walker lab in which the work in Clark *et al.* [39] was carried out. The differences observed between lifespan in this, and previous studies does raise questions as for the cause of these differences. It is unlikely that batch-differences in the cornmeal food would be enough to explain this discrepancy, especially as the flies on defined media were as long lived as their cornmeal counterparts. Perhaps different handling techniques may go some way to explain the difference, as Clark *et al.*[39] used nitrogen to anaesthetise their flies, whereas CO_2 was used here. Alternatively, there may be differences in the bacteria present in this laboratory, and so the composition of the microbiota; it has been shown that intestinal microbiota composition can vary between different labs[245,246], and that the gut microbiota has a bearing on organism health and longevity in *Drosophila*[39,199,247]. It should also be noted that whilst both this and the previous study used Canton-S wild-type flies, genetic drift is likely to have occurred within these separated populations, which could also explain the differences observed here. Unfortunately, it is impossible to determine with certainty the cause of the increased lifespan, however the consistency across the two diets, as well as between replicates, provides confidence that this is a reliable result.

The proportion of smurf flies within the surviving population is another important phenotype of ageing and organismal health, which has been shown to increase with age and to predict and precede death[39]. Three timepoints, chosen to cover young, mid-life and old flies, were used to assess the proportions of smurf flies. These ages were chosen based upon previously published lifespans of

Canton-s females flies reared on the same cornmeal media[39] which had a median lifespan of 40 days, the 'old' timepoint used here.

The proportion of smurfs on both diets encouragingly increased with age as expected, with no significant differences in the proportions between the two diets. I did however observe lower smurf proportions than in previously published data. This may be due to observer bias, as the smurf phenotype exists on a scale from very light blue smurfs, who perhaps have only recently begun losing barrier integrity, to much darker smurfs which are clearly identifiable[248]. It is possible that lighter smurfs were being scored in the published studies than I scored here. The flies were not anaesthetised for close observation down the microscope to determine staining, as CO_2 treatment is known to affect lifespan[249], instead, the flies were observed within lifespan vials which may have resulted in the less obvious 'light-smurfs' being missed. Alternatively, the lower smurf proportions may reflect the increased lifespan of these flies. Either way, the expected trend of increased proportions of smurf flies with age was replicated in this study and maintained on the defined media.

3.4.2 A diet of defined media does not prevent age-related activation of the immune system

Immune activation is another biomarker which increases with age as well as loss of intestinal barrier function[39], so, in addition to the lifespan and smurf phenotype, I measured the expression of two AMPs; *Drosomycin* (DRS) and *Diptericin* (DPT), which are expressed through the Toll and IMD immune pathways respectively. As the Toll pathway is not involved in gut-mediated immunity, both whole-fly and gut-specific samples were collected. It was expected that the DPT expression would increase with age in both the gut and the whole-fly samples[39], and that expression of DRS would increase with age and loss of intestinal barrier function in the whole-fly but not the gut samples. DRS has, however, been shown to increase specifically in the gut upon loss of intestinal barrier integrity[39], perhaps under the control of a different pathway; it has been suggested that the JAK/STAT pathway can regulate immune response and some AMPs, including *drosomycin*-like peptides, in the gut[47,79,92,250,251].

For the most part, the expected trends with age were observed on both diets, however, the gut-specific cornmeal samples did not show increased DPT expression with age, and the whole-fly defined media samples did not show the expected increase in DRS expression between 10 and 40 days, although there was a significant increase with loss of intestinal barrier function. These deviations may be explained by the later median lifespan of the flies in this study; 40 days may have

been too early in terms of biological age, as approximately 75% of the population was still alive at this point. It would be good to repeat this with an older timepoint reflecting the median age of this population, to understand whether the observed deviations are simply from samples being collected too early, however, the fact that the expected increase in AMP expression is observed on defined media with the onset of the smurf phenotype, as well as with age in most cases, gives support to the use of the defined media in our ageing research.

3.4.3 Bacterial load increases with loss of intestinal barrier integrity irrespective of diet

Expansion of intestinal bacteria has also been shown to increase with age and loss of intestinal barrier integrity and is thought to play an important role in age-related decline[39,88,89,92,247]. To see if this remains the case on the defined diet, I measured the bacterial load of the flies on both diets, at the same timepoints used previously. Additionally, the composition of the microbiota has been shown to change with age, with an expansion of *γ-proteobacteria*, in particular*,* being linked to increased barrier dysfunction[39].

Encouragingly, I did see the expected increase in internal bacterial load with the onset of the smurf phenotype on both diets, however, this was not observed with chronological age (10-40 days). This may again reflect the increased median lifespan of these flies compared to Clark *et al.*[39] as the same timepoints were used here as in the smurf proportions.

There was however an increase in the levels of bacilli bacteria on both defined and cornmeal media with both chronological age and onset of the smurf phenotype. That this is not reflected in the overall bacterial levels may indicate that this bacterial class does not make up a large enough proportion of total bacteria to influence total bacterial load. This increase in Bacilli would be masked if another class, which showed no changes in bacterial levels with age, made up a much larger proportion of total bacteria, or if the increased bacilli competed with other bacterial classes, depleting their numbers.

α-proteobacteria levels showed much greater differences between the diets, with significant increases in abundance being observed with both chronological age (10-25 and 10-40 days) and onset of the smurf phenotype on cornmeal, but not the defined, media. These differences may perhaps indicate that the defined media is less able to support α-proteobacteria, particularly at high levels, as its nutritional composition is very different from the cornmeal media. The ability of the defined media to support α-proteobacteria was not further investigated here.

Previous studies have shown an association between the specific expansion of γ-proteobacteria with increased intestinal barrier dysfunction[39]. In this study however, I was not able to quantify the levels

of this class of bacteria through qPCR, and suspect that they were too low in abundance for accurate quantification as the primers worked well with an *E. coli* standard. This may suggest that the microbial composition of flies in my study vary to those of previous studies. The fact that these flies appear to have an undetectable level of γ-proteobacteria, which has previously been linked to increased intestinal barrier dysfunction, may help to explain the increased lifespan of these flies, along with the lower proportion of smurfs and the lack of some AMPs increasing expression at 40 days. As I was unable to quantify this class of bacteria on either diet, I am unable to comment on the effect of the defined diet on this class of bacteria, however, the fact that it was undetectable on both diets indicates that the absence of this class of bacteria is disconnected from diet.

It is interesting that, at least in the cornmeal media, two bacterial classes are increasing with chronological age while total bacterial load is not. This suggests that there is a large bacterial population that we have missed in this study. Unfortunately, qPCR is not the best method for determining the composition of the microbiota, and without sequencing data this will largely remain a mystery. It does indicate however that the composition of the intestinal microbiome of our flies is disparate to that of previous studies. It is important to remain cognisant of this when comparing data to that published by other groups.

3.4.4 Lower levels of nutrient stores observed on the defined diet

The levels of nutrient storage molecules has been shown to decrease with age in *Drosophila*[22,77]. A decline in physiological reserves is also seen in human ageing, with accelerated decline observed with 'frailty'[252,253]. Frailty is an important clinical expression implying concern over an older persons vulnerability and prognosis, and the diminished ability to 'bounce back' from what would typically be deemed 'minor' stressors[252].

Before measuring the levels of physiological reserves in my flies, it was important for me to assess the mass and protein content of the flies, prior to using either one as a method of normalisation. Interestingly we found there to be a significant increase in the levels of protein in flies on the defined diet compared the cornmeal diet. The cornmeal diet contains ~22 g/L protein (according to the diet calculator (Broderick Laboratory | Johns Hopkins University | Research) assuming no batch-batch differences), the defined diet contains ~21 g/L protein. As the two diets have very similar amounts of protein, and indeed the defined diet has slightly less total protein than the cornmeal diet, it seems unlikely that this would explain the increased levels of protein within the defined media flies. The protein sources of the two diets are very different however, and the free amino acids of the defined media may result in increased protein bioavailability. Additionally, the specific proportions of amino acids in the defined media could allow for improved muscle synthesis or

maintenance. An alternative explanation is that the defined diet may lead to behavioural changes in the flies which result in altered muscle growth. Whatever the cause, it must happen early in life, as the flies are only transferred to the defined diet at approximately 5 days of age, and the increased protein compared to cornmeal flies is observed as early as 10 days of age. Because of the differences in fly protein content between the diets, it was decided that fly mass would be used for further normalisation, to better enable comparison between the diets, with the comparisons between 10 and 40 days given more weight.

I measured the free glucose and glycogen content of flies on both diets, as well as the levels of triglycerides (TAG).

Triglyceride reserves have been shown to decrease with both age and loss of intestinal barrier function[22], however the picture is not so clear with glycogen. Biteau *et al.*[77] have shown reduced levels of glycogen with age, although they didn't distinguish between smurf and non-smurf individuals[77], however Rera *et al.*[22] showed glycogen storage to remain relatively stable with age but decrease with loss of intestinal barrier function, suggesting that glycogen is lost with smurfness and not with age

Here I found a significant decrease in the levels of glycogen with age in non-smurf flies, regardless of diet. The inconsistency between the results of these three studies may reflect, as well as smurf status, differences in the metabolism of different genotypes, as the previous studies used flies in a w^{1118} background. Interestingly, as well as decreasing levels of glycogen with age on both diets, I observed that the defined media flies had significantly lower levels of glycogen than the cornmeal flies at every age. This may be due to differences in dietary sugar between the two diets (17.2g sucrose vs 19g sucrose and 38g dextrose per litre in the defined and cornmeal diets respectively). Dietary sugar is taken up by cells and used to produce energy through glycolysis, with excess glucose getting stored as glycogen as a metabolic safeguard[254,255]. The cornmeal food has a higher percentage of sugar than the defined diet and contains both sucrose and dextrose which may result in differences in sugar storage and metabolism.

Despite the differences in sugar composition between the diets, there was no difference in the levels of free glucose between the conditions, likely reflecting the tight control organisms maintain on sugar metabolism through the insulin signalling pathway (or insulin-like signalling pathway in *Drosophila*). Interestingly, some of this control may be lost with age as there was a significant decrease in the level of circulating glucose with age (10-40 days) in the cornmeal flies and a clear, if not significant, trend towards reduced levels of circulating glucose at 40 days in the defined media

flies. This contradicts one report by Westfall *et al.*[256], who showed increasing levels of circulating glucose with age, although they used Oregon-R males up to just 30 days of age. Nevertheless, in this study, glucose levels appear to follow the same trend of a decrease with age.

I found that the triglyceride levels decreased as expected with age in the flies on the cornmeal diet, and there did appear to be a trend towards decreased levels of triglycerides with age on the defined medium, however, this was not found to be significant. Interestingly, as with glycogen, the level of triglycerides was found to be lower in flies from the defined medium compared to those on the cornmeal diet. Insulin is released upon sugar consumption and, as well as glycogen storage, promotes the synthesis of fatty acids in the liver and facilitates entry of glucose into adipocytes, fat cells, where it can be used in the synthesis of glycerol[257] and triglycerides. The lower sugar content of the defined diet may therefore explain the lower levels of TAG in these flies. Unfortunately, I have not got data on the fat content of the cornmeal media, so cannot say whether it varies considerably to the defined media, and whether this may help to explain these differences.

Levels of glycogen and triglycerides are routinely shown to be depleted upon infection and expression of immune pathways[257–261]. This may go some way towards explaining the observed depletion of these nutrient stores with age, as this corresponds to the increased immune activity shown through increased levels of DRS and DPT expression. Dionne *et al.*[258] also showed increased levels of circulating glucose up to 168 hours following infection. This doesn't immediately line up with the model of increased immune activation with age resulting in depleted nutrient stores, as glucose in this study decreased with age. Having said that, it is possible that such high levels of circulating glucose are not sustainable, and chronic immune activation over 168 hours may result in decreased glucose. There was a large amount of variation within the data at 168 hours, and no further increase in circulating glucose between 144 and 168 hours post-infection[258].

While the composition of the metabolic stores within the flies seems to vary between diets, with increased protein and decreased levels of glycogen and triglycerides in defined media flies, this data provides a reference point for any future studies assessing the levels of metabolic stores in flies on defined media with e.g. genetic perturbation or changes in microbiota composition. The overall trends observed in these metabolic stores with age did, however, remain largely consistent between diets, further supporting the use of the defined media for ageing experiments.

3.4.5 Assessing bacterial contributions to lifespan

The effect of the microbiome on fly health and longevity appears to be dependent upon the nutritional composition of the fly diet. Indeed it has been shown that gut-associated microbes can

rescue the lifespan of flies on nutrient-deficient diets, or periods of undernutrition, by promoting amino acid harvest[110]. In this case, axenic flies are shorter-lived. On the other hand, studies using axenic flies on fully nutritional food have reported increased lifespans as well as improved markers of intestinal homeostasis during ageing[39,88,89,92].

To understand whether the defined diet is able to support healthy adult flies for their full lifespan without bacterial contribution, I ran a lifespan of axenic flies and found they were longer lived and had lower proportions of smurfs at every time-point compared to re-associated and conventionally reared flies. This supports the idea that the defined media is, itself, sufficient to support adult lifespan, without nutritional contribution from the gut microbiome and also demonstrates another area of consistency between diets.

3.5 Conclusions

I have shown that, for the most part, the expected phenotypes of ageing remain present in flies reared on defined media throughout their adult life, and highlighted differences which are important to be aware of. This provides confidence in the use of the defined diet for assessing the phenotypes of ageing commonly used in our lab. Namely loss of intestinal barrier function, immune activation and increased bacterial load, as well as reduced metabolic stores. I have also shown that the defined media is sufficient to support growth without bacterial contribution, indicating that it meets the nutritional requirements of adult *Drosophila*. It was critical to test this before using the defined diet when investigating the role of the microbiome, or the effect of dietary manipulations on ageing. This set of data offers a baseline for future work investigating the effects of genetic, dietary or microbiome manipulations of flies maintained on this defined food.

4 Changes in the faecal nutrient profile driven by age and microbiota status

4.1 Introduction

As mentioned in the introduction (section 1.1) a number of well-documented metabolic and body composition changes occur during ageing. Fat mass increases, whilst muscle mass decreases with age. This is in part due to changes in metabolism with a 5-25 % decrease in basal (resting) metabolic rate leading to weight gain with unchanged dietary intake[262]. These changes begin early, with body fat increasing from as early as 25 years of age until approximately age 75, where it decreases or remains stable[263–268]. Muscle mass peaks at approximately 30 years of age, with a 20-40 % decrease by the age of 70, leading to sarcopenia[268–270]. This has important implications not only for strength and mobility, but a 10 % loss of lean tissue in previously healthy adults leads to impaired immunity, an increased risk of infection and increased mortality[271,272].

The elderly can also suffer from malnutrition which is associated with increased mortality and morbidity, as well as physical decline[273]. There are well-established reasons that the elderly may consume less, including poor dentition[274,275] and changes in masticatory muscle function[276,277], reduced appetite[278] (and earlier satiety[279]), salivary changes[280–282], and swallowing issues (dysphagia)[283–286]. The intestine also undergoes many changes with age, from microbial dybiosis[39,40,287–290], to dysplasia[77,92,291–295] and loss of intestinal barrier integrity[21,22,296]. There are also changes in intestinal enzyme activity[297–300], transit time[18,301,302] and mixed reports of changes to GI architecture[303–310].

As ageing is thought of as a general decline in function, it is also possible (and even likely) that there are changes in nutrient absorption. Indeed, micronutrient uptake is affected by age[311–315]. It is incredibly difficult to directly measure nutrient absorption, however. Indeed, there is a lack of consensus regarding the independent effects of ageing on intestinal absorption due to challenges in investigating aged intestines free from disease, the lack of good *in vivo* tools to directly measure absorption, and pitfalls in the *in vitro* methods of measuring intestinal nutrient absorption. Additionally, untangling the role of the intestinal microbial population using *in vivo* methods would be difficult.

There are several methods to assess nutrient uptake, reliant on the extraction of the gut from mammalian models. For a comprehensive review of the main in-vivo and ex-vivo methods, see Luo *et al.*[316]. Briefly, the everted gut technique takes small sections of the intestine, everts them, and bathes them in media. The gut is removed at various time points and the serosal space is analysed for transported nutrients[317–320]. Another method, the ussing chamber technique, takes intestinal

sheets clamped across an ussing chamber[319–321]. The appearance of the drug (or nutrient or metabolite) is measured on the serosal (basal) side, rather than disappearance from the mucosal (apical) side. A benefit of this technique in comparison to the everted gut method, is that the electric resistance of the membrane can be measured. It also allows regional differences in absorption to be assessed. These ex-vivo techniques however have several drawbacks, from the lack of any blood or nerve supply and rapid loss of viability of the tissues during the experiment, to damage to the tissues upon extraction (and mounting or eversion), and any changes to morphology and functionality of transporter proteins. Additionally, the role of gut microbes is not well accounted for.

These methods cannot be carried out in humans, for obvious reasons. Instead, less-invasive measurements of blood, urine, breath, and stools have been used to approximate nutrient absorption. Commonly, nitrogen balance; the difference between the amount of nitrogen ingested and the amount of nitrogen present in the final undigested substrate (faeces), is used as a proxy for protein absorption[322,323], although this doesn't provide information on the relative ratios of amino acids or the activity of transporters. The appearance of labelled amino acids (e.g. $^{2}H_{5}$-phenylalanine) in blood plasma is also used as a proxy for protein absorption[322], however, this may miss those taken up in first-pass splanchnic metabolism (amino acid uptake in intestinal and hepatic tissues[324]), and those involved in gastrointestinal protein synthesis. Isotopic labelling of protein is also commonly detected as heavy ^{13}C or ^{14}C CO_2 collected during exhalation, although this carries the assumption of 100 % protein absorption[322]. Similar methods are in place for the assessment of fat[325–328] and sugar[329–334] absorption. Additionally, measurement of ingested and egested calories, as opposed to individual macronutrients, has been measured in mice[335].

More recently, intestinal organoids have been employed to study nutrient transport. These organoids are generated from healthy, surgically removed tissue. The cells are disassociated, and organoids are generated from primary crypt cells[336]. This offers advantages in terms of scale, reproducibility, and improved ease of direct measurement and/or visualisation of nutrient transporters. They also provide opportunities to assess how/whether genetic perturbation impacts nutrient transport. Despite these advantages, they do not replicate genuine intestinal function; they do not offer the same cellular and regional complexity observed within intestines, do not contain the mucus lining or interact with a microbial population. Additionally, reproducibility may be lost between organoids derived from different patients.

Because of their technical difficulty, there are relatively few measurements of macronutrient digestibility in the intestine[337]. Changes to macronutrient digestibility with age is an area particularly

scarce in research[337], despite the metabolic changes observed in the elderly, and the malnutrition common in this population.

With the development of the defined media for *Drosophila*, we wanted to design an assay to assess changes in intestinal/faecal nutrient dynamics with age. *Drosophila* lends itself to this analysis due to the aforementioned defined diet, their short lifespans, and ease of manipulation of the microbiota, as well as the conservation in intestinal function between *Drosophila* and mammalian models.

4.2 Aims and Objectives

In this chapter, I set out to develop, validate, and run an assay assessing the nutrient concentration of *Drosophila* faeces, as measured by LC-MS/MS. I aimed to assess similarities and differences in the faecal nutrient profile of young and old *Drosophila*, with and without colonisation with intestinal microbiota, to understand more about how intestinal changes with age and microbiota may impact systemic metabolic changes.

Development of this assay in *Drosophila*, and characterisation of a 'standard' faecal profile in wild-type flies with and without microbiota, will facilitate the assessment of the luminal/faecal profile upon specific genetic perturbation, and upon association with specific microbial populations. This will enable an in-depth understanding of how specific changes in gene-expression, or in microbial composition may impact intestinal nutrient dynamics, and systemic nutritional and metabolic outcomes.

4.3 Results

4.3.1 Method development: Development of the *Drosophila* undigested metabolite profiling (DUMP) assay

One thing that has not been well studied, likely due to difficulties in assessing nutrient intake, are changes in macronutrient absorption with age. We wanted to harness the power of the defined diet for *Drosophila*, where we know the macronutrient composition, in order to assess this.

To this end we designed the *Drosophila* Undigested Metabolite Profiling (DUMP) assay. The premise of which is simple; by combining the defined diet with a non-absorbable dye, we can collect faecal samples and, by measuring the concentration of the dye, calculate how much food has been ingested for the given sample. We can then combine this with mass-spectrometry data analysing the concentration of individual nutrients within the faecal sample, and thereby assess how much of each nutrient has been ingested, how much has been egested, and how this changes with e.g. age, microbiota status, genotype etc. All mass-spectrometry was performed by Rachael Dack in the Durham Bioanalytics facility.

4.3.1.1 Use of blue dye for normalisation

The same dye used for the smurf assay is used in this DUMP assay for two purposes. Firstly, there is a clear, well-validated phenotype upon loss of intestinal barrier integrity, allowing removal of smurf flies from the assay. This is important for the second purpose of the dye; data normalisation. Quantification of the amount of dye within each faecal sample provides a proxy for the amount of food consumed for each sample, and normalisation of the mass-spectrometry data to this ensures that any observed differences are due to internal changes, and not altered food consumption.

4.3.1.2 Sample collection tubes

The sample collection pipeline is shown in Figure 4.1. The collection tubes are hollow-tubes of approximately the same dimensions as the fly culture tubes. Initially polystyrene tubes were tested, however we found these reacted with the DCM:MeOH used to collect the non-polar fraction of the sample, so glass tubes were used in place.

4.3.1.3 Validation

To optimise sample collection, we wanted to know how many washes were required to collect a full sample. To do this, we set up the assay with 6 vials of 50 flies, then rinsed all the vials with 1.5 mL of milliQ water and collected the sample in a microcentrifuge tube. This was repeated 10 times, with a subsequent rinse in DCM:MeOH. The levels of amino acids and cholesterol were then measured

within each sample, however further splitting of the sample did not seem feasible, so sugar analysis was omitted from this test.

We observed that the first two washes collected over 80 % of the amino acids within the sample (Figure 4.2B). We also observed that, while cholesterol was detected in washes 1-5, that about half of the detected cholesterol was collected within the first wash, and the remaining collected within the DCM:MeOH wash that followed the 10 water washes (Figure 4.2B). Due to the time taken to collect each subsequent wash, and because the majority of the amino acids were collected in the first two water washes, two washes was taken forward.

As we wanted to collect samples from young and old flies of the same starting population and run them together on the mass spec to minimise drift, we also tested the stability of the samples for long-term storage. The aqueous and DCM:MeOH fractions were each split into two, and freeze-dried or dried under a stream of N_2 respectively. One of the two samples from each fraction was resuspended and run on the mass-spectrometer immediately, whilst the other was run after approximately one-months storage at -80 ° C.

No real difference was observed in PAU/mass of the sample following storage (Figure 4.2A) indicating that storage long-term storage at - 80° C doesn't result in degradation of the sample, and providing confidence in the storage of our samples at -80 ° C in order to run them on the mass-spec together. The exceptions to this were arginine and lysine, however further analysis determined that the late elution of the arginine and lysine corresponds with a contaminant peak, which was reduced since identification following run 1, and likely explains the difference in peak area between the two runs.

The presence of amino acids was also tested in the DCM:MeOH sample, and in the DCM extract taken from the aqueous fraction (Figure 4.2 C and D respectively). All amino acids were detected in the DCM:MeOH sample (Figure 4.2C). Interestingly cysteine was also detected here while not in the aqueous sample. In the DCM extract from the aqueous sample, mostly non-polar amino acids were detected along with acidic and basic amino acids and tyrosine and threonine (Figure 4.2D). Because of this, and the different processing required for specific analytes, it was decided that the aqueous sample would be split into three, for amino acid, sugar and cholesterol quantification.

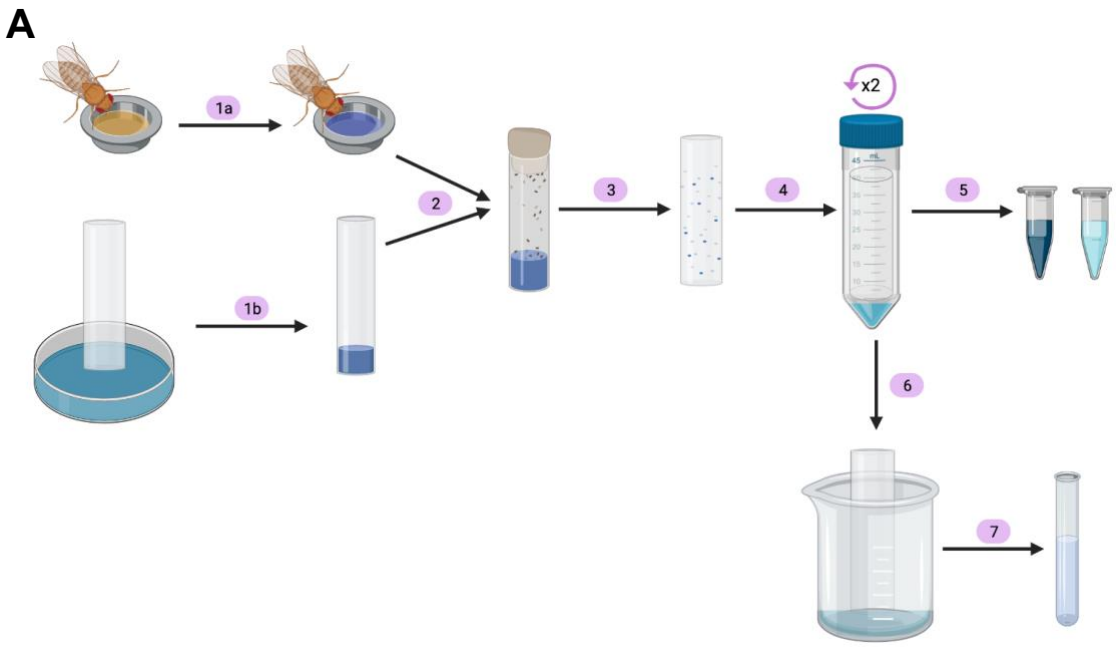
A
1a
1b
2
3
4
x2
5
6
7

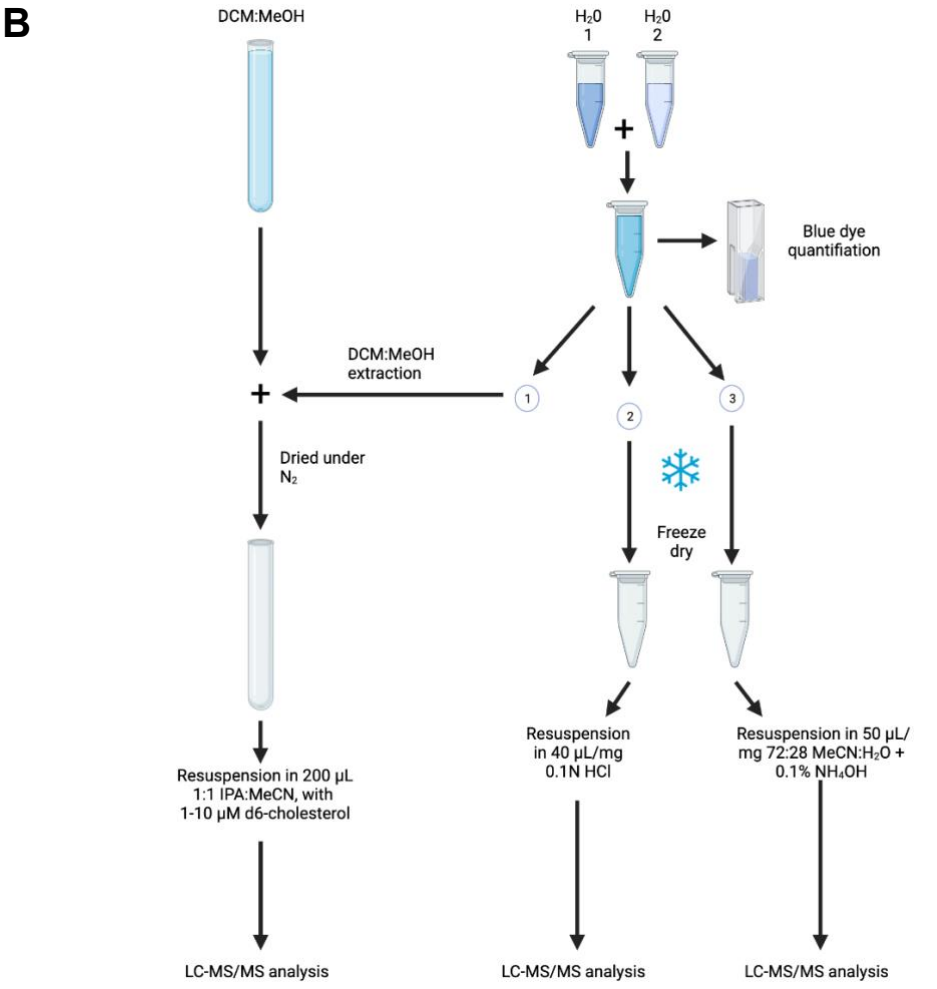
B
DCM:MeOH
H20 1
H20 2
Blue dye quantifiation
DCM:MeOH extraction
Dried under N2
Freeze dry
Resuspension in 200 µL 1:1 IPA:MeCN, with 1-10 µM d6-cholesterol
Resuspension in 40 µL/mg 0.1N HCl
Resuspension in 50 µL/mg 72:28 MeCN:H2O + 0.1% NH4OH
LC-MS/MS analysis
LC-MS/MS analysis
LC-MS/MS analysis

Figure 4.1 | Schematic of *Drosophila* Undigested Metabolite Profiling Assay

Schematic, copied from methods section 2.6, of **(A)** sample collection for the DUMP assay; 1a| Flies placed on blue food for 24h. 1b|collection vials prepared by stamping discs of food from petri-dish and securing in place with parafilm. 2|60 non-smurf flies transferred to collection tubes. 3| flies incubated at 25°C for up to 5 hours, then anaesthetised and removed with food from the bottom of the collection vials. Remaining food residue removed from collection vial base with damp white tissue, until no more blue dye visible on tissue. 4| All collection vials washed within falcon tubes with the same 1.5mL H2O to produce a concentrated sample. Vials spun down to ensure all water and sample removed to base of falcon tube. Wash was repeated for all vials with a second 1.5mL H2O. 5| water samples transferred to microfuge tubes and stored at -80°C. 6| collection vials washed in 5mL 1:1 DCM:MeOH to collect non-polar fraction. 7| DCM:MeOH sample collected in glass-storage tube to prevent reactivity with plastic vessels. Sample stored upright at -80°C. **(B)** Schematic of sample processing for the DUMP assay; the two water washes are combined and 1-2 mL removed for quantification of blue dye at 628nm. The remainder of the water washes are split three ways for 1. Cholesterol, 2. Amino acid, and 3. Sugar analysis. The non-polar fraction of the cholesterol fraction is extracted by addition of an equal volume of DCM, vortexed 2 mins and centrifuged at 1000x rpm for 15 mins. The DCM layer is collected and added to the DCM:MeOH wash sample and dried under a stream of N2. The dried sample was resuspended in 200mL 1:1 IPA:MeCN and spiked with 1-10uM d6-cholesterol prior to LC-MS/MS analysis. The amino acid and sugar samples were lyophilised, then resuspended in 0.1N HCl or 72:28 MeCN:H2O + 0.1% NH4OH respectively, prior to LC-MS/MS analysis.

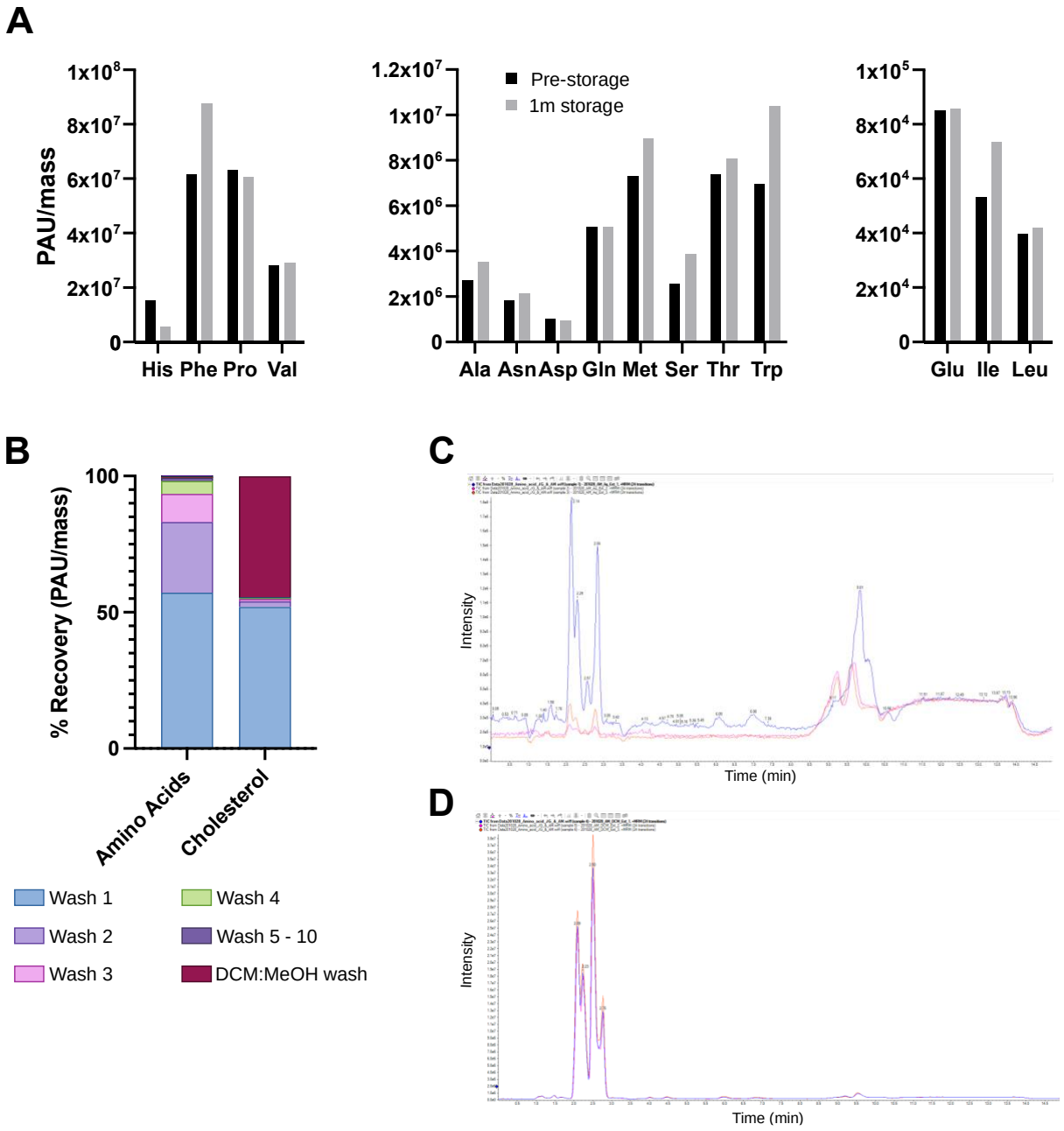

Figure 4.2. | Validation and optimisation of DUMP assay sample collection

(A) PAU/mass of amino acids before and after 1 month sample storage at -80°C. **(B)** Percent recovery; the sum of PAU/mass of all amino acids or cholesterol per wash, as a percentage of the sum of PAU/mass of all amino acids or cholesterol for all washes. No cholesterol was detected following wash 5. Amino acid mass-spectra result from **(C)** DCM:MeOH wash and **(D)** DCM extract from a fraction of the aqueous wash.

4.3.2 Changes in the macronutrient absorption/excretion profile observed with age

Following assay optimization, I wanted to assess what, if any, changes occur with age. For this I used age-matched wild-type Canton-S flies, taking faecal samples at 10 (9 - 11) and 40 (39 - 44) days of age. I then assessed the levels of amino acid and cholesterol. Attempts to measure sugar (sucrose and glucose) at this point were unsuccessful, with drops in sensitivity between replicates, high % relative standard deviation (RSD) between duplicate injections and poor peak shapes.

4.3.2.1 Faecal amino acid levels increase with age

I observed the largest changes with age in the amino acids, where there was a consistent trend towards increased concentrations in the faeces of aged flies, although not every amino acid showed significant changes with age (Figure 4.3A). As previously mentioned, no peaks were found for cysteine. This broad increase in all amino acids may indicate fundamental changes occurring within the fly, although it also creates difficulties in identifying trends and drawing conclusions.

There are however many possible reasons for these increases. The flies may be actively excreting higher levels of amino acids or be less efficient in their absorption. Additionally, the flies' extracellular protein constructs e.g. mucins[338], or indeed cells themselves may be being shed or broken down at a higher level and contributing to the luminal amino acid pool. Indeed Proline, one of the most abundant amino acids in mucins[339–343] was detected at significantly elevated levels in the faeces of aged flies.

Another likely factor affecting the faecal amino acid composition is the presence of the microbiota. As previously discussed, the internal microbial load increases with age, and this may be sufficient to explain the increased levels of faecal amino acids with age. Branched-chain amino acid (BCAA) synthesis has been shown to be essential in some bacterial species, and gut bacteria generally contain a higher proportion of BCAAs relative to other amino acids[344,345]. Indeed, we observed a significant increase in the levels of all BCAAs (isoleucine, leucine and valine) with age. Interestingly, elevated levels of BCAAs have been observed in humans with obesity and insulin resistance[346–350] and are thought to contribute to the pathogenesis of type 2 diabetes.

I also observed that all the amino acids significantly increasing in faecal output with age are neutral, excluding arginine which is basic, potentially implicating a transporter specific to neutral amino acids.

4.3.2.2 Faecal cholesterol remains stable with advancing age

No changes in the levels of cholesterol were detected with age (Figure 4.3C). This is in line with the hypothesis that the changes are driven by microbiota, as bacteria within the gut microbiota do not

commonly synthesise cholesterol and only a few genera are known to have cholesterol in their membranes. Additionally, the specificity of the mass-spectrometry should mean that even the cholesterol analogue ergosterol, found in yeast, will not be detected.

In humans, gut bacteria are thought to contribute to cholesterol metabolism through the deconjugation of bile salts through bile salts hydrolase[351–354], and through the conversion of cholesterol to coprostanol[355–357], a non-absorbable molecule excreted as faeces. Neither of these routes should, however, impact faecal levels of cholesterol in *Drosophila*, as they do not produce bile salts, and we were specifically looking at spectra for cholesterol, not any of its derivatives.

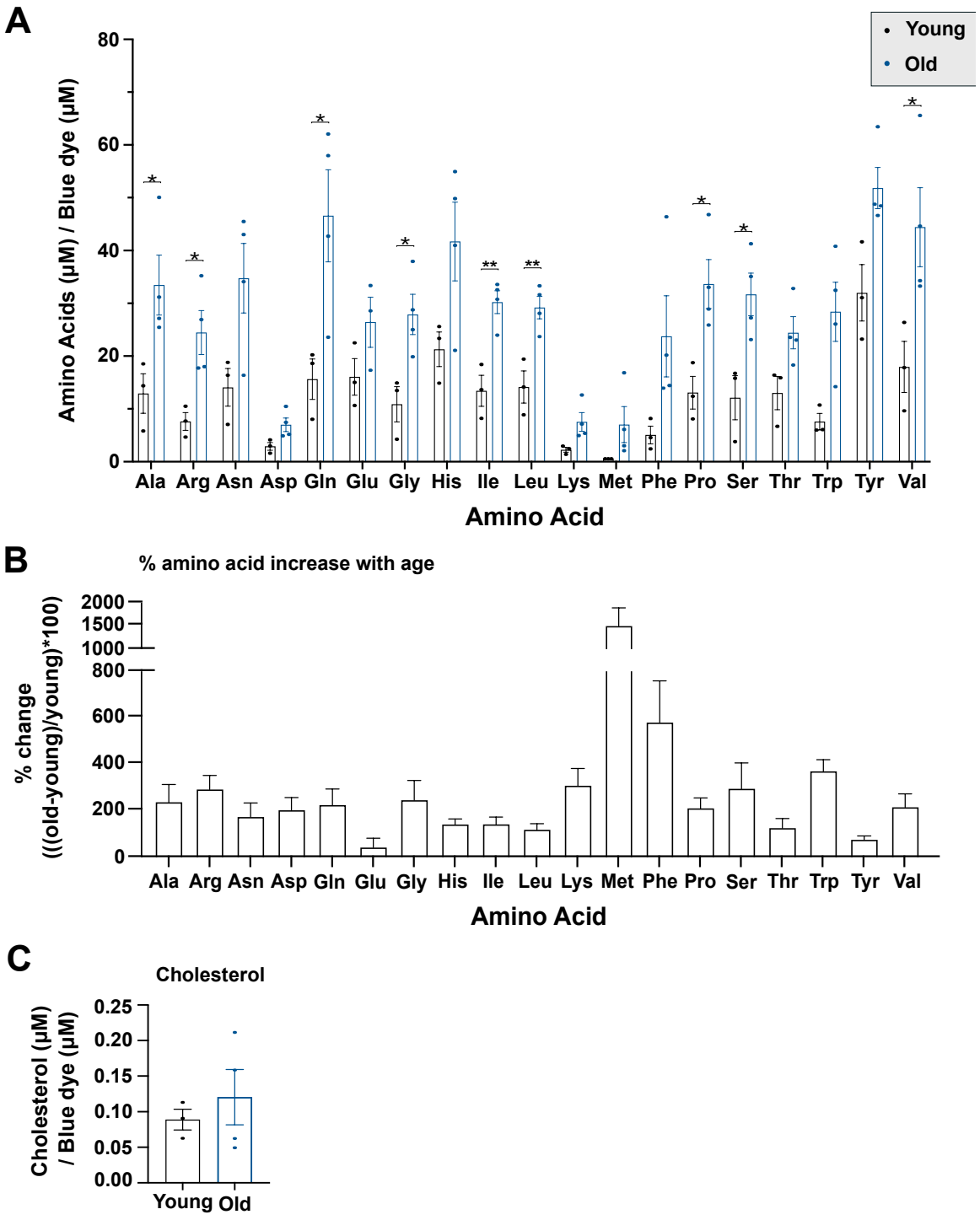

Figure 4.3. | *Drosophila* Undigested Metabolite Profiling assay uncovers changes in nutrient egestion with age

(A) Relative concentration of amino acids in the faecal deposits of young (9-11 day) and old (39-44 day) flies, normalised to the concentration of blue food dye. **(B)** percent change in relative faecal amino acid concentration calculated by (((young – old)/young)*100) using the average value for each amino acid at the young and old timepoints. **(C)** Relative concentration of cholesterol in the faecal deposits of young and old flies, normalised to the concentration of blue food dye in each faecal sample. Samples pooled from >300 mated female flies. Bar graph shows mean ± SEM. Asterisks denote the results of 2-tailed unpaired T-test (normally-distributed data) or Mann-Whitney test (not-normally distributed data; Trp and Try (A,B)), where * P<0.05, **P<0.01

4.3.3 The microbiota has a profound impact on the macronutrient absorption/excretion profile

To uncouple the contributions of the intestinal microbiota which increases in load with age, and the effects of age itself, I repeated the DUMP assay with microbiologically sterile (axenic) flies. Here, instead of just the two previous time points of 10 (9-11) and 40 (39-44) days, a third time point (52-54 days) was included to reflect the increased lifespan of our sterile flies and to provide a biological age-match to the 40-day conventional flies. 40-days in the axenic lifespan is too early to provide this biological age-match, as it falls before the rapid downward curve.

4.3.3.1 Biological rather than chronological age determines the changes in amino acid profile

To characterise the structure of the data, I performed principal component analysis on the amino acid dataset of conventional and axenic flies.

Plotting the data in respect to the first and second principal components, which explain the most variance, showed clustering by age in the conventional data set (Figure 4.4A). In the axenic dataset however, there was no separation between the 10 and 40-day data, indicating a high degree of similarity between the 10 and 40-day faecal samples (Figure 4.4B). The 52-day data however does show separation, indicating that the 52-day data is distinct from the 10 and 40-day data, and suggesting a difference between chronological and biological age. Because of this separation, the 52-day data was used for further analyses unless stated.

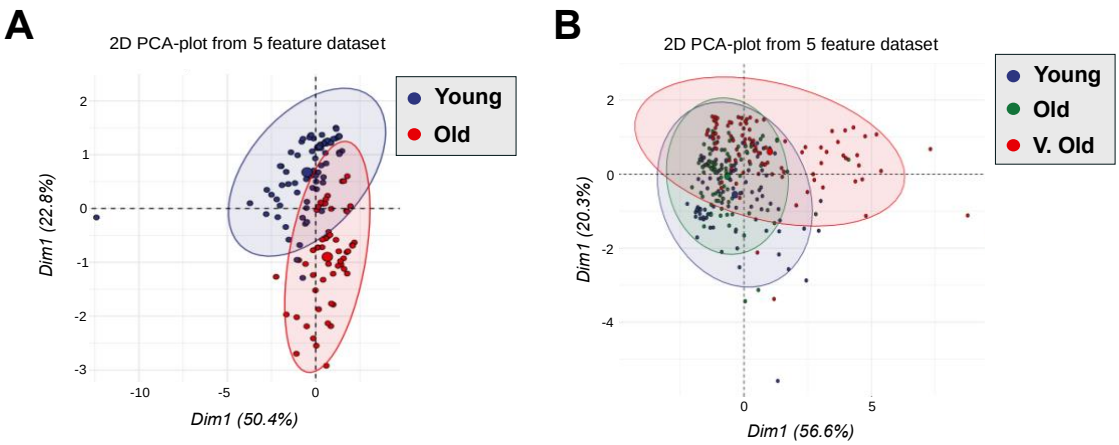

Figure 4.4. | Biological not chronological age determines sample separation

Principal component analysis plot for the overall structure of amino acid data from **(A)** conventional flies and **(B)** axenic flies plotted with respect to the first and second principal components and coloured by age. Plots show separation between **(A)** young (9-11 day) and old (39-44 day) conventional flies, and **(B)** young (9-11 day) and very old (V. Old (52-54 days)), old (38-40 days) and very old, but not young and old axenic flies.

4.3.3.2 Concentration of faecal amino acids increases with age in sterile flies

A trend towards increased faecal amino acid concentration with age remained in our sterile flies, particularly at the oldest time point (52-54 days), although this was significant for fewer amino acids than in the conventional dataset (Figure 4.5A). Additionally, the amino acids that showed significant changes with age were not consistent between axenic and conventionally reared flies, with Aspartate, Lysine and serine showing significant changes in the sterile but not the conventional flies.

Importantly, none of the amino acids were present in higher relative concentrations than in the conventional faecal samples, indicating that the microbiota must indeed be contributing significantly to the flies' faecal content.

4.3.3.3 Faecal cholesterol levels remain stable with age in the absence of microbiota

As in the faeces of conventionally reared flies, the faecal concentration of cholesterol from axenic flies remained consistent with age (Figure 4.5D). Further analysis showed there to be no significant difference in the concentration of cholesterol in the faeces of conventionally reared flies compared to sterile flies (unpaired t-test 10-day conventional vs 10-day axenic ($p > 0.289$), and 40-day conventional vs 52-day axenic ($p > 0.362$)). The consistency in cholesterol concentration between conventionally reared and sterile flies is not particularly surprising given the inability of most bacteria to synthesise cholesterol and thereby add to the nutrient pool in increasing quantities as microbial load increases with age.

4.3.3.4 Sucrose levels are depleted in axenic flies

Following the difficulties in sugar analysis of the conventional samples, the method for sugar analysis was amended for the axenic samples, with an increased oven temperature to enable better separation of closely eluting peaks, and modified dwell times. This improved the sensitivity between replicates. While the only sugar provided within the defined diet is sucrose, we analysed the levels of both sucrose and glucose, one of the monosaccharides which make up sucrose, within the faecal samples.

Interestingly, there were no significant changes in the levels of glucose within the axenic samples (Figure 4.5F), however, there was a significant difference in faecal sucrose between 10 and 40 day, but not 52 day samples (ordinary one-way Anova with Sidaks multiple comparison; 10-40 $P<0.04$, 10-52 $P>0.05$, 40-52 $P>0.05$) (Figure 4.5E). This may be due to the large amount of variance in the 10-day samples (F-test; 10-54 days $P<0.0001$). Originally, three replicates of this assay were performed, but a further two replicates were added to improve statistical power. The variability in the 10-day sucrose samples is stratified by replicate, with the first three replicates showing very high levels, and

the final two replicates showing lower levels. Whether this is due to errors within the assay, or whether the sugar samples from the first three replicates were altered through multiple mass-spec runs and freeze thaw cycles, remains to be determined.

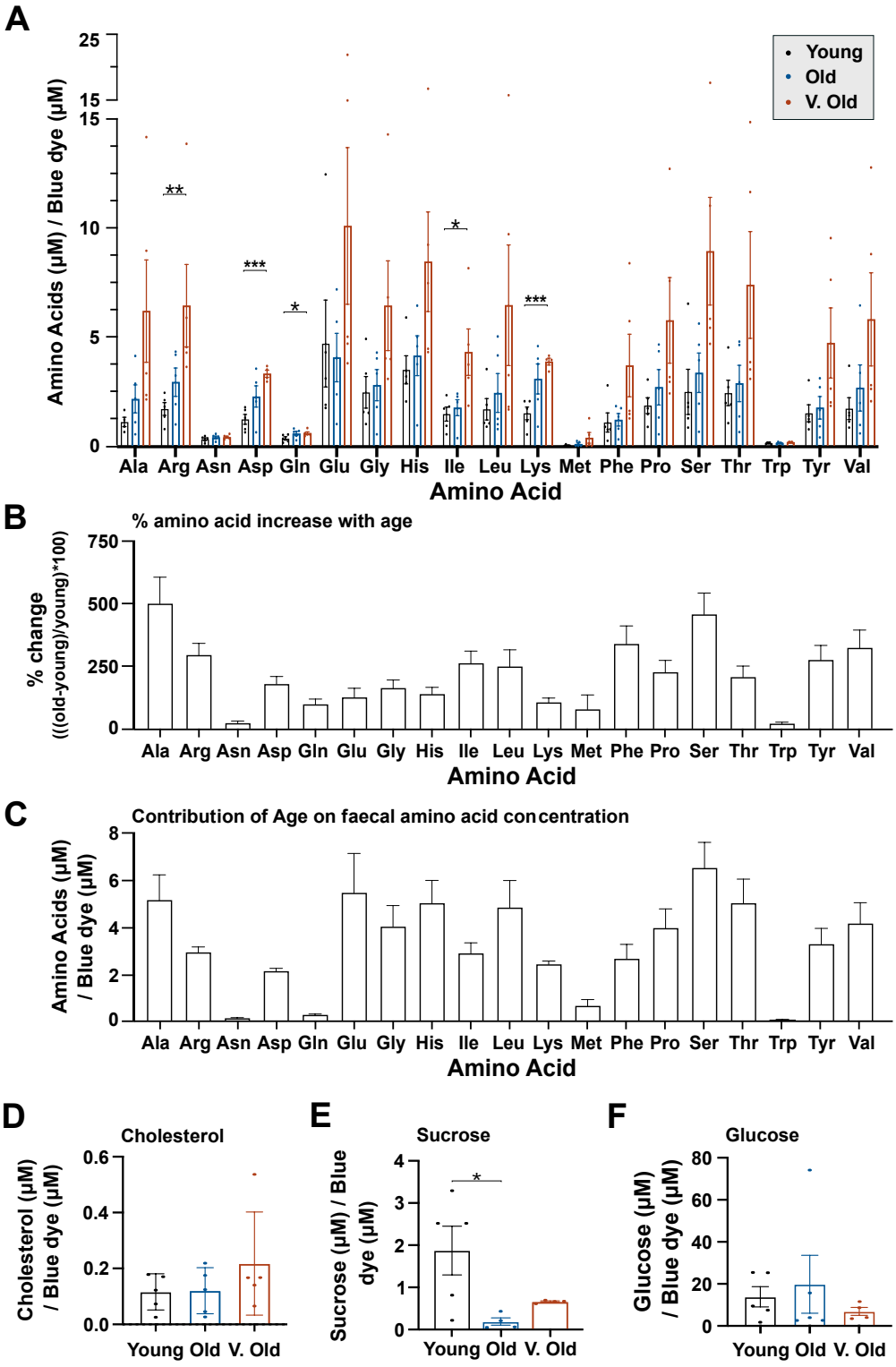

Figure 4.5 | *Drosophila* Undigested Metabolite Profiling assay uncovers changes in nutrient egestion with age in sterile flies

(A) Concentration of amino acids in the faecal deposits of young (9-11 day), old (38-40 day) and V.old (52-54 day) axenic flies, normalised to the concentration of blue food dye. **(B)** percentage change in faecal amino acid concentration between young and very old flies. Calculated by ((old-young)/young)*100. For each amino acid, comparisons were made between all the young, and all the very old concentrations, normalised to blue food dye. **(C)** The concentration of faecal amino acid, normalised to blue food dye, contributed solely by age-related changes within the fly. This was calculated for each amino acid by; axenic V. old – axenic young. The calculation was performed by subtracting each replicate of young from each replicate of V.old. **(D-F)** concentration of **(D)** cholesterol, **(E)** sucrose and **(F)** Glucose in faecal deposits of young (~10 day), old (~40 day) and V.old (~52 day) axenic flies, normalised to the concentration of blue food dye. Samples pooled from >360 mated female flies. Bar graphs show mean ± SEM. Asterisks denote the results of **(A)** a 2-tailed unpaired T-test (normally distributed data) or Mann-Whitney test (not-normally distributed data; Arg, Glu, Met, Phe, Ser and Val) between young and very old flies, or **(D-F)** an ordinary 1-way Anova, where * P<0.05, **P<0.01, *** P<0.001

4.3.3.5 Contribution of age to faecal amino acid profile

To further understand the contribution of age on the faecal amino acid profile, I looked at the percentage increase in normalised amino acid concentration with age in conventional (Figure 4.3B) and axenic (Figure 4.5B) faeces.

Interestingly, there was a larger percentage increase in most of the amino acids in the axenic faeces (Figure 4.3B (conventional) and Figure 4.5B (axenic)). Exceptions to this were asparagine, glutamine, lysine, phenylalanine and tryptophan, perhaps indicating that the microbiota is having the largest impact on these. Methionine showed the largest percentage increase in both conventional and axenic samples, although this is likely skewed by the low levels detected (Figure 4.3A (conventional) and Figure 4.5A (axenic)).

I also wanted to uncouple the effects of microbiota and age. For this, I considered just the axenic data to understand purely age-related changes in amino acid profile (Figure 4.5C).

When looking at the changes in the normalised concentration of amino acids in the axenic samples between 10 and 52 day samples, I observed the greatest increase in the relative concentration of Ser, Glu and Ala (>5 μM/μM), His, Thr, Leu and Arg (>4.5 μM/μM). The smallest changes were observed in Trp, Asn (<0.1 μM/μM), Gln and Met (<0.5 μM/μM) (Table 4.1).

To better understand the change in faecal amino acid profile with age, I ranked the faecal concentration of each amino acid at 10 and 52 days from 1-19 (high to low concentration) and calculated the rank change (young rank – old rank; Table 4.1). The relative profile of faecal amino acids appears relatively stable with age, with the majority of amino acids moving a maximum of 2 positions. This rank system did however highlight a large change in the relative amounts of alanine which, due to the large increase in normalised concentration, increased by 6 ranks. Leucine also moved up four positions, whilst proline moved down four positions despite over a 200 % increase in concentration between 10 and 52 days.

Table 4.1 | Contribution of age to faecal amino acid profile.

Average concentration (uM/uM) of 10 and 52 day (young and V..old) axenic faecal amino acids ranked 1-19 (high to low). Rank change (young-old), calculated to show the change in amino acid profile with age was also ranked 1-19 (high to low)

Amino Acid		Relative concentration (μM/μM) – Axenic		Rank		Rank change (Y-O)	Relative concentration change	
3-letter	1-letter	Young	V.Old	Young	V.Old		(uM/uM)	Rank
Ala	A	1.091	6.181	14	8	6	5.091	3
Arg	R	1.688	6.433	8	7	1	4.745	7
Asn	N	0.300	0.398	17	18	-1	0.098	18
Asp	D	1.216	3.306	13	15	-2	2.090	15
Cys	C	N/A	N/A	N/A	N/A	N/A	N/A	N/A
Gln	Q	0.336	0.577	16	17	-1	0.241	17
Glu	E	4.692	10.092	1	1	0	5.400	2
Gly	G	2.458	6.434	4	6	-2	3.976	9
His	H	3.487	8.453	2	3	-1	4.965	4
Ile	I	1.457	4.297	12	12	0	2.840	12
Leu	L	1.673	6.452	9	5	4	4.779	6
Lys	K	1.489	3.863	11	13	-2	2.374	14
Met	M	0.029	0.603	19	16	3	0.574	16
Phe	F	1.072	3.686	15	14	1	2.614	13
Pro	P	1.848	5.756	6	10	-4	3.908	10
Ser	S	2.477	8.933	3	2	1	6.456	1
Thr	T	2.421	7.385	5	4	1	4.964	5
Trp	W	0.116	0.156	18	19	-1	0.040	19
Tyr	Y	1.493	4.720	10	11	-1	3.228	11
Val	V	1.705	5.803	7	9	-2	4.098	8

4.3.4 Contribution of microbiota to faecal amino acid profile

I next wanted to assess the extent of the microbial contribution to the conventional faecal profile both directly through measurement of the microbes and their products, but also indirectly through microbiota-associated changes to the *Drosophila* intestinal absorption/excretion and cell turnover dynamics. To this end I calculated the concentration contributed by the microbiota for each amino acid in young (10 day conventional and axenic) and old (40 day conventional and 52 day axenic) flies (Figure 4.6A). This calculation was performed by comparing every conventional value to every axenic value, for each amino acid.

Interestingly tyrosine was found to be contributed at the highest levels in both young and old timepoints, however by the aged timepoint, glutamine was contributed as highly (Figure 4.6A), due to the largest increase in contributed concentration with age (>26 μM/μM) (Table 4.2). Valine, tryptophan and asparagine also showed substantial increases in microbiota-derived concentration with age (<25 μM/μM). The microbiota-contributed amino acids did not increase uniformly with age, however, indicating that there may be a microbe-specific profile.

As with changes attributed solely to age, I wanted to compare the microbiota-derived amino acid profile of young and aged flies, so I ranked the microbiota-contributed concentration of faecal amino acids from 1-19 (high-low) and calculated the rank change (young rank – old rank) (Table 4.2, Figure 4.6B).

De novo synthesis of amino acids by bacteria and yeast is associated with metabolic costs which may influence the levels of microbial contribution[358–360]. I hypothesised that amino acids with high associated metabolic costs would be synthesised at lower levels – sufficient to satisfy the needs of the source organism, but not being synthesised in excess. In addition, it would follow that absorption of lowly synthesised amino acids by *Drosophila* would be efficient to maximise intake.

To understand whether the energetic cost of *de novo* synthesis is impacting the profile of microbial contribution, I plotted the energetic cost (as calculated by Akashi and Gojobori[359]) against the rank of microbial contribution at young and old (Figure 4.6C), and found no correlation (Pearson Correlation coefficient, p=0.66 and p=0.15 for young and old ranks respectively). Indeed, tryptophan and methionine, the costliest amino acids to synthesise, increased in relative microbial contribution with

age. This may indicate increased biosynthesis, perhaps through expansion of the bacterial species containing this pathway.

As previously noted, tyrosine was contributed at the highest contribution in both young and old conventional fly faeces (Figure 4.3A), so showed no rank change.

In comparison to the age-related profile, the microbiota-contributed profile appeared more variable with age. The largest rank change was observed in tryptophan, which increased by 9 positions, although this amino acid didn't show the largest change in concentration with age.

The largest remaining rank changes (5 or more positions) were seen in glutamine, leucine and threonine which were contributed proportionally less with age, and phenylalanine whose proportional contribution increased with age (Table 4.2, Figure 4.6B).

The smallest changes in relative contributed concentration with age were seen in aspartate, lysine (<3 μM/μM increase), glutamine, methionine and threonine (<7μM/μM) (Table 4.2). This may indicate lower levels of biosynthesis of these amino acids (three of which are essential), or indeed increased uptake by the microbial populations and/or the fly.

As lysine and aspartate were available in only very small concentrations, their rank was not affected much by the low increase in available contribution. Glutamate and threonine, however, were contributed at reasonably high levels in young flies, so only a small increase in contributed concentration resulted in large rank changes (5 positions each) and a proportional decrease in availability.

Table 4.2 | Contribution of microbiota to faecal amino acid profile.

Relative microbiota-contributed-concentration calculated by subtraction of the axenic relative amino acid concentration at 10 or 52 days, from the conventional relative amino acid concentration at 10 and 40 days, was ranked from 1-19 (high to low) for young and old datasets. The rank change (young – old) was calculated to show the change in amino acid profile with age. Concentration change (young contributed relative concentration (uM/uM) – old contributed relative concentration (uM/uM)) was also ranked 1-19 (high to low).

Amino Acid		**Relative contributed concentration (μM/μM)**		**Rank**		**Rank change (Y-O)**	**Relative contributed concentration change**	
3-letter	**1-letter**	**Young**	**Old**	**Young**	**Old**		**(uM/uM)**	**Rank**
Ala	A	12.045	28.039	7	8	-1	15.994	9
Arg	R	5.937	20.273	15	15	0	14.335	10
Asn	N	13.781	31.587	5	6	-1	17.806	7
Asp	D	1.696	4.304	17	19	-2	2.608	19
Cys	C	N/A	N/A	N/A	N/A	N/A	N/A	N/A
Gln	Q	15.296	42.208	4	2	2	26.912	1
Glu	E	11.365	20.884	9	14	-5	9.518	14
Gly	G	8.419	21.167	13	13	0	12.748	12
His	H	17.799	40.128	2	4	-2	22.330	4
Ile	I	11.965	24.805	8	9	-1	12.840	11
Leu	L	12.474	21.353	6	12	-6	8.879	15
Lys	K	0.776	4.524	18	18	0	3.747	18
Met	M	0.524	8.059	19	17	2	7.535	16
Phe	F	3.982	23.320	16	10	6	19.338	5
Pro	P	11.228	30.480	10	7	3	19.253	6
Ser	S	9.640	21.621	12	11	1	11.981	13
Thr	T	10.571	17.340	11	16	-5	6.769	17
Trp	W	7.479	32.959	14	5	9	25.479	3
Tyr	Y	30.480	48.223	1	1	0	17.743	8
Val	V	16.244	41.999	3	3	0	25.755	2

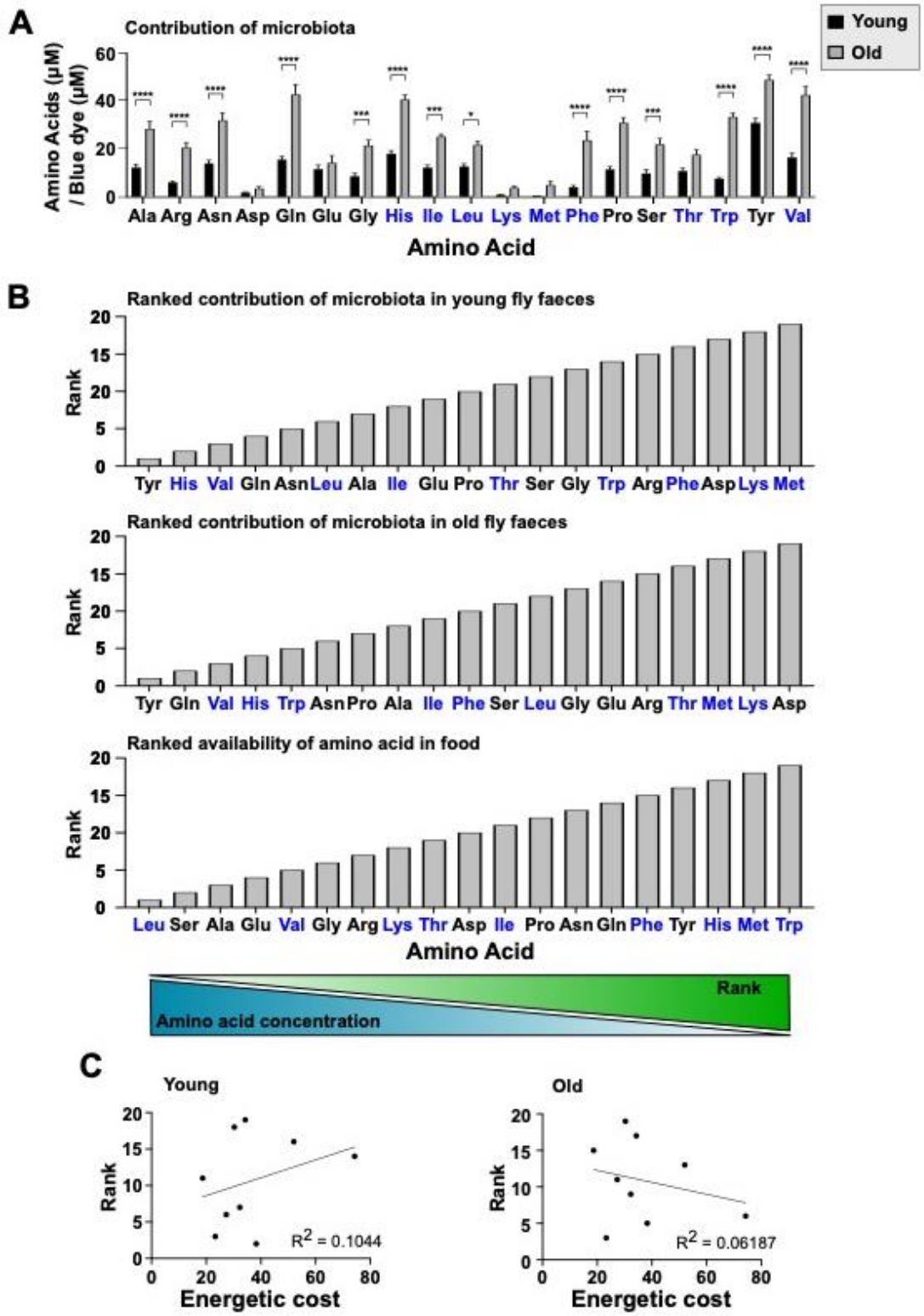

Figure 4.6. | Microbial contribution with age shifts faecal amino acid profile

(A) concentration of faecal amino acids, normalised to the concentration of blue food dye, contributed by the microbiota in young and old flies. The microbial contribution was calculated for each amino acid at the young timepoint by; Conventional concentration (9-11 days) – axenic concentration (9-11 days), and at the old timepoint by; Conventional concentration (38-40 days) – axenic concentration (52-54 days), using the

concentration of amino acid normalised to blue dye for each sample. For each amino acid, at each time point, the calculation was carried out between every conventional and every axenic measurement. **(B)** amino acids ranked from 1-19 by microbial contribution in young and old flies, and by availability within the food, where a low rank indicates a high amino acid contribution/availability. **(C)** Energetic cost of bacterial de novo amino acid synthesis plotted against the ranked microbial contribution of old and young faeces. Blue amino acid labels denote essential amino acids. Bar graph shows mean ± SEM. Asterisks denote the results of a 2-way Anova, where * P<0.05, **P<0.01, *** P<0.001

4.4 Discussion

4.4.1 DUMP assay detected age-related changes in faecal profile

Here we developed a novel assay which was able to detect changes in the faecal profile of *Drosophila* with age.

The effect of both age, and microbiota on nutrition is an understudied area, with potentially wide-ranging implications in health and disease. An area particularly lacking in research is a direct measurement of nutrients within faeces, with many studies in mice instead focusing on nutrients which have made their way to the portal vein, or plasma of mammals. These measurements can be confounded by changes in metabolism within the entire organism e.g. muscle wastage could increase serum amino acid levels. There is also the assumption that nutrients consumed as food will be bioavailable to the organism in their entirety. Focusing on post-absorptive nutrient and metabolite measurements misses valuable information regarding the nutrient environment within the intestine itself, and thereby how the microbiota, and factors such as ageing, affect initial nutrient availability.

We have shown that there are substantial changes in the faecal amino acid profile, and thus gastrointestinal nutrient levels, with both age and microbial status which may have a direct impact on healthy ageing.

Whilst we used the assay to measure the levels of macronutrients within the faecal samples for proof of principle, there is a much larger scope for this assay, which could be applied to measure the levels of other specific nutrients or metabolites, or indeed untargeted MS/MS could be applied to look at the entire faecal profile. Additionally, it would be a powerful in combination with genetic manipulation or specific association with microbes to understand nutritional changes which may be impacting the systemic responses.

This study uncovered limitations to the assay. Firstly, we typically use loss of intestinal barrier function to identify the individuals closest to death and in rapid health decline. By excluding smurf flies from the assay, in order to use the blue dye for normalisation, we are unable to compare the faecal profiles of flies undergoing rapid decline with those which are, in relative terms, healthy age-matched flies. This means we are losing valuable data, defining the differences in faecal composition, and potentially intestinal function, of these distinct groups. Additionally, there were difficulties in quantifying the levels of sugars (sucrose and glucose) within our samples, likely due to the different processing requirements of the individual nutrients. While we were able to modify the

protocol to enable improved quantification for the axenic cohort, this highlights the need to identify appropriate solvents for the specific MS/MS pipeline. Ideally, one solvent for the entire sample would be optimal, although this is virtually impossible given the varying polarities and chemical properties of different analytes.

4.4.2 Physiological changes may alter nutrient absorption/excretion dynamics

Given that increased faecal amino acid concentrations were observed in both older sterile and conventionally reared flies, physiological changes to the intestine and resulting changes to absorption/excretion dynamics may be the simplest explanation.

The architecture of the gut has been shown to change with age in several model organisms. In *C. elegans* there is a loss of intestinal nuclei and microvilli[361]. In *Drosophila*, ISC proliferation increases, resulting in an accumulation of polyploid, mis-differentiated cells, and disruption of intestinal homeostasis, basal organisation, and epithelial function[49,92,362].

In mice and rats, thicker muscular layers, distorted villi, more secretory Paneth and goblet cells, and impaired junctions between enterocytes have been observed[303,304,306,363–366]. Additionally, mice have wider and higher villi with increased age[365], whilst rats have wider and shorter villi[306]. Human studies showed no significant changes in morphology[307,308,367]. However, abnormal hyperproliferation and apoptosis were found in enterocytes of a normal elderly group, which resulted in impaired function of the aged intestine[309,368].

Associations between changes in intestinal morphology and nutrient uptake with age are, however, unclear. As an example, fatty acid uptake is increased in older rabbits despite reductions in mucosal surface area, however, it should be noted that the rabbits counted as mature were only 1 year old, whereas the life expectancy of rabbits is 8-12 years[369]. An association between intestinal morphology and protein absorption has also not been studied.

Amino acids must be carried into cells through specific membrane-spanning transporters. Expression of these transporters may be impacted by the altered intestinal structure observed with age, or by other unknown age-related reasons. Unfortunately, there is little-to-no information on the expression of such transporters with age in humans[337]. Research surrounding age-related changes in amino acid absorption is also limited in other models, although there is evidence suggesting impaired amino acid absorption with age in rats[370–373]. Additionally, while absorption itself has not been directly studied in humans, a delay in the rate of postprandial appearance of essential amino

acids has been shown in the elderly (60-75 years vs 20-25 years with matched BMI scores)[374], and lower levels of labelled amino acids have been shown to reach the bloodstream of the elderly (66-76 years vs 19-25 years) following digestion and absorption[375]. These results may indicate lower levels of absorption from the intestinal lumen and/or increased uptake and utilisation by the splanchnic tissues[376], known to occur with age for leucine[377,378], phenylalanine[324] and glutamate[379]. Impaired protein absorption may also be implicated in another study, where feeding a diet containing 1.4-1.5 g/kg body mass of protein per day, as compared to a diet containing 0.9-1 g/kg, doubled faecal nitrogen in the elderly but not younger adults on the same diet[380]. Extrapolation of these results to suggest altered protein absorption should be taken with care however, as nitrogen balance however is a function of protein intake, absorption, metabolism, utilisation and excretion[381]. Taken together, these studies build a compelling argument towards reduced protein uptake with age, consistent with our results.

On top of morphological changes, ageing is often associated with reduced gut motility, and resultant constipation[382–384]. Indeed some clinical reports have associated increased morbidity with dysfunctional gut motility and gastric emptying in the elderly[383]. Similarly, aged monkeys show reduced intestinal motility[385], as do mice[386]. Indeed, *Drosophila* also display delays in gastric emptying with age[387] and reductions in gut contractility[388], suggesting that this may be a conserved feature of ageing. Slowed passage of food through the intestine may allow increased time for nutrient absorption. It would also enable a greater build-up of microbially contributed nutrients, which might help explain the substantially higher amino acid concentrations observed in the faeces of conventionally reared aged flies. Interestingly, amino acids within the rat intestinal lumen have been shown to regulate their own absorption from a distant intestinal site by affecting transporter affinity[389]. Such regulatory systems may factor into the increased faecal amino acid concentrations observed with age; delayed passage of food may trick the intestine into believing there is a higher concentration of nutrients, resulting in reduced amino acid transporter affinity and uptake at proximal regions.

4.4.3 Microbial contribution to protein nutrition

This assay highlighted profound changes in the faecal amino acid profile of flies with and without gut microbiota. The intestinal microbiota has been implicated in health and disease and is widely studied in terms of its contribution to carbohydrate metabolism. Microbial production of short chain fatty acids (SCFAs), the main microbial fermentation products of dietary fibre and resistant starch produced

in the large intestine[390,391], are widely believed to be beneficial, not just for gut health[392–395], but also systemically as reduced levels of SCFA-producing bacteria are correlated with disease[396–403].

In contrast, the role of the gut microbiota in host amino acid metabolism is not well understood, although there is a growing understanding that the intestinal microbiota plays an important role in amino acid metabolism and protein nutrition[358].

Higher organisms have lost the metabolic pathways required for the synthesis of certain amino acids; these are the essential amino acids which must be consumed. The gut bacteria however have the ability to synthesise this pool of amino acids, although it was not known until recently whether the ability of the gut microbiota to synthesise essential amino acids had any functional significance to the host.

It has now been demonstrated in mice, that microbially synthesised essential amino acids are incorporated into skeletal muscle, although the level of contribution varied depending on the amino acid, from less than 5% (threonine, lysine and phenylalanine), up to 60% (valine)[358]. This trend remains true here, with valine being contributed at very high levels in both young and old flies and threonine and lysine contributed at relatively low levels. The DUMP assay also shows histidine to be contributed at high levels (second highest) in young flies, although its relative contribution decreases with age whereas the contribution of valine remains the same. Newsome *et al.* did not look at the level of microbial histidine contribution in mice[358], so no comparison can be made here.

De novo synthesis of amino acids by bacteria and yeast is metabolically costly, and whilst I hypothesised that the amino acids with high associated metabolic costs would be synthesised at lower levels, there was no trend to this effect upon plotting energetic cost against the rank of microbial contribution at either young or old timepoints. Indeed, tryptophan and methionine, the costliest amino acids to synthesise, increased in relative microbial contribution with age. This may indicate increased biosynthesis, perhaps through expansion of the bacterial species containing this pathway. It should be noted that such an effect may be masked, as the microbial amino acid contribution here is not only the direct measurement of the amino acids within, and synthesised by, the microbiota, but also amino acids which change indirectly through association with microbiota, e.g. by changes to intestinal amino acid absorption/excretion and cell turnover dynamics.

Additionally, metabolic mutualism, or cross-feeding of metabolites, has been shown to occur between bacterial species within the gut microbiota[404–407]. Perhaps such a system is in place for the synthesis of costly essential amino acids, reducing the individual cost to each species and enabling

the high-cost amino acids to be synthesised in high concentration. Mutualism may also exist whereby one bacterial species synthesises e.g. methionine, and receives a useful metabolite from a separate bacterial species involved in e.g. the methionine cycle. If this was the case but the second species in this interaction was depleted with age, the luminal methionine concentration is likely to increase with age.

Microbial association has also been shown to rescue *Drosophila* in periods of undernutrition, through the harvesting, and thereby concentrating, of amino acids from nutrient-poor, low-yeast diets[110]. The mechanism was determined to be increased flux to the fly, although de-novo synthesis of amino acids was not investigated in this study.

On top of more direct amino acid provision to the host, it has been shown in *Drosophila*, that association with *Lactobacillus plantarum*, sustains *Drosophila* peptidase activity within the midgut, promoting protein digestion and thereby increasing the pool of available amino acids[202].

Here we show evidence suggesting a profound provision of amino acids by the gut microbiota. While we cannot determine the mechanisms behind this increased amino acid concentration, it is likely that the microbiome acts as a nutrient store, similar to the proposed amino acid harvesting mechanism proposed by Yamada *et al.*[110], as well as contributing amino acids via *de-novo* synthesis. So, while the DUMP assay is designed to look at changes in nutrient profile at one set point in time, it will be affected by all previously consumed food. Additionally, it has been shown in mice that microbial colonisation increases protein turnover as well as cell turnover (compared to germ-free), which would add to the luminal pool of protein/amino acids[408].

It would be interesting to see the ratio of L- to D- amino acids, as bacteria are able to synthesise and use both stereoisomers, mainly as cell wall constituents. It may be that a large proportion of the faecal amino acid pool is comprised of D-amino acids, which are not useful to the host, and for which the host may not have functional transporters. Unfortunately, as the two isomers are chemically identical, it is not possible to distinguish between them with mass-spectrometry.

4.4.4 Host contribution to faecal profile

One of the additional sources of luminal protein, other than diet and the microbiota, is from the host. This could be through active excretion of nutrients or extracellular proteins, shedding of membrane-bound proteins, or shedding of the intestinal cells.

4.4.4.1 Intestinal cell shedding

The intestine is a highly dynamic organ that has to withstand mechanical and environmental pressures[409]. In humans, the intestinal epithelium is completely renewed every 2-6 days[410].

The intestinal microbiota has also been shown to impact the rate of cell proliferation in mice[411,412] and in *Drosophila*[88], considered a proxy for cell turnover. One study also showed increased levels of cell and protein turnover in mice containing a microbiota by following the half-life of proteins containing a labelled lysine[408].

It has been shown that sterols make up approximately 4% of the lipids in the lipid membrane of adult female flies[413]. Arthropods like *Drosophila* lack some of the genes required for *De novo* cholesterol synthesis, and must obtain cholesterol directly or from plant sterols which can be converted to cholesterol within the intestine[414]. Cholesterol is added directly to the defined medium and there are no additional plant sources for conversion. Additionally, the intestinal microbial population is unable to synthesise cholesterol[415], so the cholesterol in our samples could derive only from the food, or from *Drosophila*. It should thus be a good indicator of the levels of cell shedding. Counter to previous conclusions that microbial colonisation increases cell turnover, we observed no difference in the levels of cholesterol with age, or with microbial status. It may be the case that there is increased cell proliferation without a resultant increase in the shedding of aged cells into the lumen. Certainly, mis-differentiation and dysplasia of the intestine is well characterised with age[49,77,92,362], and this may be accelerated upon microbial colonisation. Indeed, this could be an additional factor in the shortened lifespans observed in conventionally colonised compared to axenic flies.

Alternatively, or additionally, changes in the absorption dynamics of cholesterol may occur with age or microbial colonisation, impacting luminal cholesterol concentration and masking any indication of altered levels of cell shedding. It is also quite possible, that shed cells are subject to the digestive enzymes within the lumen, and the individual constituents may be re-absorbed.

4.4.4.2 Host proteins

The cells of the digestive tract have specific roles, within which they secrete proteins into the intestinal lumen. ECs secrete digestive enzymes, whilst EEs secrete hormones to regulate the gut in response to internal external stimuli. ECs, EEs and EBs also secrete AMPs in response to infection[416].

Additionally, a peritrophic matrix is produced by cells of the cardia which line and protect the midgut from mechanical and microbial stress. It must also allow passage of nutrients from the internal

lumen, to the enterocytes for absorption[417]. It is formed of proteins, glycoproteins, and chitin microfibrils within a matrix of proteoglycan which, as it is continually synthesised, is likely damaged by the passage of food, and may be an energy source for resident microbes, although, to my knowledge, this is not something that has been studied in *Drosophila*. Pathogenic bacteria are, however, able to degrade the peritrophic membrane of bees[418,419]. Mucins are another protein class which is likely to impact the faecal nutrient profile. They are abundant in the lungs and digestive tract of vertebrates[420,421], but *Drosophila* also contain mucin genes which are expressed in the gastrointestinal tract[343]. Mucins are either secreted and gel-forming, or are expressed on the outer membrane of cells, with a cleavable transmembrane domain. They also contain characteristic extended tandem-repeat regions of prolines, with serines and/or threonines[422].

It is not yet known whether age or colonisation with microbiota affects the expression of mucin genes, however, there was a significant increase in the faecal concentration of both proline and serine with age in the conventionally reared flies. The microbial contribution of both proline and serine was also significant – this may indicate an indirect microbial contribution, where the microbiota stimulates mucin synthesis or breakdown. There was a non-significant increase in both proline and serine with age in the faeces of sterile flies, and in threonine concentration with age in the sterile and conventional faeces.

Whilst the peritrophic matrix, and likely mucins, provide a barrier between the cells of the intestine and the microbial community residing within, *Drosophila* must still secrete AMPs to protect against infection[423,424].

Defensins and *Drosomycin* are cysteine-rich proteins[425]. Unfortunately, this assay did not detect cysteine so there is no indication of the direction of change, if any, with either age or colonisation by the gut microbiota. *Diptericin*, *Drosocin* and *metchnikowin* are other AMPs, however these are known to be rich in proline (and glycine in the case of *Drosocin* and *Diptericin*)[425]. Both proline and glycine increase significantly with age in the conventional faeces, but not the axenic faeces. Expression of AMPs is often found to be upregulated with age in conventionally reared flies, so it is likely that they are adding to the pool of detected amino acids.

Digestive enzymes are also actively secreted into the lumen to break down carbohydrates lipids and proteins. Due to the complexity of their natural food sources, *Drosophila* has a vast assay of digestive enzymes (up to 349 based from bioinformatics searches)[426]. These enzymes are spatially expressed[34,427,428], however they all end up in the lumen and, unless broken down and re-absorbed, will leave in the faeces, impacting the faecal profile.

As well as enzymes targeting carbohydrates proteins and lipids, 15 lysozyme genes have been identified within the genome of *Drosophila* which have no known immune functions. It is instead suggested that they may be used to digest peptidoglycan, a major component of bacterial cell walls, as they are expressed in the midgut[426,429]. Flies also have chitinases and glucanases which may help digest yeast. This ability to digest structural components of the microbiota may be beneficial in an immune response, but may also explain how *Drosophila* benefits nutrients from the microbiota, particularly in the case of *Issatchenkia orientalis* which rescues *Drosophila* lifespan under periods of undernutrition by concentration of the available amino acids[110]. This concentrated pool of protein would then be available to *Drosophila* upon digestion of the microbe.

The presence of microbes also influences the secretion of digestive enzymes. Association of *Drosophila* with *Lactobacillus plantarum* sustains *Drosophila* peptidase activity within the midgut, promoting protein digestion and thereby increasing the pool of available amino acids[202]. This sustained peptidase expression would also, however directly impact the faecal protein profile. Additionally, the presence of microbiota has been shown to upregulate the expression of digestive enzymes, including amylases, proteases and maltases[430]. This may also tie into the observation of much higher faecal amino acid levels in conventionally reared than axenic flies.

4.5 Conclusion

We have successfully developed an assay to assess changes in the faecal profile of flies. From this I observed increased amino acid deposition with advanced age. This appears to be a result of biological rather than chronological age, and occurs irrespective of microbial presence.

I have explored potential host-specific intrinsic causes behind the increased faecal amino acid concentration, from age-related changes in intestinal morphology and intestinal transit, to differential protein expression with age. I have also shown that the presence of an intestinal microbiota contributes large amounts of protein, either directly through their digestion or *De novo* synthesis, or indirectly by altering host metabolism and gene expression. Whilst I only looked at the faecal profile of macronutrients as proof of principle, there is scope for this assay to be used more broadly to look at micronutrients and metabolites. It would be interesting to repeat it with gnotobiotic flies, to understand the contribution of a single bacterial species, or to repeat it with specific disease models. One drawback of the assay is that it requires healthy flies with intact intestinal barriers, excluding an important group of individuals undergoing rapid decline. I have also

highlighted difficulties in analysing sugars, something we have put down to the different processing requirements of the analytes.

5 Age-related changes in the luminal/faecal nutrient profile impact ageing and age affects the expression of intestinal amino acid transporters

5.1 Introduction

5.1.1 Protein and ageing

Current literature suggests that high protein diets are detrimental to health and lifespan. Initial studies showed that dietary restriction (DR) - the reduction of nutrient intake without causing malnutrition - was a conserved and reproducible method of lifespan extension. Subsequent studies went further to show that macronutrient balance, specifically the protein-to-carbohydrate ratio is what is important in inducing this lifespan response (high carb, low protein)[118–121,243]. Additionally, the beneficial effects of protein restriction outweigh those of restricting the intake of carbohydrate or fats[431–433], and reductions in specific amino acids, as opposed to protein as a whole, is sufficient to influence health and ageing. Reduced methionine or branched-chain amino acid (BCAA) intake in *Drosophila*[124,128,434,435], or reduced methionine, branched-chain amino acid or tryptophan intake in mice[122,123,123,125,126,129,436,437] is sufficient to improve lifespan. Furthermore, the source and quality of protein appears to be an important factor[438,439], potentially due to the balance of amino acids within the protein source.

An idea which was accepted until recently is that DR improves lifespan by redirecting limiting resources (e.g. protein) away from reproduction and towards somatic maintenance[440,441]. This belief has been challenged, however, by findings that supplementation of DR diets with methionine can improve reproduction without a cost to lifespan[124,442]. Additionally, recent work has shown that matching the proportion of amino acids within the defined media for *Drosophila*, to the proportion of amino acids within translated proteins improves early life fitness and fecundity without impacting lifespan[224].

Despite the evidence to show lifespan reductions upon high-protein diets, there are calls to suggest an increase to the dietary protein intake recommendations for the elderly to prevent or reduce age-related muscle loss and sarcopenia[443].

Muscle mass is maintained through the balance of muscle growth and muscle loss. This balance appears to be lost in the elderly, with muscle loss occurring around 0.6 % per year from between the ages of 40 and 50[444]. This loss is exacerbated by periods of disuse, from as little as a reduction in step-count, to stays in hospital[445].

Studies have shown that increasing dietary protein concentration, particularly the concentration of essential amino acids (and leucine most highly), increases muscle growth[446–449]. They have also shown that older adults must consume higher amounts of protein to stimulate muscle growth in comparison to younger adults[450–452]. This has led to the idea of anabolic resistance[453–455]; a reduced stimulation of muscle protein synthesis in response to anabolic stimuli such as exercise and dietary protein[455], perhaps due to reductions in sensitivity to the stimuli and, from this, the suggestion of increased dietary protein intake in the elderly[443].

The observed increase in faecal amino acids with age in the absence of a microbial contribution shown in section 4.3.3, may suggest less efficient amino acid uptake by the intestine as a possible mechanism for reduced muscle mass in the elderly, and a counterargument to anabolic resistance. Perhaps higher quantities of protein must be consumed to stimulate muscle growth in the elderly, as a lower proportion is absorbed and bioavailable to the muscles. More research in this area is required, however existing studies performed in rats indicate that absorption is impaired with age[370–373]. Additionally, there is evidence showing changes to changes to the postprandial availability of amino acids within the circulatory system of ageing humans (see section 4.4.2).

Taken together with the known negative effects of high protein diets on lifespan and healthspan, this may suggest that the effect of protein consumption is context-dependent. Low protein diets early in life may confer later-life benefits, but increased protein intake in later years may be required to maintain good health. These increased protein requirements may be necessary to counteract a decline in intestinal function, systemic metabolic changes, or changes to the microbiota.

5.1.2 Amino acids and their role in disease

As well as being the building blocks of proteins, amino acids have other biologically important functions within the body. Many are precursors to other important metabolites, they can be used for energy, and can often act as chemical messengers in inter-cell communication. While the 20 proteinogenic amino acids are typically consumed as whole-protein, individual amino acids, and amino acid classes impact health and disease in varied ways. Any changes to the levels of these amino acids impact, not only protein nutrition but also these additional pathways, thereby impacting health and disease in several ways.

It is not possible to talk here about all the ways in which each amino acid may be implicated in ageing and disease. Some amino acids however have established roles in ageing or disease, whilst others have strong associations with the gut microbiota, so I will talk to some of these below.

5.1.2.1 Alanine

Alanine levels have been shown to decline with age in the plasma and muscle of mice[456,457], as well as in parasitoid wasps[458]. As one of 13 glucogenic amino acids, it can be converted to glucose through gluconeogenesis via pyruvate[459]. Additionally, it can be synthesised from pyruvate, as well as from branched-chain amino acids e.g. isoleucine, leucine and valine. It constitutes a high proportion of amino acids in many proteins, and when muscle proteins break down, it's released in high quantity into the bloodstream where it is taken up by the liver in mammals.

There is increasing evidence that alanine supplementation may be beneficial, particularly in terms of metabolic diseases such as insulin resistance/diabetes and obesity. Alanine infusion into hyperglycaemic dogs was shown to improve their metabolic responses to sugar[460]; when blood sugar was elevated, insulin secretion increased with minimal changes to glucagon levels and, when fasting, the addition of alanine stimulated glucagon release without affecting insulin levels. Further to this, culturing pancreatic beta cells in cell culture media supplemented with alanine, increased glucose metabolism and insulin secretion[461]. Additionally, in mice, increasing alanine was able to prevent obesity induction through a high-fat diet[462].

In the DUMP assay (chapter 4) I observed significantly higher levels of alanine in the faeces of aged conventionally reared flies, indicating increased luminal bioavailability of this amino acid with age. Additionally, while the 10-52 day increase was not significant, likely due to the variation observed in the 52-day samples, the concentration of alanine in the sterile faeces increased 500%, potentially indicating a reduced absorptive capacity for this amino acid with age. Such a reduction in alanine absorption may explain the declining levels observed in the plasma and muscle of mice with age, and the increase in insulin resistance which often accompanies age.

5.1.2.2 BCAAs

There is conflicting evidence for the impact of branched-chain amino acids (BCAAs), leucine, isoleucine and valine, on health and ageing. BCAAs have been shown to decrease with age in humans, linked to an increased proteolytic microbiome profile[463]. Interestingly, there is also data

linking reduced levels of microbial BCAA synthesis to development of sarcopenia in a cohort of patients with liver cirrhosis[464,465]. This suggests that, even on a matched diet, patients with this characteristic microbiome may have lower amino acid uptake[464] – a potential driver of sarcopenia. Additionally, supplementation of middle-aged mice with BCAAs improved survival, as well as cardiac and skeletal muscle function[466], and in *C. elegans*, reduction of BCAA catabolism through knockdown of BCAA transferase-1 increased lifespan and resulted in increased levels of circulating BCAAs[467].

In contrast to this, elevated levels of BCAAs have been implicated in insulin resistance and obesity in mice[432] and humans[468,469]. Additionally, infusion of a cocktail of 18 amino acids, including the BCAAs leucine, isoleucine and valine, resulted in decreased insulin sensitivity[470]. Elevated circulating BCAA levels have also been associated with increased mortality in mice[432], and dietary restriction of BCAAs in *Drosophila* has been shown to improve age-associated gut pathology and extend lifespan[434].

The gut bacterial population has been implicated in BCAA availability, as gut bacteria generally contain a higher proportion of BCAAs relative to other amino acids[344]. In addition, BCAA synthesis has been shown to be essential in some bacterial species. Age-related intestinal dysbiosis may result in the expansion of some of these species. Indeed, in the DUMP assay (chapter 4) we observed significant increases in the faecal concentrations of the BCAAs isoleucine, leucine and valine in conventional flies. Proportionally, however, the microbial contribution of these BCAAs does not increase the most with age, possibly indicating that BCAA-synthesis-dependent species are not undergoing the greatest population expansion. Alternatively, expansion of these populations may occur alongside populations which utilise a large proportion of these BCAAs; interestingly, catabolism of BCAAs results in the synthesis of precursors to branched-chain fatty acids which are involved in membrane biosynthesis of inflammation-causing gram-negative bacteria[463,471,472].

Additionally, the faecal BCAA concentration increased with age in the absence of a microbiota, though only significantly in the case of isoleucine which may implicate reduced absorption/increased excretion or shedding of these amino acids.

5.1.2.3 Glutamine/glutamate

5.1.2.3.1 Glutamine

Glutamine is the most abundant amino acid in human blood, skeletal muscle and the free amino acid pool[473], and is the precursor to many physiological molecules e.g. amino acids and nucleotides[474,475].

Interestingly, glutamine levels decrease with age in fission yeast, and supplementation of glutamine is sufficient to extend lifespan[476].

Glutamine is also a potent regulator of TOR signalling[477–481], which itself is widely implicated in ageing, but it has also been implicated in intestinal permeability. Deprivation reduces the expression of tight-junction proteins[482] whilst supplementation protects tight-junction formation in caco-2 cells upon methotrexate treatment[483]. In addition to this, glutamine functions as a signalling molecule modulating programmed cell death[484], and is involved in intestinal stem cell proliferation through the activity of several MAPKs, including JNK[485,486]. Glutamine deprivation in *Drosophila* reduces lifespan and stress tolerance[487], while glutamine supplementation rescues a progeria phenotype in mice, and protects against oxidative stress driven senescence[487].

Glutamine levels are also implicated in the development and progression of Alzheimer's disease[488,489]. Supplementation can reduce inflammation-induced neuronal cell cycle activation and Tau phosphorylation in an Alzheimer's disease mouse model[489].

Interestingly, data from the DUMP assay indicates a high contribution of glutamine by microbial colonisation (Table 4.2). Glutamine was one of the most abundant amino acids in the faeces of old and young conventional flies, but one of the least abundant in axenic flies at any age. Despite this, it increased significantly between young and old in both conventionally reared and axenic faeces. It was also one of the highest amino acids contributed by microbiota, with the largest increase in microbial contribution from young to old.

5.1.2.3.2 Glutamate

The glutamate-glutamine cycle is the biochemical process by which glutamate and glutamine can be recycled within cells[490–493]. This cycle is particularly important in the central nervous system where glutamate is the major excitatory neurotransmitter. Highlighting its importance, over 90% of neurons and 40% of synapses express glutamate receptors. The glutamate-glutamine cycle enables rapid synthesis and removal of glutamate, which can be excitotoxic[494,495].

During healthy ageing, the pool of neuronal glutamate available for signalling decreases along with thinning of grey matter within the brain[496]. The density of excitatory amino acid transporters (EAATs), responsible for clearing glutamate from the synaptic cleft and preventing excitotoxicity, also decreases with age[497]. Glutamate dysregulation also appears to contribute to the onset or progression of Alzheimer's disease, and downregulation of genes involved in excitatory neurotransmission in humans, and inhibition of glutamatergic neuron excitation increased lifespan in

C. elegans[498]. Interestingly, mice deficient in the cystine/glutamate antiporter system X_c^- (SLC7A11), which transports glutamate out of cells in exchange for cysteine, showed increased lifespan[499].

Unfortunately, given the importance of glutamate and glutamine in the CNS, there is little information surrounding the role of these amino acids in peripheral organs, particularly with regards to any age-related changes. This is likely an oversight. There is emerging evidence of the importance of glutamate and glutamatergic signalling in bone homeostasis[500–502], and in cancer[503–506]. It is likely to also have importance in different organ and disease systems. Indeed, in the DUMP assay (chapter 4) there is evidence to suggest an impact of both age and microbial colonisation on glutamate metabolism. There was trend towards increased luminal glutamate concentration with both age and microbial colonisation. Indeed, glutamate was at the highest concentration in both young and very old axenic faeces, and showed the second highest increase with age. Interestingly, there was also a trend towards increased glutamate concentration with age in conventional flies, however, the microbial contribution proportionally decreased with age. Combined with the observed trend for glutamine, it may be that the microbiota is converting luminal glutamate to glutamine in conventionally colonised flies.

5.1.2.4 Methionine

Methionine is an essential amino acid and must be consumed through diet. Interestingly though, it's been shown that restricting the consumption of methionine exclusively, is sufficient to extend lifespan in rats, mice, *C. elegans* and *Drosophila*[123,126,128,129,507,508], and that methionine consumption shortens the lifespan of the Argentinian ant[509]. Additionally, the expression of methioninase, which breaks down methionine into ammonia, α-Ketoglutarate and methanethiol, is sufficient to extend the lifespan and healthspan of *Drosophila*[435].

Methionine plays an important role as an initiator of protein synthesis in both eukaryotes and prokaryotes. It is also involved in several complex metabolic pathways including the methionine cycle.

In the methionine cycle, methionine is the precursor to s-adenosyl methionine (SAM), which has methyltransferase activity. SAM can be converted to s-adenosyl-homocysteine (SAH). During ageing, SAM levels increase. Counteracting this age-related increase in SAM levels has been shown to extend lifespan in *Drosophila*[510]. SAH levels also increase with age, and knockdown of SAH hydrolases in the brain or intestine of *Drosophila* reduces SAH levels and improves healthspan and lifespan[511]. Reduced levels of SAM also activate autophagy through the inhibition of mTORC1 activity[512].

Interestingly, methionine restriction has been shown to impact the microbiota in mice[513]. A 3-month regimen of methionine restriction reduced inflammatory cytokines in the serum of aged mice, reduced intestinal permeability, and reduced bacterial endotoxin lipopolysaccharide concentration in the serum of aged mice. It also altered the composition of the microbiota, increasing the proportion of Bacteroidetes and decreasing the proportion of Firmicutes, in comparison to aged mice without the 3-month methionine restriction, and increasing the level of the SCFA producing microbe *Prevotella*[513]. This study is not alone in showing a benefit to intestinal permeability, and an increased abundance of SCFA-producing bacteria upon methionine restriction, with Yang *et al.* finding an increased abundance of Bifidobacterium, Lactobacillus and Ruminococcus, among others[514].

The microbiota may also impact methionine absorption dynamics as the levels of methionine in the portal vein of germ-free mice were found to be higher than that of conventionally reared mice[515]. This is particularly interesting as methionine is an essential amino acid that must be provided through the diet, or through the microbiota, however, this data suggests that mice with a microbiota have a lower methionine intake, though it may also suggest altered metabolism and greater utilisation of methionine by the enterocytes. Perhaps some of the lifespan benefit of methionine restriction is a result of altered microbial metabolism.

Unfortunately, this was not corroborated in the DUMP assay. There was a trend towards increased faecal levels with age in both conventional and axenic flies (chapter 4), however it was one of the least abundant amino acids in both conditions, and at every age. This may suggest that the dietary methionine supplied in the defined media is too low. There is no indication from this data, however, that the microbiota is reducing methionine availability.

5.1.2.5 Tryptophan

Tryptophan is one of the essential amino acids which must be consumed through diet. Interestingly, data from the DUMP assay suggests a large microbial tryptophan contribution. It is the lowest amino acid in abundance in axenic faeces, and relatively high in abundance in conventional faeces. There was also an apparent trend towards increased concentrations with age in conventional faeces, although this did not reach significance. Nonetheless, the tryptophan microbially contributed did increase significantly with age, and tryptophan was one of the amino acids most highly contributed.

It may be rate limiting in protein synthesis, is an important precursor to serotonin and melatonin and is highly catabolised by the kynurenine pathway, which generates NAD and several neuroactive intermediates including kynurenic acid, picolinic acid and quinolinic acid[516,517].

Due to its role in serotonin metabolism, tryptophan is thought to be a key modulator of the gut-brain axis; a bidirectional communication system between the central nervous system and the gastrointestinal tract[518,519].

As well as its role in the brain, serotonin is involved in the control of intestinal motility, and secretion within the gut[520]. Indeed, in mammals, approximately 95% of total body serotonin is provided by the gut[521], and gut-colonising bacteria within the enterococcus and pseudomonas families have been shown to synthesise serotonin from tryptophan[522,523]. Additionally, tryptophan metabolism pathways have been shown, by *in-silico* analysis of bacterial genomes and gut microbiome data, to be enriched in five-gut associated phyla; Actinobacteria, Firmicutes, Bacteroidetes, Proteobacteria and fusobacteria[524]. On top of this, the levels of serotonin synthesis in the brains of germ-free mice has been correlated with the availability of tryptophan[525], so tryptophan-producing bacteria may play a pivotal role in brain health.

Interestingly, serum serotonin levels have recently been shown to decrease with age, with a study of Korean adults identifying a significant negative correlation between serum serotonin and age (serum serotonin decreased with age)[526], and reduced levels of serotonin have been implicated in the development and progression of Alzheimer's disease[516,527].

On-top of its role in serotonin metabolism, the ratio of tryptophan-to-kynurenine (high kynurenine to low tryptophan) has been implicated in several diseases, including inflammatory bowel syndrome and other inflammatory diseases, cancer and neurodegenerative diseases[516,517,528–531].

This ratio is also robustly associated with ageing in humans[531–541], and has been suggested to be a physiological age-related change, rather than a secondary development. It may also be a suitable biomarker of inflammaging[541]. Unfortunately, the serum tryptophan:kynurenine ratio in *Drosophila* has not been measured in an ageing context, however inhibition of the kynurenine pathway, and mutants with impaired kynurenine formation have been shown to increase lifespan in *Drosophila*[542,543]. Additionally, inhibition of the kynurenine pathway in *C. elegans* delays ageing and ageing-associated decline[544]. All evidence to suggest that this is a conserved contributor to ageing.

5.1.3 Amino acid transport

While the mechanism of amino acid transport has been well studied in mammalian systems, the same cannot be said in the case of *Drosophila* and other invertebrate models. Additionally, even in mammalian systems, the knowledge base surrounds transport kinetics under healthy physiological conditions, or in aminoaciduria's where one or more transporters are non-functional. Little-to-

nothing is known about the function or expression dynamics of amino acid transporters over the course of ageing, nor what role amino acid transport may play in the ageing process, despite the growing understanding role of the of amino acids and protein in health and disease.

Amino acid transporters (AATs) were initially classified into various systems based upon substrate specificity and transport mechanisms[545]. More recently, transmembrane transporters including AATs were classified into solute carrier (SLC) families based on sequence identity[546]. To date, 65 different SLC families have been identified, of which 11 contain AATs[547]. For a full review of the current understanding of AATs and their role in health and disease, see Kandasamy *et al.*[547].

As different tissues have different amino acid requirements, they often express a different subset of amino acid transporters. For simplicity, I will speak only to the amino acid transporters most highly expressed in the mammalian intestine. Even here, the apical and basolateral sides of the absorptive cells have distinct subsets of proteins for uptake from the lumen and release into the bloodstream.

Following a meal, the peptide chains which make up proteins are cleaved by membrane-anchored peptidases resulting in a large pool of di- and tri-peptides. These oligopeptides are absorbed primarily in enterocytes by PipT1 (SLC15A1), a proton-coupled oligopeptide transporter[548], and are rapidly cleaved into individual amino acids once within the cell. Individual amino acids also result from protein digestion, and several transporters with distinct affinities for different types of amino acids e.g. neutral, hydrophilic, hydrophobic, cationic or anionic transport these from the lumen, into cells.

The main mammalian small-intestinal transporters are shown in Figure 5.1. As intracellular amino acid concentrations are often higher than those in the extracellular fluid (even the lumen, between meals), many amino acids are co-transported with one or more Na^+, H^+ or Cl^- molecules, and/or the counter transport of K^+, to maintain transport against a concentration gradient[549]. A Na^+/K^+-ATPase, along with NHE2 (SLC9A2), which facilitates the exchange of Na^+ and H^+, help cells to maintain the transmembrane gradients for efficient amino acid uptake.

5.1.3.1 Intestinal transporters on the apical membrane

On the apical membrane ACE2 (B^0AT1 or SLC6A19) couples the intake of neutral amino acids with one Na^+. This allows the heterodimer of rBAT (SLC3A1) and $B^{0,+}$AT (SLC7A9) to exchange intracellular neutral amino acids with extracellular cationic amino acids.

Proline and glycine are co-transported with a proton (H^+) by PAT1 (SLC36A1), and proline is also transported by SIT1 (SLC6A20) with $2N^+$ and Cl^-.

Anionic amino acids are co-transported by EAAT3 (SLC1A1) alongside $3Na^+$ $1H^+$ and the counter-transport of K^+.

Whilst these are the best-characterised transporters with activity in the apical membrane of the intestine, other transporters may also be involved in uptake from the lumen. As an example ASCT2, an obligatory exchanger[550] whose role within the intestine is ill-defined, may compensate for a lack of glutamate transport in cases of dicarboxylic aminoaciduria[551,552], a rare autosomal recessive inherited disorder resulting from mutations within the EAAT3 protein[553,554].

5.1.3.2 Intestinal transporters on the basolateral membrane

On the basolateral membrane, amino acid exchangers and transporters act in concert to coordinate the bulk transport of amino acids, and to maintain intracellular amino acid homeostasis.

A heterodimer of 4F2hc (SLC3A2) and LAT2 (SLC7A8) which has broad specificity for neutral amino acids, excluding proline[555,556], exchanges influx of branched-chain or aromatic amino acids, for efflux of smaller neutral amino acids[555,557].

The amino acids taken up in this obligatory exchange can be released through the action of TAT1 (SLC16A10) which transports phenylalanine, tyrosine and tryptophan from the cell[558], or through the action of LAT4 (SLC43A2) which transports methionine, isoleucine, leucine, phenylalanine and valine from the cell[559]. Additionally, the heterodimer of 4F2hc and y+LAT1 (SLC7A7) couples influx of neutral amino acids and Na^+ with efflux of cationic amino acids[560–562]. The influx of neutral amino acids is balanced by the action of the 4F2hc/LAT2 exchange mechanism.

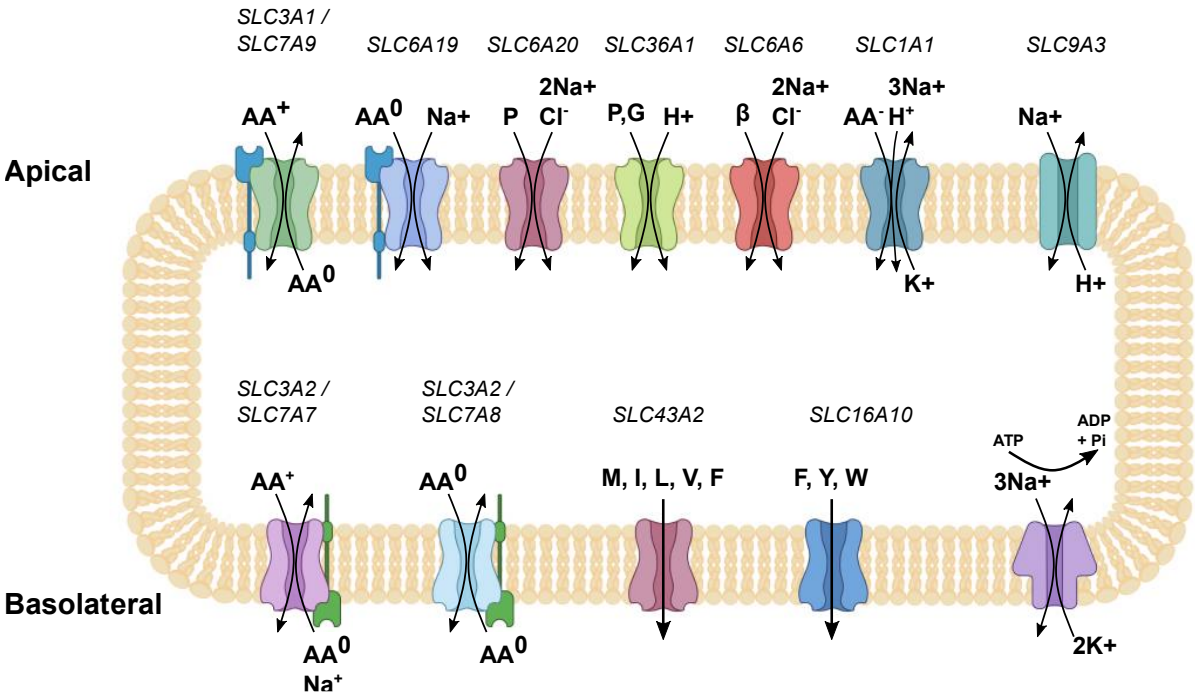

Figure 5.1 | Transporters involved in amino acid absorption in the human small intestine.

Figure adapted from Broer and Fairweather, 2019[551]. The apical membrane is shown at the top, with the basolateral membrane at the bottom. The transporters included are representative of the human small intestine, however the list is not exhaustive and other transporters are likely to be involved. Transporters are denoted by their solute-carrier denotation. Arrows indicate preferential direction of transport. Substrate groups are as follows: AA0 – neutral amino acids, AA+ - cationic amino acids, AA– - anionic amino acids, b – beta-amino acids. Individual amino acids are denoted by their one-letter symbol.

5.2 Aims and Objectives

Following the finding of increased amino acid concentrations in the faeces of aged conventional and axenic flies, I wanted to understand the impact of this increased luminal concentration on ageing. I set out to design a diet that reflected this increased luminal amino acid concentration observed with age, to assess potential impacts on lifespan and ageing phenotypes of conventional and axenic Canton-S flies.

Additionally, as increased faecal concentrations of amino acids were observed with age in the absence of a microbiota, I hypothesised that this may be due to reduced amino acid absorption through changing expression of amino acid transporters. I aimed to assay the expression of a panel of intestinal amino acid transporters with age, by RT-qPCR, and thereby see whether altered AAT expression may explain the changing faecal profile with age.

5.3 Results

5.3.1 Impact of increased intestinal amino acid levels on age and ageing phenotypes

5.3.1.1 Development of a microbial and age-associated amino acid diet

Following the results of the DUMP assay, where we observed increased levels of faecal amino acid with increased age, and with microbial composition, I wanted to understand whether the observed increases in luminal nutrient concentration would have an impact on lifespan or the microbiota.

To assess this, I used the DUMP data to design a diet that mimics the amino acid changes that occur with age in *Drosophila*. The new concentrations were calculated for each amino acid by;

Where F^{AA} is the concentration of each amino acid in the original defined medium. O^{AA} is the mean concentration of each amino acid in the 40-day conventional faeces, and Y^{AA} is the mean concentration of each amino acid in the 10-day conventional faeces.

The amino acid concentrations of this new diet, hereafter referred to as Aged AA media, are shown in Table 5.1 and the adjusted recipes for the amino acid stock solution and Aged AA media are shown in Table 5.2 and Table 5.3. An increased volume of Aged AA amino acid stock solution must be added per Litre of Aged AA media for the required concentration, as the Aged AA amino acid stock solution had to be made more dilute to ensure the amino acids remain in solution.

Table 5.1 | Concentration of amino acid in Aged AA media.

New concentrations are calculated by the difference in old and young conventional DUMP concentration, plus the original defined media amino acid concentration for each amino acid, based on the mean concentration of each amino acid at each time point.

Amino Acid	Concentration in food (mM)
Ala	18.82
Arg	14.66
Asn	14.29
Asp	10.08
Cys	2.82
Gln	17.42
Glu	34.66
Gly	15.57
His	10.65
Ile	13.83
Leu	20.22
Lys	10.98
Met	6.08
Phe	11.99
Pro	14.97
Ser	19.26
Thr	12.89
Trp	8.13
Tyr	11.39
Val	18.58

Table 5.2 | Amino acid and NaGlu stock solutions adjusted for the Aged AA diet.

Amino Acid		Grams per litre
Aged AA Amino acid stock solution:		
	Ala	9.24
	Arg	14.07
	Asn	10.41
	Asp	7.39
	Gln	14.03
	Gly	6.44
	His	9.11
	Lys	8.85
	Met	5.00
	Phe	10.91
	Pro	9.49

	Ser	11.15
	Thr	8.45
	Trp	9.15
	Val	11.99
NaGlu stock solution		
	NaGlu	820

Table 5.3 | Composition of Aged AA media.

The masses of amino acids added dry to buffer 1 are calculated by the difference in old and young conventional DUMP concentration, plus the original defined media amino acid concentration for each amino acid, based on the mean concentration of each amino acid at each time point. The volume of water is adjusted to make the total solution 1L, as an increased volume of the Aged AA stock solution is required to reach the required final amino acid concentration.

Ingredient		**Per litre**	
Buffer 1			
	Agar	20	g
	Sucrose	17.12	g
	Isoleucine	1.81	g
	Leucine	2.65	g
	Tyrosine	2.06	g
	Acetate Buffer	100	mL
	CaCl2	1	mL
	CuSO4	1	mL
	FeSO4	1	mL
	MgSO4	1	mL
	MnCl2	1	mL
	ZnSO4	1	mL
	Cholesterol	15	mL
	mQ H2O	624.5	mL
Buffer 2			
	Aged AA stock	181.5	mL
	Aged NaGlu stock	15.1	mL
	Cysteine	6.8	mL
	Sodium Folate	1	mL
	Vitamins	21	mL
	Other Nutrients	8	mL
	Propionic Acid	6	mL
	10% Nipagin	15	mL

5.3.1.2 Aged AA media shortens lifespan

To understand whether the Aged AA media, made to mimic the increase in luminal amino acid concentration observed with age in conventional flies, has an impact on lifespan, a lifespan was performed with wild-type Canton-S females on defined media and Aged AA media. I saw a significant and reproducible shortening of lifespan upon Aged AA treatment compared to defined media (Figure 5.2A, Log-rank $P < 0.0001$). This was the expected result due to the known lifespan effects of a high-protein diet.

I also looked at the proportion of flies losing intestinal barrier function at various points along the lifespan (Figure 5.2B). Unexpectedly, it appears that in early life (11-15 and 23 days), Aged AA flies maintain barrier function better than defined media flies (binomial test $P<0.01$ and $P<0.05$ respectively). This trend was reversed around the median lifespan of Aged AA flies, with an increased proportion of smurfs compared to defined media flies at 35-39 days of age (binomial test ($P<0.01$). At day 45, closer to the t50 of defined media flies there was no significant difference in the proportion of smurfs between the two diets.

As the increased luminal nutrient concentration may be impacting the microbiota, and thus the lifespan, and as the microbiota may be further increasing the luminal amino acid concentration, I also wanted to see whether this diet would affect the lifespan of axenic flies. This would provide a clearer understanding of whether the microbial amino acid concentration, or the increased luminal amino acid concentration we observed with age on the DUMP assay, is having a direct impact on lifespan. I was only able to perform one replicate of this lifespan, however there is a clear and significant reduction in lifespan on the Aged AA media, in comparison to the defined media (Figure 5.2C, Log-rank $P<0.0001$).

I also looked at the proportion of smurfs in axenic flies on the two diets (Figure 5.2D). Unlike with the conventional Canton-S flies, there were no significant differences, and no early-life benefit to the Aged AA flies in terms of the proportion of smurfs (Day 16 Binomial test $P>0.7$, Day 30 Binomial test $P>0.2$). By day 47, there is a significant increase in the proportion of Aged AA smurf flies, compared to defined media (Binomial test $P<0.01$).

It was also important to understand whether the new diet affected food consumption, as changing their eating habits to compensate for the increased protein would alter the luminal amino acid levels so they would no longer mimic the DUMP data. To assess feeding, I employed the capillary feeding assay. This usually uses a yeast-extract/sucrose solution, and measures consumption of this solution following a treatment, however as the defined media, and by extension the Aged AA media, can be

made as a liquid solution, without agar, I was able to directly measure consumption of the two diets of interest. Of note, the cholesterol fell out of solution, so this was omitted from both the liquid diets. Upon 48h of liquid feeding, there was no statistical difference in the amount of food consumed by the flies, although surprisingly there was a slight trend towards increased consumption of the Aged AA media, which would result in further inflated luminal amino acid levels.

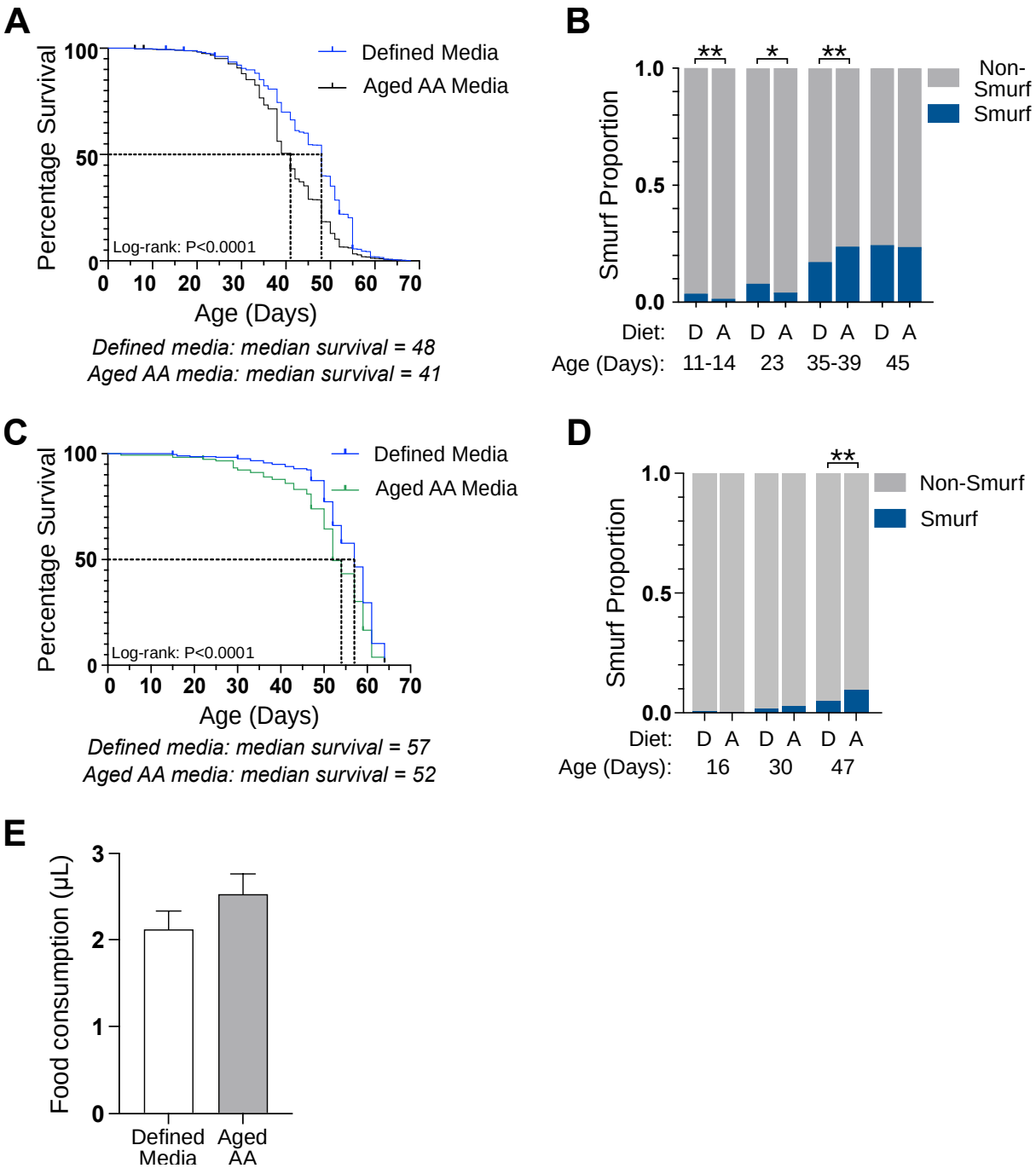

Figure 5.2 | Aged AA media reduced lifespan independent of microbial status.

(A) Combined lifespan of 2 replicates of conventionally colonised mated Canton-S females on defined media (blue) or Aged AA media (black). Dashed black line denotes the median survival. **(B)** proportion of smurf and non-smurf conventionally colonised mated Canton-S females on defined media or Aged AA media at 11-14, 23, 35-39 and 45 days of age. Combined results from two replicates at 11-14 and 35-39 days. Only one replicate of data at day 23 and day 45. **(C)** Lifespan of axenic mated Canton-S females on defined media (blue) or Aged AA media (green). Red arrows denote transition to new diet. Dashed black line denotes the median survival. **(D)** proportion of smurf and non-smurf axenic mated Canton-S females on defined media or Aged AA media at 16, 30 and 47 days. **(E)** 48 hour food consumption (mL) of groups of 10 mated female Canton-S flies fed liquid defined media or Aged AA media (omitting cholesterol) for 48 hours. **(A-D)** n > 240 flies per condition at day 1. BD+ denotes smurf flies with barrier dysfunction. BD- denotes non-smurf flies, without evidence of barrier dysfunction. Asterisks denote the result of **(B, D)** binomial tests, or **(E)** students t-test, where * P<0.05 and **P<0.01.

5.3.1.3 Aged AA media does not drive the expansion of internal bacteria

One hypothesis for the reduced lifespan of conventional flies on Aged AA media was that the increased luminal nutrient concentration would drive the expansion of the gut microbiota, and support a greater population of microbes. To test this, I measured the internal bacterial load of non-smurf Canton-S mated females at 10 and 38 days of age, and of smurfed flies at 38 days of age. Encouragingly, analysis by a 2-way Anova showed a significant main effect of age and intestinal barrier function (P<0.01) as we would expect, however, there was no significant variation in bacterial load between the two diets (2-way Anova P>0.4).

5.3.1.4 Aged AA media may impact the intestinal expression of Diptericin, but not Drosomycin in conventionally colonised, not axenic flies

Due to the reduction in lifespan, I also wanted to investigate the levels of immune activity by looking at the expression of two AMPs, DPT and DRS.

The expected increase in DPT expression was observed in the conventional flies on defined media (Figure 5.3A). I hypothesised that due to the reduced lifespan of Aged AA flies, that flies on this media would have a strong increase in the expression of DPT. Interestingly however, there was no age-related increase in the expression of DPT with age in conventional flies on the Aged AA media (Figure 5.3A), indicating that these flies aren't undergoing the expected level of immune activity through the IMD pathway.

I also assessed the expression of DPT in sterile Canton-S flies on defined or Aged AA media. I hypothesised that the levels of immune activation in these flies would be lower, as there is no microbiota to stimulate the immune pathways. Contrary to this, there is a trend towards increased DPT expression with age in flies on both diets (Figure 5.3F), although this was not significant in either case.

I also looked at the levels of DRS expression in conventional and sterile flies on both the defined and Aged AA media. No difference was observed between diets, or with age on either diet in the conventional or axenic flies.

5.3.1.5 A diet of aged AA media does not impact JAK-STAT pathway activity in comparison to defined media

I also wanted to look at the level of JAK-STAT pathway activity more directly. To do this, I quantified the expression of unpaired 3 (upd3), an activator of the JAK-STAT pathway. Chronic JAK-STAT activation is associated with several of the classical intestinal features of age-related decline[58].

In the conventionally reared flies, there was an apparent trend towards increased upd3 expression with age on both diets, although this difference was not significant. There was also no significant difference between the diets (Figure 5.3C). This trend was not maintained in the absence of a microbiota. Here we observed reduced variability with age in the axenic flies on defined media (F-test $P < 0.05$). There also appeared to be reduced variability with age in the axenic flies fed Aged AA, however this was not significant (F-test $P > 0.05$) (Figure 5.3H).

5.3.1.6 Age-related increase in JNK pathway activity is lost upon Aged AA feeding

JNK signalling in the intestine chronically increases with age, inducing over-proliferation of ISCs and apoptosis of ECs, eventually resulting in loss of intestinal integrity and dysplasia[49]. *Puckered* (*puc*) is a JNK phosphatase, expressed downstream of JNK and a readout of JNK activity. It also functions in a negative feedback loop, dephosphorylating basket, and turning off JNK activity (Figure 1.3B).

Whilst there was no significant effect of diet on the expression of *Puc* in conventional flies (*Figure* 5.3D, 2-way Anova main effect (Diet) $P = 0.88$) There was a significant increase in the levels of *puc* expression in conventional flies fed defined media (Figure 5.3D) which was not observed in the conventional flies fed Aged AA media (Figure 5.3D). There was also no significant increase in the expression of *puc* in axenic flies on either diet, although there did appear to be a trend towards increased expression with age (Figure 5.3I).

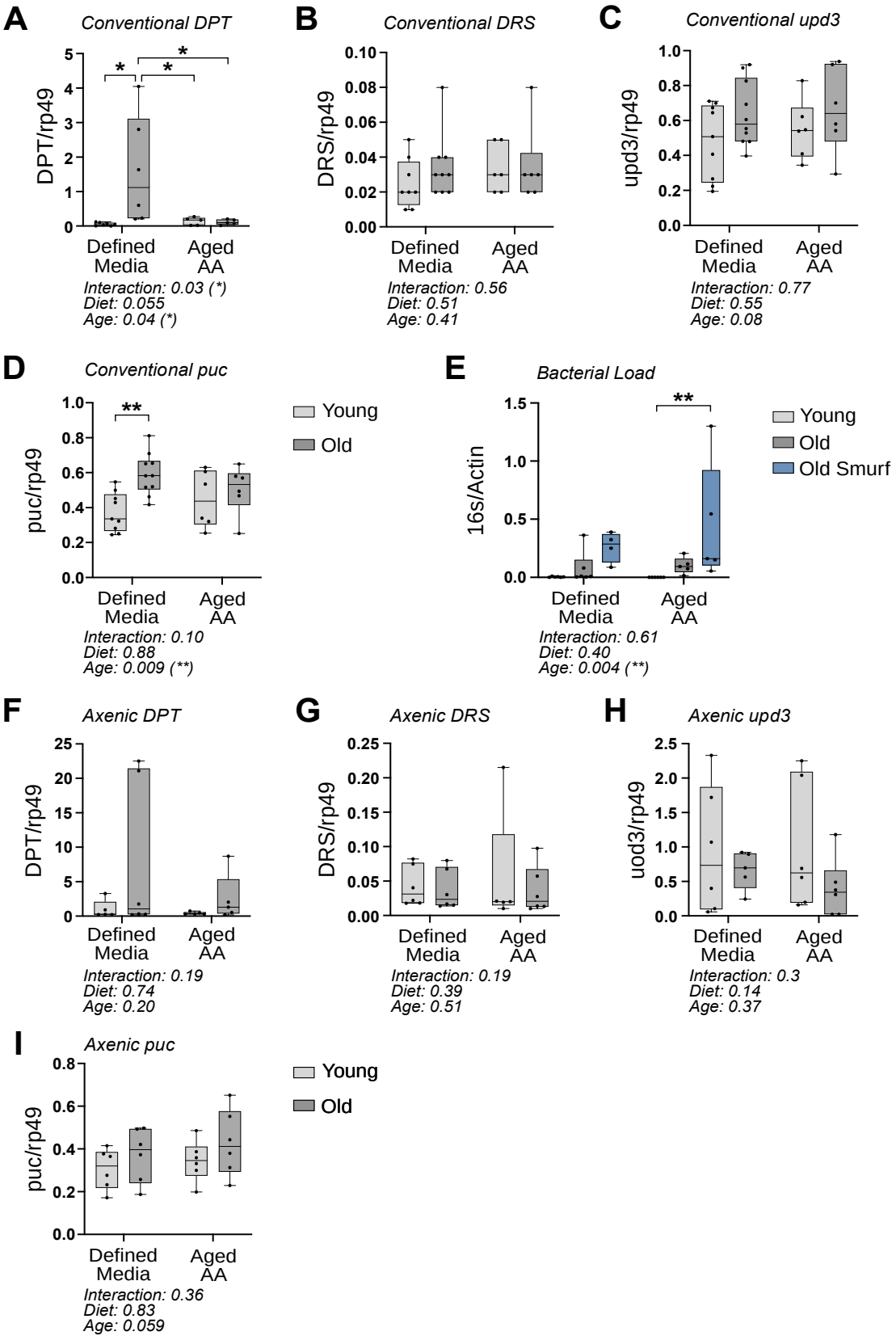

Figure 5.3 | Aged AA diet has a greater impact on the gene expression of conventionally reared than axenic flies

Intestinal gene expression levels in conventionally reared **(A-E)** and axenic **(F-I)** Canton-S flies on defined media or Aged AA media at young and old) timepoints. Expression of **(A)** diptericin (DPT), **(B)** Drosomycin (DRS), **(C)** unpaired 3 (upd3) and **(D)** puckered (puc) in the midgut of conventionally reared Canton-S females raised on defined and Aged AA media at young (10 days) and old (38 days) time-points, normalised to the expression of rp49. **(E)** Internal bacterial load of young (10 day), old (38 day) and old smurf (38 days with intestinal barrier dysfunction) mated female Canton-S females flies measured using universal primers for the 16s rRNA gene, normalised to the actin gene. Expression of **(F)** diptericin (DPT), **(G)** Drosomycin (DRS), **(H)** unpaired 3 (upd3) and **(I)** puckered (puc) in the midgut of conventionally reared Canton-S females raised on defined and Aged AA media at young (16 days) and old (45 days) time-points, normalised to the expression of rp49. n = 5-6 samples/age/condition. Box plots show the 25-75th percentiles and the median with the whiskers extending from min-max. Data from at least 5 flies/sample, with a minimum of 6 samples. Asterisks denote the result of a 2-way Anova with Tukeys multiple comparison test where * P<0.05, ** P<0.01, *** P<0.001. Results of 2-way anova displayed below each graph.

5.3.2 Age impacts the expression of several, but not all, intestinal amino acid transporters

From the DUMP assay, we observed increased levels of faecal amino acids in the absence of gut microbiota, implicating physiological changes within the fly itself.

One potential mechanism resulting in increased faecal concentrations of amino acids is a reduction in amino acid absorption or an increase in amino acid excretion. To determine whether this was a factor in the observed faecal concentrations, and in the absence of ways to directly measure absorption, I assayed the expression of amino acid transporters, required for amino acid absorption, as a proxy measurement.

First, I generated a list of validated and predicted *Drosophila* amino acid transporters; this list contained 48 genes, 21 of which were unnamed and likely poorly studied genes known by CG number alone. To select for genes which would show gut expression, I used the online databases FlyGutSeq (http://flygutseq.buchonlab.com) and FlyAtlas2 (https://flyatlas.gla.ac.uk/FlyAtlas2/index.html). Genes which showed homology to human intestinal amino acid transporters were also included (https://www.flyrnai.org/cgi-bin/DRSC_orthologs.pl). This generated a final list of 18 genes spanning 8 solute carrier families (Table 5.4).

For clarification, the top forward homolog relates to the human gene which is most homologous to the *Drosophila* gene. The top reverse homolog relates to whether the *Drosophila* gene is also most homologous to its top human ortholog. As an example, if genes A, B and C all share the top homolog X, however X is most homologous to B, then X will be the top forward and reverse homolog of B, but just the top homolog of A and C.

Table 5.4 | Final list of genes with validated or predicted amino acid transporter function and predicted intestinal expression.

Top human orthologs and weighted DIOPT[563] score determined from (https://www.flyrnai.org/cgi-bin/DRSC_orthologs.pl). The genes in grey font were not taken forward due to poor qPCR primers. 1All top orthologs, sharing the same weighted DIOPT score.

Drosophila **Gene**	**Annotation Symbol**	**Homologous human Solute carrier family**	**Top Human ortholog**	**Weighted DIOPT score**
Eaat1	CG3747	SLC1	SLC1A3	9.85
CD98hc	CG2791	SLC3	SLC3A2	5.82
CG1698	CG1698	SLC6	SLC6A16	3.94
Naat1	CG3252	SLC6	SLC6A16	3.94
CG13796	CG13796	SLC6	SLC6A14	3.94
Slimfast	CG11128	SLC7	SLC7A1	12.84
CG5535	CG5535	SLC7	SLC7A1	10.92
CG7255	CG7255	SLC7	SLC7A2	8.75
Minidiscs	CG3297	SLC7	SLC7A7	8.88
Sobremesa	CG9413	SLC7	SLC7A9	13.75
Kazachoc	CG5594	SLC12	SLC12A4	14.75
dmGlut	CG5305	SLC17	SLC17A3	5.89
CG43693	CG43693	SLC36	SLC36A1	9.9
Pathetic	CG3234	SLC36	SLC36A1-4[1]	5.92
CG8785	CG8785	SLC36	SLC36A4	7.87
CG1139	CG1139	SLC36	SLC36A1-4[1]	6.85
CG30394	CG30394	SLC38	SLC38A10	10.73

Primers were designed against all 18 genes, however 5 were rejected due to primer-dimer formation, or poor selectivity. The validated primers were then run against young (~10 day) and old (~40-day) wild-type Canton-S gut samples.

Of these 13 transporters, 6 from 4 of the families assayed showed age-related changes; the SLC1, SLC7, SLC17 and SLC36 families (Figure 5.4).

5.3.2.1 SLC1 family – Eaat1

Excitatory amino acid transporter 1 (Eaat1) is the best forward and reverse ortholog of human SLC1A3 (hEAAT1). It is also the best forward ortholog of SLC1A1 (EAAT3), SLC1A6 (EAAT4) and SLC1A7 (EAAT5), as well as SLC1A5 (ASCT2) and SLC1A4 (ASCT1) (orthologs identified using DIOPT[563]; https://www.flyrnai.org/cgi-bin/DRSC_orthologs.pl).

The EAATs transport L-glutamate with highest affinity, although L- and D- aspartate are also substrates. The amino acids are co-transported with 3 Na+ and one H+ and the counter-transport of

K+. The alanine, serine, cysteine threonine transporters (ASCT) 1 and 2 transport neutral amino acids. Indeed, despite the name, ASCT2 has the highest affinity for glutamine, and cysteine is a modulator not a substrate[564].

Despite dEaat1 being the top reverse ortholog of ASCT1 and ASCT2, its does not share the same substrates, indeed behaving as a typical Eaat1 transporter.

It is known to be highly expressed in the brain, however there is evidence to indicate a functional role in the intestine[565]. Here, I found that the levels of Eaat1 decrease with age (Figure 5.4A).

5.3.2.2 SLC17 family – dmGlut

Dietary and metabolic glutamate transporter (dmGlut) encodes a sodium-independent transmembrane glutamate transporter. It is the top forward and reverse ortholog of human SLC17A3 (hNPT4) (DIOPT[563]), however they only share a weighted score of 5.9 (DIOPT[563]).

hNTP4 is an organic anion transporter, shown to transport urate in the kidneys. Contrary to this, dmGLUT transports glutamate in a sodium independent manner. It shares the highest homology with *Drosophila* VGLUTs[566], however like Eaat1, it can be competitively inhibited by aspartate.

I observed a significantly decreased expression of dmGLUT with age in *Drosophila* intestines (Figure 5.4C).

5.3.2.3 SLC36 – CG8785, CG43693 and pathetic

The SLC36 family consists of four members; SLC36A1-4, or proton-coupled amino acid transporters (PAT) 1-4. They transport typically small amino acids e.g. alanine, proline and serine, as well as imino acids, although there are differences in the specific substrates of each of the PATs.

Three *Drosophila* proteins homologous to this family were assayed; CG8785 which had only SLC36A4 as its top forward ortholog, CG43693 which had the top forward orthologs SLC36A1 and SLC36A4, and pathetic (path) to which SLC36A1-4 were the top orthologs.

Path is expressed at the cell membrane and in endosomes[567]. In comparison to human PATs, the *Drosophila* transporter path, was found to have a much higher affinity for alanine (100 to 3000 fold higher) and lower transport capacity[568]. It also has a high affinity for glycine, but not proline[568]. Because of its low transport capacity, it is thought that path would not substantially contribute to amino acid flux. Instead it has been suggested that path acts as a transceptor; a transporter-like protein with a receptor function, to regulate signalling in response to metabolites independently of its transport capacity[567,569].

CG43693 has not been well studied. It has been shown to be expressed within the astrocytes of adult *Drosophila*[570,571], and within the ovaries[572,573], two regions with high amino acid requirements, however there is no information on its transport kinetics to date.

Like CG43693, CG8785 has not been well studied. It has been shown to be expressed within trachaea of *Drosophila*, and interestingly was shown to be upregulated following ingestion of Ecc15[250,574].

Here, I confirmed that both transporters are expressed within the adult *Drosophila* intestine. Interestingly, both were upregulated with age (Figure 5.4G and H). They both also showed increased variability with age (F-test $P<0.05$), however CG8785, orthologous to SLC36A4, showed no significant changes in expression with age.

5.3.2.4 SLC7 – slimfast and sobremesa

The SLC7 family is divided into two subgroups, the cationic amino acid transports (CAT family, SLC7A1-4), and the glycoprotein-associated amino acid transporters (the gpaAT family, SLC7A5-11). The gpaAT proteins are also the light/catalytic chains of the hetero(di)meric amino acid transporters (HAT), made up of one gpaAT, and a heavy chain protein from the SLC3 family.

SLC7A1 (CAT1) is the top forward ortholog of the *Drosophila* protein Slimfast (Slif). Slif also has the top reverse homology with SLC7A2 (CAT2) and SLC7A3 (CAT3) (DIOPT[563]). As suggested by their name, CATs transport cationic amino acids, although they appear to have a higher affinity for cationic amino acids with a long carbon backbone: arginine, lysine > ornithine > 2,4–diamino-n-butyric acid[575]. L-histidine is also a substrate for CATs at low pH[575,576].

Like the CATs, *Drosophila* Slif transports L-arginine[577], although to my knowledge, no one has tested its ability to transport lysine. Knockdown, or loss-of-function of Slif in the whole fly induces amino acid starvation phenotypes, and death of most animals at larval stages[577], and knockdown in just the fat-body results in developmental delay and growth defects in a TOR-dependent manner[577]. Expression has also been shown in the gut, indicating a role in nutrient uptake from the lumen.

Sobremesa (sbm) has the top forward and reverse homologs of SLC7A9 and SLC7A13 respectively. These are both gpaATs, however they appear to have different substrates. SLC7A9 ($b^{0,+}$AT), in a homodimer with SLC3A1 (rBAT), induces sodium independent, high-affinity transport of cationic and neutral amino acids through an obligatory exchange mechanism[578–581]. Under physiological conditions, cysteine and cationic amino acids are preferentially taken up, whereas neutral amino acids are transported outwards[578,580].

SLC7A13 (AGT1), when bound to SLC3 family members, transports glutamate and aspartate at high affinity in a sodium-independent manner[582]. It has been found to associate with SLC3A1 (rBAT) in mouse kidneys, and to transport cystine as well as glutamate and aspartate[583].

Sbm has been shown to form a heterodimer with the *Drosophila* SLC homolog CD98hc[584], and to be expressed in glia, neurons, and the gut[584]. The level of *Sbm* expression has been shown modulate the levels of ecdysone (a *Drosophila* growth hormone), potentially as a nutritional sensor[584]. The amino acid substrates of Sbm have not been elucidated, however as it shows a much higher homology to SLC7A9 than SLC7A13 (13.75 to 4.94 on DIOPT[563]), an assumption could be made that Sbm will likely exchange cationic and neutral amino acids and cysteine. Unfortunately, the primer I designed against CD98hc formed a primer-dimer so was not taken forward. It would be interesting to see if the levels of transcript for this protein of the heterodimer pair follows the same expression pattern with age, however, minidiscs (mnd) which also associates with CD98hc maintains consistent expression levels with age.

Gut expression of both *Slif* and *Sbm* was confirmed here, and interestingly both showed decreased levels of expression with age (Figure 5.4I and M). This was not seen across all the SLC7-homologous proteins, however, with the expression of *mnd*, CG7255 and CG5535 remaining consistent with age (Figure 5.4J, K and L).

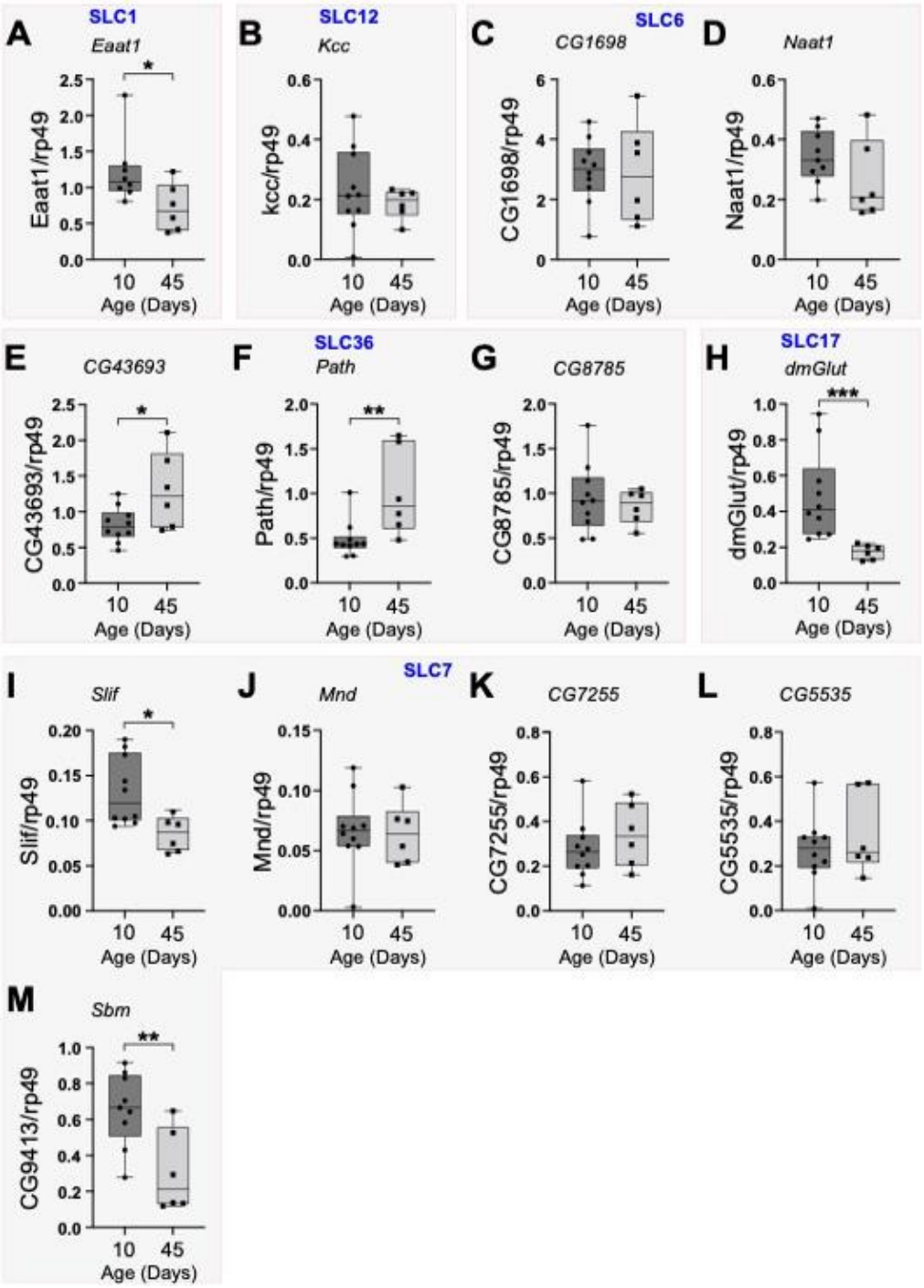

Figure 5.4 | Screen of intestinal amino acid transporter levels with age.

Levels of **(A)** Excitatory amino acid transporter 1 (Eaat1), **(B)** kazachoch (kcc,) **(C)** CG1698, **(D)** Nutrient amino acid transporter 1 (Naat1), **(E)** CG43693, **(F)** Pathetic (path), **(G)** CG8785, **(H)** dietary and metabolic glutamate transporter (dmGlut), **(I)** Slimfast (Slif), **(J)** minidiscs (mnd), **(K)** CG7255, **(L)** CG5535 and **(M)** sobremesa (sbm) at measured in Canton-S young (10 days) and old (40 days) midguts, normalised to the expression of rp49. n=8-10 samples at day 10, and n=5-6 at day 45. Boxes surround *Drosophila* orthologs of human solute carrier (SLC) families, denoted in blue. Box plots show the 25-75th percentiles and the median with the whiskers extending from min-max. Data from at least 5 flies/sample, with a minimum of 6 samples. Asterisks denote the results of 2-tailed unpaired T-test (normally-distributed data) or Mann-Whitney test (not-normally distributed data as calculated by the Shapiro-Wilk test; Eaat1 and path **(A,F)**), where * P<0.05, **P<0.01.

5.4 Discussion

5.4.1 Developed a diet that mimics the aged amino acid profile from DUMP assay

Following the result that luminal amino acid concentrations increase with age in conventionally reared and axenic flies, I wanted to design a diet to mimic this increased luminal amino acid concentration to assess whether there is a physiological impact.

Several possible ways to calculate the amino acid content of this new diet were considered. Firstly, the addition of the difference in amino acid concentration from the old and young axenic faeces to the original defined media amino acid concentrations. This would have enabled us to assess the impact of purely age-driven increases in luminal amino acid concentrations. In the future, such a diet should be used for bacterial growth experiments, for a better understanding of whether these age-related amino acid changes may lead to microbial community alterations.

Secondly, the addition of the amino acid concentrations from old conventional flies, to the original defined media amino acid concentrations. As we aimed to assess the impact of the luminal amino acid concentrations observed in old flies, however, we considered that this would not be the best representation. It would result in higher luminal amino acid levels than desired as the young conventional flies are egesting a level of amino acids which are not completely absorbed. Instead, we designed the diet based on the difference in amino acid concentration of old and young conventional flies, added to the concentration of amino acids in the original diet. This considers the observed amino acid concentration egested by young flies.

I was able to assay the effect of this diet on both conventionally colonised, and axenic flies. It should be noted that the luminal amino acid concentration of conventionally reared flies on this new diet is likely increased further by the microbial presence, as was seen in the DUMP assay (Chapter 4), although no data was collected to confirm this.

The results from the DUMP assay could also be used to assess the impact of the increased amino acids resulting from microbial colonisation, through the subtraction of axenic from conventional amino acid concentrations. I did not design experimental diets for this, however such an experiment would be best performed on axenic flies, to separate the impact on the fly from any further microbial impact.

5.4.2 Age-specific impact of high-protein diets

As detailed in the introduction, high-protein diets robustly shorten lifespan. This study corroborates the findings of this previous research. Interestingly, as this high protein diet was designed to mimic the increased luminal amino acid concentrations observed with age in conventionally reared flies, this data may suggest that the increased luminal amino acid availability with age is contributing to, or even driving, the increased mortality observed with age. Additionally, the size of the lifespan reduction was increased in conventional flies, in comparison to axenic flies (14.6 % reduction to 9.6 % reduction in median lifespan), suggesting that the presence of microbiota, or perhaps the additional amino acids that are contributed by the microbiota, is additive.

As mentioned, despite the evidence to suggest a detrimental effect of high-protein diets, there are currently calls to increase the daily recommended protein intake for elderly persons to prevent or reduce age-related muscle loss and sarcopenia[443]. With the suggestion that higher quantities of protein consumption is required to stimulate muscle growth in the elderly, as a lower proportion is absorbed and bioavailable to the muscles.

Indeed, certain amino acid transporters (AATs) assayed here were found to reduce in intestinal expression with age. This is further evidence to suggest that a reduced proportion of dietary amino acids are being absorbed, resulting in lower blood amino acid concentrations which are less able to stimulate muscle synthesis. Not all the AATs decreased in expression with age though, with many appearing stable, and some increasing with age – potentially indicative of compensatory mechanisms. It should also be mentioned that the expression of these transporters was assayed from whole-midgut samples, providing an average of the expression along the gut. The midgut can be split into additional regions based upon function[33,34], and the expression of these amino acids may be modulated differently with age in these different regions.

Here, there was no apparent late-life benefit to a high-protein diet. This may be due to additive detrimental effects of a lifelong diet of high protein, where the benefit may only be derived in old age. Diet is a key determinant of microbiota composition, and high protein diets have been shown to promote an increase in proteolytic bacteria and enrichment of opportunistic pathogenic bacteria that may promote gut dysbiosis and increase the risk of severe gastrointestinal disease[585]. This may be a contributor to the shortened lifespan of full-lifespan high-protein diets, however as the lifespan of sterile axenic flies on this diet was also reduced, it cannot be the full explanation.

Surprisingly, it appeared that there was an early-life benefit to this Aged AA high protein diet as a lower proportion of smurf flies was observed up to day 23 before the lifespans diverge. This was

consistent between replicates at days 11-14, where I had data from multiple replicates, but it should be noted that only one replicate at day 23 is used to draw this conclusion. Such a benefit may be due to sufficient protein resources bypassing the trade-off between reproduction and somatic maintenance; egg laying declines by 20 days post-mating[586]. This suggests that the impact of dietary protein content is context or age-dependent and that a more nuanced approach should perhaps be employed when studying its organismal impact.

It would be interesting to compare the lifespans of sterile flies fed defined or Aged AA media for the full lifespan, to those fed Aged AA only until the lifespans diverge, or only after day 40 to better understand the age-specific impact of high-protein diets. Day 40 is suggested as there was not a significant change in luminal amino acid concentration in the axenic DUMP cohort at this timepoint (Section 4.3.3.1).

5.4.3 Aged AA diet doesn't drive microbial expansion or inflammation

One hypothesis for why increased amino acids contribute to the increased mortality of flies on the Aged AA diet, was that increased luminal nutrients enable the expansion of the intestinal microbiota.

The composition of the intestinal microbiota is moulded by diet, and changes in nutrient load have been shown to affect microbial load in an *in vitro* gut model[587]. There is also data to show that increased caloric intake induces rapid changes in the microbial composition[588]. Additionally, one study has shown that the addition of all 20 amino acids to the diet of cows improved the growth rate of mixed ruminal bacteria[589]. It should be noted however that this was in comparison to incubation with single amino acids, or ammonium sulphate as a nitrogen source and so does not explore whether increasing amino acid concentrations enables greater bacterial growth. The most compelling evidence to suggest that the increased amino acid content of the new diet used here may impact microbial load is that nitrogen is a limiting factor for microbial growth in the large intestines of mammals, and reduced dietary protein in mice leads to a reduction in faecal bacterial concentrations[590]. The authors did not assess the impact of increased protein concentrations on microbial load or composition, however, and whether nitrogen availability is a limiting factor in *Drosophila* is unknown.

Interestingly, the utilisation preferences of the 20 amino acids vary between different bacterial species[591], and members of the Bacteriodetes phylum consume nitrogen in the large intestine more readily than other commensal microbial species[590]. This may suggest that certain bacterial species will benefit from the altered amino acid proportions, if not the increase in total amino acids, of the new diet.

While there was no apparent effect of diet on microbial load here, there was more variability in the bacterial load of old smurfs on the Aged AA media. There are many possible reasons why the increased amino acid content does not lead to the expansion of the microbiota. Firstly, nitrogen may not be a limiting factor within the *Drosophila* intestine, so the microbes would derive limited benefit from the excess amino acids. Secondly, the sugar content within the diet is low, which may impact bacterial growth rates. Thirdly, the fly may be adept at regulating the levels of microbes inhabiting/passing through the digestive tract when healthy. Finally, whilst there is no apparent difference to the microbial load, there may be changes to the composition of the underlying microbial community. If this is a shift towards opportunistic pathobionts this could explain the reduced lifespan. Such a shift would, however, be expected to result in increased immune activation which was not observed.

Whether or not the new diet alters the microbiota, the Aged AA diet did not induce increased inflammation, in terms of DRS and DPT expression. Flies on Aged AA media actually had lower DPT expression with age than those on defined media, and did not show the expected trend towards increased DPT expression with age. This may indicate that the Aged AA media is preventing age-related immune activation. There may even be a suggestion that the microbiota is preventing in some way the expected increase in DPT with age, as there is a trend towards increased DPT with age in the sterile flies.

5.4.4 Aged AA diet does not induce stress-response pathway activation

5.4.4.1 JNK pathway

As mentioned in the introduction (section 1.3.2.2.1), chronic JNK expression has been associated with the age-related deterioration of the intestinal epithelium, and age-related decline[49]. Despite this, it doesn't appear to be a driver of the shortened lifespan of flies on Aged AA media. It is possible that chronic JNK activity was induced at an earlier timepoint in Aged AA flies and reached a plateau; the old samples were collected at 38 days, and the proportion of smurf flies on the two diets levels out by 45 days of age. JNK expression is likely to increase prior to observing an increased smurf phenotype, as this increased activity drives stem cell proliferation and dysbiosis which contributes to loss of intestinal barrier function[77,92]. Additionally, as *Puc* acts in a negative feedback loop, acting as a readout of JNK activity, whilst also dephosphorylating basket and turning off JNK activity, there may be a maximum level of activity.

5.4.4.2 JAK-STAT pathway

As detailed in the introduction (section 1.3.2.2.2), chronic activation of JAK-STAT signalling in the aged *Drosophila* gut is associated with age-related metaplasia, microbial dysbiosis and functional decline of the gastrointestinal tract[58]. We saw a trend towards increased *upd3* (a readout of JAK-STAT activation) with age on both diets here, although this did not reach significance, corroborating evidence that this pathway is activated with age.

Some of this chronic activation may be due to the presence of senescent cells. In mammalian systems, the JAK pathway is more active in senescent than non-senescent cells, and inhibition of JAK-STAT signalling suppresses the senescence-associated secretory phenotype and alleviates age-related dysfunction[59–61]. While there have been extensive studies of cellular senescence in mammalian systems, there is little evidence of senescence in invertebrate models, although it has been shown that activation of the RAS oncogene with mitochondrial dysfunction can induce senescence in the *Drosophila* imaginal epithelium[62–64].

As there was no difference in the levels of *upd3* on either diet, this data suggests that changes in JAK-STAT signalling are not mediating the reduction in longevity of flies on Aged AA media. There was increased variability in the levels of *upd3* in young axenic than old axenic flies, on both diets. This may be suggestive of differences in cell proliferation amongst the samples, with reduced variability with age potentially indicative of cell cycle arrest.

5.4.5 Amino acid-induced activation of the mTOR pathway may explain the shortened lifespan

Given that the JNK and JAK-STAT pathways have not been implicated in the shortened lifespan observed on the Aged AA diet, it is likely that the lifespan effects are driven by changes to mTOR pathway activity. As mentioned in the introduction (section 1.3.3.2.2), the mTOR pathway has been widely implicated in ageing and the response to dietary restriction. It regulates cell growth and metabolism and is influenced by a variety of signals including amino acid abundance. To test whether mTORC1 activation is driving this shortened lifespan, flies on this diet could be fed on rapamycin, an mTORC1 inhibitor. If the shortened lifespan is reversed upon rapamycin feeding, this would indicate that mTORC1 is involved in the shortened lifespan. Additionally, observation of higher levels of phosphorylated-S6K by western blot would indicate increased mTORC1 activity.

Amino acids are activators of mTORC1 which drives cells towards growth. When active, mTORC1 suppresses autophagy which is one mechanism by which mTOR activity has been suggested to lead to reduced lifespan. Autophagy is beneficial during ageing as it recycles mis-folded proteins and

protein aggregates known to accumulate with age. Induction of autophagy promotes longevity[172,173,182], partially through maintenance of stem cell and intestinal homeostasis[592].

mTOR activity also suppresses apoptosis[593]. mTOR activation may exacerbate the effects of chronic JNK activation by inhibiting JNK-induced apoptosis. Interestingly, if JNK-induced apoptosis is suppressed in tumour cells, JNK signalling promotes both autonomous and non-autonomous cell proliferation, as well as tumour cell invasiveness[594]. TOR-mediated suppression of autophagy and apoptosis may accelerate tumour malignancy with age. It may also accelerate cell dysplasia, as JNK signalling will continue to promote ISC proliferation to fill the niche of damaged cells, however (damaged) ECs will not be removed. This may help explain why flies on Aged AA media have a shortened lifespan with the same level of JNK activity.

5.4.6 Age-related changes uncovered in the expression of intestinal amino acid transporters

As I observed significant changes in the luminal concentration of amino acids with age in both conventionally colonised and sterile flies, I wanted to investigate whether this could be driven by changes in amino acid absorption and, in the absence of ways to directly measure absorption, by the expression of amino acid transporters.

Amino acid transporters in humans and other mammalian systems have been relatively well characterised in terms of their kinetics and mechanisms.

There is an agricultural interest in the mechanisms of amino acid uptake, with the view to optimising weight gain in livestock. Amino acid transporters have also been well studied in terms of genetic diseases such as hartnup disease where uptake of nonpolar amino acids is affected, or other aminoaciduria's. There is also interest in the role of amino acid transporters in neuronal health and neuronal signalling, particularly as many amino acids participate in the production of neurotransmitters. Additionally, there is increasing interest in the role of some amino acid transporters as 'tranceptors', sensing and signalling amino acid availability, as well as transporting amino acid substrates[595]. In *Drosophila*, one amino acid transporter, Slimfast, has gained attention acting as a nutritional sensor[577], relaying information from the fat body to the brain to control growth.

Despite the research surrounding amino acid transport, their role in initial amino acid uptake appears largely ignored. This seems to me to be an oversight, as the metabolic and signalling functions of amino acids, on top of their nutritional benefit, rely on them reaching systemic

circulation. If we don't know if or when changes in amino acid uptake occur, it is impossible to then pinpoint the cause of certain metabolic effects in disease, or ageing.

There is evidence to suggest reduced amino acid uptake in older organisms. Absorption of tyrosine, phenylalanine and tryptophan was reduced in jejunal rings from 24-month old rats[371]. Additionally, a lower affinity for the transport of glycine, alanine and lysine was reported in another study of older rats[372,373]. This data is not consistent, however, with a different study showing lower K_t values for tryptophan and phenylalanine in 6-month compared with 12- and 27- month rats[596]. The different approaches used may explain some of the inconsistencies between these studies. Even the method of normalising or expressing the data may have an impact on qualitative differences between studies. Uptake is often expressed per intestinal weight or surface area which does not take into account potential age-associated differences[337].

Nevertheless, there are indications that amino acid uptake may be impaired with age. Indeed, I observed both increased and decreased expression of certain amino acid transporters, indicating that meaningful changes are occurring with age. These changes were not limited to transporters of specific amino acids, or transporters within particular families, indicating that the changes will impact the uptake of a broad range of amino acids.

On top of this, there is evidence suggesting changes in the expression of amino acid transporters in the muscle of the elderly[597,598]. Additionally, single nucleotide polymorphisms (SNP) in certain amino acid transporters have been associated with parameters of physical performance in the elderly. One SNP in SLC38A9 showed a survival advantage before the age of 90, but a survival disadvantage later, possibly due to antagonistic pleiotropic effects of the SNP, and remodelling of AA metabolism[599]. The top *Drosophila* ortholog to SLC38A9 (CG32081 – DIOPT[563]) did not show gut expression in FlyAtlas2, and only had a moderate weighted score in DIOPT[563] of 2.78, so primers were not made against this gene.

The suggestion that a SNP within an amino acid transporter may impact longevity, does however highlight the need for a greater understanding regarding the role of amino acid transport in ageing. Additionally, while the original study was investigating single nucleotide polymorphisms for their effect on muscles during age, the same SNP may also impact nutritional uptake if the transporter is expressed in the intestine.

5.4.6.1 Glutamate transport may be functionally relevant to ageing

Two of the transporters significantly downregulated with age transport glutamate as their primary substrate; Eaat1 and dmGlut. This may suggest that reduced systemic glutamate, or increased luminal glutamate would have a functional impact on ageing. Interestingly, glutamate was present at the highest concentration (compared to the other amino acids) in axenic faeces, and showed the second largest increase in concentration with age (Table 4.1).

Glutamate is among one of the most abundant amino acids in proteins and serves as a critical energy source for the intestine[600]. It is an important signalling molecule[601], and the major excitatory neurotransmitter of the central nervous system[602]. Excess levels of glutamate in the brain can excite cells to their death in a process referred to as "excitotoxicity"[602].

Within the intestine, increased luminal glutamate concentration has been shown to stimulate stem cell proliferation in *Drosophila*[565] and in mice[603] through activation of a metabotropic glutamate receptor (mGluR). Interestingly, high doses of glutamate in mice led to a loss of intestinal barrier function[603], whilst the highest doses (5 – 10 % L-Glu) tested by Deng *et al.* in *Drosophila* led to impaired ISC proliferation[565]. A reduced, and more physiologically relevant, glutamate concentration of 1 % however, lead to increased levels of ISC proliferation[565]. Reduced expression of intestinal glutamate receptors would lead to an increased luminal glutamate concentration. Along with increased JNK and JAK-STAT signalling, this may be sufficient to stimulate ISC proliferation, potentially driving intestinal proliferative deregulation. Additionally, L-glutamate can also be a product of the commensal microbiota[89,604], which may contribute higher amounts with age. Indeed, faecal glutamate concentrations increased with age in both conventional and axenic flies (chapter 4). It is possible that the reduced glutamate transporter expression observed here is to compensate for this increased luminal supply of glutamate however, it may further activate the mGluR receptor, driving stem cell proliferation.

5.4.6.2 Amino acid transceptor signalling may contribute to ageing

There is an increasing understanding that some amino acid transporters do not simply transport their substrates, but also act as receptors; relaying signals of nutrient availability into cells.

The concept of amino acid transceptors was first discovered in yeast, with the discovery that the amino acid permease Gap1 is necessary for cAMP-independent activation of the protein kinase A (PKA) pathway upon re-introduction of amino acid to starved cells[605]. In the case of Gap1, its signalling requires a ligand-induced conformational change which may occur during the transport cycle, but doesn't require the complete transport cycle[606]. Since this discovery, multiple transceptors

have been identified in a wide range of organisms, although they have been most widely studied in yeast; Mep2, a yeast ammonium transceptor activates PKA activity[607], and impacts filamentation of yeast[608,609]. Mek homologues in other fungal species have also been implicated in filamentation, likely through a similar mechanism[610,611]. Other nutrients activate transceptors in yeast, e.g. Pho84 for phosphate[612–614], sul1 and 2 for sulphate[615]. Additionally, a nitrate transporter in *Arabidopsis* is suggested to have a direct nitrate-sensing role, affecting root architecture[616]

In *Drosophila*, Path affects growth independent of its amino acid transport function, indicating receptor activity[568]. Similarly, human PAT1 and PAT4 appear to have transceptor activity, promoting cell proliferation and mTORC1 activity[617] in cultured cells[618,619], and when overexpressed in flies[618]. Additionally, the closely related SNAT2 activates mTORC1 activity even when transporting a non-metabolisable substrate, promoting the proliferation of the MCF7 breast cancer cell line, and L6 myotubes[620]. Unfortunately, no *Drosophila* SNAT homologues were used in this assay. There was no data to suggest gut expression of the top SNAT2 ortholog, Mahogany, and the primer designed for CG30394 – another SNAT2 ortholog, formed primer-dimers and was not taken forward.

The mosquito homologue of *Slimfast*, an AAT shown to act as an amino acid sensor in the mTORC pathway in the *Drosophila* fatbody[577], has been shown to act as a transceptor in mosquitos[621]. *Sobremesa*, a *Drosophila* AAT in the same SLC family as *Slimfast* has also been shown to modulate the levels of ecdysone, potentially as an amino acid sensor[584]. Even human Eaat1 has been proposed to have receptor signalling activity, phosphorylating ERK1/2 and activating ERK/MEK cascades in rat astrocytes in response to substrate and transported but unmetabolizable analogs[622].

Whether the transceptor activity of these transporters has a direct link to ageing remains to be determined. It is possible however that transceptor activation of mTORC1, independent of, and on top of, amino acid influx, helps to elevate mTORC pathway during the course of ageing.

5.5 Conclusion

Here I developed a diet reflecting the increased luminal amino acid concentration observed with age in conventionally reared flies. This reduced the lifespan of wild-type flies, but may show early-life benefits, indicating that the increased luminal protein content may not be entirely deleterious, although these benefits likely occur before the increased luminal amino acid concentration typically occurs.

I also showed that the expression of various predicted or confirmed, intestinally expressed amino acid transporters is altered during the course of ageing. This may impact the activity of several pathways, including mTORC1 which can be activated by amino acids, as well as systemic nutrition and metabolism, and is something that warrants additional attention.

6 Expression of the amino acid transporter Slimfast impacts longevity

6.1 Introduction

The results from the intestinal amino acid transporter screen showed a reduction in the levels of the cationic amino acid transporter *slimfast* with age. Additionally, the faecal concentrations of both cationic amino acids; arginine and lysine, increased significantly with age in axenic flies, indicating that this is a feature of ageing. The faecal concentration of arginine also increased significantly with age in conventionally reared flies, although this was not true of lysine.

6.1.1 Slimfast

Slimfast is a cationic amino acid transporter expressed at the plasma membrane[623]. It was first studied in the *Drosophila* larval fat body in the context of nutrient signalling where it was found to be important for the regulation of growth, with knockdown of *Slif* in the fat body sufficient to reduce larval growth[577]. Interestingly, this response was specific to knockdown in the larval fat body, with no growth defect observed upon knockdown in the imaginal discs, salivary gland or larval gut[577].

Whilst a systemic growth defect was not observed upon knockdown in wing imaginal discs, closer examination showed that these cells were able to respond to amino acid deprivation, resulting from *Slif* knockdown, in a cell-autonomous manner through the mTOR pathway[577].

The systemic growth defect upon fat-body knockdown also relied upon the inhibition of local mTOR activity[577,624]; overexpression of *dS6K*, a major downstream component of the mTOR pathway, partially rescued the growth defects of fat-body *Slif* knockdown. Additionally, expression of a dominant-negative *Drosophila* TOR, or inhibition of mTOR activation through co-overexpression of *TSC1* and *TSC2* resulted in similar developmental delay and growth defects reminiscent of *Slif* downregulation[577].

Localisation of Slif to the membrane is in part controlled through the mTOR pathway. Activation of TOR, through overexpression of *Rheb*, increases surface levels of Slif whereas inhibition of mTOR activity through the expression of *TSC1* and *TSC2* decreases Slif levels[623]. At least some of this dynamic control is mediated through endocytosis recycling Slif from the membrane, as disruption of endocytosis increases the levels of Slif at the cell surface. This disruption of endocytosis also prevents the reduction of membrane-bound Slif observed upon mTOR inhibition[623].

The systemic growth defect upon fat-body knockdown also leads to the downregulation of PI3K signalling in peripheral tissues. Insulin signalling activates the PI3K pathway, however no changes were observed in the expression of *dilps* required to bind and activate the insulin receptor and activate PI3K. The authors instead hypothesised that the *Drosophila* acid-labile subunit (*dALS*) ortholog expressed in the fat body and median neurosecretory cells in the larval brain, may be the direct target of the fat-body nutrient sensor mechanism[577], as it is downregulated in starvation conditions, and strongly downregulated in the fat-body upon *Slif* knockdown. dALS has subsequently been shown to interact with dilps to regulate growth and metabolism[625]. Interestingly, the human homolog of *Slimfast*; *SLC7A1* or cationic amino acid transporter 1 (*CAT1*), is not responsive to insulin in human muscle cells, indicating that Slimfast likely acts upstream of the IIS-AMPK pathway[626].

In mammals, circulating insulin growth factor 1 (IGF-1) is bound in a ternary complex with IGF binding partners (IGF-BPs) and an acid labile subunit (ALS)[305,627]. Depletion of dALS may prevent circulation of dilps, which may enable the systemic signal resulting from local *Slif* knockdown.

Slif also has an apparent role in the control of food intake. Knockdown in particular neuronal populations reduces food intake in the presence of a protein-rich diet[628]. Interestingly, even fat-body knockdown of *Slif* impacts feeding behaviour, reducing a 'protein intake-induced feeding inhibition' effect[629], likely through nutrient sensor mechanisms explored by Colombini *et al.*[577].

CAT1 has also been linked to mTORC1 signalling[630]. N-methyl-D-aspartate (NMDA) receptor activation leads to reductions in the cell-surface levels of CAT1 and the closely related CAT3, as well as reductions in mTORC1 activity. This reduction in mTOR function was shown to be mediated by the reduction in CAT1 and CAT3 levels, as knockdown or *CAT1* and *CAT3* blocks the influence of NMDA receptor activation on mTOR function[630]. Amino acid availability also mediates *CAT1* expression, with reduced availability resulting in upregulation of *CAT1* via a mechanism which requires eIF2α phosphorylation[631–635]. eIF2α is downstream of mTORC1. Additionally, it has been shown that CAT1 has a TATA-less promotor and instead contains an amino acid response element[633].

CAT1 also has a role in immune function. It is important for T-cell function and is upregulated in CD8+ T-cells as well as naïve and memory T-cells[636], although It doesn't appear to have an important role in macrophages[637]. Increased expression of *CAT1* and arginine availability has also been implicated in the progression of rheumatoid arthritis in mice[638], an auto-immune disease[639].

Mis-regulation of *CAT1* expression has also been implicated in ovarian cancer, where it is negatively associated with relapse-free survival[640], as well as in the progression of colorectal cancer[641–643],

liver[644–646] and breast cancer[647]. Interestingly, expression of *CAT1* is decreased in a cell model of amyotrophic lateral sclerosis[648], indicating that the levels of CAT1 must be tightly regulated to maintain health. Any potential role in ageing, however, is yet to be uncovered.

6.1.2 Cationic amino acids and ageing

6.1.2.1 Arginine

Arginine is considered a semi-essential amino acid, essential in children and conditionally essential in adults[649,650]. It constitutes 5-7 % of dietary amino acid intake, and about 60 % of this is absorbed during the first pass effect in the splanchnic bed[651].

Arginine is important in immunity, stimulating the proliferation of young human T-lymphocytes to aid in wound healing[652,653]. Additionally, oral administration of L- but not D-arginine has also been shown to enhance the healing rate of acetic acid-induced ulcers in a dose-dependent manner, and arginine has been shown to improve intestinal immunity phenotypes in mice, through modulation of the microbiota[654]. Increasing luminal arginine through supplementation or through a reduction in arginase-1 which catalyses the conversion of arginine to ornithine, also increases the diversity of murine microbiota[655,656]. Bacteroidetes[655] and Bifidobacterium[654] species in particular were shown to be enhanced. These microbial changes improve the phenotypes of colitis[655] and enhance pulmonary antimicrobial activities[654]. They also improve intestinal damage and intestinal immunity promoted by increased intestinal production of Secretory IgA in the lumen[654]. The benefits can also be passed on through faecal transplantation from mice with arginine supplementation to mice without, whereas antibiotic treatment prevents the improved colitis phenotypes[655,657].

In terms of ageing, reduced levels of arginine (as well as lysine) are associated with ageing skeletal muscle, and it has been suggested that interventions aimed at maintaining skeletal levels of the cationic amino acids may be useful therapeutic strategies to minimise biological ageing[658]. Arginine has also been shown to have a positive association with species lifespan in a study of fibroblasts taken from a range of primate, avian and rodent species[659], and supplementation of arginine increases the lifespan of *C. elegans*[660].

Despite the evidence for the beneficial effects of arginine, arginine supplementation has been shown to increase the secretion of IGF-1[661] and growth hormone[662], which have both been shown to have pro-ageing functions in mice[663–665]. It also stimulates mTOR pathway activity[666] which is associated with ageing. Increased arginine levels have been found in aged *Drosophila*[667], and

supplementation of 20mM arginine to the diet of *Drosophila* leads to a lifespan reduction, and reduced fecundity[668]. This highlights the need for caution when assessing the impact of interventions, such as arginine supplementation, on lifespan effects as well as health outcomes occurring over the relative-short-term. Additionally, the mode of supplementation (intravenous or dietary), as well as the source (pure L-arginine, animal protein or plant protein), may impact health outcomes.

6.1.2.2 Lysine

The other major cationic amino acid, lysine, is essential throughout all stages of life. A higher proportion of absorbed lysine makes it into the bloodstream in comparison to arginine, with approximately 30 % taken up in first-pass metabolism.

Lysine has been shown to have a positive association with species lifespan in a study of fibroblasts taken from a range of primate, avian and rodent species[659], and to protect caco-2 intestinal epithelial cells from oxidative stress[669]. High lysine levels have also been linked to longevity in humans[670] and, as mentioned, levels of lysine in murine skeletal muscle decrease with age[658]. Additionally, during ageing, the intracellular levels of 16 proteinogenic amino acids decrease in yeast; glutamine to the greatest extent, followed by glutamate and lysine[671]. Lysine also decreases with age in *C. elegans*[672–674], and it has been shown that lysine supplementation yields small increases in lifespan[660]

The impact of changes in luminal lysine availability has not been studied in humans. Supplementation of lysine and methionine in lambs has, however, been shown to protect intestinal mucosa and integrity, enhance innate immune responses, as well as alter microbial composition[675], similarly to the aforementioned response to increased luminal arginine. Lysine restriction also impacts the intestinal microbial composition of pigs[676] and reduces the expression of SLC7 transporters[676]. The impact of lysine on human microbiota has not been studied, however, so whether this is a conserved response is unknown.

6.2 Aims and objectives

In this chapter, I set out to understand whether changes to the expression of intestinal *Slimfast* have a physiological impact on ageing. I previously observed a reduced expression of this transporter with age. I also previously observed an increased faecal concentration of its substrates, arginine and lysine, with age in sterile flies, as well as a significantly increased concentration of arginine in conventional flies.

The expression of amino acid transporters has not previously been investigated in an ageing context, I wanted to understand the functional significance of this downregulation.

My first aim was to characterise the expression of *Slif* under physiological conditions in the intestine. I first assessed the expression of *Slif* along the length of the gastrointestinal tract. I also assessed the expression of *Slif* with age in axenic flies to understand whether the presence of microbiota impacts the intestinal expression of this transporter.

I next wanted to understand the impact of modulating intestinal *Slif* expression. For this, I utilised the *UAS-gal4* GeneSwitch system to knockdown or increase the expression of *Slif*, and observed the impact of these manipulations on lifespan, loss of intestinal barrier, gene expression and internal bacterial load.

Additionally, I investigated potential links between *Slif* expression and the age-related activation of JNK, JAK-stat and IMD pathways.

6.3 Results

6.3.1 The amino acid transporter *Slimfast* is expressed along the *Drosophila* midgut

Following the finding that *Slimfast* expression decreases with age in conventionally colonised Canton-S intestines (Figure 6.1A), I wanted to characterise its expression pattern along the midgut. For this, I assayed the levels of *Slimfast* in regional gut samples of Canton-S females previously collected within the lab, as well as in whole-gut samples from the same cohort of flies. *Slif* showed expression along the length of the midgut, with much lower expression observed in the hindgut (Figure 6.1C-E). This is consistent with the view that the midgut is the centre of absorption.

By contrast to the original assay showing reduced *Slif* expression with age, it did not decrease significantly in the whole-gut samples from this collection (Figure 6.1C), although there was a significant reduction in expression upon loss of intestinal barrier function. I initially considered that this may be due to differences in the gut regions included, with the whole-gut samples including the crop, hindgut and tubules, which were absent in the midgut samples used in the original screen. However, counter to expectations, expression increased in the anterior midgut and posterior midgut between 10 and 40 days of age (Figure 6.1D, E). Another clear difference between the two sample sets was the diet of the flies. The original samples were collected from flies raised on defined media for adulthood (Figure 6.1A) whereas the whole gut and regional samples were collected from flies fed cornmeal media for their full lives (Figure 6.1C-F). This may indicate that diet is an important determinant of amino acid transporter expression levels.

As well as understanding whether there was regional *Slif* expression, I wanted to understand whether the changes in *Slif* expression observed with age in the original screen were a result of microbial colonisation and the changing microbial dynamics with age. Particularly considering the differences in *Slif* expression with age on flies raised on different diets. To do this I assayed the levels of *Slif* in the midgut (cardia to midgut-hindgut junction) of sterile Canton-S mated females raised on sterile defined media through adulthood. Here there was a significant reduction in the levels of *Slif* expression with age (Figure 6.1B), indicating that this change is independent of the microbiota and consistent between flies reared on the same diet.

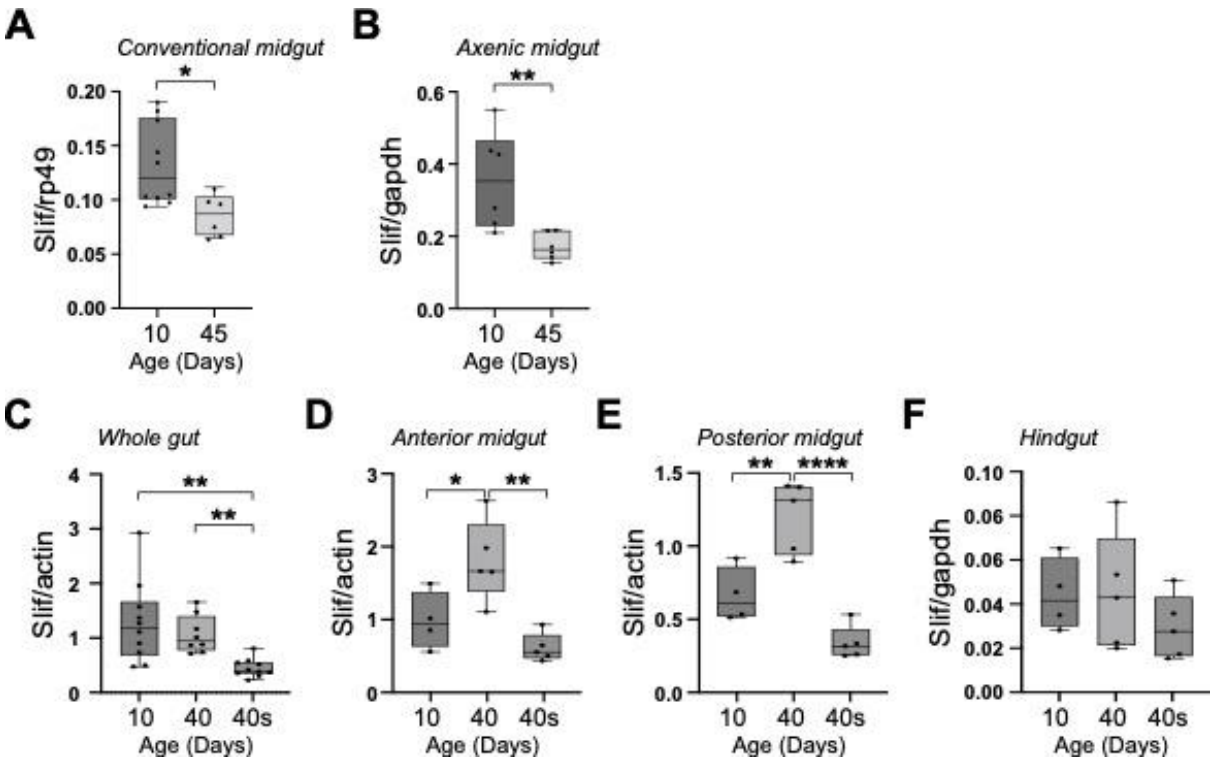

Figure 6.1 | Expression of Slimfast in Canton-S *Drosophila* intestines.

(A) Expression of Slif, normalised to rp49, in the midgut of conventionally colonised Canton-S females at 10 and 45 days of age. Graph taken from Figure 5.4. **(B)** Expression of Slif, normalised to gapdh, in the midgut of axenic Canton-S females at 10 and 45 days of age. **(C-F)** Expression of Slif in conventionally colonised Canton-S samples from flies raised on cornmeal medium, at 10 and 40 days of age, including also 40 day old smurf flies (40s). Samples as follows: **(C)** whole-gut (crop, cardia, midgut, tubules and hindgut), **(D)** anterior midgut, **(E)** posterior midgut and **(F)** hindgut. **(A,B)** n = 6-10 samples of 5 midguts (cardia to midgut-hindgut junction). **(C)** n=8-10 samples of 3 whole guts. **(D-F)** n = 4-5 samples containing 20 gut regions per sample. Box plots show the 25-75th percentiles and the median with the whiskers extending from min-max. Asterisks denote the result of **(A, B)** an unpaired t-test, **(C)** a kruskal-wallis test, or **(D-F)** a one-way Anova, where * P<0.05, ** P<0.01, *** P<0.001, **** P<0.0001.

6.3.2 *Slif* knockdown increases survival, potentially as a DR mimic

Following the observation of decreased intestinal *Slif* expression with age, I knocked down its expression specifically in the intestine for the full lifespan, using the *Slif-antisense line (Slif^{anti})*, developed by Colombani *et al.*[577], and the TIGS driver to determine whether the age-reduction in *Slif* expression is functionally relevant.

While I expected to see a lifespan reduction upon *Slif* knockdown, I instead observed a reproducible lifespan extension compared to the vehicle control (Figure 6.2A).

I reasoned that the reduced expression of *Slif* observed in late life is not well replicated by a full-life knockdown. To better recapitulate physiological conditions, and understand the impact of the later

life reduction in *Slimfast* expression, I knocked intestinal *Slif* expression down from day 35 (Figure 6.2A). The lifespan effect of this late-life knockdown was less clear, with two replicates showing a 1-day extension or matched median lifespan compared to control, and another replicate showing a decreased survival. The reasons for this variability in response are undetermined, however, they may occur from differences in the point of lifespan of knockdown initiation. Instead of initiating knockdown at the same chronological time, knocking *Slif* down at the same point within the lifespan i.e. T_{90} may have provided a more reproducible effect.

These results do however indicate that the lifespan benefit of full-life *Slimfast* knockdown occurs early in life, or requires full-life intervention. One possible reason for this is that the control *Slif* levels are already decreasing by the time of late-life knockdown, resulting in a decreased difference in expression between control and knockdown groups.

Interestingly, when looking at the proportions of smurf flies in these three groups, the lifespan effect was not reflected. Indeed there was a small but significant increase in the proportion of smurfs in the knockdown flies at 13 days (Figure 6.2B), but no other timepoint showed any difference in smurf proportions between control and knockdown groups.

To ensure that the lifespan effect is not an artefact from changes to food consumption, I performed a capillary feeding (cafe) assay, and found no observable difference in the volume of food consumed (unpaired t-test, $P>0.05$, Figure 6.2C).

I considered that changes to intestinal *Slif* expression may alter the luminal nutrient availability, and thus impact the intestinal microbial community. Indeed, it appears that intestinal *Slif* knockdown may result in a reduction in microbial load. This was only significant however following loss of intestinal barrier function (Figure 6.2D, Ordinary one-way Anova, $P < 0.01$). This reduced bacterial load does not appear to impact the expression of AMPs (Figure 6.2E, F); there were no significant changes to the expression of either DRS or DPT upon *Slif* knockdown. A trend towards increased DPT levels was observed with age regardless of Slif expression, although there was a lot of variability, and this was not significant.

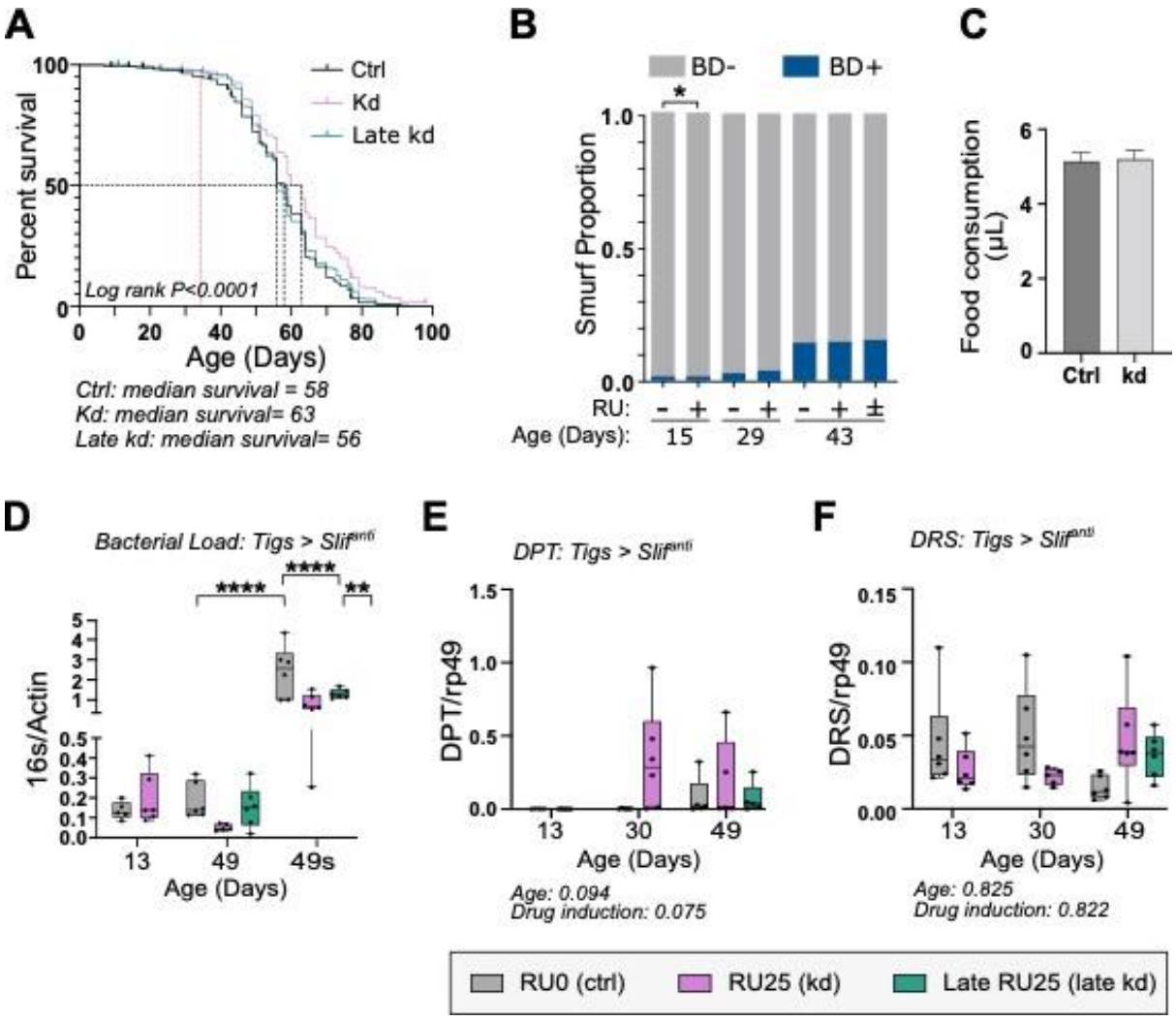

Figure 6.2 | Full-life intestinal Slif knockdown increased lifespan, without impacting intestinal barrier dysfunction or readouts of immune activity.

(A) Combined lifespan of 2 replicates of conventionally colonised mated TIGS > Slif^{anti} females on defined media with ethanol (control (ctrl); black), 25uM Ru-486 (knockdown (kd); yellow), or transferred from ethanol to RU-486 at 35 days of age (Late knockdown; green). Dashed black line denotes the median survival. Dashed red line denotes the transfer from ethanol media to RU media. **(B)** Proportion of smurf and non-smurf conventionally colonised TIGS > Slif^{anti} flies on control defined media or RU treated media to induce Slif knockdown, at 15, 29 and 43 days of age. BD+ denotes smurf flies with barrier dysfunction. BD- denotes non-smurf flies, without evidence of barrier dysfunction. Addition of RU, and subsequent knockdown denoted by +. Late knockdown flies denoted by ±. **(C)** 48 hour food consumption (uL) of groups of 10 mated TIGS>Slif^{anti} flies fed liquid defined media (omitting cholesterol) for 48 hours, following 72h induction of knockdown or control treatment. **(D)** Internal bacterial load of 13 day, 49 day and 49 days smurf (49S) mated female TIGS>Slif^{anti} females, with and without induction of intestinal Slif knockdown, and with late induction of Slif knockdown (green). Internal bacterial load measured using universal primers for the 16s rRNA gene, normalised to the actin gene. Expression of **(E)** diptericin (DPT) and **(F)** Drosomycin (DRS) in the midgut of conventionally reared TIGS>Slifanti with and without induction of knockdown, at 13, 30 and 49 days of age (flies with late induction of knockdown also shown at 49 days. Knockdown induced at 35 days of age). Expression normalised to the expression of rp49. (A-B) n > 285 flies per condition, per replicate at day 1. **(C)** n=6 vials of 10 flies per condition. **(D-F)** n=5-6 samples of **(D)** genomic DNA from 5 flies or **(E,F)** cDNA from 5 midguts (cardia to midgut-hindgut junction) per age per condition. Bar graphs show the mean ± SEM. Box plots show the 25-75th percentiles and the median with the whiskers extending from min-max. Asterisks denote the result of **(B)**

binomial tests, **(C)** unpaired t-test, **(D)** Ordinary one-way Anova with Holm Sidaks multiple comparison, or **(E, F)** 2-way Anova with Tukeys multiple comparisons, where * P<0.05, **P<0.01, ***P<0.001 and ****P<0.0001. **(D-F)** multiple comparisons within treatment groups, or between groups at one age only are shown. Result of 2-way Anova main source of variation is shown below each graph.

6.3.3 Inconsistent effect of *Slif* overexpression

Another way of assessing the physiological effect of age-reduced intestinal *Slif* expression is to observe the effects of intestinal *Slif* overexpression.

As with the *Slif* knockdown, I overexpressed *Slimfast* for the full adult lifespan. From the two replicates of this lifespan performed, I gained inconsistent results, with one replicate showing a lifespan-shortening effect of 4 days upon *Slif* overexpression (Figure 6.3A), and the other showing a lifespan extension of 3 days (Figure 6.3C). Induction of late-life *Slif* overexpression was included in the second replicate with the aim of rescuing just the age-related decrease in *Slif*. This late-life overexpression matched the lifespan of the full-life overexpression (Figure 6.3C).

The proportion of smurfs for each replicate matched the lifespan effect observed, with higher smurf proportions for the overexpression lifespan of replicate 1, although this was not significant (Figure 6.3B). Replicate 2, which showed an increased lifespan upon *Slif* overexpression, had a lower proportion of smurfs in both the full-lifespan overexpression, and late-life overexpression lifespans, compared to the control (Figure 6.3D).

The reasons for the differences observed between replicates is unclear. Both lifespans were maintained on defined media, which reduced batch variation in the original paper[222]. They were run at different times of the year, something which has been shown to impact lifespan previously[677]. Replicate 1 was begun in October, and replicate 2 began in May the following year. There were issues with the temperature of the lab when replicate 1 was started, with temperatures reaching up to 29°C. Whilst the flies were maintained in an incubator held at 25°C, they were exposed to the laboratory temperature during sorting, and flipping. Whilst this was fixed by December, such variation in temperature could conceivably alter the flies' response to genetic perturbation, as well as the level of knockdown. If this is indeed the reason for the variability between the replicates, it may indicate a role of *Slimfast* in heatshock response.

All the genomic DNA and cDNA samples were collected from replicate 2, which was performed under more stable conditions so, unless mentioned, all data corresponds to the lifespan and smurf proportions from this replicate.

Despite the reduced proportion of smurfs upon *Slif* overexpression, there was no difference between control or either of the overexpression groups, on bacterial load, or AMP expression (2-way anova, Figure 6.3E, F and G). I observed a significant increase in the expression of *Diptericin* with age (2-way Anova, Figure 6.3F), and stable *Drosomycin* levels with age (Figure 6.3G) in both the control and *Slif* overexpression groups, indicating the typical immune activation pathways are activated.

There was a trend towards increased bacterial load with age and loss of intestinal barrier function, although this was only significant in the late-RU group (Figure 6.3A, Ordinary one-way Anova, $P < 0.01$), but there was no difference in the bacterial load of *Eaat1* knockdown flies compared to ethanol controls.

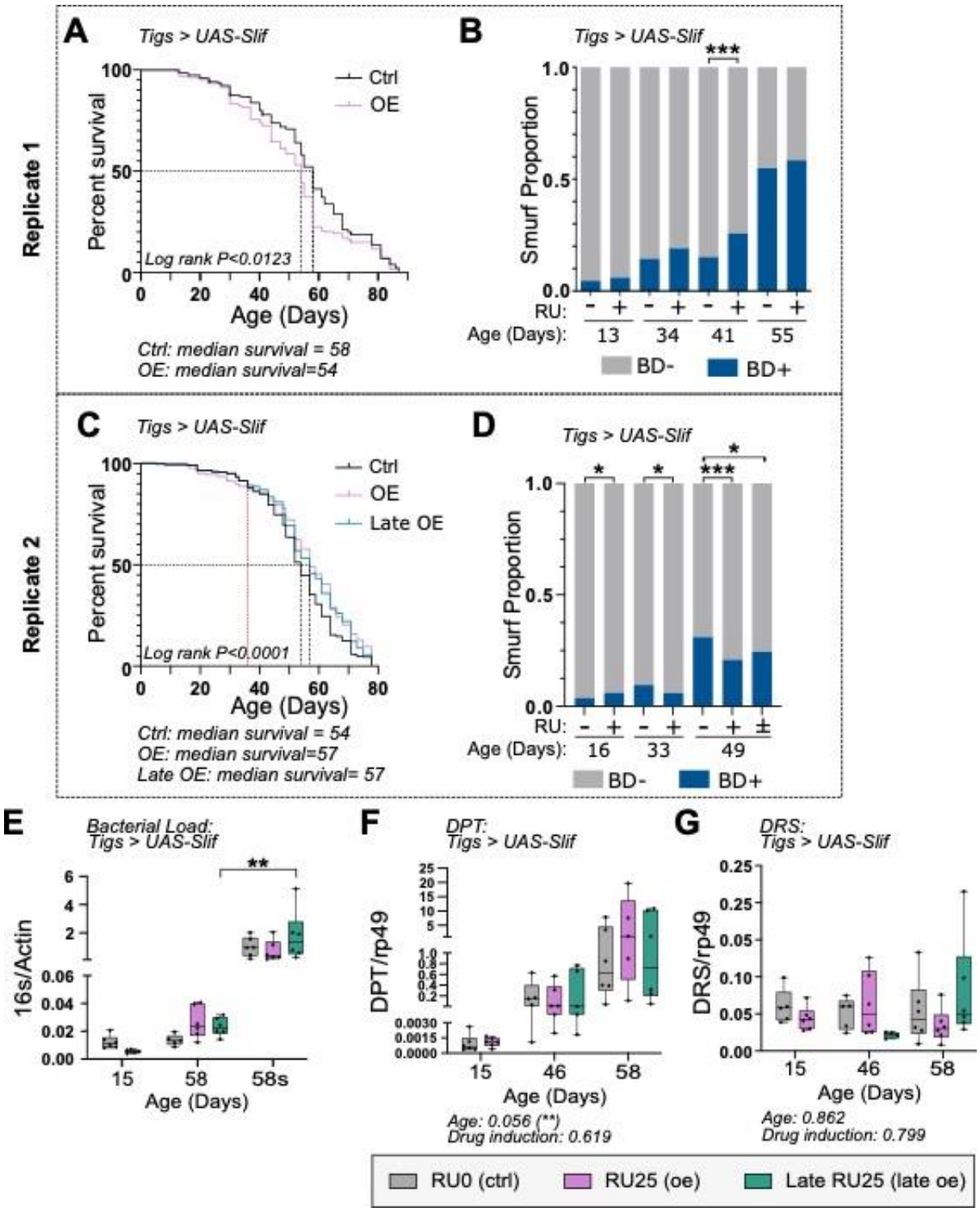

Figure 6.3 | Full-life intestinal Slif overexpression increased lifespan, without impacting intestinal barrier dysfunction or readouts of immune activity.

(A, C) 2 lifespan replicates of conventionally colonised mated TIGS > UAS-Slif females on defined media with ethanol (control (ctrl); black), 25uM RU (overexpression (oe); yellow), or **(C)** transferred from ethanol to RU-486 at 35 days of age (Late overexpression; green). Dashed black line denotes the median survival. Dashed red line denotes the transfer from ethanol media to RU media. **(B,D)** Proportion of smurf and non-smurf conventionally colonised TIGS > UAS-Slif flies on control defined media or RU treated media to induce Slif

overexpression, at **(B)** 13, 34, 41 and 55 days of age, and **(D)** 16, 33 and 49 days of age. BD+ denotes smurf flies with barrier dysfunction. BD- denotes non-smurf flies, without evidence of barrier dysfunction. Addition of RU, and subsequent overexpression denoted by +. Late overexpression flies denoted by ±. The proportions of smurfs in **(B)** were taken from flies in lifespan **(A)**, and the proportion of smurfs in **(D)** were taken from flies in lifespan **(C)**. **(E)** Internal bacterial load of 13 day, 49 day and 49 days smurf flies (49S) mated female TIGS>UAS-Slif females, with and without induction of intestinal Slif overexpression, and with late induction of Slif overexpression (green). Internal bacterial load measured using universal primers for the 16s rRNA gene, normalised to the actin gene. Expression of **(F)** diptericin (DPT) and **(G)** Drosomycin (DRS) in the midgut of conventionally reared TIGS>UAS-Slif with and without induction of overexpression, at 13, 30 and 49 days of age (flies with late induction of overexpression also shown at 49 days. Overexpression induced at 35 days of age). Expression normalised to the expression of rp49. **(A-D)** n > 285 flies per condition, per replicate at day 1. **(E-G)** n = 5-6 Samples of **(E)** genomic extraction from 5 whole flies or **(F, G)** cDNA from 5 midguts (cardia to midgut-hindgut junction). Box plots show the 25-75th percentiles and the median with the whiskers extending from min-max. Asterisks denote the result of **(B, D)** binomial tests, **(E)** ordinary one-way Anova with Holm-Sidak multiple comparisons, or **(F, G)** 2-way Anova with Tukeys multiple comparisons, where * P<0.05, **P<0.01, ***P<0.001 and ****P<0.0001. **(D-E)** multiple comparisons within treatment groups, or between groups at one age only are shown. Result of 2-way Anova main source of variation shown below each graph.

6.3.4 *Slif* expression modulated by the JNK pathway

Due to the changes in *Slif* expression with age, I wanted to understand whether manipulations in any age-related pathways impacted *Slif* expression. Other members of the lab were driving knock-down and overexpression of JNK, JAK-STAT and IMD pathway constituents in the intestine (using the TIGS driver), and collecting gut samples. Unfortunately, only two of these manipulations; induction of constitutive hep.CA expression, and overexpression of PGRP, proved successful.

Driving expression of a constitutively active Hep.CA chronically activates the JNK pathway, through phosphorylation of Basket. Interestingly, activation of the JNK pathway significantly reduced Slif expression (Figure 6.4A). This is in line with my results showing decreased *Slif* expression with age (Figure 6.1 A and B) and research showing chronic JNK activation with age[49].

Puc is a readout of JNK pathway activity. Interestingly, while not significant, a trend towards increased *puc* levels with age remained in both the control and knockdown flies, with no observable or statistical effect of knockdown (Figure 6.4B). *Puc* expression also increased with age when *Slif* was overexpressed, although while the results of a 2-way anova showed age to be statistically significant, post-hoc tests showed significance only between days 15 and 46 (Figure 6.4C). There was increased variability in the results at day 58. This may indicate that *puc* expression peaks during the period of rapid decline (Figure 6.4C) then plateaus.

Taken together the data suggests that *Slif* is controlled downstream of JNK, but does not itself impact JNK pathway activity.

6.3.5 *Slif* expression is not regulated by immune signalling and does not impact age-related immune activation

PGRP functions upstream of the IMD pathway, which is activated with age in conventionally colonised flies. Activation of the IMD pathway through overexpression of *PGRP* did not impact *Slif* levels (Figure 6.4D). This is consistent with the fact that *Slif* levels are reduced with age in both conventionally reared (Figure 6.1A) and sterile intestines (Figure 6.1B) where age-related immune activation is lower.

There was also no significant effect of knockdown or overexpression of *Slif* on *Diptericin* levels (Figure 6.2E, Figure 6.3F), an AMP in the IMD pathway, or on the levels of *Drosomycin* (Figure 6.2F, Figure 6.3G), an AMP typically expressed through toll pathway activity.

6.3.6 Knockdown, but not overexpression of *Slif*, impacts JAK-STAT signalling

Upd3 is a JAK-STAT ligand. We expect to see increased activation with advanced age, and this was observed in both the control and knockdown flies (Figure 6.4E, 2-way Anova Age effect $P<0.0001$), and the control and overexpression flies (Figure 6.4F, 2-way Anova Age effect $P<0.0027$). Interestingly though, despite the increased median lifespan observed upon *Slif* knockdown, the knockdown flies showed increased levels of *upd3* (Figure 6.4E, 2-way Anova, Drug induction effect $P<0.027$). This increase only appears to occur upon full-life knockdown of *Slif* however, as the late knockdown sample at day 49 completely overlaps with the control expression levels. Additionally, while knockdown explained some of the variation in *upd3* levels, there was no significant interaction between *Slif* overexpression and *upd3* expression (Figure 6.4F).

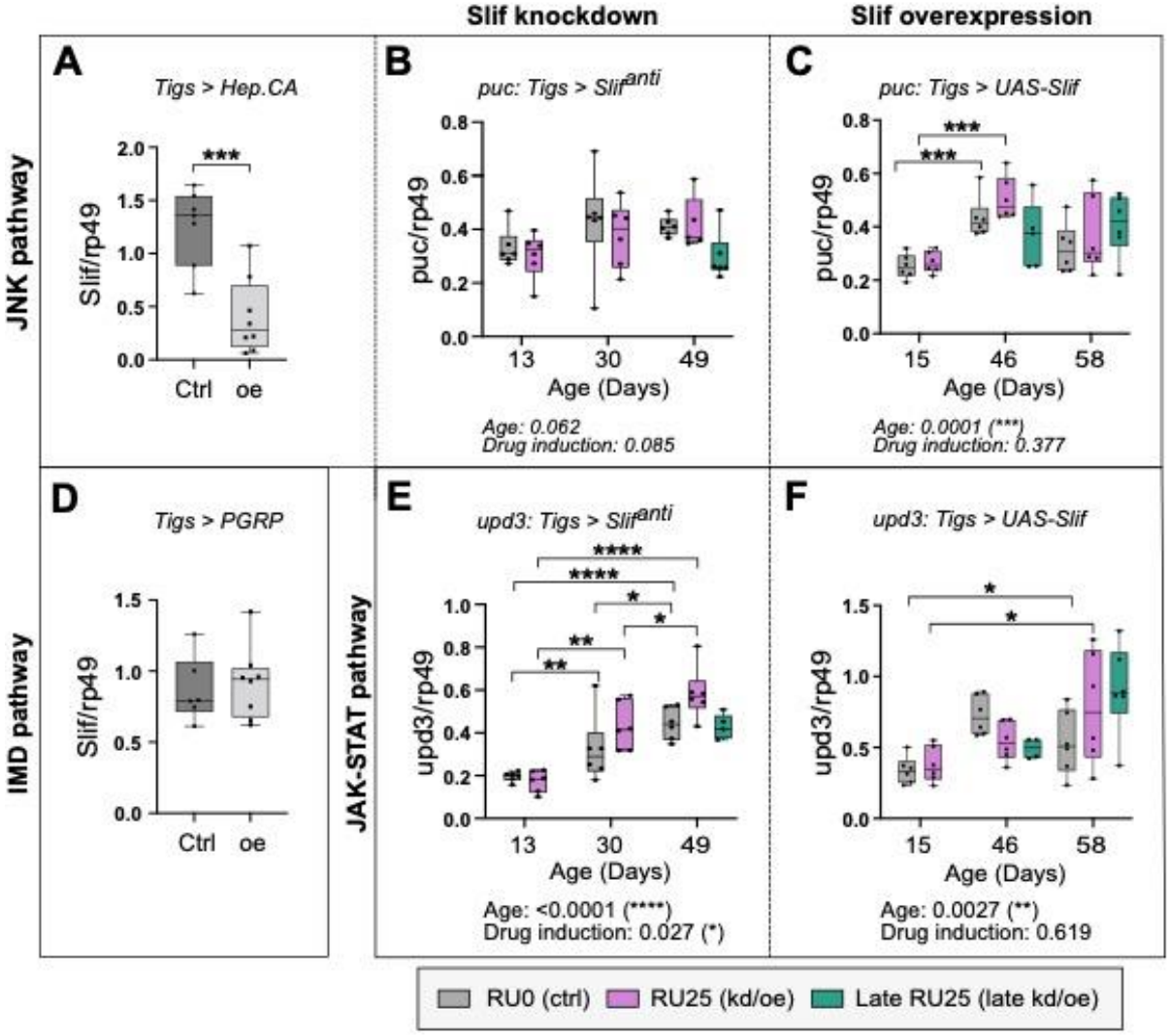

Figure 6.4 | Interaction of Slimfast with age-related signalling pathways.

(A-C) show manipulations to, or readouts of, the JNK pathway. **(A)** expression of Slif normalised to rp49 in whole-gut samples of constitutively active hep.CA driven by TIGS geneswitch driver. Ctrl denotes control, where expression of Hep.CA was not driven. oe denotes overexpression, where addition of RU-486 to the fly food drove the expression of a constitutively active Hep.CA. n=7-8 samples of 5 whole guts **(B, C)** The expression of puc, a readout of JNK pathway activity, with age, normalised to rp49, in the midgut of **(B)** Slif knockdown flies (TIGS>Slif^{anti}) and **(C)** Slif overexpression flies (TIGS > UAS-Slif). The results of a 2-way anova are shown below. **(D)** expression of Slif normalised to rp49 in whole-gut samples of PGRP overexpression flies (TIGS > PGRP). Overexpression of PGRP drives IMD pathway activity. Ctrl denotes control, where overexpression of PGRP was not driven. oe denotes overexpression, where addition of RU-486 to the fly food drove expression of a PGRP in the fly gut. n=7-8 samples of 5 whole guts. **(E, F)** The expression of upd3, a readout of JAK-STAT pathway activity, with age, normalised to rp49, in the midgut of **(E)** Slif knockdown flies (TIGS>Slifanti) and **(F)** Slif overexpression flies (TIGS > UAS-Slif). The results of a 2-way anova are shown below. **(B, C, E, F)** RU25 denotes the addition of RU-486 to the fly food at a concentration of 25mg/ml, to drive knockdown or overexpression of Slimfast. n=5-6 samples of 5 midguts (cardia to midgut-hindgut junction). Box plots show the 25-75th percentiles and the median with the whiskers extending from min-max. Asterisks denote the result of **(B, C, E, F)** multiple comparisons from a 2-way Anova with Tukeys post-hoc test, or **(A, D)** an unpaired t-test, where * P<0.05, ** P<0.01, *** P<0.001, **** P<0.0001. Result of 2-way Anova main source of variation shown below each graph

6.4 Discussion

6.4.1 Characterisation of *Slimfast* expression and regulation

Slimfast has previously been shown by *in-situ* hybridisation, to be highly expressed in the fat body and gut[577], however regional variation in the expression of *Slif* along the gut has not been investigated to this point. Interestingly, the expression of *Slif* appears reasonably consistent along the midgut, albeit with a trend towards increased expression in the anterior midgut. As the midgut was roughly halved, this does not rule out more regionalised expression based upon function[34], for example at the copper cell region. Unfortunately, without a *Slif* antibody, fluorescently-tagged, or *Slif-gal4* line we were unable to assess variation in Slif protein or expression levels along the length of the gut via microscopy. An antibody or fluorescently-tagged protein would be most advantageous, as gene expression levels do not always equate to protein levels. Such lines may also enable the identification of subcellular localisation; Slif has been shown, by antibody staining, to be expressed at the plasma membrane of adipose cells in the fat body and degraded by endocyosis[623], however, whether it is also expressed on intracellular organelles is yet to be determined.

The midgut is considered to be the absorptive region of the gut[426], analogous to the small intestine, so it is not surprising that *Slif* expression in the hindgut is much lower. Unfortunately, housekeeping genes for the crop were not stable with age, so we do not have a reliable readout of crop expression.

Interestingly, in the samples from Canton-S females fed cornmeal media, the anterior and posterior midgut expression increases between days 10 and 40, but is reduced in day 40 smurfs, whereas expression decreases between days 10 and day 45 in midgut samples from flies on defined media. One possibility for this is the inclusion of early smurfs in the aged defined media samples. There was an apparent lower proportion of smurfs on the defined than cornmeal diet, when first assessing ageing phenotypes on defined media. Whilst this difference was not significant (section 3.3.1.2), it may be possible that early smurfs are not being detected on defined media, and consequently more of these early smurfs are included in the old samples.

Alternatively, these differences may indicate that diet, or resultant microbial changes, impact the expression of amino acid transporters with age. Nevertheless, changes in microbial load with age cannot explain the reduced *Slif* expression observed with age on defined media, as this remained significant in the absence of microbiota. Instead, it appears that advancing age drives a reduction in *Slif* expression.

6.4.2 Increased luminal concentration of *Slif* substrates may explain the lifespan extension upon knockdown

As mentioned, *Slimfast* is highly homologous to human SLC7 transporters, which transport arginine, lysine and ornithine. Indeed *Slif* has itself been shown to transport arginine[577]. No work has been done to assess the substrate affinity of *Drosophila Slif* however, although the mosquito *Slimfast* homolog was found to transport L- and D- arginine at the highest affinity, and lysine and histidine at equal lower affinities[621].

6.4.2.1 Arginine

As mentioned in the introduction, increased luminal arginine concentrations lead to microbial and immune changes in mice[654,655,655–657].

Knockdown of *Slimfast* would also increase luminal arginine concentrations, but whether such changes underlie the observed increase in lifespan upon *Slif* knockdown remains to be determined. Nevertheless, there are indications to this effect; firstly, there was a significant impact of *Slif* knockdown upon the bacterial load of smurf flies. Unfortunately, as the resultant microbiota was not sequenced, we do not have information about community changes which may be driving these differences. Secondly, we observed a trend towards increased *Diptericin* expression with age upon *Slif* knockdown which is reminiscent of the increased immune activity mentioned above.

This effect only appears to occur upon increased, not reduced luminal arginine, as there were no changes in bacterial load or diptericin levels upon *Slif* overexpression. This effect also appears to rely on early, or full-life reduction in *Slif*, as late-life knockdown resulted in a shortened lifespan. This may indicate that the arginine and lysine-driven microbial changes only occur early in life, perhaps before the microbiota is too established. This could be tested by performing *Slif*-knockdown in axenic or gnotobiotic flies, or by treating flies with antibiotics prior to *Slif* knockdown at various points within the lifespan to enable the establishment of a new microbial population based upon new luminal nutrient concentrations and potential immune changes. It would also be interesting to have a better understanding of potential microbial changes which may occur through *Slif* knockdown by sequencing. Additionally, utilisation of the DUMP assay with *Slif* knockdown flies would be useful for confirmation of luminal changes in the concentration of cationic amino acids. This would be most useful in axenic flies, without the additional impact of potential microbial changes driven by *Slif* knockdown.

6.4.2.2 Lysine

As another SLC7 substrate, *Slif* is expected to transport lysine, thus knockdown of *Slif* is expected to result in increased luminal lysine.

The impact of changes in luminal lysine availability has not been studied in humans however, as mentioned, both supplementation and reduction of dietary lysine results in microbial composition changes in mammalian systems[675,676]. It was also noted that lysine restriction resulted in reduced expression of SLC7 transporters[676], likely further reducing lysine availability. Could it be that this reduction in SLC7 transporter expression is mediated by the microbiota to restore luminal levels of this amino acid for microbial metabolism? Further analysis by Yin and colleagues showed that the altered microbiota was involved in host metabolism and, in particular, amino acid metabolism[678]. mTOR phosphorylation was not altered, however, lysine restriction inhibited AMPK signalling[678], potentially implicating the AMPK pathway in the regulation of *Slif* expression. Unfortunately, I have no data on investigating AMPK pathway activity upon *Slif* modulation, or on *Slif* expression upon AMPK pathway manipulation.

Taken together with the results from this study, there is evidence to suggest that the lifespan effect observed upon full-life *Slif* knockdown may be, at least in part, modulated by the microbiota. This could be tested by performing *Slif*-knockdown in axenic or gnotobiotic flies. It would also be interesting to have a better understanding of potential microbial changes which may occur through *Slif* knockdown by sequencing. Additionally, as mentioned above with arginine, utilisation of the DUMP assay alongside *Slif* knockdown in axenic flies, for confirmation of luminal lysine changes would be useful. This may also identify unexpected changes in the faecal profile from potential compensatory mechanisms regulating the expression and transport efficiency of other intestinal transporters.

6.4.3 *Slimfast* as a nutrient sensor

Slimfast has also been shown to act as a nutrient sensor, in an mTOR dependent manner, in the fat body during larval development, with knockdown of *Slif* in the fat body resulting in humoral signals that systemically inhibit PI3K signalling[577]. In the previously published study, a 90% reduction in dietary arginine was not sufficient to affect larval growth, although it did enhance the effect of fat-body Slif knockdown[577]. It may then, be the case that intestinal *Slif* knockdown would not reduce systemic arginine levels sufficiently to induce this humoral response initiated by the fat body,

however, such a nutrient-sensing mechanism may also play a role in the intestine, the first source of nutrition, and may impact lifespan.

mTOR regulates both the localisation of *Slif* to the plasma membrane of adipose tissues and its endocytic degradation[623], likely to promote the uptake of nutrients required for cell growth. A study assessing arginine uptake in S2 cells, however, determined that reduced mTOR activity increased rather than decreased arginine uptake[679]. The reasons for this are not clear. It may be that other signals also impact *Slimfast* expression to promote uptake in low nutrient conditions, or that the affinity of the transporter can be modulated in some way. Evidence here indicates that the JNK pathway can also regulate *Slif* expression (See below).

Interestingly, while *Slif* knockdown appears to have a strong effect in the fat body[577,623], gut and even muscle[680], overexpression of *Slif* in the differentiating eye, or on the dorsal surface of the wing does not result in any changes in growth[568]. This may suggest that the nutrient-sensing pathway downstream of *Slif* is more sensitive to reduced than plentiful nutrients, and may explain some of the inconsistency observed in the overexpression lifespans here. It is also possible that overexpression of *Slif* may lead to increased protein, but that other mechanisms prevent its targeting to the membrane.

6.4.4 *Slif* links the age-related JNK and JAK-STAT pathways

As mentioned (section 1.3.2.2.1), the JNK pathway is responsible for cell-proliferative and apoptotic responses to tissue damage due to stress[46]. Phosphorylation of the *Drosophila* JNK, *basket*, leads to the activation and transcription of several genes including *puc* which limits JNK activity in a negative feedback loop. JNK activity is upregulated with age, associated with loss of intestinal integrity and dysplasia[49].

JNK activity also mediates transcription of the cytokine *upd3* which itself is a JAK-STAT ligand.

JNK pathway activation through the expression of a constitutively active Hep.CA, which phosphorylates *basket,* resulted in reduced *Slif* expression. Interestingly, reduced *Slif* expression in turn leads to increased levels of *upd3* but not *puc*, implicating *Slif* as an intermediate factor mediating *upd3* expression and JAK-STAT pathway activity from JNK signal activation (Figure 6.5). *Slif* knockdown in the fat body has previously been shown to upregulate expression of the JAK-STAT ligand *upd2*, but not *upd1*[681].

Chronic JAK-STAT pathway activation is also associated with age[65]. That *Slif* knockdown results in lifespan extension alongside increased JAK-STAT pathway activation is counter to expectation. This unusual result may be explained through arginine levels. As mentioned above, increased luminal arginine sculpts the microbiota[655,656], resulting in reduced intestinal damage[654,655]. This may protect intestinal barrier function even upon chronic JAK-STAT activity.

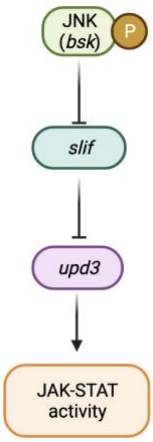

Figure 6.5 | Schematic of JNK signalling cascade indicating Slif as an intermediate factor between JNK and JAK-STAT pathways.

Activation of the *Drosophila* JNK basket (bsk) inhibits the expression of Slif. Slif expression inhibits upd3 expression, and thus JAK-STAT pathway activation. JNK inhibition of Slif expression, therefore, leads to increased upd3 expression and JAK-STAT activation.

6.5 Conclusion

I have shown that the cationic amino acid transporter *Slimfast* is expressed along the length of the midgut, with reduced expression in the hindgut. Expression of *Slimfast* decreases with age in wild-type flies fed defined media, irrespective of microbiota status, however, diet may impact expression levels. Reduction of its expression leads to lifespan extension, which may be driven by increased luminal arginine levels which positively modulate the microbiota in mammalian systems, or through dietary restriction mechanisms via the mTOR pathway as late-life knockdown did not confer the same benefit.

While *Slif* has been shown to be regulated through the mTOR pathway and arginine is known to be a potent activator of mTOR, the evidence here suggests that the JNK pathway also regulates its expression. *Slif* appears to be an intermediate factor, downstream from JNK activation, but

upstream of *upd3* transcription and JAK-STAT signalling. The decreased *Slif* expression with age may therefore be driven by increasing JNK pathway activity. Reduced *Slif* expression, in turn, leads to increased levels of upd3 and JAK-STAT activity.

Amino acid availability has been implicated in ageing, particularly through the activation of mTORC1. This data however highlights an important link between intestinal amino acid transport and other known age-related pathways, which has, until now, been a neglected area of research.

There is also an apparent acceptance within the field that dietary nutrients are efficiently absorbed and transported from the intestine to the rest of the body. Data here suggests that this process may not remain efficient with age. This may have consequences on the physiology and ageing of different peripheral organs and may contribute to the increased frailty and mortality observed upon advancing age.

7 Expression of the amino acid transporter Eaat1 impacts longevity and stem cell proliferation

7.1 Introduction

7.1.1 Importance of Glutamate

The results from the intestinal amino acid transporter screen indicate that glutamate transport may be affected by the ageing process, with the expression of both *Eaat1* and *dmGlut* reducing with advancing age (section 5.1.3).

L-glutamate is among the most abundant amino acids in dietary protein (8-10%) and represents a major source of energy for the intestine[682]. ~80% of dietary glu absorbed is removed during the first pass effect in the splanchnic bed, contributing to energy production and generally supporting intestinal function[683,684]. Glutamate also participates in gut protein synthesis, both as a proteinogenic amino acid, and as a precursor to the synthesis of other amino acids such as proline and arginine, as well as glutathione[600]. In support of the importance of L-glutamate, supplementation improves small intestinal architecture of weaning piglets[685], however, it is also an important energy source in many cancers[506].

Glutamate is also the most abundant neurotransmitter in the CNS, with glutamate receptors present on 90% of neurons, and 40% of synapses[496,686,687], however excess glutamate can lead to excitotoxicity; a persistent activation of NMDA and α-amino-3-hydroxy-5-methyl-4-isoxazolepropionic (AMPA) receptors resulting in a lethal influx of extracellular calcium[688]. This excitotoxic cell death can lead to neurologic deficits due to the progressive dysfunction and loss of neurons, and is linked to neurodegenerative diseases including alzheimers disease and multiple sclerosis[689–692]. Interestingly, reduced concentrations of glutamate have been detected in the brains of older individuals[693,694], and reductions in glutamate can be detected as early as 31 years of age[695].

In the DUMP assay, there was a trend towards increased luminal glutamate concentration with both age and microbial colonisation (section 4), and the results from assaying intestinal amino acid transporter expression (section 5) indicate that this may be caused by reduced intestinal glutamate uptake with age.

7.1.1.1 Glutamate and glutamine concentrations are tightly linked

Glutamate is also a large contributor to the glutamate-glutamine cycle. The enzymes glutamine synthetase and mitochondrial glutaminase, catalyse the reaction from glutamate to glutamine[696,697]. Interestingly, while glutamate increased non-significantly in the faeces of conventional and axenic

flies, glutamine concentration increased significantly (section 4). Bacteria can also contribute to the conversion of glutamate to glutamine by glutamine-amidotransferases or glutaminases[698]. This may explain the switch in relative microbial contribution and axenic faecal concentrations; glutamate is present at the highest concentration in the faeces of young and old axenic flies, whilst glutamine is present at low abundance. The relative microbial contribution of glutamine, however, increases the most of all the amino acids with age, whilst the relative microbial contribution (rank change) of glutamate decreases.

Glutamine has been more widely implicated with ageing than glutamate. Glutamine levels decrease with age in fission yeast, and supplementation of glutamine can extend lifespan[476]. Additionally, glutamine deprivation in *Drosophila* reduces lifespan and stress tolerance[487], while glutamine supplementation rescues a progeria phenotype in mice, and protects against oxidative stress-driven senescence[487]. Reduced glutamine levels are also implicated in the development and progression of Alzheimer's disease[488,489], where supplementation can reduce inflammation-induced neuronal cell cycle activation and tau phosphorylation in an Alzheimer's disease (AD) mouse model[489].

On the other hand, a rat model of type-2 diabetes shows high serum glutamine concentration[699], and increased serum glutamine may contribute to autism-spectrum-like behaviours[700]. There may be an optimal balance of glutamine, with concentrations above and below this threshold deleterious to health and longevity in different ways. It should be noted, however, that the observed changes in serum glutamine levels in these models may be biomarkers, rather than drivers, of disease. Both studies observed changes in microbiota composition which may both increase glutamine availability and contribute to disease via separate mechanisms.

Glutamine has also been implicated in the maintenance of intestinal barrier integrity, which is linked to longevity in flies and mice[22,39,40]. Deprivation of glutamine reduces expression of tight-junction proteins[482] whilst supplementation protects tight-junction formation in caco-2 cells upon methotrexate treatment[483]. Long-term glutamine treatment, initiated before advanced age in rats also beneficially impacts enterocytes, resulting in increased gut mass and improving villus height, and leading to improved body weight maintenance[701]. In addition to this, glutamine functions as a signalling molecule modulating programmed cell death[484], and is involved in intestinal stem cell proliferation through the activity of several MAPKs, including JNK[485,486].

7.1.2 Glutamate transport in *Drosophila*

There are multiple glutamate transporters in *Drosophila*; Eaat1, Eaat2, dmGlut, vesicular glutamate transporter (VGLUT), glutamate carriers (GC) 1 and 2, and aralar1 (determined by GO search of "L-glutamate transmembrane transport" in flybase http://flybase.org/ ; accessed June 2020). Of these, only Eaat1, Eaat2 and dmGlut are localised to the cell membrane[566,702]. GC1, GC2 and aralar are involved in glutamate transport across mitochondrial membranes[703,704] and VGLUT is localised to vesicles[705].

Eaat2 was found to be a selective aspartate and taurine transporter, with a much lower affinity for glutamate transport compared to all other known EAAT proteins[706], leaving just Eaat1 and dmGlut as high-affinity transporters of glutamate across the plasma membrane.

dmGlut is homologous to the SLC17 family of transporters, with the highest homology to SLC17A3 (DIOPT[563]), a voltage-driven transporter that excretes intracellular urate and organic anions from the blood into renal tubule cells[707]. dmGlut functions quite differently, transporting glutamate into *Drosophila* cells in a sodium-independent manner, with a K_m of 69.4 μM[708]. Knockout by P-element insertion is lethal during embryogenesis, suggesting an essential function to this gene[709]. Additionally, overexpression of *dmGlut* can lead to megamitochondrial formation[566,708]. Unfortunately, this is the current extent of the knowledge on dmGlut.

Eaat1 is homologous to the human Excitatory amino acid transporter family (*EAAT*), which is discussed further below. As Eaat2 transports aspartate and taurine over glutamate, the two *Drosophila* Eaats are not considered to be functionally redundant. EAAT proteins typically transport glutamate with a K_m of 45-66 μM, and aspartate with a K_m of 54-60 μM[710,711], whereas *Drosophila* Eaat2 transports aspartate with a K_m of 15-45 μM and glutamate with a K_m of 185 μM[706]. In comparison to dmGlut, more is known about this family of proteins in mammalian and *Drosophila* systems, particularly in terms of their role in glutamate clearing in the central nervous system. This has led to increased availability of genetic tools to enable the characterisation of the gene. For this reason, and because of the evidence to suggest the importance of glutamate transport with age, Eaat1 was chosen as a candidate for further characterisation.

7.1.3 Eaat1 structure and homology

As mentioned, *Drosophila* Eaat1 is a 'high-affinity' glutamate transporter homologous to the human excitatory amino acid transporters. Five EAATs have been identified in mammalian systems; EAAT1

(GLAST, SLC1A1)[712,713], EAAT2 (GLT, SLC1A2)[714], EAAT3 (EAAC, SLC1A1)[715], EAAT4 (SLC1A6)[716] and EAAT5 (SLC1A7)[717]. All the EAAT proteins catalyse transmembrane transport of L-glutamate and L- and D-aspartate, coupled with influx of three sodium ions (Na^+), efflux of potassium ions (K^+), and use of an extracellular H^+ gradient[718–727]. At equilibrium, under standard physiological conditions, this coupling is able to support a 10^6 fold gradient of glutamate across the cell membrane[726,728].

The five mammalian EAATs share 50-60 % sequence identity within species, and 30-40 % identity with the remaining members of the SLC1 family; the alanine-serine-cysteine-transporters ASCT1 and ASCT2[729–732]. EAATs also share ~37 % sequence identity with GltPh, a glutamate transporter homolog from Pyrococcus horikoshii[718,719,733]. Most of the information surrounding EAAT transport mechanisms comes from the crystal structure of this bacterial homolog. It has been shown that EAATs form homotrimers, where each monomer is independently functional and capable of substrate transport[718,719,733]. EAAT3 and EAAT4 may also be able to assemble as heterotrimers, impacting cell-localisation[734]. More recently, crystal structures of human EAAT2 have been determined, confirming the trimeric structure, with each protomer consisting of 8 transmembrane domains[722].

Interestingly, in addition to ligand transport and ion channel activity, protein-protein interactions at both the N- and C- terminal domains of EAATs suggest a potential transceptor function for EAATs. Interactions between the EAATs and the actin cytoskeleton, as well as mitogen-activated protein kinase (MAPK) cascades have been reported[622,735–737].

The five mammalian EAATs have specific localisations, with EAAT1 the major glutamate transporter in the cerebellum[738], 6-fold more abundant here than EAAT2 and 10-fold more than EAAT4[738]. In the rest of the brain regions, EAAT2 is most abundant and is responsible for ~90-95 % of glutamate uptake in the forebrain. *EAAT2* is predominantly expressed in astrocytes[738], and represents up to 1 % of total brain protein[739]. Outside of the brain, *EAAT1* is also expressed in the heart[740], placenta[741], bone osteocytes[742] and mammary glands[743]. *EAAT2* is expressed in the placenta[741] and mammary glands[743].

EAAT3 is expressed in neurons in the hippocampus, cerebellum and basal ganglia[744–748], but at ~100-fold lower expression compared to *EAAT1* and *EAAT2*[748]. Interestingly, a large proportion is intracellular, thought to be rapidly mobilized to the plasma membrane when required. It is also expressed in the kidney, where it plays a role in dicarboxylic amino acid reabsorption[715,749,750], and the intestine[712,714,748], heart[740], placenta[741] and enteric neurons[751].

EAAT4 and *EAAT5* expression is highly localised, with the majority of *EAAT4* expressed in Purkinje cells of the cerebellum[752], and *EAAT5* exclusively expressed in the retina[717].

As mentioned, *Drosophila* contains just one functional EAAT ortholog, Eaat1. It must perform many of the roles of the distinct human EAAT genes, and is known to be highly expressed in glial cells[753,754], malpighian tubules[755] and intestine[565]. It may also be expressed in other tissues.

7.1.3.1 Eaat1 and glutamate: disease and age relevance

Given the important role of EAAT proteins in clearing glutamate from the synaptic cleft and preventing excitotoxicity, it is no surprise that dysregulation of EAATs, and other glutamate transporters, has been linked to neurological disorders including schizophrenia[756–760] and amyotrophic lateral sclerosis (ALS)[761–764]. Reduced *EAAT2* expression has also been implicated as a key process in the progression of Alzheimers disease however despite extensive research into glutamatergic changes in mouse models of Alzheimers disease[765], there is a lack of studies investigating the role of EAAT proteins in Alzheimer's disease in humans.

Interestingly, while there is a lack of research investigating changes in the expression of EAAT proteins with age, a decrease in astrocytic expression of *EAAT1* and *EAAT2*, but not neuronal *EAAT3* expression has been observed as a feature in aged rats, and a generally decreased expression of *EAAT2* was observed in other aged animals[766–768]. It has been hypothesised that a reduced glutamate uptake capacity with age may be the most important risk factor in neurodegenerative diseases[769].

Although the mechanisms of glutamatergic signalling were characterised primarily in the CNS, and thus the bulk of research into glutamate and glutamate transport focuses on this system, the importance of glutamate signalling in non-neuronal tissues is gaining more recognition in the literature.

Glutamate signalling has been implicated in the transformation and progression of several cancers, often through the activation of cell-surface glutamate receptors[503,505,506,770–773]. Interestingly, re-expression of *EAAT2* significantly prevents cell proliferation in several glioma cell lines[774], and the association between EAAT proteins and cancer is not limited to neuronal cancers[503,506,770,775]. Release of glutamate from cancer has been linked to the progression of glioma[776], cancer-induced bone pain[777,778], and may be linked to bone metastasis[779].

Additionally, glutamine is often preferred over glucose as a fuel for cancer cells as it both fulfils energy requirements and serves as an intermediate for the synthesis of many macromolecules. As mentioned above, glutamate can be converted to glutamine by glutamine synthetase[696] or

mitochondrial glutaminase[697], and thus is an important source of glutamine to cancer cells. Indeed, a glutaminase inhibitor is in clinical trials for the treatment of a number of malignancies[773,780–783], and glutamine synthetase is considered a potential therapeutic target[784].

Whilst the field is beginning to recognise the importance of glutamate and glutamatergic signalling beyond the CNS, there is still a clear gap in the research, particularly in the context of ageing.

7.1.4 Glutamate sensing

Changes in glutamate concentration can be sensed by glutamate receptors on the surface membrane. There are two types of glutamate receptor; ionotropic glutamate receptors (iGluRs) which are ligand-gated ion channels, and metabotropic glutamate receptors (mGluRs) which are G-protein coupled receptors.

There are three groups of iGluRs; NMDA, AMPA and kainite receptors, which are predominantly expressed at synaptic termini. Binding of glutamate enables cation flux, resulting in membrane depolarization. Overactivation of these receptors, through dysregulation of glutamate dynamics, results in excitotoxic cell death which, as mentioned above (section 7.1.1), is implicated in ageing.

Unlike ionotropic glutamate receptors, metabotropic glutamate receptors modulate cell excitability and synaptic transmission via secondary messenger signalling pathways through activation of G-proteins. Humans have at least 8 mGluR's, split into three groups on the basis of their sequence homology, pharmacological profile and transduction pathways[785]. In general, the different groups are also coupled to different G-proteins, with Group I (mGluR1 and mGluR5) coupled to G_{aq}, and groups II (mGluR2 and mGluR3) and III (mGluR4, mGlur5 and mGluR7) coupled to $G_{i/o}$ proteins[785]. This coupling leads to alternative downstream signalling. Activation of group I mGluRs, results in activation of phospholipase C, whereas group II and III activation leads to inhibition of adenylyl cyclase and cAMP formation, which limits downstream protein kinase A (PKA) activation[785].

In comparison to the 8 mGluR's in humans, *Drosophila* has just two loci with mGluR homology. Only one of these is activated by glutamate[786], thus *Drosophila* is considered to have only one functional mGluR. This functional mGluR (hereby denoted as dmGluR), shares the highest homology to group II mammalian mGluRs[787], although it is coupled to both G_i and G_q G-proteins[788,789]. In confirmation of the higher degree of homology to group II mGluR's, dmGluR also inhibits Adenylate cyclase activity.

mGluR's are widely expressed in the CNS, and their expression was once considered to be restricted to neuronal cells[790]. They are now known to be expressed in many peripheral organs, including bone[791], skin[792,793], pancreas[794,795], liver[796], heart[797], thymus[798], intestine[603,799,800] and embryonic stem cells[801] suggesting that their role is wider than simply neurotransmission. Indeed, they are also widely implicated in calcium signalling in neurons[802–806] and astrocytes[807–810], and there are indications of a role of mGluR's and calcium signalling in bone cells[811] and in stem cell differentiation[565,603,812,813].

Interestingly, aside from sharing a ligand, mGluR's and EAATs appear to be linked. EAAT3 and mGluR5 were shown to colocalise in rat hippocampal cultures[814]. Additionally, activation of groups I and II mGluRs have been shown to modulate the expression of EAATs; activation of group I mGluRs down-regulates the expression and protein levels of EAAT1 and EAAT3, whilst stimulation of group II mGluRs up-regulates EAAT1 and EAAT3 gene expression and protein levels[815]. The direction of response may also depend on the length of mGluR stimulation. Evidence suggests that acute activation of group I mGluRs actually leads to an acute increase in EAAT2 activity and glutamate import[816], and that it is chronic activation which leads to the reductions in EAAT levels[815,817].

7.2 Aims and objectives

In this chapter, I set out to understand whether changes to the expression of intestinal *Eaat1* has a physiological impact on ageing. I previously observed a reduced expression of two intestinal glutamate transporters with age and, as the expression of amino acid transporters has not previously been investigated in an ageing context, I wanted to understand the functional significance of this downregulation. I focused exclusively on the high-affinity glutamate transporter Eaat1 due to the availability of genetic tools at my disposal.

My first aim was to characterise the expression of *Eaat1* under physiological conditions in the intestine. I first assessed the localisation of Eaat1, both at the level of individual cells, as well as in the whole gastrointestinal tract to gain insights into its function. I also assessed the expression of *Eaat1* with age in axenic flies to understand whether the presence of microbiota impacts the intestinal expression of this transporter.

I next wanted to understand the impact of modulating intestinal *Eaat1* expression. For this, I utilised the *UAS-gal4* GeneSwitch system to knockdown or increase expression of *Eaat1*, and observed the

impact of these manipulations on lifespan, loss of intestinal barrier, gene expression and internal bacterial load.

Additionally, due to reports of increased luminal glutamate driving the division of intestinal stem cells through mGluR activation, I aimed to investigate the impact of *Eaat1* overexpression and knockdown, which should impact intestinal glutamate concentrations, on ISC proliferation.

7.3 Results

7.3.1 The amino acid transporter *Eaat1* is expressed along the *Drosophila* midgut

Following the finding that *Eaat1* expression decreases with age in conventionally colonised Canton-S intestines (Figure 5.4A, Figure 7.1A), I wanted to characterise its expression pattern along the midgut. For this, I assayed the levels of *Eaat1* in regional gut samples of Canton-S females previously collected within the lab, as well as in whole-gut samples from the same cohort of flies.

Expression was observed along the length of the midgut, with much lower expression in the posterior midgut (Figure 7.1E) than in the anterior midgut (Figure 7.1D). Interestingly, the different regions of the gut showed different patterns of *Eaat1* expression with age. There was a significant increase in the levels of *Eaat1* in the anterior midgut at day 40, however upon loss of intestinal barrier function, this was reversed (Figure 7.1D). The posterior midgut also showed a trend towards increased levels at day 40 however, this was significantly reduced upon loss of intestinal barrier function (Figure 7.1E). Conversely, in the hindgut, expression remained stable with age (Figure 7.1F). Unfortunately, while crop samples were collected, I was unable to find a housekeeping gene which remained stable with age. It would also be interesting to look at the expression dynamics of *Eaat1* in the tubules with age, as amino acid transporters are often highly expressed in mammalian kidneys, and Eaat1 has been shown to be expressed in the tubules[755].

As well as assaying gene expression levels, I utilised the Eaat1-venus flies donated by the van Meyel lab[230] to assess Eaat1 protein expression along the length of the gut. The guts were stained with an anti-GFP antibody that recognises venus, to enhance the venus signal, and images of whole guts were taken down a fluorescent dissection microscope (Leica stereo fluor M165FC). Pixel intensity was then measured in different regions along the gut (Figure 7.1H). The regions measured included the five anatomical regions of the midgut identified in Buchon *et al.* 2013[34], as well as the crop, cardia and hindgut (HG). I also measured the pixel intensity along the whole gut (WG). Pixel intensity was measured in Fiji (ImageJ). The line tool was used to draw along the centre of the guts, for the length of each sample, and the average intensity along the length of the line was recorded. Signal intensity was increased where sections of the gut overlapped, so these regions were omitted. The only region showing statistical significance from the whole-gut was the crop which displayed much higher levels of Eaat1 protein. Median Eaat1 protein levels were below the whole-gut median in the cardia, and midgut regions 4 and 5 (Figure 7.1G), in agreement with the gene-expression levels suggesting lower Eaat1 expression in the posterior than anterior midgut (Figure 7.1E and D).

7.3.2 Variation in *Eaat1* expression in young intestines may mask age-related changes

The pattern of expression with age was not consistent between the whole-gut samples collected previously in my lab, compared to the midgut data from the transporter screen (Figure 7.1C and A). In the whole-gut data, there is a significant reduction in expression upon loss of intestinal barrier function, however a significant reduction in *Eaat1* levels was not observed between day 10 and day 40 samples with intact barrier function (Figure 7.1C).

The 10-day samples did however show a large amount of variance compared to the 40 day samples (F-test, P = 0.0272), which may mask age-related changes in expression. The difference in expression pattern with age between these whole-gut samples (Figure 7.1C), and the midgut samples used in the screen (Figure 7.1A), may be due to differences in the gut regions included within the sample. These whole-gut samples include the crop, hindgut and tubules, which were absent in the midgut samples used in the original screen. Additionally, while all the samples were collected from mated Canton-S female flies, the two sample groups were raised on different media, with the whole-gut flies on cornmeal media for their full lifespans, and the midgut flies raised on defined media throughout adulthood. Whilst the difference in the proportion of smurfs was not significantly different between flies on defined or cornmeal media at either age, there was a trend towards lower proportions on defined media (section 3.3.1.2). It may therefore be possible that early smurfs are not being detected on defined media due to differences in e.g. food consumption, and thus being included in the old samples. This may account for the changes observed with age on defined media, but only with loss of intestinal barrier function on cornmeal flies.

Midgut samples taken from sterile Canton-S females also showed a large amount of variance in 10-day samples compared to 45 day samples (F-test P = 0.0074) (Figure 7.1B). It may be the case that there is more dynamic *Eaat1* expression in young flies, perhaps in relation to food consumption, and that in older flies, *Eaat1* expression remains more constant regardless of i.e. food intake. There appears to be a trend towards reduced *Eaat1* expression with age in the absence of microbiota, although this did not reach significance (Figure 7.1B, t-test P = 0.0529), indicating that the observed changes in *Eaat1* expression are an effect of age, rather than age-related microbial changes.

7.3.3 Eaat1 shows localisation to the apical membrane

I also wanted to utilise the Eaat1-venus flies to assess the cellular localisation of Eaat1. Eaat1-venus guts stained with DAPI, phalloidin and an anti-GFP antibody that recognises venus, to enhance the venus signal, were imaged on a fluorescent confocal microscope (Zeiss 800). As the Eaat1

localisation data indicated higher levels of Eaat1 in the anterior midgut, this was the region imaged. I hypothesised that Eaat1 would be localised to the apical membrane, however this was not clear in the z-projection (required to intensify GFP signal (Figure 7.1I)), as the z-stack was taken from the top of the intestine down towards to lumen. To counteract this, I used the reslice function in Fiji (imageJ) to generate a new z-stack, with the z-stack in the previous y plane (Figure 7.1J). By doing this on reduced sections of the original image, I was able to more clearly visualise the Eaat1 localisation (Figure 7.1I'). Eaat1 appears diffuse within the cell with stronger, more punctate signal, at the apical membrane. This punctate pattern is interesting, potentially indicating rafts of Eaat1 on the apical membrane, or perhaps containment of Eaat1 inside vesicles, prior to membrane fusion, indicative of dynamic Eaat1 localisation. More in-depth analysis of subcellular Eaat1 localisation, and localisation dynamics would be of great interest.

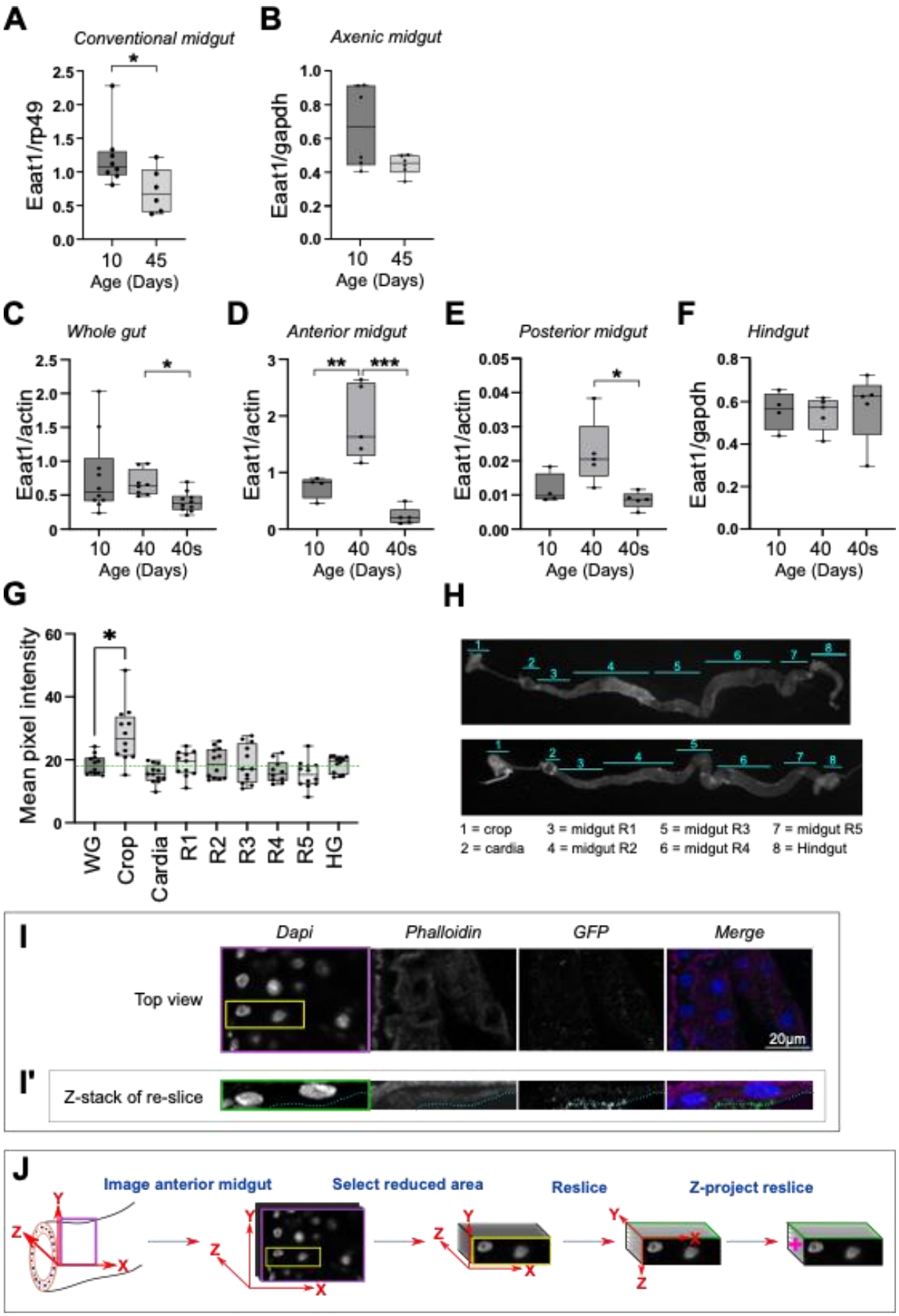
A
Conventional midgut
Eaat1/rp49
Age (Days)
B
Axenic midgut
Eaat1/gapdh
Age (Days)
C
Whole gut
Eaat1/actin
Age (Days)
D
Anterior midgut
Eaat1/actin
Age (Days)
E
Posterior midgut
Eaat1/actin
Age (Days)
F
Hindgut
Eaat1/gapdh
Age (Days)
G
Mean pixel intensity
WG
Crop
Cardia
R1
R2
R3
R4
R5
HG
H
1 = crop
2 = cardia
3 = midgut R1
4 = midgut R2
5 = midgut R3
6 = midgut R4
7 = midgut R5
8 = Hindgut
I
Dapi
Phalloidin
GFP
Merge
Top view
20µm
I'
Z-stack of re-slice
J
Image anterior midgut
Select reduced area
Reslice
Z-project reslice

Figure 7.1 | Intestinal expression of Eaat1

(A) Expression of Eaat1, normalised to rp49, in the midgut of conventionally colonised Canton-S females at 10 and 45 days of age; n=6-8 samples/age. Graph taken from Figure 5.4**. (B)** Expression of Eaat1, normalised to gapdh, in the midgut of axenic Canton-S females at 10 and 45 days of age; n=6 samples/age. (C-F) Expression of Eaat1 in conventionally colonised Canton-S samples from flies raised on cornmeal medium, at 10 and 40 days of age, including also 40 day old smurf flies (40s). **(C)** whole-gut (crop, cardia, midgut, tubules and hindgut; n=8-10 samples/age, **(D)** anterior midgut **(E)** posterior midgut **(F)** hindgut. (D-F) n = 4-5 samples/age of 20 gut regions**. (G)** pixel intensity, as measured on Fiji, of GFP in different regions of GFP stained Eaat1-venus 10F female flies, between 7 and 15 days of age. n=12 guts. The green line denotes the mean whole-gut pixel intensity. WG denotes whole gut. HG denotes hindgut. The regions crop, cardia, R2, R2, R3, R4, R5 and R5 correspond to regions 1-8 in **(H)**; representative images of GFP-stained venus-tagged Eaat1 10F female intestines. The numbered blue lines indicate the different regions measured, and the legend denotes how the numbers correspond to the regions in **(G). (I)** Representative images from Eaat1-venus guts stained with DAPI, GFP and phalloidin. GFP enhances the signal of venus-tagged Eaat1, phalloidin stains F-actin, and DAPI stains the nuclei. White arrows indicate the locations of some punctate GFP expression. **(I')** z-stack from re-sliced region of **(I)**. The dotted line indicates the border of the intestinal lining (left) and the intestinal lumen (lower right). **(J)** Schematic of image-processing procedure to reslice and z-project the acquired image stack in imageJ Fiji to look laterally across the cell. Original images were acquired inversely on Zeiss 800 confocal microscope. Z-stacks were taken from the top of the gut, into the lumen. A couple of nuclei were selected using the rectangle tool. This section was resliced (image -> stacks -> reslice) to generate a z-stack ventrally. This changes the X-Y-Z axis orientation. The resultant stack was then z-projected to generate a maximal projection across the cells. Box plots show the 25-75th percentiles and the median with the whiskers extending from min-max. Asterisks denote the result of **(A, B)** an unpaired t-test, **(C)** a kruskal-wallis test, or **(D-F)** a one-way Anova, where * P<0.05, ** P<0.01, *** P<0.001, **** P<0.0001.

7.3.4 Knockdown of *Eaat1* reduces lifespan dependent on the level of knockdown

Following the observation that expression of *Eaat1* decreases with age, I wanted to understand whether this reduced expression has a physiological effect.

For this I knocked down *Eaat1* levels in the intestine using the TIGS driver, and two separate *Eaat1* knockdown lines; *Eaat1* TRiP (BDSC 43287), and *Eaat1* shRNAi (VDRC 330103). No lifespan effect was observed upon induction of knockdown using the *Eaat1* TRiP line (Figure 7.2A) although there was an increased proportion of smurfs at 10 and 29 days upon *Eaat1* knockdown (Figure 7.2B). In contrast, knockdown of *Eaat1* expression using the *Eaat1* shRNAi line resulted in a reproducible median lifespan reduction of 6 and 12 days (Figure 7.2D and F), and an increased proportion of smurfs, although not at every timepoint (Figure 7.2E and G).

The difference in lifespan response upon *Eaat1* knockdown may be due to the level of knockdown achieved. *Eaat1* shRNAi results in a much stronger level of knockdown compared to *Eaat1* TRiP (Figure 7.2H compared to C). This may suggest that only low levels of *Eaat1* are required to fulfil its function, or perhaps that another transporter is able to compensate for the reduced *Eaat1* levels up to a certain point.

7.3.5 Inconsistent effect of late-life *Eaat1* knockdown

As reduced *Eaat1* levels appear with advanced age in wild-type flies, I wanted to understand the impact of knocking down *Eaat1* expression only in later life. Here I transferred flies from ethanol control food, onto RU-486 food to induce knockdown, at 35 days of age. In replicate 1, this was at T_{95}, and the full-life knockdown lifespan had already diverged from the control lifespan (Figure 7.2D). In the second replicate, 35 days was at T_{90} and the control and full-life knockdown lifespans were still tracking each other.

Induction of late-life knockdown extended lifespan, compared to control, by 6 days (Figure 7.2D) in the first replicate, indicating that the observed reduction in *Eaat1* levels with age may be an adaptation or response to increase organismal health and thereby longevity. Late-life knockdown had the opposite result in the second replicate, however, resulting in a lifespan reduction of 14 days compared to the control, and 2 days compared to full-life knockdown (Figure 7.2F).

This inconsistency in response may be due to the point within the lifespan that knockdown is induced. It is also possible that this reversal in response could be due to differences within microbial composition, with knockdown advantageous in the presence or absence of specific microbial populations. Perhaps those which synthesise or utilise Eaat1 substrates most highly, although as these lifespans were conducted relatively close together, such variation is questionable as we would not expect much microbial fluctuation within the stocks.

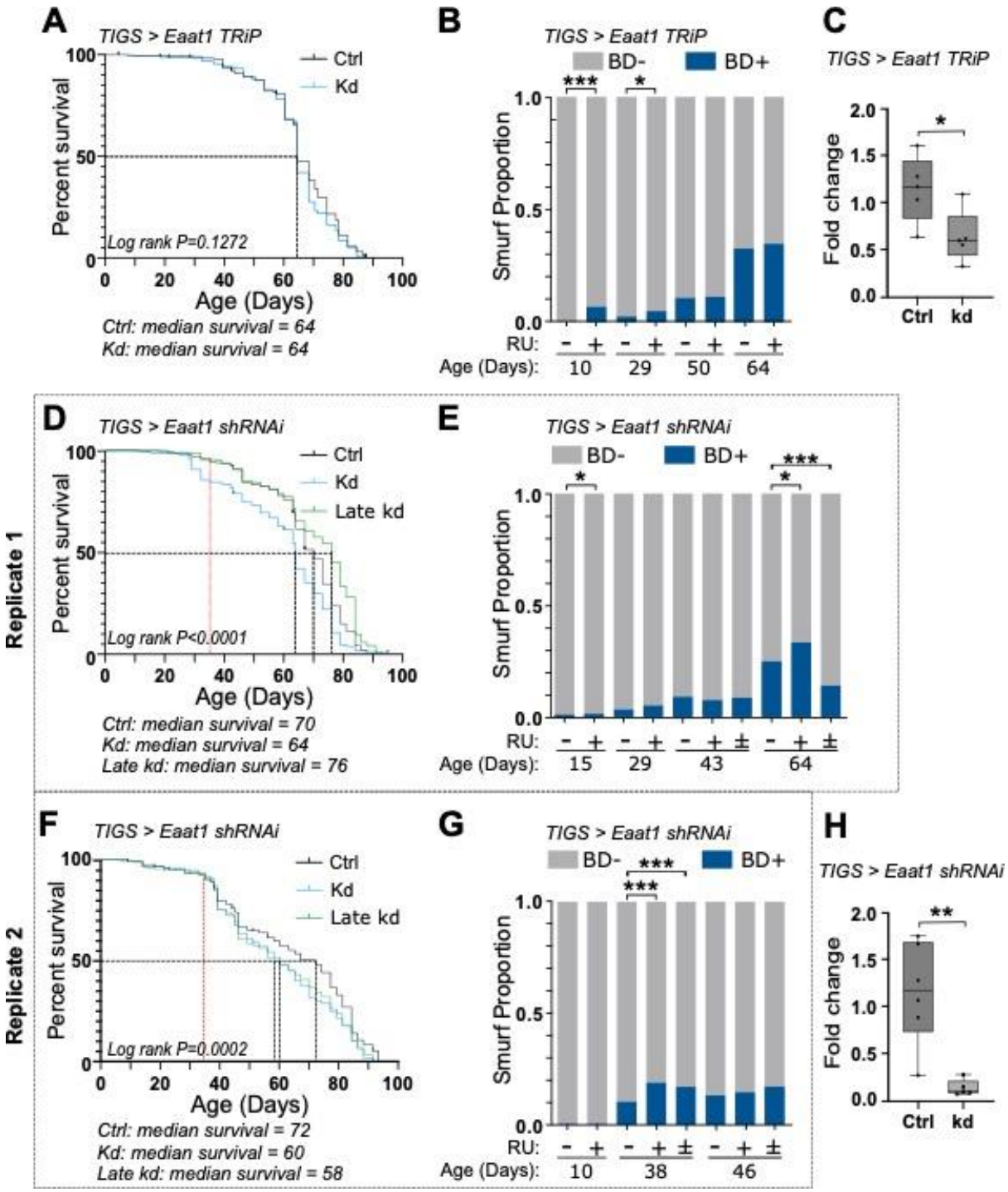
A
TIGS > Eaat1 TRiP
Ctrl
Kd
Percent survival
Log rank P=0.1272
Age (Days)
Ctrl: median survival = 64
Kd: median survival = 64
B
TIGS > Eaat1 TRiP
BD-
BD+
Smurf Proportion
RU:
Age (Days):
C
TIGS > Eaat1 TRiP
Fold change
Ctrl
kd
D
TIGS > Eaat1 shRNAi
Late kd
Log rank P<0.0001
Ctrl: median survival = 70
Kd: median survival = 64
Late kd: median survival = 76
E
TIGS > Eaat1 shRNAi
Replicate 1
F
TIGS > Eaat1 shRNAi
Log rank P=0.0002
Ctrl: median survival = 72
Kd: median survival = 60
Late kd: median survival = 58
G
TIGS > Eaat1 shRNAi
Replicate 2
H
TIGS > Eaat1 shRNAi

Figure 7.2 | Lifespan shortening effect of intestinal Eaat1 knockdown dependent on the strength and length of knockdown

(A) lifespan and **(B)** corresponding smurf proportion of Tigs > Eaat1 TRiP on defined media. **(B)** proportion of smurfs observed in Tigs > Eaat1 TRiP. **(C)** expression of Eaat1 in whole-gut Tigs > Eaat1 TRiP samples, depicted as fold-change, relative to the expression of rp49. **(D, F)** 2 lifespan replicates and **(E, G)** corresponding smurf proportions, of Tigs > Eaat1 shRNAi flies on defined media. **(F)** expression of Eaat1 in whole-gut Tigs > Eaat1 shRNAi samples, depicted as fold-change, relative to the expression of alpha-tubulin. For all lifespans (**A, D, F**), dashed black line denotes median survival. Ethanol (control (ctrl); black), 25uM Ru-486 (knockdown (kd); blue) or **(D, F)** transferred from ethanol to 25mM RU-486 at 35 days of age (Late kd; green). For all smurf proportions **(B, E, G)** BD+ denotes smurf flies with barrier dysfunction. *BD- denotes non-smurf flies, without evidence of barrier dysfunction*. Addition of RU, and subsequent knockdown denoted by +. Late knockdown flies denoted by ±. **(A, B, D, E, F, G)** n > 285 flies per condition, per replicate at day 1. **(C, H)** n=6 samples of 5 midguts/condition. Box plots show the 25-75th percentiles and the median with the whiskers extending from min-max. Asterisks denote the result of **(B, E, G)** *binomial tests, or **(C, H)** unpaired t-test, where * P<0.05, **P<0.01, ***P<0.001 and ****P<0.0001.*

7.3.6 *Eaat1* knockdown does not impact AMP expression or bacterial load

I hypothesised that *Eaat1* knockdown may result in changes to microbial load, with knock-on effects to antimicrobial peptide expression, by increasing the luminal availability of *Eaat1* substrates.

Bacterial genomic DNA was isolated from whole-fly samples and assayed by qPCR with universal 16s primers, and levels of *Diptericin* and *Drosomycin* were assayed by RT-qPCR from dissected midguts (cardia to midgut-hindgut junction). Midguts were dissected from the same cohort of flies as the second *Eaat1* shRNAi lifespan (Figure 7.3F), and bacterial genomic DNA samples were taken from an independent cohort of flies.

There was a trend towards increased bacterial load with age, and a significant increase in bacterial load upon loss of intestinal barrier function (Figure 7.3A, Ordinary one-way Anova, $P < 0.05$), but there was no difference in the bacterial load of *Eaat1* knockdown flies compared to ethanol controls.

Looking at the levels of DPT, the expected increase in expression with age was observed (Figure 7.3B, 2-way anova, $P = 0.04$), and there was no statistically significant effect of *Eaat1* knockdown, although at day 46 expression did appear lower and less variable in Eaat1 knockdown than control flies.

There was no significant effect of either age or *Eaat1* expression on DRS levels (Figure 7.3C), although late induction of *Eaat1* knockdown appeared to lead to a non-significant reduction in DRS

levels and expression variance. Late-life knockdown results should however be taken with caution due to the variable lifespan results of this intervention.

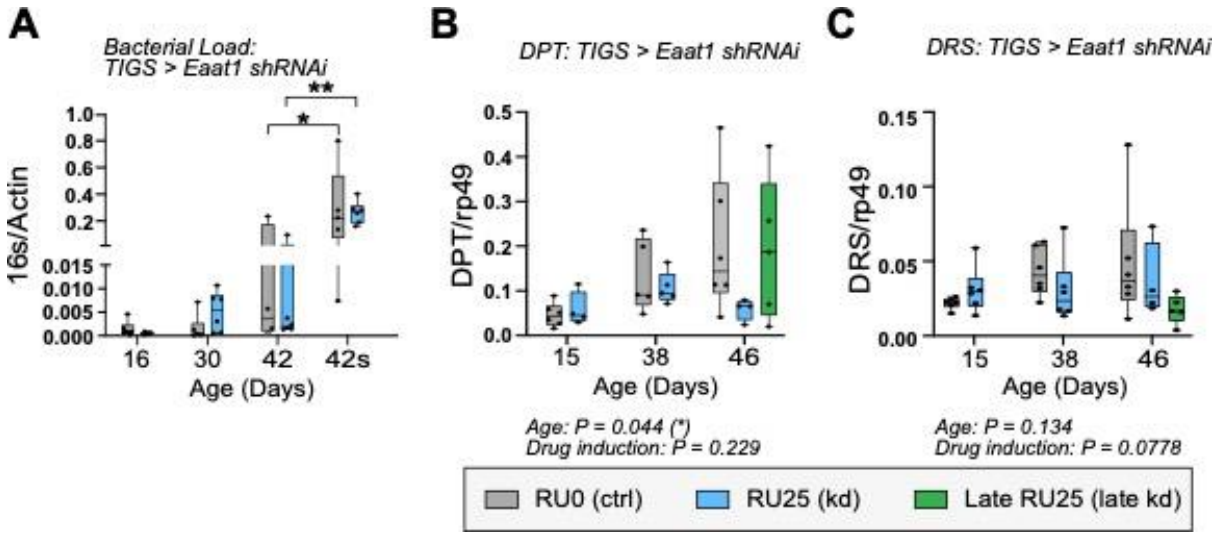

Figure 7.3 | Eaat1 knockdown does not impact the expression of AMPs, or internal bacterial load changes expected with age

(A) Internal bacterial load of 16 day, 30 day, 42 day and 42 days smurf (49S) mated female TIGS>Eaat1 shRNAi females, with and without induction of intestinal slif knockdown. Internal bacterial load measured using universal primers for the 16s rRNA gene, normalised to the actin gene. Expression of **(B)** diptericin (DPT) and **(C)** Drosomycin (DRS) in the midgut of conventionally reared TIGS>Eaat1 shRNAi with and without induction of knockdown, at 15, 38 and 45 days of age (flies with late induction of knockdown also shown at 45 days. Knockdown induced at 35 days of age). Expression normalised to the expression of rp49. n = 4-6 samples/age/condition. Box plots show the 25-75th percentiles and the median with the whiskers extending from min-max. Asterisks denote the result of (A) an ordinary one-way Anova with Holm Sidaks multiple comparison or **(B, C)** a 2-way Anova with Tukeys multiple comparisons, where * P<0.05 and **P<0.01. multiple comparisons within treatment groups, or between groups at one age only are shown. Result of 2-way Anova source of variation shown below each graph.

7.3.7 Inconsistent effect of *Eaat1* overexpression

As there is decreased intestinal *Eaat1* expression with age, and full-life knockdown leads to a lifespan reduction, I wanted to assess whether rescuing this reduced expression through overexpression of *Eaat1* would increase lifespan.

As with the *Eaat1* knockdown, I overexpressed *Eaat1* for the full adult lifespan. From the two replicates of this lifespan performed, I gained inconsistent results, with one replicate showing a lifespan-shortening effect of 7 days upon *Eaat1* overexpression (Figure 7.4A), and the other showing a lifespan extension of 9 days (Figure 7.4C). Induction of late-life *Eaat1* overexpression was included in the second replicate with the aim of rescuing just the age-related decrease in *Eaat1*. This late-life

overexpression increased lifespan by 7 days compared to control, and reduced it by 2 days compared to full-life overexpression (Figure 7.4C).

The proportion of smurfs for each replicate matched the lifespan effect observed, with higher smurf proportions upon eaat1 overexpression compared to control in replicate 1, although this was only significant at day 43, and the proportions equalised by day 50 (Figure 7.4B). Replicate 2, which showed an increased lifespan upon *Eaat1* overexpression, had a lower proportion of smurfs upon *Eaat1* overexpression compared to control, although this was only significant at day 46 (Figure 7.4D). Interestingly, despite the full-life knockdown having the longest lifespan, the proportion of smurfs following late induction of overexpression was lower than that of the full-life induction, although whether this is significant has not been tested (Figure 7.4D).

The reasons for the differences observed between replicates is unclear. Both lifespans were maintained on defined media, which reduced batch variation in the diet[222]. As with the *Slimfast* overexpression lifespans (section 6.3.3), these were run at different times of the year, replicate 1 beginning in October, and replicate 2 in May of the following year. There were issues with the temperature of the lab when replicate 1 was started, with temperatures reaching up to 29°C. Whilst the flies were maintained in an incubator held at 25°C, they were exposed to the laboratory temperature during sorting and flipping. Such variation in temperature could conceivably alter the flies' response to genetic perturbation, as well as the level of knockdown.

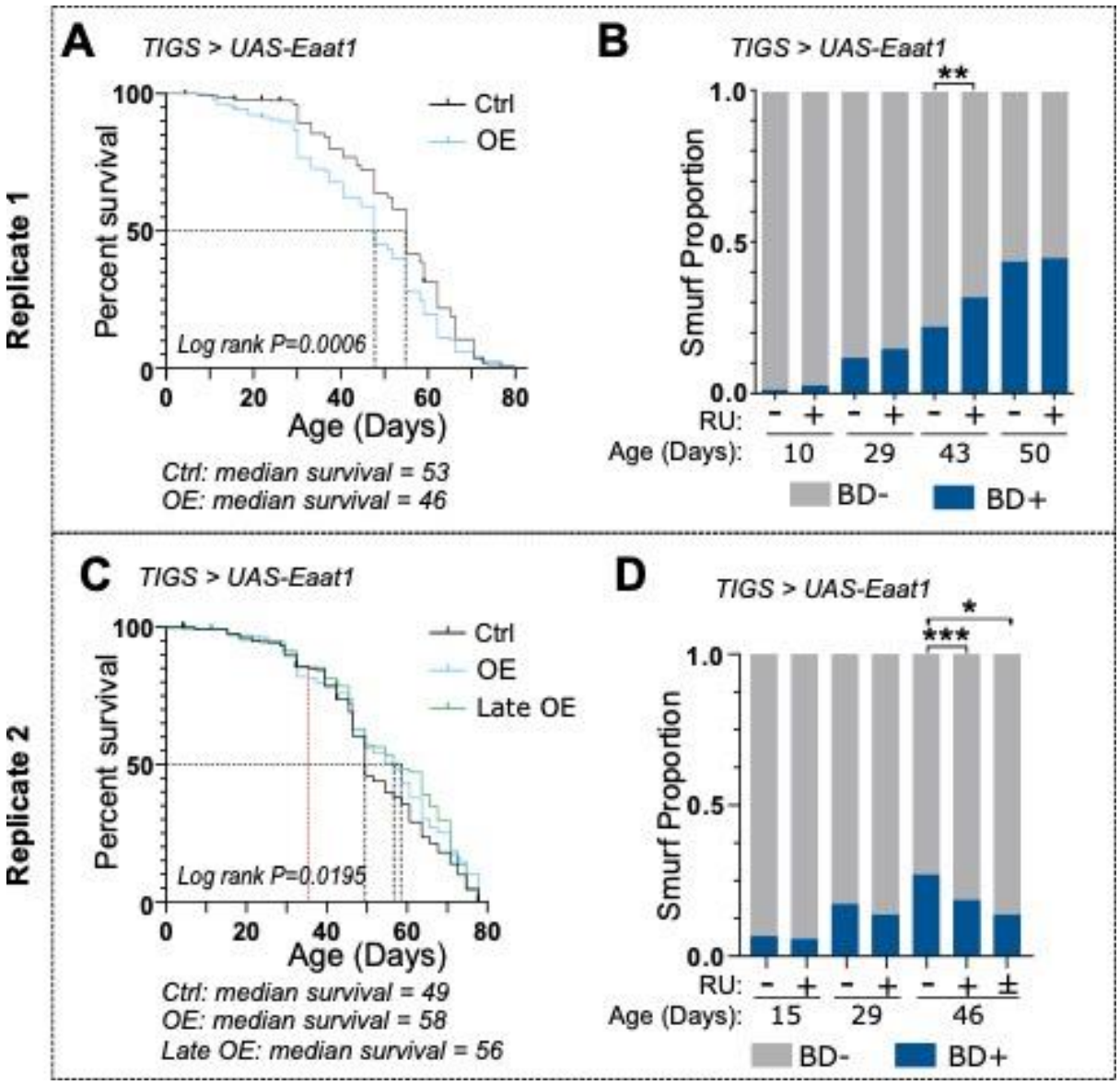

Figure 7.4 | Inconsistent lifespan effect of Eaat1 overexpression on lifespan and intestinal barrier integrity

(A, C) 2 lifespan replicates of conventionally colonised mated TIGS > UAS-Eaat1 females on defined media with ethanol (control (ctrl); black), 25uM Ru-486 (overexpression (or); blue), or **(C)** transferred from ethanol to RU-486 at 35 days of age (Late overexpression; green). Dashed black line denotes the median survival. Dashed red line denotes the transfer from ethanol media to RU media. **(B, D)** Proportion of smurf and non-smurf conventionally colonised TIGS > UAS-Eaat1 flies on control defined media or RU treated media to induce slif overexpression, at **(B)** 10, 29, 43 and 50 days of age, and **(D)** 15, 29 and 49 days of age. Addition of RU, and subsequent overexpression denoted by '+'. Late overexpression flies denoted by '±'. The proportions of smurfs in **(B)** were taken from flies in lifespan **(A),** and the proportion of smurfs in **(D)** were taken from flies in lifespan **(C).** BD+ denotes smurf flies with barrier dysfunction. BD- denotes non-smurf flies with no evidence of barrier dysfunction. n > 285 flies per condition, per replicate at day 1. Asterisks denote the result of **(B, D**) binomial tests, where * P<0.05, **P<0.01, ***P<0.001 and ****P<0.0001.

7.3.8 *Eaat1* overexpression does not impact AMP expression or bacterial load

I hypothesised that *Eaat1* overexpression may result in changes to microbial load, with knock-on effects on antimicrobial peptide expression, by reducing the luminal availability of *Eaat1* substrates.

Bacterial genomic DNA was isolated from whole-fly samples and assayed by qPCR with universal 16s primers, and levels of D*iptericin* and *Drosomycin* were assayed by RT-qPCR from dissected midguts (cardia to midgut-hindgut junction). Samples were collected from the same cohort of flies as the second *UAS-Eaat1* lifespan (Figure 7.4C)

There was a trend towards increased bacterial load with age, and a significant increase in bacterial load upon loss of intestinal barrier function (Figure 7.5A, Ordinary one-way Anova, $P < 0.05$), but there was no difference in the bacterial load of *Eaat1* overexpression flies compared to ethanol controls.

The expected increase in *DPT* expression with age was observed (Figure 7.5B, 2-way anova, $P = 0.035$), and there was no statistically significant effect of *Eaat1* overexpression, although, at day 29 DPT expression did appear lower and less variable in Eaat1 overexpression than control flies, but this was reversed at day 46 and was not found to be significant by post-hoc tests.

There was also no effect of age on *DRS* expression (2-way Anova, $P > 0.2$), as expected. Additionally, overexpression of *Eaat1* did not impact *DRS* expression levels (Figure 7.5C, 2-way Anova, $P > 0.3$).

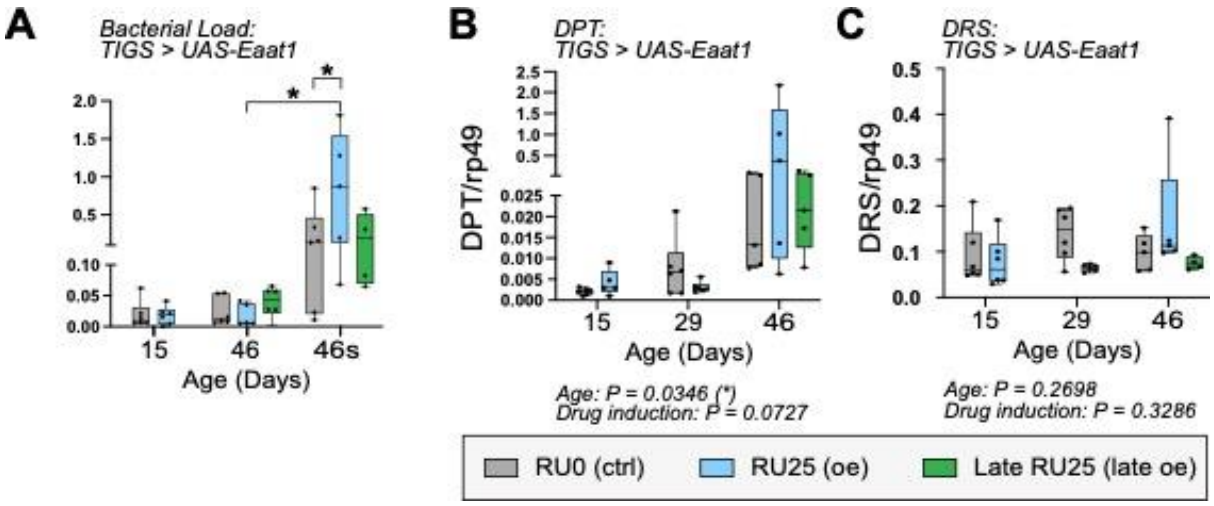

Figure 7.5 | Eaat1 overexpression does not impact intestinal barrier dysfunction or readouts of immune activity.

(A) Internal bacterial load of 15 day, 46 day and 46 days smurf flies (49S) mated female TIGS>UAS-Eaat1 females, with and without induction of intestinal Eaat1 overexpression, and with late induction of Eaat1

overexpression (green). Internal bacterial load measured using universal primers for the 16s rRNA gene, normalised to the actin gene. Expression of **(B)** diptericin (DPT) and **(C)** Drosomycin (DRS) in the midgut of conventionally reared TIGS>UAS-Eaat1 flies with and without induction of overexpression, at 15, 29 and 46 days of age (flies with late induction of overexpression also shown at 46 days. Overexpression induced at 35 days of age). Expression normalised to the expression of rp49. n=4-6 samples/age/condition. Asterisks denote the result of **(A)** an ordinary one-way Anova with Holm Sidaks multiple comparison, and **(B, C)** a 2-way Anova with Tukeys multiple comparisons, where * P<0.05, **P<0.01, ***P<0.001 and ****P<0.0001. Result of 2-way Anova source of variation shown below each graph.

7.3.9 *Eaat1* expression does not impact JNK signalling

Due to the changes in *Eaat1* expression with age, I wanted to understand whether manipulations in any age-related pathways impact *Eaat1* expression, or conversely whether changes in *Eaat1* impact the activity of these age-related pathways. As mentioned previously, other members of the lab drove JNK pathway activity by inducing the expression of a constitutively active *Hep.CA.*

Assaying the expression of *Eaat1* in dissected guts from *TIGS>UAS-Hep.CA* flies with and without induction of the transgene, by RT-qPCR, showed no change in the expression of *Eaat1* upon JNK pathway activity (Figure 7.6A, unpaired t-test, P > 0.05). Additionally, assaying the levels of *Puc* expression in midgut samples from *Eaat1* knockdown and overexpression flies showed there to be no effect of *Eaat1* expression levels (*Eaat1* knockdown; Figure 7.6B, 2-way Anova P > 0.05 and *Eaat1* overexpression; Figure 7.6C, 2-way Anova P > 0.05). The expected increase in *puc* expression with age was preserved in *Eaat1* overexpression guts (Figure 7.6C, 2-way Anova P = 0.0019), however there was no significant effect of age in the *Eaat1* knockdown flies (Figure 7.6B, 2-way Anova P > 0.05).

7.3.10 Eaat1 expression does not impact immune response pathways

As previously discussed, PGRP functions upstream of the IMD pathway, which is activated with age in conventionally colonised flies. Activation of the IMD pathway through overexpression of PGRP did not impact *Eaat1* levels (Figure 7.6D).

There was also no significant effect of knockdown or overexpression of *Eaat1* on *Diptericin* levels (Figure 7.3B and Figure 7.5B) an AMP regulated by the IMD pathway, or on the levels of *Drosomycin* (Figure 7.3C and Figure 7.5C), an AMP typically expressed through toll pathway activity.

7.3.11 Eaat1 expression levels impact JAK-STAT pathway activity

Upd3 is a JAK-STAT ligand. We expect to see increased activation with advanced age, however, while there appeared to be a trend towards increased expression with increased age, this was not found to be significant in either the *Eaat1* knockdown or overexpression flies (knockdown; Figure 7.6E, 2-way Anova $P > 0.25$ and overexpression; Figure 7.6F, 2-way Anova $P > 0.07$). Interestingly, there was a significant effect of overexpression on the levels of *upd3* when overexpression was induced (Figure 7.6F, 2-way Anova $P < 0.05$), with mean *upd3* expression lower in *Eaat1* overexpression guts. Additionally, when only including days 15 and 38 in the analysis, *Eaat1* knockdown significantly increases upd3 levels (2-way anova $P = 0.0071$, tukeys post-hoc test $P<0.05$ at day 15 and day 38). This is not significant when including the entire dataset as the P-value is adjusted based on the number of comparisons made. Unfortunately, only 3 samples where knockdown was induced were useable at day 45 which due to the large variance in *upd3* expression across samples of each group, may be the reason knockdown induction does not remain significant when this time point is accounted for.

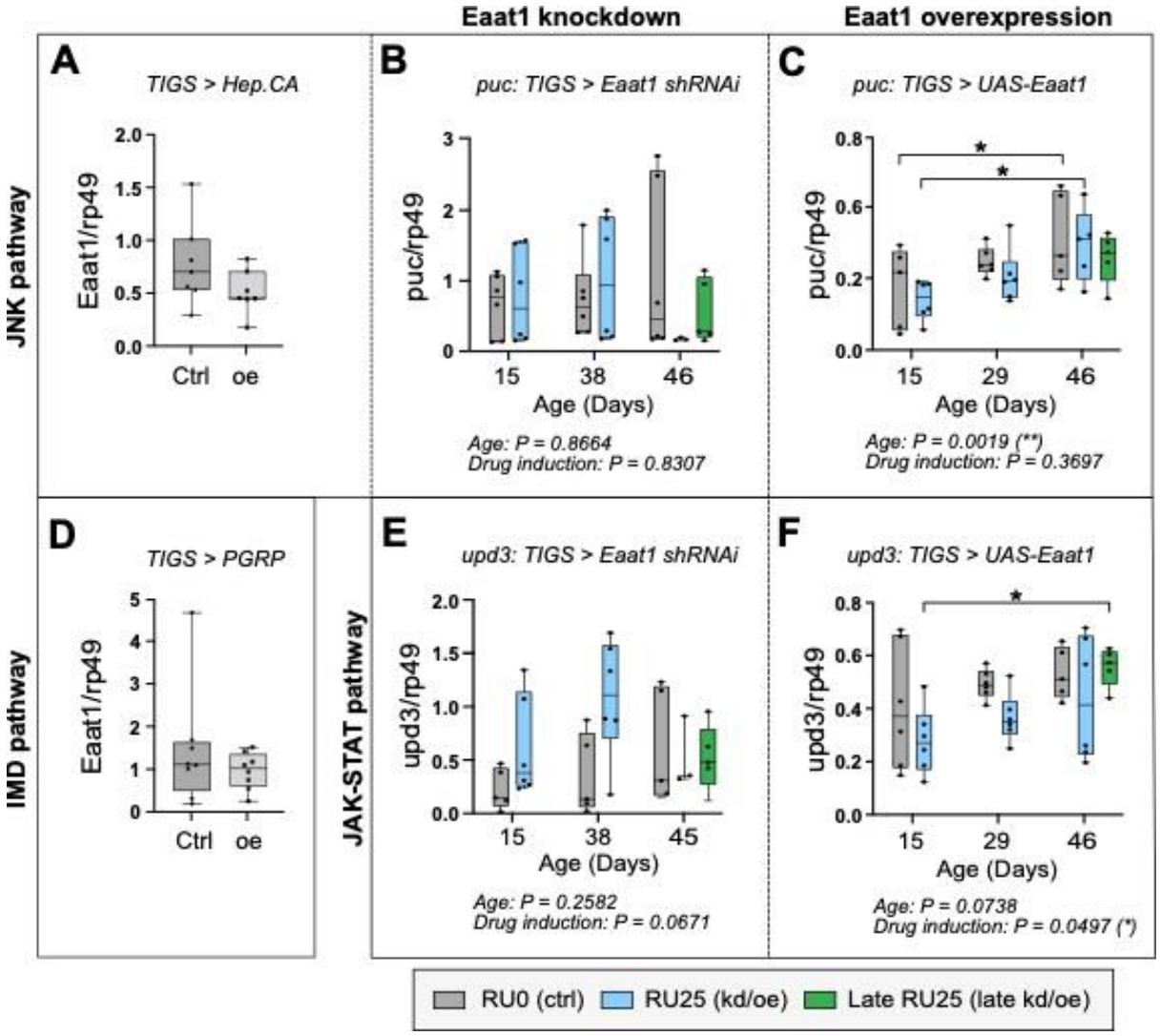

Figure 7.6 | Eaat1 expression, impacts JAK-STAT but not JNK or IMD pathway activity

(A-C) show manipulations to, or readouts of, the JNK pathway. **(A)** expression of Eaat1 normalised to rp49 in whole-gut samples of constitutively active hep.CA driven by TIGS geneswitch driver. Ctrl denotes control, where expression of Hep.CA was not driven. oe denotes overexpression, where addition of RU-486 to the fly food drove expression of a constitutively active Hep.CA. **(B,C)** The expression of puc, a readout of JNK pathway activity, with age, normalised to rp49, in the midgut of **(B)** Eaat1 knockdown flies (TIGS>Eaat1 shRNAi) and **(C)** Eaat1 overexpression flies (TIGS > UAS-Eaat1). The results of a 2-way anova are shown below. **(D)** expression of Eaat1 normalised to rp49 in whole-gut samples of PGRP overexpression flies (TIGS > PGRP). Overexpression of PGRP drives IMD pathway activity. Ctrl denotes control, where overexpression of PGRP was not driven. oe denotes overexpression, where addition of RU-486 to the fly food drove expression of a PGRP in the fly gut. **(E, F)** The expression of upd3, a readout of JAK-STAT pathway activity, with age, normalised to rp49, in the midgut of **(E)** Eaat1 knockdown flies (TIGS>Eaat1 shRNAi) and **(F)** Eaat1 overexpression flies (TIGS > UAS-Eaat1). The results of a 2-way anova are shown below. **(B, C, E, F)** RU25 denotes the addition of RU-486 to the fly food at a concentration of 25mg/ml, to drive knockdown or overexpression of Eaat1. n=3-8 samples(/age)/condition Box plots show the 25-75th percentiles and the median with the whiskers extending from min-max. Asterisks denote the result of **(B, C, E, F)** multiple comparisons from a 2-way Anova with Tukeys post-hoc test, **(A)** an unpaired t-test, or **(D)** a Mann-whitney test where * P<0.05, ** P<0.01, *** P<0.001, **** P<0.0001.

7.3.12 Eaat1 expression impacts intestinal stem cell proliferation

A previous study by Deng *et al.* 2015[565] found that knocking *Eaat1* down specifically in the enterocytes, using an enterocyte specific driver (*NP1::gal4*) resulted in increased cell proliferation. They went on to show that increased luminal glutamate levels, which would result from the Eaat1 knockdown, stimulate metabotropic glutamate receptors on stem and progenitor cells, stimulating proliferation.

I wanted to see whether this result would be replicated, so whole-guts from *TIGS>Eaat1 shRNAi* flies, with and without induced knockdown, were stained against a mitotic marker, phosphorylated histone-H3 (PH3), to quantify intestinal stem cell proliferation.

To my surprise, I found a significant reduction in stem cell proliferation upon *Eaat1* knockdown, which was reproducible across 3 replicates, each of 6-15 guts (Figure 7.7A, mann-whitney $P < 0.0001$). This is in contradiction to the results of the previous study. I hypothesised that this may be a result of the different drivers used, with TIGS being expressed in enterocytes as well as a stem cells[818], whilst *NP1::gal4* is restricted to enterocytes. To assess whether knockdown of *Eaat1* in ISCs is sufficient to reverse the expected result and reduce stem cell proliferation, pH3 counts were taken from *5961-GS>Eaat1 shRNAi* flies, with and without induced knockdown. We once again found a significant reduction in stem cell proliferation upon stem-cell-specific knockdown (Figure 7.7B, mann-whitney $P < 0.05$). Of note, the study by Deng *et al*.[565] used the *Eaat1-TRiP* (BDSC 43287) line which showed lower levels of knockdown than the *Eaat1 shRNAi* line used here (Figure 7.2C and H), which may have an impact on the observed results.

I also assessed the level of ISC proliferation in *TIGS>UAS-Eaat1* flies, with and without induction of *Eaat1* overexpression. In alignment with the finding that eaat1 knockdown driven by TIGS reduces ISC proliferation, TIGS driven overexpression results in a significant increase in stem-cell proliferation (Figure 7.7C, Mann-whitney $P < 0.05$), suggesting that it is the driver and not the strength of knockdown leading to the differences between this study and that by Deng and colleagues[565]. It should be noted that this result is from only one replicate, of which only 3 guts were viable for the control group.

This data adds to previous work implicating L-glutamate in stem cell proliferation, and suggests that ISC-specific expression of *Eaat1* is required for induction of stem-cell proliferation. This may indicate that mGluR's are only one arm of the ISC replicative response to L-glutamate.

7.3.13 Eaat1 responds dynamically to changes in luminal L-glutamate concentration

Due to the variability in *Eaat1* expression, particularly in young flies, I hypothesised that *Eaat1* levels may be modulated according to the levels of substrate available within the lumen. To test this hypothesis, I fed Canton-S mated females defined media, with varying concentrations of NaGlu, where 1x NaGlu is the concentration within standard defined media and assessed the expression of *Eaat1* in dissected midguts by RT-qPCR. There was a trend towards increased levels of *Eaat1* on diets containing lower NaGlu, although this was only significant at 0.5xNaGlu (Figure 7.7E, one-way Anova $P< 0.05$). This suggests that the expression of *Eaat1* is dynamically regulated according to glutamate availability, increasing *Eaat1* expression when NaGlu concentrations are low, to compensate for the reduced availability.

I was also interested to see whether changes in NaGlu concentration would impact ISC proliferation. pH3 counts were taken from the same cohort of Canton-S females on the defined media with varying NaGlu concentrations. Increasing dietary L-glutamate concentration has previously been shown to increase stem cell proliferation[565]. Whilst there was a trend towards increased ISC proliferation with increased concentrations of dietary NaGlu, this was not found to be significant (Figure 7.7D, 1-way anova $P > 0.05$). The reason for this discrepancy is likely the concentrations used, with the previous study using a diet containing 1% L-Glutamate[565], where the highest concentration of NaGlu used here is over 12-fold lower. Indeed, when the previous study used a more comparable 0.1 % glutamate diet, they observed a modest and not-significant increase in ISC proliferation. The concentrations chosen here are more physiologically relevant, as faecal glutamate concentrations doubled in sterile flies, and only increased by 1/3 with age in conventional flies (chapter 4).

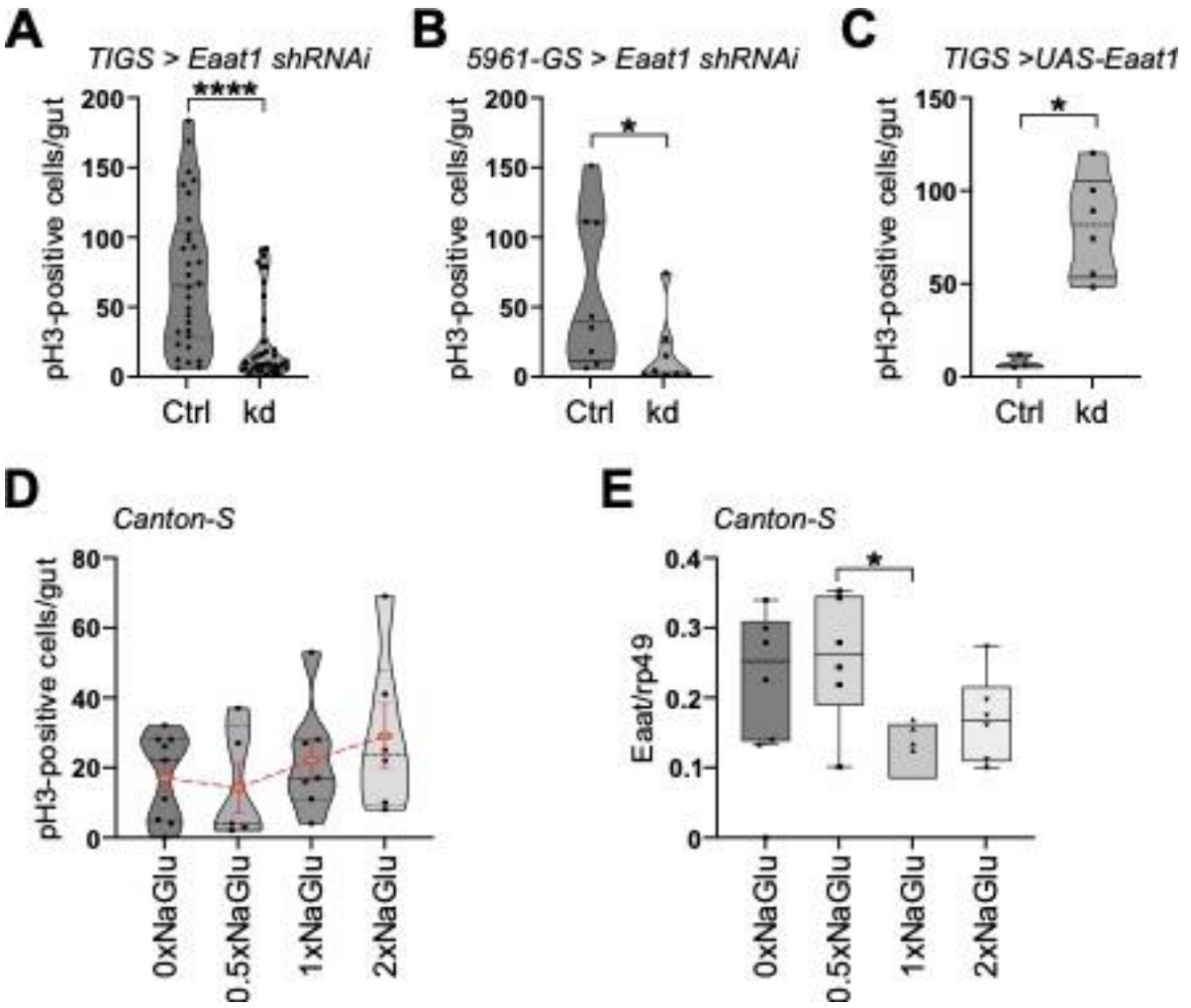

Figure 7.7 | Changes to intestinal glutamate concentration through Eaat1 expression or dietary NaGlu concentration impact intestinal proliferation.

Quantification of changes in mitotic indices of intestines where **(A)** Eaat1 was knocked down in the enterocytes and stem cells; TIGS > Eaat1 shRNAi, **(B)** Eaat1 was knocked down in the stem and progenitor cells; 5961-GS > Eaat1 shRNA, **(C)** Eaat1 was overexpressed in the enterocytes and stem cells; TIGS > UAS-Eaat1 flies and **(D)** Canton-S flies were fed defined media containing different concentrations of NaGlu**. (A-C)** The number of pH3 cells was compared between vehicle control and drug-induced (A and B) knockdown or **(C)** overexpression. **(D)** the number of pH3 positive cells was compared to the control diet (standard defined media) 1xNaGlu. **(E)** the expression of Eaat1 was quantified in midgut samples taken from Canton-S females fed defined media containing varying concentrations of NaGlu. 1xNaGlu (standard defined media) was the control. Eaat1 expression levels were normalised to the levels of rp49. The red point depicts the mean±SEM. Violin plots show the median (bold dashed line) and the 25-75th percentiles (dotted line). Box plots show the 25-75th percentiles and the median with the whiskers extending from min-max. n > 3 guts (pH3 counts) or n > 5 samples (qPCR) per condition. Asterisks denote the results of **(A-C)** a Mann-Whitney or (**D, E)** a one-way Anova, where * P<0.05, ** P<0.01, *** P<0.001, **** P<0.0001

7.4 Discussion

7.4.1 Characterisation of eaat1 expression and regulation

As the presence and role of Eaat1 in the *Drosophila* intestine has not been well studied, I characterised the expression of *Eaat1* along the length of the intestine by RT-qPCR and immunofluorescence. While in mice, *EAAT3* expression increases towards the end of the small intestine, with poor expression in the duodenum and jejunum, and very high expression in the brush border of the ileum[819], previous data using *Eaat1-gal4>UAS*-eGFP flies has shown highest expression in the anterior midgut of *Drosophila*[565]. My RT-qPCR expression data is in agreement with much lower expression in the posterior than anterior midgut, however this trend was less clear when assessing protein levels - highlighting the caveat that expression levels do not always equate to protein levels.

EAAT1 has been shown to localise towards the membrane of EAAT1-GFP transfected SL2 cells[566], a non-neuronal *Drosophila* cell-line. Additionally, the study by Hu *et al.* showed very clear EAAT3 localisation on the brush-border membrane of the ileum in mice, however they also identified cytoplasmic EAAT3 protein in the colon[819]. Given the variation in EAAT3 subcellular localisation in mice, and the indication of higher *Eaat1* expression in the *Drosophila* anterior midgut, I wanted to assess the localisation of Eaat1 in this region. There was a clear localisation to the apical membrane of cells consistent with its role in nutrient absorption, however there also appeared to be punctate dots of cytoplasmic expression. This perhaps indicates a dynamic regulatory process involving endocytic shuttling of the transporter to the membrane, or a store of Eaat1 within the cells. The cytoplasmic EAAT3 in mice was hypothesised to represent a pool of EAAT3 protein awaiting mobilisation when required[819].

RT-qPCR data hinted that expression of *Eaat1* is regulated according to substrate availability. Such dynamic expression of *Eaat1* in response to substrate levels, may help to explain some of the variability observed, particularly in the young gut samples. However, changing gene expression is not the only way to regulate substrate intake. Controlling receptor localisation is potentially a faster mechanism to adapt to changes in substrate availability; internalising Eaat1 when L-glutamate is plentiful, and shuttling it to the membrane in times of scarcity.

The apparent cytoplasmic expression may also indicate an association with intracellular organelles, indeed, human EAAT1 and EAAT2 have been detected on ribosomes and rough endoplasmic reticulum of human brain tissue, and EAAT2 has also been detected on outer mitochondrial membranes[820]. This association of EAAT2 is consistent with a previous report that it exists in a

multiprotein complex in close association with mitochondria[821]. Additionally, subsequent research has shown human EAAT1[822] and EAAT3[823] to associate with mitochondria, participating in glutamate stimulated ATP production[823]. That several of the human EAATs associate with mitochondria, suggests that this association is likely to be conserved. This is something that warrants further interrogation through co-localisation studies.

Given its role in amino acid absorption, it has been assumed that Eaat1 is expressed exclusively on absorptive enterocytes. My data however suggests that there is some level ISC expression as knockdown of *Eaat1* in stem and progenitor cells resulted in a clear phenotype. Whether this is a low-level of expression in all ISC's or expression only in a subset of ISCs remains to be determined. Additionally, as ISCs are not absorptive cells, and there is evidence to suggest localisation of EAAT proteins with subcellular organelles, it is possible that ISC EAAT1 has a different pattern of subcellular localisation which is more easily missed by immunofluorescence.

7.4.2 Discordance between JAK-STAT signalling and ISC proliferation may lead to premature death upon Eaat1 knockdown

Unpaired 3 (*Upd3*) is a cytokine ligand produced by ECs and EBs upon damage or shedding, responsible for activating the JAK-STAT pathway in progenitor cells to induce proliferation[47]. Released *upd3* binds to the receptor *Domeless* on stem and progenitor cell membranes. *Upd3* also provides an indirect readout of the stress-response JNK pathway, and is upregulated by IMD and Toll activation.

Here however changes in the expression of *Eaat1* did not impact *puc*, a readout of the JNK pathway, *DRS*, a readout of the Toll pathway or *DPT* a readout of the IMD pathway. Additionally, activation of the JNK or IMD pathways did not affect expression of Eaat1. Despite this, *Eaat1* appears to impact *upd3* levels; *Eaat1* knockdown increased *upd3* levels, whereas *Eaat1* overexpression reduced *upd3* expression. This increased *upd3* expression upon knockdown would be expected to activate JAK-STAT signalling and promote ISC proliferation. Unexpectedly, however, *Eaat1* knockdown appears to reproducibly reduce ISC proliferation, and the opposite of this atypical association is observed upon *Eaat1* overexpression. This unexpected response may be due to the cell types involved, with the ISC proliferative effect seemingly dependent on ISC *Eaat1* levels.

This may indicate varying degrees of strength of different ISC proliferative signals, with certain signals taking precedence. It may also indicate that variations in *Eaat1* expression have different

effects depending on cell type. It would be interesting to assess the levels of *upd3* expression when *Eaat1* knockdown is driven in stem and progenitor cells, but not ECs, using the *5961-GS* driver line. Any apparent difference in response between cell types may be due to Eaat1 localisation, or interaction with different proteins and pathways. As it stands, however, such interactions or even differential localisation patterns remain to be determined.

The cause of the reduced lifespan observed upon *Eaat1* knockdown remains unclear. It is possible that the observed late-life reduction in *Eaat1* is a mechanism to prevent excessive proliferation, however the reduction in cell proliferation, combined with increased *upd3* levels may indicate that ISC proliferation is dampened such that damaged and shed cells are not being replaced. It would be interesting to look at the proportions of different cell types, cell density and gut size following an extended period of *Eaat1* knockdown, to see if any of these measures are impacted.

7.4.3 A new model for the mechanism of stem-cell roles of Eaat1

7.4.3.1 Metabotropic glutamate receptors and Eaat1

Glutamate has been implicated in driving ISC expression through activation of metabotropic glutamate receptors (mGluR) in mice[603] and in *Drosophila*[565]. It has also been linked to proliferation in cancer cells[773,824,825]. Additionally, expression of *mGluR's* is sensitive to luminal L-glutamate concentration, with supplementation of L-Glutamate resulting in increased expression of porcine *mGluR1* and *mGluR4*[685].

Human mGluRs contain at least 8 different proteins which have been classified into three groups on the basis of their sequence homology, pharmacological profile and transduction pathways[785]. In contrast, *Drosophila* is considered to have only one functional mGluR; dmGluR, which shares the highest homology to group II mammalian mGluRs[787].

Interestingly, group I and group II mGluRs have been shown to impact the expression of *EAAT1* and *EAAT3* in opposite directions. Stimulation of group I mGluRs by agonists down-regulates expression and protein levels of the EAAT proteins, whilst stimulation of group II mGluRs up-regulates EAAT expression and protein levels, with these changes blocked by selective antagonists of each group[815].

7.4.3.2 Homeostatic calcium signalling

Calcium oscillations in non-excitable cells are generated through the through influx and efflux of calcium from the ER or extracellular space. Store-operated calcium entry (SOCE) is the mechanism by which calcium concentrations in the ER, and by extension the cytoplasm, is dynamically

controlled[826–828]. Cytoplasmic calcium concentrations are reduced as sarco-endoplasmic reticulum ATPase (SERCA) pumps cytosolic Ca^{2+} into the ER, and sodium-calcium exchanger (NCX) or plasma membrane calcium ATPase (PMCA) pump cytosolic ca^{2+} out of the cell[826–828]. A decrease in ER calcium is sensed by stromal interaction molecule (STIM), an ER membrane protein that opens the plasma membrane Ca^{2+} channel Orai, allowing influx of extracellular calcium into the cytoplasm[826–828]. This process is conserved in *Drosophila*[565].

Changes to the frequency of oscillation, specifically a prolonged increase in cytosolic calcium, has been shown to stimulate ISC proliferation[565]. These changes have been shown to occur upon activation of several proliferative stimuli, including overexpression of the InR or JNK pathways, or knockdown of *Notch*[565].

7.4.3.3 EAAT1 and NCX

As mentioned, there is compelling evidence that EAAT proteins are found on internal membranes, as well as the plasma membrane. Interestingly, mitochondrial co-localisation of EAAT3 and the sodium/calcium exchanger 1 (NCX1) has been shown in human neuronal, glial and cardiac muscle[823], as well as at the plasma membrane[829]. NCX1 is involved in the extrusion of calcium from the cell, or into the mitochondria, however reversal of its transport has been shown to occur upon high levels of sodium[830–835]. Interestingly, in mitochondria activity of EAAT3 is sustained by its association with NCX[823]. A similar dependency may exist at the plasma membrane[829,836].

EAAT transports glutamate into cells alongside $3Na^{+}$, so it is possible that increased EAAT levels and subsequent increased glutamate transport result in high Na^{+} levels and a reversal of the direction of NCX transport[836]. This may be sufficient to prolong high intracellular Ca^{2+} levels sufficiently to induce proliferation.

7.4.3.4 Adaptations to the proposed model

Deng and colleagues[565] proposed that enterocyte-specific knockdown of *Eaat1* leads to increased luminal glutamate concentrations which activate dmGluRs on ISCs, and result in a prolonged increase in cytosolic calcium and promotion of ISC proliferation.

I present a new model (Figure 7.8), whereby increasing luminal glutamate through diet or EC-specific *Eaat1* knockdown, leads to activation of dmGluR and consequent upregulation of *Eaat1* in ISCs. I suggest that upon increased *Eaat1* expression, driven by dmGluR activation, increased co-transport of glutamate with $3Na^{+}$ leads to reversal of NCX transport at the plasma membrane, prolonged periods of high cytosolic Ca^{2+}, and subsequent cell proliferation. In contrast, loss or reduction of

Eaat1 expression in ISCs suppresses proliferation by preventing the reversal of NCX transport and the subsequent high cytosolic Ca^{2+}. This suggests a permissive role of Eaat1 in homeostasis.

I believe the evidence for these amendments is compelling. I have shown that ISC expression of *Eaat1* is required for the previously observed increase in ISC proliferation upon EC-specific knockdown of the transporter[565]. *dmGluR* shared the highest homology with *mGluR* group II which, upon stimulation, up-regulate the expression of EAAT proteins. It has been shown through co-immunoprecipitation and affinity binding assays, that mGluR1 and a subunit of the NMDA receptor in humans interact[837]. Whether such an association between dmGluR and Eaat1 exists in ISCs remains to be determined, however, it may help explain the apparent link between the two proteins and ISC proliferation. Additionally, colocalization and mutual activity dependency has been shown between human EAAT3 and NCX1 on neuronal, glial and cardiac mitochondria[823], as well as the plasma membrane[829], and the reversal of NCX transport is known to occur in conditions of high Na^+ resulting in inward flow of Ca^{2+} into the cell. A local high Na^+ concentration is likely to occur when NCX is in association with EAAT proteins, which co-transport $3Na^+$ alongside each glutamate molecule.

Certain aspects of this model remain to be tested. First and foremost, whether ISC knockdown or overexpression of *dmGluR* does indeed result in reduced or increased *Eaat1* levels respectively. This may be hard to detect by RT-qPCR due to the low proportion of ISCs to ECs, where Eaat1 is also expressed. Concurrent EC-specific knockdown of *Eaat1* may be required alongside ISC overexpression of *dmGluR* in order to detect ISC-specific changes in *Eaat1* expression. Additionally, to my knowledge, association of NCX and Eaat1 has not been shown in *Drosophila*, nor any co-localisation of dmGluR and Eaat1, so this requires further investigation.

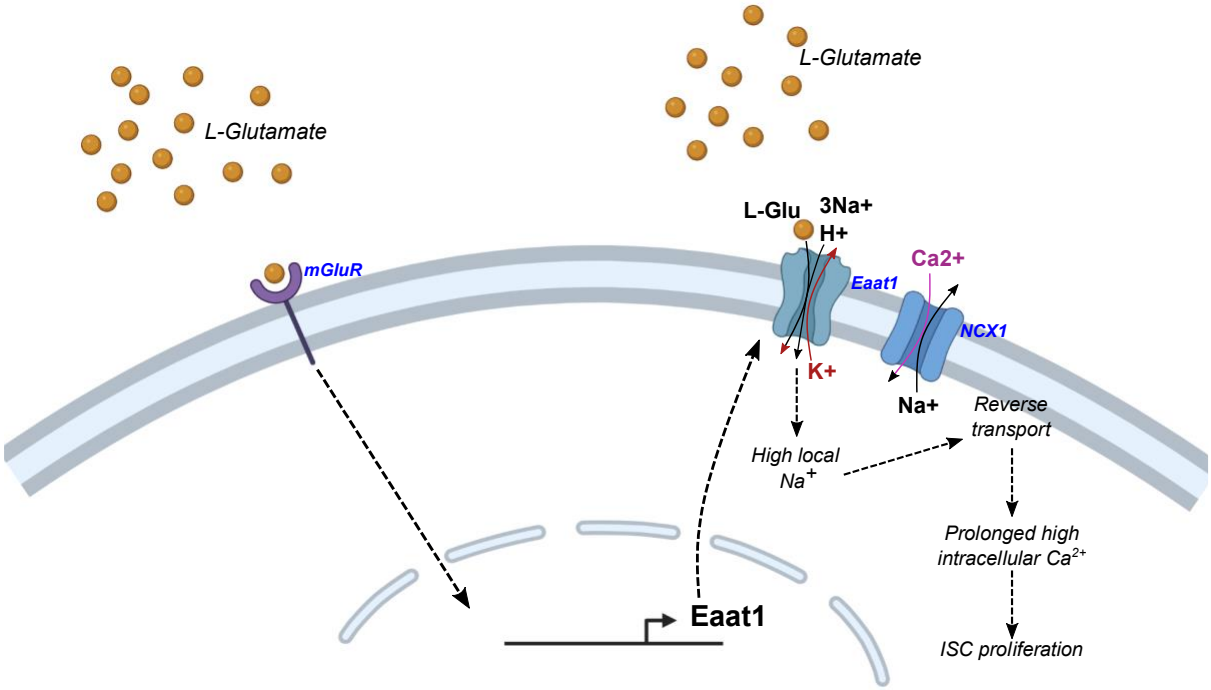

Figure 7.8 | High L-Glutamate levels drive intestinal stem cell division through Eaat1 mediated transport and reversal of NCX1 transport

High luminal L-glutamate stimulated mGluR receptor on ISC cell membranes and activating transcription of Eaat1. Eaat1-mediated L-glutamate transport creates a high local sodium (Na+) concentration which drives the sodium-calcium transporter (NCX1) towards transport reversal; sodium efflux and calcium influx. NCX1 transport reversal results in prolonged high intracellular calcium, and stimulates ISC proliferation.

7.5 Conclusion

Here I have characterised the expression profile of *Eaat1* in the *Drosophila* intestine, highlighting differences in the intestinal localisation of this transporter between *Drosophila* and mice. I have also provided evidence that, as well as its role and expression in enterocytes, Eaat1 has an important role in stem cells. Proper regulation of intestinal *Eaat1* expression is required for optimised survival, with knockdown of this transporter reducing lifespan, potentially through dysregulated stem cell proliferation. Overexpression of the transporter also resulted in a lifespan effect, although the direction of this effect was not consistent between replicates. Lifespan effects upon modulation of *Eaat1* expression also indicate that glutamate may impact lifespan, as well as glutamine which has previously been linked to lifespan and intestinal health.

On top of this, I have put forward amendments to the previously proposed model, that increased luminal glutamate increases stem cell proliferation through activation of a metabotropic glutamate receptor, and prolonged elevation of cytosolic calcium. I have shown that stem-cell Eaat1 levels are

important for this proliferative response, and suggested a new model, whereby stimulation of mGluR increases stem-cell Eaat1 levels. Interaction between Eaat1 and NCX, and increased glutamate transport, results in a high local sodium concentration, driving reversal of transport by NCX and promoting internal flux of calcium into the stem cells. This internal calcium transport prolongs the period of high cytosolic calcium concentrations, and thus promotes proliferation.

8 Thesis Discussion

8.1 The DUMP assay and protein management

It has been understood in the field that the intestine undergoes several changes with age which contribute to mortality[22,39,49,51,88,92]. The basic function of the intestine as an absorptive organ, however, is largely ignored. Despite this, the metabolic changes observed with increased age may begin at the point of nutrient uptake, rather than just changes to metabolism.

In this thesis, I aimed to utilise the defined media for *Drosophila* to interrogate age-related changes to intestinal nutrient dynamics. To begin, I characterised the ageing phenotypes of flies fed on defined media, providing a baseline to enable comparison between results from this, and our labs standard media (chapter 3). Confidence in the use of this media with ageing enabled the development of the DUMP assay, to assess the luminal/faecal nutrient profile of *Drosophila* (chapter 4).

Here, I observed changes to faecal amino acid dynamics, indicative of reduced uptake with advancing age. It is generally accepted that dietary needs change with age, specifically that the elderly population have a lower caloric requirement as they have lower energy expenditure. This, however, is based upon the assumption that they are absorbing ingested nutrients at the same efficiency as younger individuals, although this this may not always be true. Indeed, data here may support existing calls to increase the recommended daily amount of protein for the elderly, to prevent muscle loss.

Reductions in nutrient uptake, as this data indicates, would likely impact systemic metabolism. In mammals reduced concentrations of amino acids in the blood, reduces the stimulus for muscle growth, resulting in muscle loss over time. Additionally higher concentrations of protein must be ingested in the elderly to stimulate muscle growth. As well as contributing to sarcopenia and frailty, this has wider implications on systemic metabolism as skeletal muscle plays a central role in the regulation of systemic energy homeostasis, and metabolic syndrome[838,839].

This data may suggest that dietary interventions could prevent or be useful in the management of the loss of muscle mass and sarcopenia. A diet designed to mimic the increased luminal concentration of amino acids observed with advanced age, resulted in early life benefits despite an overall reduction in lifespan (chapter 5). This may indicate that the detrimental effects commonly observed upon high protein intake are age and context-dependent. It could be that high protein diets have an additive effect which leads to lifespan reductions. An interventional high-protein diet

should be tested in middle-aged to old flies, to assess whether late-life increases in protein lead to health benefits. Climbing assays may be particularly useful here to assess motility and muscle mass, or biochemical assays to measure organismal protein levels.

As well as impacting protein synthesis and systemic nutrition, amino acids also impact signalling pathways. Most notably mTORC1, who's activation results in reductions to lifespan. mTORC1 activity was not measured here, nor the levels of autophagy or apoptosis which are linked to mTORC1. Balancing protein intake to promote muscle maintenance, whilst preventing over-activation of mTOR may be key to promoting healthy longevity. This may be tested through co-feeding of the aged AA diet alongside rapamycin, the mTORC1 inhibitor, particularly in later life. If this is successful in maintaining muscle mass, as well as longevity, then it may have huge translational and therapeutic potential.

8.1.1 The DUMP assay and the microbiota

The DUMP assay (chapter 4) also showed that the microbiota greatly impacts the luminal/faecal amino acid concentrations, however the role or impact of the microbiota in nutritional requirements at different ages is an additional area which would benefit from further research. The factors that result in the observed increase in amino acid concentration remain unclear. As mentioned, the assay may be measuring amino acids within, or produced by, the intestinal microbiota. Microbial colonisation may also impact the luminal/faecal nutrient profile indirectly by changing host dynamics, although ultimately, it Is likely a combination of these options.

It is widely accepted that the composition of the microbiota changes with age, although the impact this may have on nutrition has not been assessed to date. Correlations between the microbiota and frailty have however been uncovered[101,290,840], as well as sarcopenia[831] and metabolic syndrome[841]. A deeper understanding of the nutritional impact of different microbial species or phyla may be important when assessing their impact on the health and longevity of individuals.

Running the DUMP assay with gnotobiotic flies, associated with single bacterial species or simple mixes of microbes, may enable a deeper understanding of their direct contributions. It should be noted however that there is likely to be mutualism between bacterial species which may be missed by such an approach. The DUMP assay, or similar, could also be employed in mammalian models, utilising chemically defined diets specific to the species, to assess whether these changes are conserved between species.

Additionally, whilst we used the DUMP assay to determine changes to faecal macronutrient levels, it could be more widely applied using untargeted metabolomics approaches. This may enable detection of far greater changes. Combining such a technique with gnotobiotic flies could be a powerful tool in understanding the various ways in which microbial species interact with host diet, and impact the host. Whilst we used this assay to determine changes in the faecal profile with age and microbial colonisation, it could also be used to assess changes upon genetic manipulation, dietary supplementation etc. or even upon infection. Further to this, the female *Drosophila* intestine undergoes remodelling following mating. It is thought that this remodelling enables increased nutrient uptake to support egg production, however the DUMP assay would enable quantification of these changes, and may provide important insights into this process. Changes to nutrient absorption in disease models could also be quantified, e.g. models of cachexia or obesity/diabetes.

8.2 Amino acid transporters and ageing

Following the observation that luminal/faecal amino acid concentrations increase with age, I assayed the expression of several predicted amino acid transporters in the intestine of wild-type flies with age (chapter 5). I observed changes in the expression of a large subset of these transporters with age, which may explain some of the observed changes in the DUMP assay. The direction of change in expression was not consistent, however, potentially implicating compensatory mechanisms.

Whether such changes in amino acid transport occur with age in mammals has not been published, although there are changes to intestinal amino acid transporter expression at different stages of development, and ageing is associated with a general decline in function, so it would not be surprising if this was conserved.

If such changes were found to be conserved across species, then amino acid transporters may lend themselves as druggable targets for the prevention or treatment of sarcopenia and frailty, as well as other metabolic changes and malnutrition observed with age.

The expression of *Slimfast*, and *Eaat1*, decreased with age and both were followed up for further characterisation (chapters 6 and 7).

Interestingly, whilst these two transporters are specific for very different substrates, they both appeared to be associated with expression of *upd3.* Knockdown of Slif resulted in increased *upd3*, whilst JNK activation resulted in reductions in *Slif*, potentially implicating *Slif* as an intermediate factor linking the JNK and JAK-STAT pathways. A similar trend towards increased *upd3* expression upon *Eaat1* knockdown was also observed. This may highlight a nutritional dependency of the JAK-

STAT pathway. Intestinal JAK-STAT activity has been shown to be reliant on enteral nutrient intake in studies using mice, and this activation is important in maintaining immune function[842]. This may be mediated through expression or activation of amino acid transporters, as there is evidence to suggest that Eaat1 is upregulated under low glutamate conditions.

Intestinal knockdown of *Slif* intriguingly extended lifespan, possibly through increased luminal arginine levels. If true, this highlights the impact of individual amino acids on healthy longevity, suggests that we may be looking too broadly at the role of protein, and that the role of individual amino acids should be considered, on top of the impact of whole-protein. If this lifespan extension was indeed mediated through increased luminal arginine, and conserved arginine supplementation would be easy to implement in a population setting. Additional work is required however to determine the mechanisms by which slif knockdown leads to lifespan extension.

The lifespan extension observed upon *Slif* knockdown may also be a consequence of reduced mTOR activity as it has previously been shown to interact with this pathway[623,679]. Additionally, intestinal knockdown of Slif may impact it's nutrient sensor role in the fat body[577], by reducing extracellular cationic amino acid concentrations.

In contrast, intestinal knockdown of Eaat1 resulted in lifespan reduction. This may be through an increased luminal glutamate concentration, as glutamate has been linked to ISC proliferation[565,603]. Stem-cell expression of Eaat1 was also shown to be important for ISC proliferation, however, and a new model was proposed linking ISC Eaat1 to mGluR and NCX1, to control ISC proliferation in response to luminal glutamate concentrations.

The interactions between Eaat1, ISC proliferation and JAK-STAT activity, and between Slif, JNK, JAK-STAT and mTOR, highlight the importance of nutrition in determining the activity of a wide range of signalling pathways. It also highlights potential transceptor functions of these transporters, and the impact of changing nutrient dynamics with age – some of which is driven by microbial changes.

A more complete understanding of the pathways impacted by specific amino acid transporters, as well as an improved understanding of AAT regulation, may enable the development of targeted therapeutic interventions to specifically modulate transporter activity and dynamics. This may be a powerful way to modulate health and lifespan effects.

8.3 A collective view

Protein is an important determinant of lifespan, however here I have uncovered additional, novel mechanisms by which it imparts its effect. Not only do individual amino acids impact nutrition directly, but they also have a profound impact indirectly. They can activate signalling pathways such as mTORC1 which is widely associated with lifespan, they may modulate the microbiota, and impact expression of amino acid transporters. Expression and activation of amino acid transporters appears to have a much wider than expected impact, possibly through transceptor functions. This may result in amino acid transporters becoming druggable targets for the modulation of varied signalling pathways. Indeed, small molecule drugs already exist for SLC7A5 and SLC7A7, as well as the peptide transporter SLC6A14[843].

Changes to protein absorption with age, as indicated here, may underlie the malnourishment, sarcopenia and frailty commonly observed with ageing, as well as wider metabolic changes. Understanding what drives these changes with age may enable the development of better treatments and preventative measures. Data here indicate that changes to the expression of amino acid transporters may underpin some of these changes, although not all transporters were downregulated with age. Interestingly, the downregulation of some transporters results in a wider-than-expected impact, affecting intestinal homeostasis through modulation of JAK-STAT pathway activation and ISC proliferation. Transporter downregulation also likely impacts nutrient signalling pathways, although this was not tested, and may impact the composition of the microbiota.

The microbiota was shown to make a large contribution to the luminal/faecal amino acid profile, which may impact host nutrition. Changes in the microbiota associated with ageing may, therefore, also affect host nutrition. It is possible that the microbiota would play a role in amino acid transporter expression, or that changes to the expression of amino acid transporters would impact the microbial community although broad changes in bacterial load were not observed here.

An improved understanding of the individual, and combined role of specific nutrients, transporters and the microbiota, as well as the downstream effector pathways is required, in order to determine rational dietary interventions, or identify druggable targets for the treatment or prevention of age-related metabolic changes.

8.4 Limitations to this work

It is important to be aware of the limitations of any work, and the work presented here is not without it's own limitations. The statistical analyses presented here were particularly stringent, to

prevent from overstating any results. Non-parametric testing often was performed based upon the results of normality tests, however the sample sizes were too small for this to be reliable, and thus parametric testing could have been employed throughout. Additionally, more information could have been gained from the data through the use of other statistical models, for example generalised linear models may have enabled greater comparison between different conditions, such as age and treatment/gene expression, as compared to the pairwise comparisons employed within.

As mentioned previously, there were also limitations to the DUMP assay developed. Not only is it unable to include smurf flies, an important cohort for understanding age-related decline, but the source of the measured amino acids is unclear. It is assumed that whole proteins are not being detected through this assay due to the chromatography separation prior to mass-spectrometry analysis, although this is something that should be tested. Pulse feeding isotopically-labelled amino acids may go some way to untangling the contribution of absorption, egestion and the microbiota.

Another limitation is that potential changes to feeding were not measured upon each AAT manipulation. It is therefore possible that the observations made here are, at least in part, due to changes in food consumption, as opposed to the changes in gene expression.

9 Future Perspectives

Several questions remain for our research group, not limited to the following:

1) What is the impact of amino acid transporter modulation, or the Aged AA diet on nutrient signalling pathways?
2) How do changes to the expression of amino acid transporters impact systemic metabolism?
3) What drives the changes in amino acid transporter expression with age?
4) How do these changes impact the microbial community, and do microbial composition, or microbial products impact these changes?
5) Are these changes conserved in other organisms?

Future experiments to answer some of these questions, would include pairing the dietary or gene expression changes, e.g. the Aged AA diet, or Eaat1 overexpression, with rapamycin treatment. Rapamycin is an mTORC1 inhibitor, and thus if mTORC1 activity is driving the lifespan effects observed within this thesis, then blocking mTORC1 by rapamycin would reduce or prevent these changes. In the case of the Aged AA diet, if the reduced lifespan is driven by mTORC1 activation, the feeding of Aged AA containing rapamycin should prevent this reduced lifespan. Assessing the levels

of phosphorylated S6k would also provide information on nutrient signalling pathways. Western blotting of different tissues, e.g. the fatbody or brain, to assess the levels of phosphorylated S6k, would provide information of the systemic effect upon gastrointestinal gene expression changes, or dietary changes. Additionally, assessing the levels of nutrient stores e.g. TAG, glycogen etc. as was performed in chapter 3, would provide insight into the impact of intestinal AAT manipulation on systemic nutrition.

On top of this, metagenomic sequencing and subsequent bioinformatics analyses, would enable identification of enrichment or depletion of intestinal microbial species upon dietary or intestinal gene-expression changes. Importantly, it would also enable characterisation of changes in microbial pathways and enrichment or loss or specific e.g. metabolic genes.

Once we have a better understanding of these questions, particularly whether these changes are conserved amongst organisms, we will have a far greater understanding of the nutritional changes underlying age-related decline. This is important as ageing is associated with so many metabolic changes, including sarcopenia and frailty.
The hope is, that this research will provide a solid rationale for targeted dietary interventions, updated dietary recommendations for the elderly, or the identification of potential druggable targets e.g. specific amino acid transports, for the treatment or prevention of these metabolic changes.

As highlighted in this thesis, however, amino acid transporters and their amino acid substrates, have additional functions beyond nutrition. These roles must also be understood and considered when studying the impact of modulating their activity, and selecting them as druggable targets.

11 Bibliography

1. Garmany, A., Yamada, S. & Terzic, A. Longevity leap: mind the healthspan gap. *npj Regen Med* **6**, 1–7 (2021).
2. McLeod, M., Breen, L., Hamilton, D. L. & Philp, A. Live strong and prosper: the importance of skeletal muscle strength for healthy ageing. *Biogerontology* **17**, 497–510 (2016).
3. Partridge, L., Deelen, J. & Slagboom, P. E. Facing up to the global challenges of ageing. *Nature* **561**, 45–56 (2018).
4. Adams, M. D. *et al.* The genome sequence of Drosophila melanogaster. *Science* **287**, 2185–2195 (2000).
5. Bakula, M. The persistence of a microbial flora during postembryogenesis of Drosophila melanogaster. *Journal of Invertebrate Pathology* **14**, 365–374 (1969).
6. Bozcuk, A. N. DNA synthesis in the absence of somatic cell division associated with ageing in Drosophila subobscura. *Exp Gerontol* **7**, 147–156 (1972).
7. Demerec, M. *Biology of Drosophila*. (CSHL Press, 1994).
8. Kaufman, T. C. A Short History and Description of Drosophila melanogaster Classical Genetics: Chromosome Aberrations, Forward Genetic Screens, and the Nature of Mutations. *Genetics* **206**, 665–689 (2017).
9. Brand, A. H. & Perrimon, N. Targeted gene expression as a means of altering cell fates and generating dominant phenotypes. *Development* **118**, 401–415 (1993).
10. Golic, K. G. & Lindquist, S. The FLP recombinase of yeast catalyzes site-specific recombination in the Drosophila genome. *Cell* **59**, 499–509 (1989).
11. Golic, K. G. Site-Specific Recombination Between Homologous Chromosomes in Drosophila. *Science* **252**, 958–961 (1991).
12. Xu, T. & Rubin, G. M. Analysis of genetic mosaics in developing and adult Drosophila tissues. *Development* **117**, 1223–1237 (1993).

13. Osterwalder, T., Yoon, K. S., White, B. H. & Keshishian, H. A conditional tissue-specific transgene expression system using inducible GAL4. *Proc Natl Acad Sci U S A* **98**, 12596–12601 (2001).

14. Roman, G., Endo, K., Zong, L. & Davis, R. L. P[Switch], a system for spatial and temporal control of gene expression in Drosophila melanogaster. *Proc Natl Acad Sci U S A* **98**, 12602–12607 (2001).

15. Port, F. *et al.* A large-scale resource for tissue-specific CRISPR mutagenesis in Drosophila. *eLife* **9**, e53865 (2020).

16. McClure, C. D. *et al.* An auxin-inducible, GAL4-compatible, gene expression system for Drosophila. *eLife* **11**, e67598 (2022).

17. Moens, E. & Veldhoen, M. Epithelial barrier biology: good fences make good neighbours. *Immunology* **135**, 1–8 (2012).

18. Madsen, J. L. & Graff, J. Effects of ageing on gastrointestinal motor function. *Age and Ageing* **33**, 154–159 (2004).

19. Hollander, D. & Tarnawski, H. Aging-associated increase in intestinal absorption of macromolecules. *Gerontology* **31**, 133–137 (1985).

20. Ma, T. Y., Hollander, D., Dadufalza, V. & Krugliak, P. Effect of aging and caloric restriction on intestinal permeability. *Experimental Gerontology* **27**, 321–333 (1992).

21. Tran, L. & Meerveld, B. G.-V. Age-Associated Remodeling of the Intestinal Epithelial Barrier. *The Journals of Gerontology Series A: Biological Sciences and Medical Sciences* **68**, 1045 (2013).

22. Rera, M., Clark, R. I. & Walker, D. W. Intestinal barrier dysfunction links metabolic and inflammatory markers of aging to death in Drosophila. *Proc Natl Acad Sci U S A* **109**, 21528–21533 (2012).

23. Franceschi, C. *et al.* Inflammaging and anti-inflammaging: a systemic perspective on aging and longevity emerged from studies in humans. *Mech Ageing Dev* **128**, 92–105 (2007).

24. Franceschi, C. & Campisi, J. Chronic inflammation (inflammaging) and its potential contribution to age-associated diseases. *J Gerontol A Biol Sci Med Sci* **69 Suppl 1**, S4-9 (2014).

25. Guigoz, Y., Doré, J. & Schiffrin, E. J. The inflammatory status of old age can be nurtured from the intestinal environment. *Curr Opin Clin Nutr Metab Care* **11**, 13–20 (2008).

26. Yatsunenko, T. *et al.* Human gut microbiome viewed across age and geography. *Nature* **486**, 222–227 (2012).

27. Claesson, M. J. *et al.* Composition, variability, and temporal stability of the intestinal microbiota of the elderly. *PNAS* **108**, 4586–4591 (2011).

28. Claesson, M. J. *et al.* Gut microbiota composition correlates with diet and health in the elderly. *Nature* **488**, 178–184 (2012).

29. Mariat, D. *et al.* The Firmicutes/Bacteroidetes ratio of the human microbiota changes with age. *BMC Microbiol* **9**, 123 (2009).

30. Leite, G. *et al.* Age and the aging process significantly alter the small bowel microbiome. *Cell Reports* **36**, 109765 (2021).

31. Smith, E. R. Epidemiology of gastrointestinal disorders. *Can Fam Physician* **24**, 1007–1011 (1978).

32. Sperber, A. D. *et al.* Worldwide Prevalence and Burden of Functional Gastrointestinal Disorders, Results of Rome Foundation Global Study. *Gastroenterology* **160**, 99-114.e3 (2021).

33. Buchon, N. & Osman, D. All for one and one for all: Regionalization of the Drosophila intestine. *Insect Biochemistry and Molecular Biology* **67**, 2–8 (2015).

34. Buchon, N. *et al.* Morphological and Molecular Characterization of Adult Midgut Compartmentalization in Drosophila. *Cell Reports* **3**, 1725–1738 (2013).

35. de Navascués, J. *et al.* Drosophila midgut homeostasis involves neutral competition between symmetrically dividing intestinal stem cells. *EMBO J* **31**, 2473–2485 (2012).

36. Hung, R. J. *et al.* A cell atlas of the adult Drosophila midgut. *Proceedings of the National Academy of Sciences of the United States of America* **117**, (2020).

37. Amcheslavsky, A. *et al.* Enteroendocrine Cells Support Intestinal Stem Cell-Mediated Homeostasis In Drosophila. *Cell Rep* **9**, 32–39 (2014).

38. López-Otín, C., Blasco, M. A., Partridge, L., Serrano, M. & Kroemer, G. The Hallmarks of Aging. *Cell* **153**, 1194–1217 (2013).

39. Clark, R. I. *et al.* Distinct Shifts in Microbiota Composition during Drosophila Aging Impair Intestinal Function and Drive Mortality. *Cell Rep* **12**, 1656–1667 (2015).

40. Thevaranjan, N. *et al.* Age-Associated Microbial Dysbiosis Promotes Intestinal Permeability, Systemic Inflammation, and Macrophage Dysfunction. *Cell Host Microbe* **21**, 455-466.e4 (2017).

41. Angarita, S. A. K. *et al.* Quantitative Measure of Intestinal Permeability Using Blue Food Coloring. *J Surg Res* **233**, 20–25 (2019).

42. Salazar, A. M. *et al.* Intestinal Snakeskin Limits Microbial Dysbiosis during Aging and Promotes Longevity. *iScience* **9**, 229–243 (2018).

43. Gan, T. *et al.* JNK Signaling in Drosophila Aging and Longevity. *Int J Mol Sci* **22**, 9649 (2021).

44. Bode, A. M. & Dong, Z. The Functional Contrariety of JNK. *Mol Carcinog* **46**, 591–598 (2007).

45. Biteau, B., Karpac, J., Hwangbo, D. & Jasper, H. Regulation of Drosophila lifespan by JNK signaling. *Exp Gerontol* **46**, 349–354 (2011).

46. Pinal, N., Calleja, M. & Morata, G. Pro-apoptotic and pro-proliferation functions of the JNK pathway of Drosophila: roles in cell competition, tumorigenesis and regeneration. *Open Biol* **9**, 180256 (2019).

47. Jiang, H. *et al.* Cytokine/Jak/Stat signaling mediates regeneration and homeostasis in the Drosophila midgut. *Cell* **137**, 1343–1355 (2009).

48. Wang, M. C., Bohmann, D. & Jasper, H. JNK extends life span and limits growth by antagonizing cellular and organism-wide responses to insulin signaling. *Cell* **121**, 115–125 (2005).

49. Biteau, B., Hochmuth, C. E. & Jasper, H. JNK activity in somatic stem cells causes loss of tissue homeostasis in the aging Drosophila gut. *Cell Stem Cell* **3**, 442–455 (2008).

50. Mundorf, J., Donohoe, C. D., McClure, C. D., Southall, T. D. & Uhlirova, M. Ets21c Governs Tissue Renewal, Stress Tolerance, and Aging in the Drosophila Intestine. *Cell Rep* **27**, 3019-3033.e5 (2019).

51. La Marca, J. E. & Richardson, H. E. Two-Faced: Roles of JNK Signalling During Tumourigenesis in the Drosophila Model. *Front Cell Dev Biol* **8**, 42 (2020).

52. Brown, S., Hu, N. & Hombría, J. C. Identification of the first invertebrate interleukin JAK/STAT receptor, the Drosophila gene domeless. *Curr Biol* **11**, 1700–1705 (2001).

53. Brown, S., Hu, N. & Hombría, J. C.-G. Novel level of signalling control in the JAK/STAT pathway revealed by in situ visualisation of protein-protein interaction during Drosophila development. *Development* **130**, 3077–3084 (2003).

54. Chen, H.-W. *et al.* mom identifies a receptor for the Drosophila JAK/STAT signal transduction pathway and encodes a protein distantly related to the mammalian cytokine receptor family. *Genes Dev* **16**, 388–398 (2002).

55. Binari, R. & Perrimon, N. Stripe-specific regulation of pair-rule genes by hopscotch, a putative Jak family tyrosine kinase in Drosophila. *Genes Dev* **8**, 300–312 (1994).

56. Hou, X. S., Melnick, M. B. & Perrimon, N. Marelle acts downstream of the Drosophila HOP/JAK kinase and encodes a protein similar to the mammalian STATs. *Cell* **84**, 411–419 (1996).

57. Yan, R., Small, S., Desplan, C., Dearolf, C. R. & Darnell, J. E. Identification of a Stat gene that functions in Drosophila development. *Cell* **84**, 421–430 (1996).

58. Li, H., Qi, Y. & Jasper, H. Preventing Age-Related Decline of Gut Compartmentalization Limits Microbiota Dysbiosis and Extends Lifespan. *Cell Host Microbe* **19**, 240–253 (2016).

59. Xu, M., Tchkonia, T. & Kirkland, J. L. Perspective: Targeting the JAK/STAT pathway to fight age-related dysfunction. *Pharmacol Res* **111**, 152–154 (2016).

60. Xu, M. *et al.* JAK inhibition alleviates the cellular senescence-associated secretory phenotype and frailty in old age. *Proceedings of the National Academy of Sciences* **112**, E6301–E6310 (2015).

61. Xu, M. *et al.* Targeting senescent cells enhances adipogenesis and metabolic function in old age. *Elife* **4**, e12997 (2015).

62. Ohsawa, S. *et al.* Mitochondrial defect drives non-autonomous tumour progression through Hippo signalling in Drosophila. *Nature* **490**, 547–551 (2012).

63. Nakamura, M., Ohsawa, S. & Igaki, T. Mitochondrial defects trigger proliferation of neighbouring cells via a senescence-associated secretory phenotype in Drosophila. *Nat Commun* **5**, 5264 (2014).

64. Ito, T. & Igaki, T. Dissecting cellular senescence and SASP in Drosophila. *Inflammation and Regeneration* **36**, 25 (2016).

65. Moskalev, A., Proshkina, E., Zhavoronkov, A. & Shaposhnikov, M. Effects of unpaired 1 gene overexpression on the lifespan of Drosophila melanogaster. *BMC Systems Biology* **13**, 16 (2019).

66. Panda, A. *et al.* Human innate immunosenescence: causes and consequences for immunity in old age. *Trends Immunol* **30**, 325–333 (2009).

67. Aw, D., Silva, A. B. & Palmer, D. B. Immunosenescence: emerging challenges for an ageing population. *Immunology* **120**, 435–446 (2007).

68. Eleftherianos, I. & Castillo, J. C. Molecular mechanisms of aging and immune system regulation in Drosophila. *Int J Mol Sci* **13**, 9826–9844 (2012).

69. Min, K.-J. & Tatar, M. Unraveling the Molecular Mechanism of Immunosenescence in Drosophila. *Int J Mol Sci* **19**, E2472 (2018).

70. DeVeale, B., Brummel, T. & Seroude, L. Immunity and aging: the enemy within? *Aging Cell* **3**, 195–208 (2004).

71. Müller, L., Fülöp, T. & Pawelec, G. Immunosenescence in vertebrates and invertebrates. *Immun Ageing* **10**, 12 (2013).

72. Solana, R., Pawelec, G. & Tarazona, R. Aging and innate immunity. *Immunity* **24**, 491–494 (2006).

73. Yoshikawa, T. T. Epidemiology and unique aspects of aging and infectious diseases. *Clin Infect Dis* **30**, 931–933 (2000).

74. Kline, K. A. & Bowdish, D. M. E. Infection in an aging population. *Curr Opin Microbiol* **29**, 63–67 (2016).

75. Ferrandon, D. *et al.* A drosomycin-GFP reporter transgene reveals a local immune response in Drosophila that is not dependent on the Toll pathway. *EMBO J* **17**, 1217–1227 (1998).

76. Zerofsky, M., Harel, E., Silverman, N. & Tatar, M. Aging of the innate immune response in Drosophila melanogaster. *Aging Cell* **4**, 103–108 (2005).

77. Biteau, B. *et al.* Lifespan extension by preserving proliferative homeostasis in Drosophila. *PLoS Genet* **6**, e1001159 (2010).

78. Kim, S.-H. & Lee, W.-J. Role of DUOX in gut inflammation: lessons from Drosophila model of gut-microbiota interactions. *Front Cell Infect Microbiol* **3**, 116 (2014).

79. Chakrabarti, S. *et al.* Remote Control of Intestinal Stem Cell Activity by Haemocytes in Drosophila. *PLOS Genetics* **12**, e1006089 (2016).

80. Landis, G. N. *et al.* Similar gene expression patterns characterize aging and oxidative stress in Drosophila melanogaster. *PNAS* **101**, 7663–7668 (2004).

81. Moskalev, A. & Shaposhnikov, M. Pharmacological inhibition of NF-κB prolongs lifespan of Drosophila melanogaster. *Aging (Albany NY)* **3**, 391–394 (2011).

82. Pletcher, S. D. *et al.* Genome-wide transcript profiles in aging and calorically restricted Drosophila melanogaster. *Curr Biol* **12**, 712–723 (2002).

83. Seroude, L., Brummel, T., Kapahi, P. & Benzer, S. Spatio-temporal analysis of gene expression during aging in Drosophila melanogaster. *Aging Cell* **1**, 47–56 (2002).

84. Ganesan, S., Aggarwal, K., Paquette, N. & Silverman, N. NF-κB/Rel proteins and the humoral immune responses of Drosophila melanogaster. *Curr Top Microbiol Immunol* **349**, 25–60 (2011).

85. Felix, T. M., Hughes, K. A., Stone, E. A., Drnevich, J. M. & Leips, J. Age-Specific Variation in Immune Response in Drosophila melanogaster Has a Genetic Basis. *Genetics* **191**, 989–1002 (2012).

86. Mackenzie, D. K., Bussière, L. F. & Tinsley, M. C. Senescence of the cellular immune response in Drosophila melanogaster. *Exp Gerontol* **46**, 853–859 (2011).

87. Buchon, N., Silverman, N. & Cherry, S. Immunity in Drosophila melanogaster — from microbial recognition to whole- organism physiology. *Nat Rev Immunol* **14**, 796–810 (2014).

88. Broderick, N. A., Buchon, N. & Lemaitre, B. Microbiota-Induced Changes in Drosophila melanogaster Host Gene Expression and Gut Morphology. *mBio* **5**, (2014).

89. Guo, L., Karpac, J., Tran, S. L. & Jasper, H. PGRP-SC2 Promotes Gut Immune Homeostasis to Limit Commensal Dysbiosis and Extend Lifespan. *Cell* **156**, 109–122 (2014).

90. Ren, C., Webster, P., Finkel, S. E. & Tower, J. Increased internal and external bacterial load during Drosophila aging without life-span trade-off. *Cell Metab* **6**, 144–152 (2007).

91. Freund, A., Laberge, R.-M., Demaria, M. & Campisi, J. Lamin B1 loss is a senescence-associated biomarker. *Mol Biol Cell* **23**, 2066–2075 (2012).

92. Buchon, N., Broderick, N. A., Chakrabarti, S. & Lemaitre, B. Invasive and indigenous microbiota impact intestinal stem cell activity through multiple pathways in Drosophila. *Genes & Development* **23**, 2333–2344 (2009).

93. Bodogai, M. *et al.* Commensal bacteria contribute to insulin resistance in aging by activating innate B1a cells. *Sci Transl Med* **10**, eaat4271 (2018).

94. Smith, P. *et al.* Regulation of life span by the gut microbiota in the short-lived African turquoise killifish. *Elife* **6**, e27014 (2017).

95. Frank, D. N. *et al.* Molecular-phylogenetic characterization of microbial community imbalances in human inflammatory bowel diseases. *Proc Natl Acad Sci U S A* **104**, 13780–13785 (2007).

96. Dubinsky, M. C. *et al.* Serum immune responses predict rapid disease progression among children with Crohn's disease: immune responses predict disease progression. *Am J Gastroenterol* **101**, 360–367 (2006).

97. O'Keefe, S. J. D. *et al.* Products of the colonic microbiota mediate the effects of diet on colon cancer risk. *J Nutr* **139**, 2044–2048 (2009).

98. Sampson, T. R. *et al.* Gut Microbiota Regulate Motor Deficits and Neuroinflammation in a Model of Parkinson's Disease. *Cell* **167**, 1469-1480.e12 (2016).

99. Hu, X., Wang, T. & Jin, F. Alzheimer's disease and gut microbiota. *Sci China Life Sci* **59**, 1006–1023 (2016).

100. Barlow, G. M., Yu, A. & Mathur, R. Role of the Gut Microbiome in Obesity and Diabetes Mellitus. *Nutr Clin Pract* **30**, 787–797 (2015).

101. Jackson, M. A. *et al.* Signatures of early frailty in the gut microbiota. *Genome Medicine* **8**, 8 (2016).

102. van Tongeren, S. P., Slaets, J. P. J., Harmsen, H. J. M. & Welling, G. W. Fecal microbiota composition and frailty. *Appl Environ Microbiol* **71**, 6438–6442 (2005).

103. Scher, J. U. *et al.* Expansion of intestinal Prevotella copri correlates with enhanced susceptibility to arthritis. *Elife* **2**, e01202 (2013).

104. Wilmanski, T. *et al.* Gut microbiome pattern reflects healthy ageing and predicts survival in humans. *Nat Metab* **3**, 274–286 (2021).

105. Cheng, J., Palva, A. M., de Vos, W. M. & Satokari, R. Contribution of the intestinal microbiota to human health: from birth to 100 years of age. *Curr Top Microbiol Immunol* **358**, 323–346 (2013).

106. Clemente, J. C., Ursell, L. K., Parfrey, L. W. & Knight, R. The impact of the gut microbiota on human health: an integrative view. *Cell* **148**, 1258–1270 (2012).

107. Biagi, E. *et al.* Through ageing, and beyond: gut microbiota and inflammatory status in seniors and centenarians. *PLoS One* **5**, e10667 (2010).

108. Carvalho, F. A. *et al.* Transient inability to manage proteobacteria promotes chronic gut inflammation in TLR5-deficient mice. *Cell Host Microbe* **12**, 139–152 (2012).

109. Broderick, N. A., Buchon, N. & Lemaitre, B. Microbiota-Induced Changes in Drosophila melanogaster Host Gene Expression and Gut Morphology. *mBio* **5**, e01117-14.

110. Yamada, R., Deshpande, S. A., Bruce, K. D., Mak, E. M. & Ja, W. W. Microbes Promote Amino Acid Harvest to Rescue Undernutrition in Drosophila. *Cell Reports* **10**, 865–872 (2015).

111. Koenig, J. E. *et al.* Succession of microbial consortia in the developing infant gut microbiome. *PNAS* **108**, 4578–4585 (2011).

112. Johnson, A. J. *et al.* Daily Sampling Reveals Personalized Diet-Microbiome Associations in Humans. *Cell Host Microbe* **25**, 789-802.e5 (2019).

113. David, L. A. *et al.* Diet rapidly and reproducibly alters the human gut microbiome. *Nature* **505**, 559–563 (2014).

114. Lin, S.-J., Defossez, P.-A. & Guarente, L. Requirement of NAD and SIR2 for Life-Span Extension by Calorie Restriction in Saccharomyces cerevisiae. *Science* **289**, 2126–2128 (2000).

115. Piper, M. D. W. & Partridge, L. Dietary Restriction in Drosophila: Delayed Aging or Experimental Artefact? *PLOS Genetics* **3**, e57 (2007).

116. Green, C. L., Lamming, D. W. & Fontana, L. Molecular mechanisms of dietary restriction promoting health and longevity. *Nat Rev Mol Cell Biol* **23**, 56–73 (2022).

117. Swindel, W. R. Dietary restriction in rats and mice: a meta-analysis and review of the evidence for genotype-dependent effects on lifespan. *Ageing research reviews* **11**, (2012).

118. Lee, K. P. *et al.* Lifespan and reproduction in Drosophila: New insights from nutritional geometry. *PNAS* **105**, 2498–2503 (2008).

119. Jensen, K., McClure, C., Priest, N. K. & Hunt, J. Sex-specific effects of protein and carbohydrate intake on reproduction but not lifespan in Drosophila melanogaster. *Aging Cell* **14**, 605–615 (2015).

120. Fanson, B. G., Weldon, C. W., Pérez-Staples, D., Simpson, S. J. & Taylor, P. W. Nutrients, not caloric restriction, extend lifespan in Queensland fruit flies (Bactrocera tryoni). *Aging Cell* **8**, 514–523 (2009).

121. Harrison, S. J., Raubenheimer, D., Simpson, S. J., Godin, J.-G. J. & Bertram, S. M. Towards a synthesis of frameworks in nutritional ecology: interacting effects of protein, carbohydrate and phosphorus on field cricket fitness. *Proceedings of the Royal Society B: Biological Sciences* **281**, 20140539 (2014).

122. Ooka, H., Segall, P. E. & Timiras, P. S. Histology and survival in age-delayed low-tryptophan-fed rats. *Mechanisms of Ageing and Development* **43**, 79–98 (1988).

123. Orentreich, N., Matias, J. R., DeFelice, A. & Zimmerman, J. A. Low methionine ingestion by rats extends life span. *J Nutr* **123**, 269–274 (1993).

124. Grandison, R. C., Piper, M. D. W. & Partridge, L. Amino-acid imbalance explains extension of lifespan by dietary restriction in Drosophila. *Nature* **462**, 1061–1064 (2009).

125. Zimmerman, J. A., Malloy, V., Krajcik, R. & Orentreich, N. Nutritional control of aging. *Exp Gerontol* **38**, 47–52 (2003).

126. Richie, J. P. *et al.* Methionine restriction increases blood glutathione and longevity in F344 rats. *FASEB J* **8**, 1302–1307 (1994).

127. De Marte, M. L. & Enesco, H. E. Influence of low tryptophan diet on survival and organ growth in mice. *Mech Ageing Dev* **36**, 161–171 (1986).

128. Lee, B. C. *et al.* Methionine restriction extends lifespan of Drosophila melanogaster under conditions of low amino acid status. *Nat Commun* **5**, 3592 (2014).

129. Miller, R. A. *et al.* Methionine-deficient diet extends mouse lifespan, slows immune and lens aging, alters glucose, T4, IGF-I and insulin levels, and increases hepatocyte MIF levels and stress resistance. *Aging Cell* **4**, 119–125 (2005).

130. Levine, M. E. *et al.* Low Protein Intake Is Associated with a Major Reduction in IGF-1, Cancer, and Overall Mortality in the 65 and Younger but Not Older Population. *Cell Metabolism* **19**, 407–417 (2014).

131. Kenyon, C., Chang, J., Gensch, E., Rudner, A. & Tabtiang, R. A C. elegans mutant that lives twice as long as wild type. *Nature* **366**, 461–464 (1993).

132. Barbieri, M., Bonafè, M., Franceschi, C. & Paolisso, G. Insulin/IGF-I-signaling pathway: an evolutionarily conserved mechanism of longevity from yeast to humans. *Am J Physiol Endocrinol Metab* **285**, E1064-1071 (2003).

133. Wolkow, C. A., Muñoz, M. J., Riddle, D. L. & Ruvkun, G. Insulin receptor substrate and p55 orthologous adaptor proteins function in the Caenorhabditis elegans daf-2/insulin-like signaling pathway. *J Biol Chem* **277**, 49591–49597 (2002).

134. Böhni, R. *et al.* Autonomous control of cell and organ size by CHICO, a Drosophila homolog of vertebrate IRS1-4. *Cell* **97**, 865–875 (1999).

135. Brogiolo, W. *et al.* An evolutionarily conserved function of the Drosophila insulin receptor and insulin-like peptides in growth control. *Curr Biol* **11**, 213–221 (2001).

136. Morris, J. Z., Tissenbaum, H. A. & Ruvkun, G. A phosphatidylinositol-3-OH kinase family member regulating longevity and diapause in Caenorhabditis elegans. *Nature* **382**, 536–539 (1996).

137. Ogg, S. *et al.* The Fork head transcription factor DAF-16 transduces insulin-like metabolic and longevity signals in C. elegans. *Nature* **389**, 994–999 (1997).

138. Huang, H. *et al.* PTEN affects cell size, cell proliferation and apoptosis during Drosophila eye development. *Development* **126**, 5365–5372 (1999).

139. Goberdhan, D. C., Paricio, N., Goodman, E. C., Mlodzik, M. & Wilson, C. Drosophila tumor suppressor PTEN controls cell size and number by antagonizing the Chico/PI3-kinase signaling pathway. *Genes Dev* **13**, 3244–3258 (1999).

140. Gao, X., Neufeld, T. P. & Pan, D. Drosophila PTEN regulates cell growth and proliferation through PI3K-dependent and -independent pathways. *Dev Biol* **221**, 404–418 (2000).

141. Maehama, T. & Dixon, J. E. The tumor suppressor, PTEN/MMAC1, dephosphorylates the lipid second messenger, phosphatidylinositol 3,4,5-trisphosphate. *J Biol Chem* **273**, 13375–13378 (1998).

142. Garelli, A., Gontijo, A. M., Miguela, V., Caparros, E. & Dominguez, M. Imaginal discs secrete insulin-like peptide 8 to mediate plasticity of growth and maturation. *Science* **336**, 579–582 (2012).

143. Grönke, S., Clarke, D.-F., Broughton, S., Andrews, T. D. & Partridge, L. Molecular evolution and functional characterization of Drosophila insulin-like peptides. *PLoS Genet* **6**, e1000857 (2010).

144. Broughton, S. *et al.* Reduction of DILP2 in Drosophila triages a metabolic phenotype from lifespan revealing redundancy and compensation among DILPs. *PLoS One* **3**, e3721 (2008).

145. Broughton, S. J. *et al.* Longer lifespan, altered metabolism, and stress resistance in Drosophila from ablation of cells making insulin-like ligands. *Proc Natl Acad Sci U S A* **102**, 3105–3110 (2005).

146. Tatar, M. *et al.* A mutant Drosophila insulin receptor homolog that extends life-span and impairs neuroendocrine function. *Science* **292**, 107–110 (2001).

147. Clancy, D. J. *et al.* Extension of life-span by loss of CHICO, a Drosophila insulin receptor substrate protein. *Science* **292**, 104–106 (2001).

148. Tu, M.-P., Epstein, D. & Tatar, M. The demography of slow aging in male and female Drosophila mutant for the insulin-receptor substrate homologue chico. *Aging Cell* **1**, 75–80 (2002).

149. Hwangbo, D. S., Gershman, B., Tu, M.-P., Palmer, M. & Tatar, M. Drosophila dFOXO controls lifespan and regulates insulin signalling in brain and fat body. *Nature* **429**, 562–566 (2004).

150. Demontis, F. & Perrimon, N. FOXO/4E-BP signaling in Drosophila muscles regulates organism-wide proteostasis during aging. *Cell* **143**, 813–825 (2010).

151. Giannakou, M. E. *et al.* Long-lived Drosophila with overexpressed dFOXO in adult fat body. *Science* **305**, 361 (2004).

152. Ismail, M. Z. B. H. *et al.* The Drosophila Insulin Receptor Independently Modulates Lifespan and Locomotor Senescence. *PLOS ONE* **10**, e0125312 (2015).

153. Essers, P. *et al.* Reduced insulin/insulin-like growth factor signaling decreases translation in Drosophila and mice. *Sci Rep* **6**, 30290 (2016).

154. Murphy, C. T. & Hu, P. J. *Insulin/insulin-like growth factor signaling in C. elegans*. *WormBook: The Online Review of C. elegans Biology [Internet]* (WormBook, 2018).

155. Selman, C. *et al.* Evidence for lifespan extension and delayed age-related biomarkers in insulin receptor substrate 1 null mice. *FASEB J* **22**, 807–818 (2008).

156. Templeman, N. M. *et al.* Reduced Circulating Insulin Enhances Insulin Sensitivity in Old Mice and Extends Lifespan. *Cell Reports* **20**, 451–463 (2017).

157. Clancy, D. J., Gems, D., Hafen, E., Leevers, S. J. & Partridge, L. Dietary restriction in long-lived dwarf flies. *Science* **296**, 319 (2002).

158. Lakowski, B. & Hekimi, S. The genetics of caloric restriction in Caenorhabditis elegans. *Proc Natl Acad Sci U S A* **95**, 13091–13096 (1998).

159. Houthoofd, K., Braeckman, B. P., Johnson, T. E. & Vanfleteren, J. R. Life extension via dietary restriction is independent of the Ins/IGF-1 signalling pathway in Caenorhabditis elegans. *Exp Gerontol* **38**, 947–954 (2003).

160. Min, K.-J., Yamamoto, R., Buch, S., Pankratz, M. & Tatar, M. Drosophila lifespan control by dietary restriction independent of insulin-like signaling. *Aging Cell* **7**, 199–206 (2008).

161. Hafen, E. Cancer, type 2 diabetes, and ageing: news from flies and worms. *Swiss Med Wkly* **134**, 711–719 (2004).

162. Partridge, L., Alic, N., Bjedov, I. & Piper, M. D. W. Ageing in Drosophila: The role of the insulin/Igf and TOR signalling network. *Experimental Gerontology* **46**, 376–381 (2011).

163. Karpac, J. & Jasper, H. Insulin and JNK: optimizing metabolic homeostasis and lifespan. *Trends Endocrinol Metab* **20**, 100–106 (2009).

164. Bjedov, I. *et al.* Fine-tuning autophagy maximises lifespan and is associated with changes in mitochondrial gene expression in Drosophila. *PLOS Genetics* **16**, e1009083 (2020).

165. Papadopoli, D. *et al.* mTOR as a central regulator of lifespan and aging. *F1000Res* **8**, F1000 Faculty Rev-998 (2019).

166. Wang, T., Blumhagen, R., Lao, U., Kuo, Y. & Edgar, B. A. LST8 Regulates Cell Growth via Target-of-Rapamycin Complex 2 (TORC2). *Mol Cell Biol* **32**, 2203–2213 (2012).

167. Glatter, T. *et al.* Modularity and hormone sensitivity of the Drosophila melanogaster insulin receptor/target of rapamycin interaction proteome. *Mol Syst Biol* **7**, 547 (2011).

168. Dh, K. *et al.* mTOR interacts with raptor to form a nutrient-sensitive complex that signals to the cell growth machinery. *Cell* **110**, (2002).

169. Saxton, R. A. & Sabatini, D. M. mTOR Signaling in Growth, Metabolism, and Disease. *Cell* **168**, 960–976 (2017).

170. Sarbassov, D. D. *et al.* Rictor, a novel binding partner of mTOR, defines a rapamycin-insensitive and raptor-independent pathway that regulates the cytoskeleton. *Curr Biol* **14**, 1296–1302 (2004).

171. Yang, Q., Inoki, K., Ikenoue, T. & Guan, K.-L. Identification of Sin1 as an essential TORC2 component required for complex formation and kinase activity. *Genes Dev* **20**, 2820–2832 (2006).

172. Bareja, A., Lee, D. E. & White, J. P. Maximizing Longevity and Healthspan: Multiple Approaches All Converging on Autophagy. *Frontiers in Cell and Developmental Biology* **7**, (2019).

173. Hansen, M., Rubinsztein, D. C. & Walker, D. W. Autophagy as a promoter of longevity: insights from model organisms. *Nat Rev Mol Cell Biol* **19**, 579–593 (2018).

174. Dyachok, J., Earnest, S., Iturraran, E. N., Cobb, M. H. & Ross, E. M. Amino Acids Regulate mTORC1 by an Obligate Two-step Mechanism. *J Biol Chem* **291**, 22414–22426 (2016).

175. Wolfson, R. L. *et al.* Sestrin2 is a leucine sensor for the mTORC1 pathway. *Science* **351**, 43–48 (2016).

176. Valenstein, M. L. *et al.* Structure of the nutrient-sensing hub GATOR2. *Nature* **607**, 610–616 (2022).

177. Cai, W., Wei, Y., Jarnik, M., Reich, J. & Lilly, M. A. The GATOR2 Component Wdr24 Regulates TORC1 Activity and Lysosome Function. *PLoS Genet* **12**, e1006036 (2016).

178. Wang, S. *et al.* Lysosomal amino acid transporter SLC38A9 signals arginine sufficiency to mTORC1. *Science* **347**, 188–194 (2015).

179. Rebsamen, M. & Superti-Furga, G. SLC38A9: A lysosomal amino acid transporter at the core of the amino acid-sensing machinery that controls MTORC1. *Autophagy* **12**, 1061–1062 (2016).

180. Wyant, G. A. *et al.* mTORC1 activator SLC38A9 is required to efflux essential amino acids from lysosomes and use protein as a nutrient. *Cell* **171**, 642-654.e12 (2017).

181. Bjedov, I. *et al.* Mechanisms of Life Span Extension by Rapamycin in the Fruit Fly Drosophila melanogaster. *Cell Metab* **11**, 35–46 (2010).

182. Juricic, P. *et al.* Long-lasting geroprotection from brief rapamycin treatment in early adulthood by persistently increased intestinal autophagy. *Nat Aging* **2**, 824–836 (2022).

183. Schinaman, J. M., Rana, A., Ja, W. W., Clark, R. I. & Walker, D. W. Rapamycin modulates tissue aging and lifespan independently of the gut microbiota in Drosophila. *Sci Rep* **9**, 7824 (2019).

184. Strong, R. *et al.* Rapamycin-mediated mouse lifespan extension: Late-life dosage regimes with sex-specific effects. *Aging Cell* **19**, e13269 (2020).

185. Bitto, A. *et al.* Transient rapamycin treatment can increase lifespan and healthspan in middle-aged mice. *Elife* **5**, e16351 (2016).

186. Harrison, D. E. *et al.* Rapamycin fed late in life extends lifespan in genetically heterogeneous mice. *Nature* **460**, 392–395 (2009).

187. von Frieling, J. & Roeder, T. Factors that affect the translation of dietary restriction into a longer life. *IUBMB Life* **72**, 814–824 (2020).

188. Bjedov, I. & Rallis, C. The Target of Rapamycin Signalling Pathway in Ageing and Lifespan Regulation. *Genes* **11**, 1043 (2020).

189. Robida-Stubbs, S. *et al.* TOR signaling and rapamycin influence longevity by regulating SKN-1/Nrf and DAF-16/FoxO. *Cell Metab* **15**, 713–724 (2012).

190. Selman, C. *et al.* Ribosomal Protein S6 Kinase 1 Signaling Regulates Mammalian Life Span. *Science* **326**, 140–144 (2009).

191. Luong, N. *et al.* Activated FOXO-mediated insulin resistance is blocked by reduction of TOR activity. *Cell Metab* **4**, 133–142 (2006).

192. Kapahi, P. *et al.* Regulation of lifespan in Drosophila by modulation of genes in the TOR signaling pathway. *Curr Biol* **14**, 885–890 (2004).

193. Vellai, T. *et al.* Genetics: influence of TOR kinase on lifespan in C. elegans. *Nature* **426**, 620 (2003).

194. Hansen, M. *et al.* Lifespan extension by conditions that inhibit translation in Caenorhabditis elegans. *Aging Cell* **6**, 95–110 (2007).

195. Kaeberlein, M., Burtner, C. R. & Kennedy, B. K. Recent developments in yeast aging. *PLoS Genet* **3**, e84 (2007).

196. Muegge, B. D. *et al.* Diet drives convergence in gut microbiome functions across mammalian phylogeny and within humans. *Science* **332**, 970–974 (2011).

197. Holmes, A. J. *et al.* Diet-Microbiome Interactions in Health Are Controlled by Intestinal Nitrogen Source Constraints. *Cell Metab* **25**, 140–151 (2017).

198. Catterson, J. H. *et al.* Short-Term, Intermittent Fasting Induces Long-Lasting Gut Health and TOR-Independent Lifespan Extension. *Curr Biol* **28**, 1714-1724.e4 (2018).

199. Keebaugh, E. S., Yamada, R., Obadia, B., Ludington, W. B. & Ja, W. W. Microbial Quantity Impacts Drosophila Nutrition, Development, and Lifespan. *iScience* **4**, 247–259 (2018).

200. Storelli, G. *et al.* Lactobacillus plantarum Promotes Drosophila Systemic Growth by Modulating Hormonal Signals through TOR-Dependent Nutrient Sensing. *Cell Metabolism* **14**, 403–414 (2011).

201. Storelli, G. *et al.* Drosophila Perpetuates Nutritional Mutualism by Promoting the Fitness of Its Intestinal Symbiont Lactobacillus plantarum. *Cell Metabolism* **27**, 362-377.e8 (2018).

202. Erkosar, B. *et al.* Pathogen Virulence Impedes Mutualist-Mediated Enhancement of Host Juvenile Growth via Inhibition of Protein Digestion. *Cell Host Microbe* **18**, 445–455 (2015).

203. Téfit, M. A. & Leulier, F. Lactobacillus plantarum favors the early emergence of fit and fertile adult Drosophila upon chronic undernutrition. *J Exp Biol* **220**, 900–907 (2017).

204. Sannino, D. R., Dobson, A. J., Edwards, K., Angert, E. R. & Buchon, N. The Drosophila melanogaster Gut Microbiota Provisions Thiamine to Its Host. *mBio* **9**, e00155-18 (2018).

205. Consuegra, J. *et al.* Drosophila-associated bacteria differentially shape the nutritional requirements of their host during juvenile growth. *PLOS Biology* **18**, e3000681 (2020).

206. Schwarzer, M. *et al.* Lactobacillus plantarum strain maintains growth of infant mice during chronic undernutrition. *Science* **351**, 854–857 (2016).

207. Dai, Z.-L., Zhang, J., Wu, G. & Zhu, W.-Y. Utilization of amino acids by bacteria from the pig small intestine. *Amino Acids* **39**, 1201–1215 (2010).

208. Conly, J. M. & Stein, K. The production of menaquinones (vitamin K2) by intestinal bacteria and their role in maintaining coagulation homeostasis. *Prog Food Nutr Sci* **16**, 307–343 (1992).

209. McCann, A. *et al.* Exploratory analysis of covariation of microbiota-derived vitamin K and cognition in older adults. *The American Journal of Clinical Nutrition* **110**, 1404–1415 (2019).

210. Wagatsuma, K. *et al.* Diversity of Gut Microbiota Affecting Serum Level of Undercarboxylated Osteocalcin in Patients with Crohn's Disease. *Nutrients* **11**, 1541 (2019).

211. Frick, P. G., Riedler, G. & Brögli, H. Dose response and minimal daily requirement for vitamin K in man. *J Appl Physiol* **23**, 387–389 (1967).

212. Beulens, J. W. J. *et al.* High dietary menaquinone intake is associated with reduced coronary calcification. *Atherosclerosis* **203**, 489–493 (2009).

213. Kurosu, M. & Begari, E. Vitamin K2 in electron transport system: are enzymes involved in vitamin K2 biosynthesis promising drug targets? *Molecules* **15**, 1531–1553 (2010).

214. Schultz, J., St LAWRENCE, P. & Newmeyer, D. A chemically defined medium for the growth of Drosophila melanogaster. *Anat Rec* **96**, 540 (1946).

215. SANG, J. H. The Quantitative Nutritional Requirements of Drosophila Melanogaster. *Journal of Experimental Biology* **33**, 45–72 (1956).

216. SANG, J. H. & KING, R. C. Nutritional Requirements of Axenically Cultured Drosophila Melanogaster Adults. *Journal of Experimental Biology* **38**, 793–809 (1961).

217. Ashburner, M. & Novitski, E. *The Genetics and biology of Drosophila*. (Academic Press, 1976).

218. Troen, A. M. *et al.* Lifespan modification by glucose and methionine in Drosophila melanogaster fed a chemically defined diet. *Age (Dordr)* **29**, 29–39 (2007).

219. Troen, A. M. *et al.* Erratum to: Lifespan modification by glucose and methionine in Drosophila melanogaster fed a chemically defined diet. *Age (Dordr)* **32**, 123 (2010).

220. Shchedrina, V. A. *et al.* Analyses of Fruit Flies That Do Not Express Selenoproteins or Express the Mouse Selenoprotein, Methionine Sulfoxide Reductase B1, Reveal a Role of Selenoproteins in Stress Resistance. *J Biol Chem* **286**, 29449–29461 (2011).

221. Piper, M., Piper, M. & Partridge, L. Preparation of a holidic medium for Drosophila melanogaster. *Protocol Exchange* (2013) doi:10.1038/protex.2013.082.

222. Piper, M. D. W. *et al.* A holidic medium for Drosophila melanogaster. *Nat Methods* **11**, 100–105 (2014).

223. Lee, W.-C. & Micchelli, C. A. Development and Characterization of a Chemically Defined Food for Drosophila. *PLOS ONE* **8**, e67308 (2013).

224. Piper, M. D. W. *et al.* Matching Dietary Amino Acid Balance to the In Silico-Translated Exome Optimizes Growth and Reproduction without Cost to Lifespan. *Cell Metab* **25**, 610–621 (2017).

225. Zanco, B., Mirth, C. K., Sgrò, C. M. & Piper, M. D. A dietary sterol trade-off determines lifespan responses to dietary restriction in Drosophila melanogaster females. *eLife* **10**, e62335 (2021).

226. Z, C.-S. *et al.* Cellular metabolic reprogramming controls sugar appetite in Drosophila. *Nature metabolism* **2**, (2020).

227. Norvaisas P *et al.* Host-Microbe-Drug-Nutrient Screen Identifies Bacterial Effectors of Metformin Therapy. *Cell* **178**, (2019).

228. Viitanen, A. *et al.* An image analysis method for regionally defined cellular phenotyping of the Drosophila midgut. *Cell Reports Methods* **1**, 100059 (2021).

229. Kabil, H., Kabil, O., Banerjee, R., Harshman, L. G. & Pletcher, S. D. Increased transsulfuration mediates longevity and dietary restriction in Drosophila. *Proc Natl Acad Sci U S A* **108**, 16831–16836 (2011).

230. Parinejad, N., Peco, E., Ferreira, T., Stacey, S. M. & van Meyel, D. J. Disruption of an EAAT-Mediated Chloride Channel in a Drosophila Model of Ataxia. *J Neurosci* **36**, 7640–7647 (2016).

231. Lewis, E. A new standard food medium. *Drosophila Information Service* 117–118 (1960).

232. Rera, M. *et al.* Modulation of Longevity and Tissue Homeostasis by the Drosophila PGC-1 Homolog. *Cell Metabolism* **14**, 623–634 (2011).

233. Hunter, G. L. *et al.* A role for actomyosin contractility in Notch signaling. *BMC Biology* **17**, 12 (2019).

234. Tennessen, J. M., Barry, W. E., Cox, J. & Thummel, C. S. Methods for studying metabolism in Drosophila. *Methods (San Diego, Calif.)* **68**, 105–15 (2014).

235. Deshpande, S. A. *et al.* Quantifying Drosophila food intake: comparative analysis of current methodology. *Nat Methods* **11**, 535–540 (2014).

236. Ja, W. W. *et al.* Prandiology of Drosophila and the CAFE assay. *Proceedings of the National Academy of Sciences* **104**, 8253–8256 (2007).

237. WIGGLESWORTH, V. B. The Utilization of Reserve Substances in Drosophila During Flight. *Journal of Experimental Biology* **26**, 150–163 (1949).

238. Tennessen, J. M., Barry, W. E., Cox, J. & Thummel, C. S. Methods for studying metabolism in Drosophila. *Methods* **68**, 105–115 (2014).

239. Heier, C. & Kühnlein, R. P. Triacylglycerol Metabolism in Drosophila melanogaster. *Genetics* **210**, (2018).

240. Partridge, L., Piper, M. D. W. & Mair, W. Dietary restriction in Drosophila. *Mech Ageing Dev* **126**, 938–950 (2005).

241. Simpson, S. J. & Raubenheimer, D. Macronutrient balance and lifespan. *Aging (Albany NY)* **1**, 875–880 (2009).

242. Bruce, K. D. *et al.* High carbohydrate-low protein consumption maximizes Drosophila lifespan. *Exp Gerontol* **48**, 1129–1135 (2013).

243. Lee, K. P. Dietary protein:carbohydrate balance is a critical modulator of lifespan and reproduction in Drosophila melanogaster: a test using a chemically defined diet. *J Insect Physiol* **75**, 12–19 (2015).

244. Strilbytska, O. *et al.* Parental dietary protein-to-carbohydrate ratio affects offspring lifespan and metabolism in drosophila. *Comp Biochem Physiol A Mol Integr Physiol* **241**, 110622 (2020).

245. Wong, A. C.-N., Chaston, J. M. & Douglas, A. E. The inconstant gut microbiota of Drosophila species revealed by 16S rRNA gene analysis. *ISME J* **7**, 1922–1932 (2013).

246. Chandler, J. A., Lang, J. M., Bhatnagar, S., Eisen, J. A. & Kopp, A. Bacterial Communities of Diverse Drosophila Species: Ecological Context of a Host–Microbe Model System. *PLOS Genetics* **7**, e1002272 (2011).

247. Lee, H.-Y., Lee, S.-H., Lee, J.-H., Lee, W.-J. & Min, K.-J. The role of commensal microbes in the lifespan of Drosophila melanogaster. *Aging (Albany NY)* **11**, 4611–4640 (2019).

248. Martins, R. R., McCracken, A. W., Simons, M. J. P., Henriques, C. M. & Rera, M. How to Catch a Smurf? – Ageing and Beyond… In vivo Assessment of Intestinal Permeability in Multiple Model Organisms. *Bio Protoc* **8**, e2722 (2018).

249. Shen, J. *et al.* CO2 anesthesia on Drosophila survival in aging research. *Archives of Insect Biochemistry and Physiology* **103**, e21639 (2020).

250. Buchon, N., Broderick, N. A., Poidevin, M., Pradervand, S. & Lemaitre, B. Drosophila intestinal response to bacterial infection: activation of host defense and stem cell proliferation. *Cell Host Microbe* **5**, 200–211 (2009).

251. Cronin, S. J. F. *et al.* Genome-wide RNAi screen identifies genes involved in intestinal pathogenic bacterial infection. *Science* **325**, 340–343 (2009).

252. Clegg, A., Young, J., Iliffe, S., Rikkert, M. O. & Rockwood, K. Frailty in elderly people. *The Lancet* **381**, 752–762 (2013).

253. Ferrucci, L. *et al.* Biomarkers of frailty in older persons. *J Endocrinol Invest* **25**, 10–15 (2002).

254. Yamada, T., Habara, O., Kubo, H. & Nishimura, T. Fat body glycogen serves as a metabolic safeguard for the maintenance of sugar levels in Drosophila. *Development* **145**, dev158865 (2018).

255. Yamada, T., Habara, O., Kubo, H. & Nishimura, T. Correction: Fat body glycogen serves as a metabolic safeguard for the maintenance of sugar levels in Drosophila (doi:10.1242/dev.158865). *Development* **145**, (2018).

256. Westfall, S., Lomis, N. & Prakash, S. Longevity extension in Drosophila through gut-brain communication. *Sci Rep* **8**, 8362 (2018).

257. DiAngelo, J. R. & Birnbaum, M. J. Regulation of fat cell mass by insulin in Drosophila melanogaster. *Mol Cell Biol* **29**, 6341–6352 (2009).

258. Dionne, M. S., Pham, L. N., Shirasu-Hiza, M. & Schneider, D. S. Akt and FOXO dysregulation contribute to infection-induced wasting in Drosophila. *Curr Biol* **16**, 1977–1985 (2006).

259. Davoodi, S. *et al.* The Immune Deficiency Pathway Regulates Metabolic Homeostasis in Drosophila. *J Immunol* **202**, 2747–2759 (2019).

260. Roth, S. W., Bitterman, M. D., Birnbaum, M. J. & Bland, M. L. Innate Immune Signaling in Drosophila Blocks Insulin Signaling by Uncoupling PI(3,4,5)P3 Production and Akt Activation. *Cell Rep* **22**, 2550–2556 (2018).

261. Suzawa, M., Muhammad, N. M., Joseph, B. S. & Bland, M. L. The Toll Signaling Pathway Targets the Insulin-like Peptide Dilp6 to Inhibit Growth in Drosophila. *Cell Rep* **28**, 1439-1446.e5 (2019).

262. St-Onge, M.-P. & Gallagher, D. Body composition changes with aging: The cause or the result of alterations in metabolic rate and macronutrient oxidation? *Nutrition* **26**, 152–155 (2010).

263. Silver, A. J., Guillen, C. P., Kahl, M. J. & Morley, J. E. Effect of aging on body fat. *J Am Geriatr Soc* **41**, 211–213 (1993).

264. Baumgartner, R. N., Stauber, P. M., McHugh, D., Koehler, K. M. & Garry, P. J. Cross-sectional age differences in body composition in persons 60+ years of age. *J Gerontol A Biol Sci Med Sci* **50**, M307-316 (1995).

265. Kyle, U. G. *et al.* Total body mass, fat mass, fat-free mass, and skeletal muscle in older people: cross-sectional differences in 60-year-old persons. *J Am Geriatr Soc* **49**, 1633–1640 (2001).

266. Wilson, P. W. F. & Kannel, W. B. Obesity, Diabetes, and Risk of Cardiovascular Disease in the Elderly. *The American Journal of Geriatric Cardiology* **11**, 119–124 (2002).

267. Hunter, G. R., Gower, B. A. & Kane, B. L. Age Related Shift in Visceral Fat. *Int J Body Compos Res* **8**, 103–108 (2010).

268. JafariNasabian, P., Inglis, J. E., Reilly, W., Kelly, O. J. & Ilich, J. Z. Aging human body: changes in bone, muscle and body fat with consequent changes in nutrient intake. *Journal of Endocrinology* **234**, R37–R51 (2017).

269. Kalyani, R. R., Corriere, M. & Ferrucci, L. Age-related and disease-related muscle loss: the effect of diabetes, obesity, and other diseases. *The Lancet Diabetes & Endocrinology* **2**, 819–829 (2014).

270. Cohn, S. H. *et al.* Compartmental body composition based on total-body nitrogen, potassium, and calcium. *American Journal of Physiology-Endocrinology and Metabolism* **239**, E524–E530 (1980).

271. Broadwin, J., Goodman-Gruen, D. & Slymen, D. Ability of fat and fat-free mass percentages to predict functional disability in older men and women. *J Am Geriatr Soc* **49**, 1641–1645 (2001).

272. Landers, K. A., Hunter, G. R., Wetzstein, C. J., Bamman, M. M. & Weinsier, R. L. The interrelationship among muscle mass, strength, and the ability to perform physical tasks of daily living in younger and older women. *J Gerontol A Biol Sci Med Sci* **56**, B443-448 (2001).

273. Norman, K., Haß, U. & Pirlich, M. Malnutrition in Older Adults—Recent Advances and Remaining Challenges. *Nutrients* **13**, 2764 (2021).

274. Nakanishi, N. *et al.* Associations between self-assessed masticatory disability and health of community-residing elderly people. *Community Dent Oral Epidemiol* **27**, 366–371 (1999).

275. Müller, F., Naharro, M. & Carlsson, G. E. What are the prevalence and incidence of tooth loss in the adult and elderly population in Europe? *Clin Oral Implants Res* **18 Suppl 3**, 2–14 (2007).

276. Palinkas, M. *et al.* Age and gender influence on maximal bite force and masticatory muscles thickness. *Arch Oral Biol* **55**, 797–802 (2010).

277. Newton, J. P., Yemm, R., Abel, R. W. & Menhinick, S. Changes in human jaw muscles with age and dental state. *Gerodontology* **10**, 16–22 (1993).

278. Pilgrim, A., Robinson, S., Sayer, A. A. & Roberts, H. An overview of appetite decline in older people. *Nurs Older People* **27**, 29–35 (2015).

279. Clarkston, W. K. *et al.* Evidence for the anorexia of aging: gastrointestinal transit and hunger in healthy elderly vs. young adults. *Am J Physiol* **272**, R243-248 (1997).

280. Astor, F. C., Hanft, K. L. & Ciocon, J. O. Xerostomia: a prevalent condition in the elderly. *Ear Nose Throat J* **78**, 476–479 (1999).

281. Ichikawa, K. *et al.* Relationships between the amount of saliva and medications in elderly individuals. *Gerodontology* **28**, 116–120 (2011).

282. Smith, C. H. *et al.* Effect of aging on stimulated salivary flow in adults. *J Am Geriatr Soc* **61**, 805–808 (2013).

283. Keller, H. H. Malnutrition in institutionalized elderly: how and why? *J Am Geriatr Soc* **41**, 1212–1218 (1993).

284. Mowé, M., Bøhmer, T. & Kindt, E. Reduced nutritional status in an elderly population (> 70 y) is probable before disease and possibly contributes to the development of disease. *Am J Clin Nutr* **59**, 317–324 (1994).

285. Smith, G. A., Logemann, J. A., Burghardt, W. R., Zecker, W. G. & Rademaker, A. W. Oral and oropharyngeal perceptions of fluid viscosity across the age span. *Dysphagia* **21**, (2006).

286. Logemann, J. A. Effects of aging on the swallowing mechanism. *Otolaryngologic clinics of North America* **23**, (1990).

287. Lee, H.-Y., Lee, S.-H. & Min, K.-J. The Increased Abundance of Commensal Microbes Decreases Drosophila melanogaster Lifespan through an Age-Related Intestinal Barrier Dysfunction. *Insects* **13**, 219 (2022).

288. Wu, C.-S. *et al.* Age-dependent remodeling of gut microbiome and host serum metabolome in mice. *Aging (Albany NY)* **13**, 6330–6345 (2021).

289. Meng, C., Feng, S., Hao, Z., Dong, C. & Liu, H. Changes in gut microbiota composition with age and correlations with gut inflammation in rats. *PLOS ONE* **17**, e0265430 (2022).

290. Haran, J. P. & McCormick, B. A. Aging, Frailty, and the Microbiome—How Dysbiosis Influences Human Aging and Disease. *Gastroenterology* **160**, 507–523 (2021).

291. Resende, L. P., Monteiro, A., Brás, R., Lopes, T. & Sunkel, C. E. Aneuploidy in intestinal stem cells promotes gut dysplasia in Drosophila. *J Cell Biol* **217**, 3930–3946 (2018).

292. Ryo, J. H. *et al.* Innate immune homeostasis by the homeobox gene caudal and commensal-gut mutualism in Drosophila. *Science (New York, N.Y.)* **319**, (2008).

293. Radtke, F. & Clevers, H. Self-Renewal and Cancer of the Gut: Two Sides of a Coin. *Science* **307**, 1904–1909 (2005).

294. Radtke, F., Clevers, H. & Riccio, O. From Gut Homeostasis to Cancer. *Current Molecular Medicine* **6**, 275–289 (2006).

295. Moorefield, E. C. *et al.* Aging effects on intestinal homeostasis associated with expansion and dysfunction of intestinal epithelial stem cells. *Aging (Albany NY)* **9**, 1898–1915 (2017).

296. Untersmayr, E., Brandt, A., Koidl, L. & Bergheim, I. The Intestinal Barrier Dysfunction as Driving Factor of Inflammaging. *Nutrients* **14**, (2022).

297. Feldman, M., Cryer, B., McArthur, K., Huet, B. & Lee, E. Effects of aging and gastritis on gastric acid and pepsin secretion in humans: A prospective study. *Gastroenterology* **110**, 1043–1052 (1996).

298. Lee, M.-F., Russell, R. M., Montgomery, R. K. & Krasinski, S. D. Total Intestinal Lactase and Sucrase Activities Are Reduced in Aged Rats. *The Journal of Nutrition* **127**, 1382–1387 (1997).

299. Vellas, B. *et al.* Exocrine pancreatic secretion in the elderly. *Int J Pancreatol* **3**, 497–502 (1988).

300. Detel, D., Baticic, L. & Varljen, J. The Influence of Age on Intestinal Dipeptidyl Peptidase IV (DPP IV/CD26), Disaccharidases, and Alkaline Phosphatase Enzyme Activity in C57BL/6 Mice. *Experimental Aging Research* **34**, 49–62 (2007).

301. Brogna, A., Ferrara, R., Bucceri, A. M., Lanteri, E. & Catalano, F. Influence of aging on gastrointestinal transit time. An ultrasonographic and radiologic study. *Invest Radiol* **34**, 357–359 (1999).

302. Kim, S.-E. Colonic Slow Transit Can Cause Changes in the Gut Environment Observed in the Elderly. *J Neurogastroenterol Motil* **23**, 3–4 (2017).

303. Höhn, P., Gabbert, H. & Wagner, R. Differentiation and aging of the rat intestinal mucosa. II. Morphological, enzyme histochemical and disc electrophoretic aspects of the aging of the small intestinal mucosa. *Mech Ageing Dev* **7**, 217–226 (1978).

304. Martin, K., Kirkwood, T. B. & Potten, C. S. Age changes in stem cells of murine small intestinal crypts. *Exp Cell Res* **241**, 316–323 (1998).

305. Duan, C. Specifying the cellular responses to IGF signals: roles of IGF-binding proteins. *J Endocrinol* **175**, 41–54 (2002).

306. Hassan, Z. A. *et al.* Morphological alterations in the jejunal mucosa of aged rats and the possible protective role of green tea. *Folia Histochem Cytobiol* **55**, 124–139 (2017).

307. Lipski, P. S., Bennett, M. K., Kelly, P. J. & James, O. F. Ageing and duodenal morphometry. *J Clin Pathol* **45**, 450–452 (1992).

308. Corazza, G. R., Frazzoni, M., Gatto, M. R. A. & Gasbarrini, G. Ageing and Small-Bowel Mucosa: A Morphometric Study. *GER* **32**, 60–65 (1986).

309. Ciccocioppo, R. *et al.* Small bowel enterocyte apoptosis and proliferation are increased in the elderly. *Gerontology* **48**, 204–208 (2002).

310. Soenen, S., Rayner, C. K., Jones, K. L. & Horowitz, M. The ageing gastrointestinal tract. *Curr Opin Clin Nutr Metab Care* **19**, 12–18 (2016).

311. ter Borg, S. *et al.* Micronutrient intakes and potential inadequacies of community-dwelling older adults: a systematic review. *Br J Nutr* **113**, 1195–1206 (2015).

312. Bullamore, J. R., Wilkinson, R., Gallagher, J. C., Nordin, B. E. C. & Marshall, D. H. Effect of Age on Calcium Absorption. *The Lancet* **296**, 535–537 (1970).

313. Veldurthy, V. *et al.* Vitamin D, calcium homeostasis and aging. *Bone Res* **4**, 1–7 (2016).

314. Stover, P. J. Vitamin B12 and older adults. *Curr Opin Clin Nutr Metab Care* **13**, 24–27 (2010).

315. Russell, R. M. Factors in Aging that Effect the Bioavailability of Nutrients. *The Journal of Nutrition* **131**, 1359S-1361S (2001).

316. Luo, Z. *et al.* Ex vivo and in situ approaches used to study intestinal absorption. *Journal of Pharmacological and Toxicological Methods* **68**, 208–216 (2013).

317. Wilson, T. H. & Wiseman, G. The use of sacs of everted small intestine for the study of the transference of substances from the mucosal to the serosal surface. *J Physiol* **123**, 116–125 (1954).

318. Barthe, L., Woodley, J. F., Kenworthy, S. & Houin, G. An improved everted gut sac as a simple and accurate technique to measure paracellular transport across the small intestine. *Eur J Drug Metab Pharmacokinet* **23**, 313–323 (1998).

319. Balimane, P. V., Chong, S. & Morrison, R. A. Current methodologies used for evaluation of intestinal permeability and absorption. *J Pharmacol Toxicol Methods* **44**, 301–312 (2000).

320. Liu, W. *et al.* Developments in Methods for Measuring the Intestinal Absorption of Nanoparticle-Bound Drugs. *Int J Mol Sci* **17**, 1171 (2016).

321. Ussing, H. H. & Zerahn, K. Active transport of sodium as the source of electric current in the short-circuited isolated frog skin. *Acta Physiol Scand* **23**, 110–127 (1951).

322. Moughan, P. J. & Wolfe, R. R. Determination of Dietary Amino Acid Digestibility in Humans. *The Journal of Nutrition* **149**, 2101–2109 (2019).

323. Trommelen, J., Tomé, D. & van Loon, L. J. C. Gut amino acid absorption in humans: Concepts and relevance for postprandial metabolism. *Clinical Nutrition Open Science* **36**, 43–55 (2021).

324. Volpi, E., Mittendorfer, B., Wolf, S. E. & Wolfe, R. R. Oral amino acids stimulate muscle protein anabolism in the elderly despite higher first-pass splanchnic extraction. *Am J Physiol* **277**, E513-520 (1999).

325. Hill, P. G. Faecal fat: time to give it up. *Ann Clin Biochem* **38**, 164–167 (2001).

326. Jandacek, R. J., Ramirez, M. M. & Crouse, J. R. Effects of partial replacement of dietary fat by olestra on dietary cholesterol absorption in man. *Metabolism* **39**, 848–852 (1990).

327. Hoving, J., Wilson, J. H., Valkema, A. J. & Woldring, M. G. Estimation of fat absorption from single fecal specimens using 131I-triolein and 75Se-triether. A study in rats with and without induced steatorrhea. *Gastroenterology* **72**, 406–412 (1977).

328. Jandacek, R. J., Heubi, J. E. & Tso, P. A novel, noninvasive method for the measurement of intestinal fat absorption. *Gastroenterology* **127**, 139–144 (2004).

329. Dencker, H., Göthlin, J., Meeuwisse, G. & Tranberg, K.-G. Human Intestinal Absorption of Glucose Measured by Portal Catheterization. *Scandinavian Journal of Gastroenterology* **7**, 451–453 (1972).

330. Lifschitz, C. H. *et al.* A carbon-13 breath test to characterize glucose absorption and utilization in children. *J Pediatr Gastroenterol Nutr* **7**, 842–847 (1988).

331. Sun, S. Z. & Empie, M. W. Fructose metabolism in humans – what isotopic tracer studies tell us. *Nutr Metab (Lond)* **9**, 89 (2012).

332. Beyreiss, K., Hoepffner, W., Scheerschmidt, G. & Müller, F. Digestion and absorption rates of lactose, glucose, galactose, and fructose in three infants with congenital glucose-galactose malabsorption: perfusion studies. *J Pediatr Gastroenterol Nutr* **4**, 887–892 (1985).

333. Lindquist, B. L. & Wranne, L. Problems in analysis of faecal sugar. *Arch Dis Child* **51**, 319–321 (1976).

334. Ford, J. D. & Haworth, J. C. The fecal excretion of sugars in children. *The Journal of Pediatrics* **63**, 988–990 (1963).

335. Basolo, A. *et al.* Procedures for Measuring Excreted and Ingested Calories to Assess Nutrient Absorption Using Bomb Calorimetry. *Obesity (Silver Spring)* **28**, 2315–2322 (2020).

336. Zietek, T. *et al.* Organoids to Study Intestinal Nutrient Transport, Drug Uptake and Metabolism – Update to the Human Model and Expansion of Applications. *Frontiers in Bioengineering and Biotechnology* **8**, (2020).

337. Rémond, D. *et al.* Understanding the gastrointestinal tract of the elderly to develop dietary solutions that prevent malnutrition. *Oncotarget* **6**, 13858–13898 (2015).

338. Gibson, G. R., Probert, H. M., Loo, J. V., Rastall, R. A. & Roberfroid, M. B. Dietary modulation of the human colonic microbiota: updating the concept of prebiotics. *Nutr Res Rev* **17**, 259–275 (2004).

339. Faure, M. *et al.* Specific Amino Acids Increase Mucin Synthesis and Microbiota in Dextran Sulfate Sodium–Treated Rats. *The Journal of Nutrition* **136**, 1558–1564 (2006).

340. Faure, M. *et al.* Development of a rapid and convenient method to purify mucins and determine their in vivo synthesis rate in rats. *Anal Biochem* **307**, 244–251 (2002).

341. Neutra MR, F. J. Gastrointestinal mucus: synthesis, secretion and function. in *Physiology of the gastrointestinal tract* 975–1009 (Raven Press, 1987).

342. Huang, Y., Li, L. & Rong, Y. S. JiangShi: a widely distributed Mucin-like protein essential for Drosophila development. *G3 (Bethesda)* **12**, jkac126 (2022).

343. Syed, Z. A., Härd, T., Uv, A. & van Dijk-Härd, I. F. A Potential Role for Drosophila Mucins in Development and Physiology. *PLoS One* **3**, e3041 (2008).

344. Dai, Z.-L., Wu, G. & Zhu, W.-Y. Amino acid metabolism in intestinal bacteria: links between gut ecology and host health. *Front Biosci (Landmark Ed)* **16**, 1768–1786 (2011).

345. Agus, A., Clément, K. & Sokol, H. Gut microbiota-derived metabolites as central regulators in metabolic disorders. *Gut* **70**, 1174–1182 (2021).

346. Ridaura, V. K. *et al.* Gut Microbiota from Twins Discordant for Obesity Modulate Metabolism in Mice. *Science* **341**, 1241214 (2013).

347. Pedersen, H. K. *et al.* Human gut microbes impact host serum metabolome and insulin sensitivity. *Nature* **535**, 376–381 (2016).

348. Liu, R. *et al.* Gut microbiome and serum metabolome alterations in obesity and after weight-loss intervention. *Nat Med* **23**, 859–868 (2017).

349. Zhou, M. *et al.* Targeting BCAA Catabolism to Treat Obesity-Associated Insulin Resistance. *Diabetes* **68**, 1730–1746 (2019).

350. Fan, Y. & Pedersen, O. Gut microbiota in human metabolic health and disease. *Nat Rev Microbiol* **19**, 55–71 (2021).

351. Schoeler, M. & Caesar, R. Dietary lipids, gut microbiota and lipid metabolism. *Rev Endocr Metab Disord* **20**, 461–472 (2019).

352. Le Roy, T. *et al.* The intestinal microbiota regulates host cholesterol homeostasis. *BMC Biol* **17**, 94 (2019).

353. Rabot, S. *et al.* Germ-free C57BL/6J mice are resistant to high-fat-diet-induced insulin resistance and have altered cholesterol metabolism. *FASEB J* **24**, 4948–4959 (2010).

354. Kriaa, A. *et al.* Microbial impact on cholesterol and bile acid metabolism: current status and future prospects. *J Lipid Res* **60**, 323–332 (2019).

355. Benno, P. *et al.* Examination of intestinal conversion of cholesterol to coprostanol in 633 healthy subjects reveals an age- and sex-dependent pattern. *Microbial Ecology in Health and Disease* **17**, 200–204 (2005).

356. Kenny, D. J. *et al.* Cholesterol Metabolism by Uncultured Human Gut Bacteria Influences Host Cholesterol Level. *Cell Host & Microbe* **28**, 245-257.e6 (2020).

357. Juste, C. & Gérard, P. Cholesterol-to-Coprostanol Conversion by the Gut Microbiota: What We Know, Suspect, and Ignore. *Microorganisms* **9**, 1881 (2021).

358. Newsome, S. D. *et al.* Isotopic and genetic methods reveal the role of the gut microbiome in mammalian host essential amino acid metabolism. *Proceedings of the Royal Society B: Biological Sciences* **287**, 20192995 (2020).

359. Akashi, H. & Gojobori, T. Metabolic efficiency and amino acid composition in the proteomes of Escherichia coli and Bacillus subtilis. *Proceedings of the National Academy of Sciences* **99**, 3695–3700 (2002).

360. Barton, M. D., Delneri, D., Oliver, S. G., Rattray, M. & Bergman, C. M. Evolutionary Systems Biology of Amino Acid Biosynthetic Cost in Yeast. *PLoS One* **5**, e11935 (2010).

361. McGee, M. D. *et al.* Loss of intestinal nuclei and intestinal integrity in aging C. elegans. *Aging Cell* **10**, 699–710 (2011).

362. Choi, N.-H., Kim, J.-G., Yang, D.-J., Kim, Y.-S. & Yoo, M.-A. Age-related changes in Drosophila midgut are associated with PVF2, a PDGF/VEGF-like growth factor. *Aging Cell* **7**, 318–334 (2008).

363. Holt, P. R., Yeh, K. Y. & Kotler, D. P. Altered controls of proliferation in proximal small intestine of the senescent rat. *Proc Natl Acad Sci U S A* **85**, 2771–2775 (1988).

364. Wang, L., Li, J., Li, Q., Zhang, J. & Duan, X.-L. Morphological changes of cell proliferation and apoptosis in rat jejunal mucosa at different ages. *World J Gastroenterol* **9**, 2060–2064 (2003).

365. Rosa, E. F. *et al.* Habitual exercise program protects murine intestinal, skeletal, and cardiac muscles against aging. *J Appl Physiol (1985)* **99**, 1569–1575 (2005).

366. Nalapareddy, K. *et al.* Canonical Wnt Signaling Ameliorates Aging of Intestinal Stem Cells. *Cell Rep* **18**, 2608–2621 (2017).

367. Webster, S. G. & Leeming, J. T. The appearance of the small bowel mucosa in old age. *Age Ageing* **4**, 168–174 (1975).

368. Corazza, G. R. *et al.* Proliferating cell nuclear antigen expression is increased in small bowel epithelium in the elderly. *Mech Ageing Dev* **104**, 1–9 (1998).

369. Sengupta, P. & Dutta, S. Mapping the Age of Laboratory Rabbit Strains to Human. *Int J Prev Med* **11**, 194 (2020).

370. Meier, J. & Sturm, A. The Intestinal Epithelial Barrier: Does It Become Impaired with Age? *Dig Dis* **27**, 240–245 (2009).

371. Navab, F. & Winter, C. G. Effect of aging on intestinal absorption of aromatic amino acids in vitro in the rat. *American Journal of Physiology-Gastrointestinal and Liver Physiology* **254**, G630–G636 (1988).

372. Pénzes, L. Intestinal absorption of glycine, l-alanine and l-leucine in the old rat. *Experimental Gerontology* **9**, 245–252 (1974).

373. Vinardell, M. P. Age influences on amino acid intestinal transport. *Comparative Biochemistry and Physiology Part A: Physiology* **103**, 169–171 (1992).

374. Milan, A. M. *et al.* Older Adults Have Delayed Amino Acid Absorption after a High Protein Mixed Breakfast Meal. *J Nutr Health Aging* **19**, 839–845 (2015).

375. Gorissen, S. H. M. *et al.* Protein Type, Protein Dose, and Age Modulate Dietary Protein Digestion and Phenylalanine Absorption Kinetics and Plasma Phenylalanine Availability in Humans. *The Journal of Nutrition* **150**, 2041–2050 (2020).

376. Ten Have, G. A. M., Engelen, M. P. K. J., Luiking, Y. C. & Deutz, N. E. P. Absorption kinetics of amino acids, peptides, and intact proteins. *Int J Sport Nutr Exerc Metab* **17 Suppl**, S23-36 (2007).

377. Boirie, Y., Gachon, P. & Beaufrère, B. Splanchnic and whole-body leucine kinetics in young and elderly men. *Am J Clin Nutr* **65**, 489–495 (1997).

378. Jourdan, M., Deutz, N. E. P., Cynober, L. & Aussel, C. Features, Causes and Consequences of Splanchnic Sequestration of Amino Acid in Old Rats. *PLoS One* **6**, e27002 (2011).

379. Rutten, E. P. A. *et al.* Decreased whole-body and splanchnic glutamate metabolism in healthy elderly men and patients with chronic obstructive pulmonary disease in the postabsorptive state and in response to feeding. *J Nutr* **135**, 2166–2170 (2005).

380. Werner, I. & Hambraeus, L. The digestive capacity of elderly people. The effect of a high protein diet. *Acta Soc Med Ups* **76**, 239–242 (1971).

381. Danford, D. E. & Munro, H. N. *Nutrition, Aging, and the Elderly*. (Springer Science & Business Media, 2013).

382. Gidwaney, N. G., Bajpai, M. & Chokhavatia, S. S. Gastrointestinal Dysmotility in the Elderly. *Journal of Clinical Gastroenterology* **50**, 819–827 (2016).

383. Soenen, S., Rayner, C. K., Horowitz, M. & Jones, K. L. Gastric Emptying in the Elderly. *Clinics in Geriatric Medicine* **31**, 339–353 (2015).

384. Saad, R. J., Semler, J. R., Wilding, G. E. & Chey, W. D. 896 The Effect of Age on Regional and Whole Gut Transit Times in Healthy Adults. *Gastroenterology* **5 Supplement 1**, S-127 (2010).

385. Mitchell, E. L. *et al.* Reduced intestinal motility, mucosal barrier function, and inflammation in aged monkeys. *J Nutr Health Aging* **21**, 354–361 (2017).

386. Sun, T. *et al.* Aging-dependent decrease in the numbers of enteric neurons, interstitial cells of Cajal and expression of connexin43 in various regions of gastrointestinal tract. *Aging (Albany NY)* **10**, 3851–3865 (2018).

387. Xi, J. *et al.* The TORC1 inhibitor Nprl2 protects age-related digestive function in Drosophila. *Aging (Albany NY)* **11**, 9811–9828 (2019).

388. El Husseiny, I. M., El Kholy, S., Mohamed, A. Z., Meshrif, W. S. & Elbrense, H. Alterations in biogenic amines levels associated with age-related muscular tissue impairment in Drosophila melanogaster. *Saudi Journal of Biological Sciences* **29**, 3739–3748 (2022).

389. Mourad, F. H. *et al.* Amino acids in the rat intestinal lumen regulate their own absorption from a distant intestinal site. *Am J Physiol Gastrointest Liver Physiol* **297**, G292-298 (2009).

390. Louis, P. & Flint, H. J. Diversity, metabolism and microbial ecology of butyrate-producing bacteria from the human large intestine. *FEMS Microbiology Letters* **294**, 1–8 (2009).

391. Miller, T. L. & Wolin, M. J. Pathways of acetate, propionate, and butyrate formation by the human fecal microbial flora. *Applied and Environmental Microbiology* **62**, 1589–1592 (1996).

392. O'Keefe, S. J. D. Diet, microorganisms and their metabolites, and colon cancer. *Nat Rev Gastroenterol Hepatol* **13**, 691–706 (2016).

393. Gaudier, E., Rival, M., Buisine, M. P., Robineau, I. & Hoebler, C. C. Butyrate enemas upregulate MUC Genes expression but decrease adherent mucus thickness in mice colon. *Physiological Research* **58**, 111 (2009).

394. Peng, L., Li, Z.-R., Green, R. S., Holzman, I. R. & Lin, J. Butyrate Enhances the Intestinal Barrier by Facilitating Tight Junction Assembly via Activation of AMP-Activated Protein Kinase in Caco-2 Cell Monolayers. *The Journal of Nutrition* **139**, 1619–1625 (2009).

395. Lewis, K. *et al.* Enhanced translocation of bacteria across metabolically stressed epithelia is reduced by butyrate†. *Inflammatory Bowel Diseases* **16**, 1138–1148 (2010).

396. Karlsson, F. H. *et al.* Symptomatic atherosclerosis is associated with an altered gut metagenome. *Nat Commun* **3**, 1245 (2012).

397. Mell, B. *et al.* Evidence for a link between gut microbiota and hypertension in the Dahl rat. *Physiological Genomics* **47**, 187–197 (2015).

398. Yang, T. *et al.* Gut Dysbiosis Is Linked to Hypertension. *Hypertension* **65**, 1331–1340 (2015).

399. Tan, J. *et al.* Chapter Three - The Role of Short-Chain Fatty Acids in Health and Disease. in *Advances in Immunology* (ed. Alt, F. W.) vol. 121 91–119 (Academic Press, 2014).

400. Dalile, B., Van Oudenhove, L., Vervliet, B. & Verbeke, K. The role of short-chain fatty acids in microbiota–gut–brain communication. *Nat Rev Gastroenterol Hepatol* **16**, 461–478 (2019).

401. Wang, L. *et al.* Elevated Fecal Short Chain Fatty Acid and Ammonia Concentrations in Children with Autism Spectrum Disorder. *Dig Dis Sci* **57**, 2096–2102 (2012).

402. Ho, L. *et al.* Protective roles of intestinal microbiota derived short chain fatty acids in Alzheimer's disease-type beta-amyloid neuropathological mechanisms. *Expert Review of Neurotherapeutics* **18**, 83–90 (2018).

403. Skonieczna-Żydecka, K. *et al.* Faecal Short Chain Fatty Acids Profile is Changed in Polish Depressive Women. *Nutrients* **10**, 1939 (2018).

404. Adair, K. L. & Douglas, A. E. Making a microbiome: the many determinants of host-associated microbial community composition. *Current Opinion in Microbiology* **35**, 23–29 (2017).

405. Abreu, N. A. & Taga, M. E. Decoding molecular interactions in microbial communities. *FEMS Microbiology Reviews* **40**, 648–663 (2016).

406. Fischbach, M. A. & Sonnenburg, J. L. Eating For Two: How Metabolism Establishes Interspecies Interactions in the Gut. *Cell Host & Microbe* **10**, 336–347 (2011).

407. Sommer, A. J. & Newell, P. D. Metabolic Basis for Mutualism between Gut Bacteria and Its Impact on the Drosophila melanogaster Host. *Appl Environ Microbiol* **85**, e01882-18 (2019).

408. Arike, L. *et al.* Protein Turnover in Epithelial Cells and Mucus along the Gastrointestinal Tract Is Coordinated by the Spatial Location and Microbiota. *Cell Reports* **30**, 1077-1087.e3 (2020).

409. Gayer, C. P. & Basson, M. D. The effects of mechanical forces on intestinal physiology and pathology. *Cell Signal* **21**, 1237–1244 (2009).

410. Mayhew, T. M., Myklebust, R., Whybrow, A. & Jenkins, R. Epithelial integrity, cell death and cell loss in mammalian small intestine. *Histol Histopathol* **14**, 257–267 (1999).

411. Smith, K., McCoy, K. D. & Macpherson, A. J. Use of axenic animals in studying the adaptation of mammals to their commensal intestinal microbiota. *Seminars in Immunology* **19**, 59–69 (2007).

412. Reikvam, D. H. *et al.* Depletion of Murine Intestinal Microbiota: Effects on Gut Mucosa and Epithelial Gene Expression. *PLOS ONE* **6**, e17996 (2011).

413. Guan, X. L. *et al.* Biochemical Membrane Lipidomics during Drosophila Development. *Developmental Cell* **24**, 98–111 (2013).

414. Clark, A. J. & Block, K. The absence of sterol synthesis in insects. *J Biol Chem* **234**, 2578–2582 (1959).

415. Huang, Z. & London, E. Cholesterol lipids and cholesterol-containing lipid rafts in bacteria. *Chem Phys Lipids* **199**, 11–16 (2016).

416. Dutta, D. *et al.* Regional Cell-Specific Transcriptome Mapping Reveals Regulatory Complexity in the Adult Drosophila Midgut. *Cell Reports* **12**, 346–358 (2015).

417. Lehane, M. J. Peritrophic Matrix Structure and Function. *Annual Review of Entomology* **42**, 525–550 (1997).

418. Garcia-Gonzalez, E. & Genersch, E. Honey bee larval peritrophic matrix degradation during infection with Paenibacillus larvae, the aetiological agent of American foulbrood of honey bees, is a key step in pathogenesis. *Environmental Microbiology* **15**, 2894–2901 (2013).

419. Nakamura, K. *et al.* Peritrophic matrix-degrading proteins are dispensable virulence factors in a virulent Melissococcus plutonius strain. *Sci Rep* **11**, 8798 (2021).

420. Forstner, J. F. Intestinal Mucins in Health and Disease. *DIG* **17**, 234–263 (1978).

421. Hollingsworth, M. A. & Swanson, B. J. Mucins in cancer: protection and control of the cell surface. *Nat Rev Cancer* **4**, 45–60 (2004).

422. Perez-Vilar, J. & Hill, R. L. The Structure and Assembly of Secreted Mucins * 210. *Journal of Biological Chemistry* **274**, 31751–31754 (1999).

423. Charroux, B. & Royet, J. Drosophila immune response: From systemic antimicrobial peptide production in fat body cells to local defense in the intestinal tract. *Fly (Austin)* **4**, 40–47 (2010).

424. Loch, G. *et al.* Antimicrobial peptides extend lifespan in Drosophila. *PLoS One* **12**, e0176689 (2017).

425. Bulet, P., Hetru, C., Dimarcq, J.-L. & Hoffmann, D. Antimicrobial peptides in insects; structure and function. *Developmental & Comparative Immunology* **23**, 329–344 (1999).

426. Miguel-Aliaga, I., Jasper, H. & Lemaitre, B. Anatomy and Physiology of the Digestive Tract of Drosophila melanogaster. *Genetics* **210**, 357–396 (2018).

427. Abraham, I. & Doane, W. W. Genetic regulation of tissue-specific expression of amylase structural genes in Drosophila melanogaster. *Proceedings of the National Academy of Sciences* **75**, 4446–4450 (1978).

428. Dutta, D., Buchon, N., Xiang, J. & Edgar, B. A. Regional Cell Specific RNA Expression Profiling of FACS Isolated Drosophila Intestinal Cell Populations. *Current Protocols in Stem Cell Biology* **34**, 2F.2.1-2F.2.14 (2015).

429. Kylsten, P., Kimbrell, D. A., Daffre, S., Samakovlis, C. & Hultmark, D. The lysozyme locus in Drosophila melanogaster: different genes are expressed in midgut and salivary glands. *Molec. Gen. Genet.* **232**, 335–343 (1992).

430. Combe, B. E. *et al.* Drosophila Microbiota Modulates Host Metabolic Gene Expression via IMD/NF-κB Signaling. *PLOS ONE* **9**, e94729 (2014).

431. Nakagawa, S., Lagisz, M., Hector, K. L. & Spencer, H. G. Comparative and meta-analytic insights into life extension via dietary restriction. *Aging Cell* **11**, 401–409 (2012).

432. Solon-Biet, S. M. *et al.* The ratio of macronutrients, not caloric intake, dictates cardiometabolic health, aging, and longevity in ad libitum-fed mice. *Cell Metab* **19**, 418–430 (2014).

433. Mirzaei, H., Suarez, J. A. & Longo, V. D. Protein and amino acid restriction, aging and disease: from yeast to humans. *Trends in Endocrinology & Metabolism* **25**, 558–566 (2014).

434. Juricic, P., Grönke, S. & Partridge, L. Branched-Chain Amino Acids Have Equivalent Effects to Other Essential Amino Acids on Lifespan and Aging-Related Traits in Drosophila. *J Gerontol A Biol Sci Med Sci* **75**, 24–31 (2020).

435. Parkhitko, A. A. *et al.* A genetic model of methionine restriction extends Drosophila health- and lifespan. *Proceedings of the National Academy of Sciences* **118**, e2110387118 (2021).

436. Segall, P. Long-term tryptophan restriction and aging in the rat. *Aktuelle Gerontol* **7**, 535–538 (1977).

437. Richardson, N. E. *et al.* Lifelong restriction of dietary branched-chain amino acids has sex-specific benefits for frailty and life span in mice. *Nat Aging* **1**, 73–86 (2021).

438. Hertzler, S. R., Lieblein-Boff, J. C., Weiler, M. & Allgeier, C. Plant Proteins: Assessing Their Nutritional Quality and Effects on Health and Physical Function. *Nutrients* **12**, 3704 (2020).

439. Berrazaga, I., Micard, V., Gueugneau, M. & Walrand, S. The Role of the Anabolic Properties of Plant- versus Animal-Based Protein Sources in Supporting Muscle Mass Maintenance: A Critical Review. *Nutrients* **11**, (2019).

440. Williams, G. C. Natural Selection, the Costs of Reproduction, and a Refinement of Lack's Principle. *The American Naturalist* **100**, 687–690 (1966).

441. Kirkwood, T. B. Evolution of ageing. *Nature* **270**, 301–304 (1977).

442. Dick, K. B., Ross, C. R. & Yampolsky, L. Y. Genetic variation of dietary restriction and the effects of nutrient-free water and amino acid supplements on lifespan and fecundity of Drosophila. *Genet Res (Camb)* **93**, 265–273 (2011).

443. Govindaraju, T., Sahle, B. W., McCaffrey, T. A., McNeil, J. J. & Owen, A. J. Dietary Patterns and Quality of Life in Older Adults: A Systematic Review. *Nutrients* **10**, E971 (2018).

444. Janssen, I. Evolution of sarcopenia research. *Appl Physiol Nutr Metab* **35**, 707–712 (2010).

445. Suetta, C. *et al.* Effects of aging on human skeletal muscle after immobilization and retraining. *J Appl Physiol (1985)* **107**, 1172–1180 (2009).

446. Volpi, E., Kobayashi, H., Sheffield-Moore, M., Mittendorfer, B. & Wolfe, R. R. Essential amino acids are primarily responsible for the amino acid stimulation of muscle protein anabolism in healthy elderly adults. *The American Journal of Clinical Nutrition* **78**, 250–258 (2003).

447. Smith, K., Reynolds, N., Downie, S., Patel, A. & Rennie, M. J. Effects of flooding amino acids on incorporation of labeled amino acids into human muscle protein. *Am J Physiol* **275**, E73-78 (1998).

448. Martínez-Arnau, F. M. *et al.* Effects of Leucine Administration in Sarcopenia: A Randomized and Placebo-controlled Clinical Trial. *Nutrients* **12**, 932 (2020).

449. Devries, M. C. *et al.* Protein leucine content is a determinant of shorter- and longer-term muscle protein synthetic responses at rest and following resistance exercise in healthy older women: a randomized, controlled trial. *The American Journal of Clinical Nutrition* **107**, 217–226 (2018).

450. Volpi, E., Mittendorfer, B., Rasmussen, B. B. & Wolfe, R. R. The Response of Muscle Protein Anabolism to Combined Hyperaminoacidemia and Glucose-Induced Hyperinsulinemia Is

Impaired in the Elderly1. *The Journal of Clinical Endocrinology & Metabolism* **85**, 4481–4490 (2000).

451. Katsanos, C. S., Kobayashi, H., Sheffield-Moore, M., Aarsland, A. & Wolfe, R. R. Aging is associated with diminished accretion of muscle proteins after the ingestion of a small bolus of essential amino acids. *The American Journal of Clinical Nutrition* **82**, 1065–1073 (2005).
452. Katsanos, C. S., Kobayashi, H., Sheffield-Moore, M., Aarsland, A. & Wolfe, R. R. A high proportion of leucine is required for optimal stimulation of the rate of muscle protein synthesis by essential amino acids in the elderly. *American Journal of Physiology-Endocrinology and Metabolism* **291**, E381–E387 (2006).
453. Rennie, M. J. Anabolic resistance: the effects of aging, sexual dimorphism, and immobilization on human muscle protein turnoverThis paper is one of a selection of papers published in this Special Issue, entitled 14th International Biochemistry of Exercise Conference – Muscles as Molecular and Metabolic Machines, and has undergone the Journal's usual peer review process. *Appl. Physiol. Nutr. Metab.* **34**, 377–381 (2009).
454. Phillips, B. E., Hill, D. S. & Atherton, P. J. Regulation of muscle protein synthesis in humans. *Current Opinion in Clinical Nutrition & Metabolic Care* **15**, 58–63 (2012).
455. Paulussen, K. J. M. *et al.* Anabolic Resistance of Muscle Protein Turnover Comes in Various Shapes and Sizes. *Front Nutr* **8**, 615849 (2021).
456. Houtkooper, R. H. *et al.* The metabolic footprint of aging in mice. *Sci Rep* **1**, 134 (2011).
457. Uchitomi, R. *et al.* Metabolomic Analysis of Skeletal Muscle in Aged Mice. *Sci Rep* **9**, 10425 (2019).
458. Kapranas, A., Snart, C. J. P., Williams, H., Hardy, I. C. W. & Barrett, D. A. Metabolomics of aging assessed in individual parasitoid wasps. *Sci Rep* **6**, 34848 (2016).
459. Kraus-Friedmann, N. Hormonal regulation of hepatic gluconeogenesis. *Physiol Rev* **64**, 170–259 (1984).

460. Müller, W. A., Faloona, G. R. & Unger, R. H. The effect of alanine on glucagon secretion. *J Clin Invest* **50**, 2215–2218 (1971).

461. Brennan, L. *et al.* A nuclear magnetic resonance-based demonstration of substantial oxidative L-alanine metabolism and L-alanine-enhanced glucose metabolism in a clonal pancreatic beta-cell line: metabolism of L-alanine is important to the regulation of insulin secretion. *Diabetes* **51**, 1714–1721 (2002).

462. Freudenberg, A., Petzke, K. J. & Klaus, S. Dietary l-leucine and l-alanine supplementation have similar acute effects in the prevention of high-fat diet-induced obesity. *Amino Acids* **44**, 519–528 (2013).

463. Rampelli, S. *et al.* Functional metagenomic profiling of intestinal microbiome in extreme ageing. *Aging (Albany NY)* **5**, 902–912 (2013).

464. Yamamoto, K. *et al.* Patients with low muscle mass have characteristic microbiome with low potential for amino acid synthesis in chronic liver disease. *Sci Rep* **12**, 3674 (2022).

465. Ponziani, F. R. *et al.* Characterization of the gut-liver-muscle axis in cirrhotic patients with sarcopenia. *Liver Int* **41**, 1320–1334 (2021).

466. D'Antona, G. *et al.* Branched-Chain Amino Acid Supplementation Promotes Survival and Supports Cardiac and Skeletal Muscle Mitochondrial Biogenesis in Middle-Aged Mice. *Cell Metabolism* **12**, 362–372 (2010).

467. Mansfeld, J. *et al.* Branched-chain amino acid catabolism is a conserved regulator of physiological ageing. *Nat Commun* **6**, 10043 (2015).

468. Tai, E. S. *et al.* Insulin resistance is associated with a metabolic profile of altered protein metabolism in Chinese and Asian-Indian men. *Diabetologia* **53**, 757–767 (2010).

469. Wang, T. J. *et al.* Metabolite profiles and the risk of developing diabetes. *Nat Med* **17**, 448–453 (2011).

470. Tremblay, F. *et al.* Overactivation of S6 Kinase 1 as a Cause of Human Insulin Resistance During Increased Amino Acid Availability. *Diabetes* **54**, 2674–2684 (2005).

471. Beck, H. C., Hansen, A. M. & Lauritsen, F. R. Catabolism of leucine to branched-chain fatty acids in Staphylococcus xylosus. *J Appl Microbiol* **96**, 1185–1193 (2004).

472. Kaneda, T. Iso- and anteiso-fatty acids in bacteria: biosynthesis, function, and taxonomic significance. *Microbiol Rev* **55**, 288–302 (1991).

473. Calder, P. C. Glutamine and the immune system. *Clin Nutr* **13**, 2–8 (1994).

474. Starr, M. S. A comparative study of the utilization of glucose, acetate, glutamine and GABA as precursors of amino acids by retinal of the rat, frog, rabbit and pigeon. *Biochem Pharmacol* **24**, 1193–1197 (1975).

475. Lacey, J. M. & Wilmore, D. W. Is glutamine a conditionally essential amino acid? *Nutr Rev* **48**, 297–309 (1990).

476. Rallis, C. *et al.* Amino Acids Whose Intracellular Levels Change Most During Aging Alter Chronological Life Span of Fission Yeast. *J Gerontol A Biol Sci Med Sci* **76**, 205–210 (2021).

477. Jewell, J. L. *et al.* Metabolism. Differential regulation of mTORC1 by leucine and glutamine. *Science* **347**, 194–198 (2015).

478. Zhu, M., Qin, Y., Gao, C., Yan, H. & Wang, X. L-Glutamate drives porcine intestinal epithelial renewal by increasing stem cell activity via upregulation of the EGFR-ERK-mTORC1 pathway. *Food Funct.* **11**, 2714–2724 (2020).

479. Bernfeld, E. *et al.* Phospholipase D-dependent mTOR complex 1 (mTORC1) activation by glutamine. *J Biol Chem* **293**, 16390–16401 (2018).

480. Crespo, J. L., Powers, T., Fowler, B. & Hall, M. N. The TOR-controlled transcription activators GLN3, RTG1, and RTG3 are regulated in response to intracellular levels of glutamine. *Proc Natl Acad Sci U S A* **99**, 6784–6789 (2002).

481. Zhai, Y. *et al.* Activation of the TOR Signalling Pathway by Glutamine Regulates Insect Fecundity. *Sci Rep* **5**, 10694 (2015).

482. Li, N., Lewis, P., Samuelson, D., Liboni, K. & Neu, J. Glutamine regulates Caco-2 cell tight junction proteins. *Am J Physiol Gastrointest Liver Physiol* **287**, G726-733 (2004).

483. Beutheu, S., Ghouzali, I., Galas, L., Déchelotte, P. & Coëffier, M. Glutamine and arginine improve permeability and tight junction protein expression in methotrexate-treated Caco-2 cells. *Clinical Nutrition* **32**, 863–869 (2013).

484. Fuchs, B. C. & Bode, B. P. Stressing out over survival: glutamine as an apoptotic modulator. *J Surg Res* **131**, 26–40 (2006).

485. Rhoads, J. M. *et al.* L-glutamine stimulates intestinal cell proliferation and activates mitogen-activated protein kinases. *Am J Physiol* **272**, G943-953 (1997).

486. Kim, M.-H. & Kim, H. The Roles of Glutamine in the Intestine and Its Implication in Intestinal Diseases. *Int J Mol Sci* **18**, 1051 (2017).

487. Zhou, J. *et al.* Glutamine Availability Regulates the Development of Aging Mediated by mTOR Signaling and Autophagy. *Front Pharmacol* **13**, 924081 (2022).

488. Adams, C. D. Circulating Glutamine and Alzheimer's Disease: A Mendelian Randomization Study. *Clin Interv Aging* **15**, 185–193 (2020).

489. Chen, J. & Herrup, K. Glutamine acts as a neuroprotectant against DNA damage, beta-amyloid and H2O2-induced stress. *PLoS One* **7**, e33177 (2012).

490. Hertz, L. The Glutamate–Glutamine (GABA) Cycle: Importance of Late Postnatal Development and Potential Reciprocal Interactions between Biosynthesis and Degradation. *Frontiers in Endocrinology* **4**, (2013).

491. Hertz, L. & Rothman, D. L. Glucose, Lactate, β-Hydroxybutyrate, Acetate, GABA, and Succinate as Substrates for Synthesis of Glutamate and GABA in the Glutamine–Glutamate/GABA Cycle. in *The Glutamate/GABA-Glutamine Cycle: Amino Acid Neurotransmitter Homeostasis* (eds.

Schousboe, A. & Sonnewald, U.) 9–42 (Springer International Publishing, 2016). doi:10.1007/978-3-319-45096-4_2.

492. Bak, L. K., Schousboe, A. & Waagepetersen, H. S. The glutamate/GABA-glutamine cycle: aspects of transport, neurotransmitter homeostasis and ammonia transfer. *Journal of Neurochemistry* **98**, 641–653 (2006).

493. Andersen, J. V. *et al.* Glutamate metabolism and recycling at the excitatory synapse in health and neurodegeneration. *Neuropharmacology* **196**, 108719 (2021).

494. Hardingham, G. E. & Bading, H. Synaptic versus extrasynaptic NMDA receptor signalling: implications for neurodegenerative disorders. *Nat Rev Neurosci* **11**, 682–696 (2010).

495. Castañeda-Cabral, J. L., López-Ortega, J. G., Fajardo-Fregoso, B. F., Beas-Zárate, C. & Ureña-Guerrero, M. E. Glutamate induced neonatal excitotoxicity modifies the expression level of EAAT1 (GLAST) and EAAT2 (GLT-1) proteins in various brain regions of the adult rat. *Neurosci Lett* **735**, 135237 (2020).

496. Gasiorowska, A. *et al.* The Biology and Pathobiology of Glutamatergic, Cholinergic, and Dopaminergic Signaling in the Aging Brain. *Front Aging Neurosci* **13**, 654931 (2021).

497. Segovia, G., Porras, A., Del Arco, A. & Mora, F. Glutamatergic neurotransmission in aging: a critical perspective. *Mech Ageing Dev* **122**, 1–29 (2001).

498. Zullo, J. M. *et al.* Regulation of Lifespan by Neural Excitation and REST. *Nature* **574**, 359–364 (2019).

499. Verbruggen, L. *et al.* Lifespan extension with preservation of hippocampal function in aged system xc−-deficient male mice. *Mol Psychiatry* **27**, 2355–2368 (2022).

500. Brakspear, K. S. & Mason, D. J. Glutamate signaling in bone. *Front Endocrinol (Lausanne)* **3**, 97 (2012).

501. Cowan, R. W., Seidlitz, E. P. & Singh, G. Glutamate Signaling in Healthy and Diseased Bone. *Front Endocrinol (Lausanne)* **3**, 89 (2012).

502. Blais, A. *et al.* Monosodium Glutamate Supplementation Improves Bone Status in Mice Under Moderate Protein Restriction. *JBMR Plus* **3**, e10224 (2019).

503. Guo, W. *et al.* Dysregulated Glutamate Transporter SLC1A1 Propels Cystine Uptake via Xc− for Glutathione Synthesis in Lung Cancer. *Cancer Research* **81**, 552–566 (2021).

504. Hu, H. *et al.* Hypoxia-inducible factors enhance glutamate signaling in cancer cells. *Oncotarget* **5**, 8853–8868 (2014).

505. Prickett, T. D. & Samuels, Y. Molecular Pathways: Dysregulated Glutamatergic Signaling Pathways in Cancer. *Clinical Cancer Research* **18**, 4240–4246 (2012).

506. Yi, H., Talmon, G. & Wang, J. Glutamate in cancers: from metabolism to signaling. *J Biomed Res* **34**, 260–270 (2020).

507. Sun, L., Sadighi Akha, A. A., Miller, R. A. & Harper, J. M. Life-Span Extension in Mice by Preweaning Food Restriction and by Methionine Restriction in Middle Age. *The Journals of Gerontology: Series A* **64A**, 711–722 (2009).

508. Cabreiro, F. *et al.* Metformin Retards Aging in C. elegans by Altering Microbial Folate and Methionine Metabolism. *Cell* **153**, 228–239 (2013).

509. Arganda, S. *et al.* Parsing the life-shortening effects of dietary protein: effects of individual amino acids. *Proceedings of the Royal Society B: Biological Sciences* **284**, 20162052 (2017).

510. Obata, F. & Miura, M. Enhancing S-adenosyl-methionine catabolism extends Drosophila lifespan. *Nat Commun* **6**, 8332 (2015).

511. Parkhitko, A. A., Jouandin, P., Mohr, S. E. & Perrimon, N. Methionine metabolism and methyltransferases in the regulation of aging and lifespan extension across species. *Aging Cell* **18**, e13034 (2019).

512. Gu, X. *et al.* SAMTOR is an S-adenosylmethionine sensor for the mTORC1 pathway. *Science* **358**, 813–818 (2017).

513. Ren, B. *et al.* Methionine Restriction Improves Gut Barrier Function by Reshaping Diurnal Rhythms of Inflammation-Related Microbes in Aged Mice. *Frontiers in Nutrition* **8**, (2021).

514. Yang, Y. *et al.* Dietary methionine restriction improves the gut microbiota and reduces intestinal permeability and inflammation in high-fat-fed mice. *Food Funct.* **10**, 5952–5968 (2019).

515. Mardinoglu, A. *et al.* The gut microbiota modulates host amino acid and glutathione metabolism in mice. *Molecular Systems Biology* **11**, 834 (2015).

516. Whiley, L. *et al.* Metabolic phenotyping reveals a reduction in the bioavailability of serotonin and kynurenine pathway metabolites in both the urine and serum of individuals living with Alzheimer's disease. *Alzheimer's Research & Therapy* **13**, 20 (2021).

517. Wnorowski, A., Wnorowska, S., Kurzepa, J. & Parada-Turska, J. Alterations in Kynurenine and NAD+ Salvage Pathways during the Successful Treatment of Inflammatory Bowel Disease Suggest HCAR3 and NNMT as Potential Drug Targets. *Int J Mol Sci* **22**, 13497 (2021).

518. Evrensel, A., Ünsalver, B. Ö. & Ceylan, M. E. Immune-Kynurenine Pathways and the Gut Microbiota-Brain Axis in Anxiety Disorders. *Adv Exp Med Biol* **1191**, 155–167 (2020).

519. Kennedy, P. J., Cryan, J. F., Dinan, T. G. & Clarke, G. Kynurenine pathway metabolism and the microbiota-gut-brain axis. *Neuropharmacology* **112**, 399–412 (2017).

520. Costedio, M. M., Hyman, N. & Mawe, G. M. Serotonin and its role in colonic function and in gastrointestinal disorders. *Dis Colon Rectum* **50**, 376–388 (2007).

521. Richard, D. M. *et al.* L-Tryptophan: Basic Metabolic Functions, Behavioral Research and Therapeutic Indications. *Int J Tryptophan Res* **2**, 45–60 (2009).

522. Lyte, M. Probiotics function mechanistically as delivery vehicles for neuroactive compounds: Microbial endocrinology in the design and use of probiotics. *Bioessays* **33**, 574–581 (2011).

523. Knecht, L. D. *et al.* Serotonin Activates Bacterial Quorum Sensing and Enhances the Virulence of Pseudomonas aeruginosa in the Host. *EBioMedicine* **9**, 161–169 (2016).

524. Kaur, H., Bose, C. & Mande, S. S. Tryptophan Metabolism by Gut Microbiome and Gut-Brain-Axis: An in silico Analysis. *Frontiers in Neuroscience* **13**, (2019).

525. Clarke, G. *et al.* The microbiome-gut-brain axis during early life regulates the hippocampal serotonergic system in a sex-dependent manner. *Mol Psychiatry* **18**, 666–673 (2013).

526. Choi, W. *et al.* Interaction effect of serum serotonin level and age on the 12-week pharmacotherapeutic response in patients with depressive disorders. *Sci Rep* **11**, 24226 (2021).

527. Geldenhuys, W. J. & Van der Schyf, C. J. Role of serotonin in Alzheimer's disease: a new therapeutic target? *CNS Drugs* **25**, 765–781 (2011).

528. Stone, T. W. & Darlington, L. G. Endogenous kynurenines as targets for drug discovery and development. *Nat Rev Drug Discov* **1**, 609–620 (2002).

529. Haq, S., Grondin, J. A. & Khan, W. I. Tryptophan-derived serotonin-kynurenine balance in immune activation and intestinal inflammation. *The FASEB Journal* **35**, e21888 (2021).

530. Gouasmi, R. *et al.* The Kynurenine Pathway and Cancer: Why Keep It Simple When You Can Make It Complicated. *Cancers (Basel)* **14**, 2793 (2022).

531. Sorgdrager, F. J. H. *et al.* Age- and disease-specific changes of the kynurenine pathway in Parkinson's and Alzheimer's disease. *J Neurochem* **151**, 656–668 (2019).

532. Capuron, L. *et al.* Chronic Low-Grade Inflammation in Elderly Persons Is Associated with Altered Tryptophan and Tyrosine Metabolism: Role in Neuropsychiatric Symptoms. *Biological Psychiatry* **70**, 175–182 (2011).

533. Collino, S. *et al.* Metabolic Signatures of Extreme Longevity in Northern Italian Centenarians Reveal a Complex Remodeling of Lipids, Amino Acids, and Gut Microbiota Metabolism. *PLOS ONE* **8**, e56564 (2013).

534. Frick, B., Schroecksnadel, K., Neurauter, G., Leblhuber, F. & Fuchs, D. Increasing production of homocysteine and neopterin and degradation of tryptophan with older age. *Clinical Biochemistry* **37**, 684–687 (2004).

535. Niinisalo, P. *et al.* Indoleamine 2,3-dioxygenase activity associates with cardiovascular risk factors: The Health 2000 study. *Scandinavian Journal of Clinical and Laboratory Investigation* **68**, 767–770 (2008).

536. Pertovaara, M. *et al.* Indoleamine 2,3-dioxygenase activity in nonagenarians is markedly increased and predicts mortality. *Mechanisms of Ageing and Development* **127**, 497–499 (2006).

537. Ramos-Chávez, L. A. *et al.* Low Serum Tryptophan Levels as an Indicator of Global Cognitive Performance in Nondemented Women over 50 Years of Age. *Oxidative Medicine and Cellular Longevity* **2018**, e8604718 (2018).

538. Rist, M. J. *et al.* Metabolite patterns predicting sex and age in participants of the Karlsruhe Metabolomics and Nutrition (KarMeN) study. *PLOS ONE* **12**, e0183228 (2017).

539. Theofylaktopoulou, D. *et al.* A community-based study on determinants of circulating markers of cellular immune activation and kynurenines: the Hordaland Health Study. *Clinical & Experimental Immunology* **173**, 121–130 (2013).

540. Yu, Z. *et al.* Human serum metabolic profiles are age dependent. *Aging Cell* **11**, 960–967 (2012).

541. Sorgdrager, F. J. H., Naudé, P. J. W., Kema, I. P., Nollen, E. A. & Deyn, P. P. D. Tryptophan Metabolism in Inflammaging: From Biomarker to Therapeutic Target. *Frontiers in Immunology* **10**, (2019).

542. Oxenkrug, G., Navrotskaya, V., Vorobyova, L. & Summergrad, P. Extension of life span of Drosophila melanogaster by the inhibitors of tryptophan-kynurenine metabolism. *Fly (Austin)* **5**, 307–309 (2011).

543. Oxenkrug, G. F. The extended life span of Drosophila melanogaster eye-color (white and vermilion) mutants with impaired formation of kynurenine. *J Neural Transm* **117**, 23–26 (2010).

544. van der Goot, A. T. *et al.* Delaying aging and the aging-associated decline in protein homeostasis by inhibition of tryptophan degradation. *Proc Natl Acad Sci U S A* **109**, 14912–14917 (2012).

545. Christensen, H. N. Role of amino acid transport and countertransport in nutrition and metabolism. *Physiol Rev* **70**, 43–77 (1990).

546. Hediger, M. A., Clémençon, B., Burrier, R. E. & Bruford, E. A. The ABCs of membrane transporters in health and disease (SLC series): introduction. *Mol Aspects Med* **34**, 95–107 (2013).

547. Kandasamy, P., Gyimesi, G., Kanai, Y. & Hediger, M. A. Amino acid transporters revisited: New views in health and disease. *Trends Biochem Sci* **43**, 752–789 (2018).

548. Fei, Y. J. *et al.* Expression cloning of a mammalian proton-coupled oligopeptide transporter. *Nature* **368**, 563–566 (1994).

549. Bröer, S. Adaptation of plasma membrane amino acid transport mechanisms to physiological demands. *Pflugers Arch* **444**, 457–466 (2002).

550. Bröer, A., Wagner, C., Lang, F. & Bröer, S. Neutral amino acid transporter ASCT2 displays substrate-induced Na+ exchange and a substrate-gated anion conductance. *Biochem J* **346 Pt 3**, 705–710 (2000).

551. Bröer, S. & Fairweather, S. J. Amino Acid Transport Across the Mammalian Intestine. *Compr Physiol* **9**, 343–373 (2018).

552. Munck, B. G. & Munck, L. K. Effects of pH changes on systems ASC and B in rabbit ileum. *Am J Physiol* **276**, G173-184 (1999).

553. Teijema, H. L., van Gelderen, H. H., Giesberts, M. A. & Laurent de Angulo, M. S. Dicarboxylic aminoaciduria: an inborn error of glutamate and aspartate transport with metabolic implications, in combination with a hyperprolinemia. *Metabolism* **23**, 115–123 (1974).

554. Melançon, S. B., Dallaire, L., Lemieux, B., Robitaille, P. & Potier, M. Dicarboxylic aminoaciduria: an inborn error of amino acid conservation. *J Pediatr* **91**, 422–427 (1977).

555. Pineda, M. *et al.* Identification of a membrane protein, LAT-2, that Co-expresses with 4F2 heavy chain, an L-type amino acid transport activity with broad specificity for small and large zwitterionic amino acids. *J Biol Chem* **274**, 19738–19744 (1999).

556. Segawa, H. *et al.* Identification and functional characterization of a Na+-independent neutral amino acid transporter with broad substrate selectivity. *J Biol Chem* **274**, 19745–19751 (1999).

557. Meier, C., Ristic, Z., Klauser, S. & Verrey, F. Activation of system L heterodimeric amino acid exchangers by intracellular substrates. *EMBO J* **21**, 580–589 (2002).

558. Kim, D. K. *et al.* Expression cloning of a Na+-independent aromatic amino acid transporter with structural similarity to H+/monocarboxylate transporters. *J Biol Chem* **276**, 17221–17228 (2001).

559. Bodoy, S. *et al.* Identification of LAT4, a novel amino acid transporter with system L activity. *J Biol Chem* **280**, 12002–12011 (2005).

560. Torrents, D. *et al.* Identification and characterization of a membrane protein (y+L amino acid transporter-1) that associates with 4F2hc to encode the amino acid transport activity y+L. A candidate gene for lysinuric protein intolerance. *J Biol Chem* **273**, 32437–32445 (1998).

561. Pfeiffer, R. *et al.* Amino acid transport of y+L-type by heterodimers of 4F2hc/CD98 and members of the glycoprotein-associated amino acid transporter family. *EMBO J* **18**, 49–57 (1999).

562. Bauch, C. & Verrey, F. Apical heterodimeric cystine and cationic amino acid transporter expressed in MDCK cells. *American Journal of Physiology-Renal Physiology* **283**, F181–F189 (2002).

563. Hu, Y. *et al.* An integrative approach to ortholog prediction for disease-focused and other functional studies. *BMC bioinformatics* **12**, (2011).

564. Scalise, M., Pochini, L., Console, L., Losso, M. A. & Indiveri, C. The Human SLC1A5 (ASCT2) Amino Acid Transporter: From Function to Structure and Role in Cell Biology. *Frontiers in Cell and Developmental Biology* **6**, (2018).

565. Deng, H., Gerencser, A. A. & Jasper, H. Signal integration by Ca 2+ regulates intestinal stem-cell activity. *Nature* **528**, 212–217 (2015).

566. Shim, M. S. *et al.* I(2)01810 is a novel type of glutamate transporter that is responsible for megamitochondrial formation. *Biochem J* **439**, 277–286 (2011).

567. Lin, W.-Y. *et al.* The SLC36 transporter Pathetic is required for extreme dendrite growth in Drosophila sensory neurons. *Genes Dev.* **29**, 1120–1135 (2015).

568. Goberdhan, D. C. I., Meredith, D., Boyd, C. A. R. & Wilson, C. PAT-related amino acid transporters regulate growth via a novel mechanism that does not require bulk transport of amino acids. *Development* **132**, 2365–2375 (2005).

569. Thevelein, J. M. & Voordeckers, K. Functioning and evolutionary significance of nutrient transceptors. *Mol Biol Evol* **26**, 2407–2414 (2009).

570. Huang, Y., Ng, F. S. & Jackson, F. R. Comparison of Larval and Adult Drosophila Astrocytes Reveals Stage-Specific Gene Expression Profiles. *G3 Genes|Genomes|Genetics* **5**, 551–558 (2015).

571. Ng, F. S. *et al.* TRAP-seq Profiling and RNAi-Based Genetic Screens Identify Conserved Glial Genes Required for Adult Drosophila Behavior. *Frontiers in Molecular Neuroscience* **9**, (2016).

572. Jambor, H. *et al.* Systematic imaging reveals features and changing localization of mRNAs in Drosophila development. *eLife* **4**, e05003 (2015).

573. Slaidina, M., Banisch, T. U., Gupta, S. & Lehmann, R. A single-cell atlas of the developing Drosophila ovary identifies follicle stem cell progenitors. *Genes Dev.* **34**, 239–249 (2020).

574. Whitaker, R. *et al.* Dietary switch reveals fast coordinated gene expression changes in *Drosophila melanogaster*. *Aging* **6**, 355–368 (2014).

575. Closs, E. I., Boissel, J.-P., Habermeier, A. & Rotmann, A. Structure and Function of Cationic Amino Acid Transporters (CATs). *J Membrane Biol* **213**, 67–77 (2006).

576. Kim, J. W., Closs, E. I., Albritton, L. M. & Cunningham, J. M. Transport of cationic amino acids by the mouse ecotropic retrovirus receptor. *Nature* **352**, 725–728 (1991).

577. Colombani, J. *et al.* A Nutrient Sensor Mechanism Controls Drosophila Growth. *Cell* **114**, 739–749 (2003).

578. Verrey, F. *et al.* CATs and HATs: the SLC7 family of amino acid transporters. *Pflugers Arch* **447**, 532–542 (2004).

579. Pfeiffer, R. *et al.* Luminal Heterodimeric Amino Acid Transporter Defective in Cystinuria. *MBoC* **10**, 4135–4147 (1999).

580. Chillarón, J. *et al.* Obligatory Amino Acid Exchange via Systems bo,+-like and y+L-like: A Tertiary Active Transport Mechanism for Renal Reasborption of Cystine and Dibasic Amino Acids. *Journal of Biological Chemistry* **271**, 17761–17770 (1996).

581. Busch, A. E. *et al.* Opposite directed currents induced by the transport of dibasic and neutral amino acids in Xenopus oocytes expressing the protein rBAT. *Journal of Biological Chemistry* **269**, 25581–25586 (1994).

582. Matsuo, H. *et al.* Identification of a novel Na+-independent acidic amino acid transporter with structural similarity to the member of a heterodimeric amino acid transporter family associated with unknown heavy chains. *J Biol Chem* **277**, 21017–21026 (2002).

583. Nagamori, S. *et al.* Novel cystine transporter in renal proximal tubule identified as a missing partner of cystinuria-related plasma membrane protein rBAT/SLC3A1. *Proc Natl Acad Sci U S A* **113**, 775–780 (2016).

584. Galagovsky, D. *et al.* Sobremesa L-type Amino Acid Transporter Expressed in Glia Is Essential for Proper Timing of Development and Brain Growth. *Cell Reports* **24**, 3156-3166.e4 (2018).

585. Wu, S. *et al.* Effect of Dietary Protein and Processing on Gut Microbiota—A Systematic Review. *Nutrients* **14**, 453 (2022).

586. Rogina, B. *et al.* Distinct Biological Epochs in the Reproductive Life of Female Drosophila melanogaster. *Mech Ageing Dev* **128**, 477–485 (2007).

587. Minnebo, Y., De Paepe, K., Raes, J. & de Wiele, T. V. Nutrient load acts as a driver of gut microbiota load, community composition and metabolic functionality in the simulator of the human intestinal microbial ecosystem. *FEMS Microbiology Ecology* **97**, fiab111 (2021).

588. Jumpertz, R. *et al.* Energy-balance studies reveal associations between gut microbes, caloric load, and nutrient absorption in humans. *Am J Clin Nutr* **94**, 58–65 (2011).

589. Kajikawa, H., Mitsumori, M. & Ohmomo, S. Stimulatory and inhibitory effects of protein amino acids on growth rate and efficiency of mixed ruminal bacteria. *J Dairy Sci* **85**, 2015–2022 (2002).

590. Reese, A. T. *et al.* Microbial nitrogen limitation in the mammalian large intestine. *Nat Microbiol* **3**, 1441–1450 (2018).

591. Liu, Y.-K., Kuo, H.-C., Lai, C.-H. & Chou, C.-C. Single amino acid utilization for bacterial categorization. *Sci Rep* **10**, 12686 (2020).

592. Nagy, P., Sándor, G. O. & Juhász, G. Autophagy maintains stem cells and intestinal homeostasis in Drosophila. *Sci Rep* **8**, 4644 (2018).

593. Zou, Z., Tao, T., Li, H. & Zhu, X. mTOR signaling pathway and mTOR inhibitors in cancer: progress and challenges. *Cell & Bioscience* **10**, 31 (2020).

594. Uhlirova, M., Jasper, H. & Bohmann, D. Non-cell-autonomous induction of tissue overgrowth by JNK/Ras cooperation in a Drosophila tumor model. *Proc Natl Acad Sci U S A* **102**, 13123–13128 (2005).

595. Hundal, H. S. & Taylor, P. M. Amino acid transceptors: gate keepers of nutrient exchange and regulators of nutrient signaling. *American Journal of Physiology-Endocrinology and Metabolism* **296**, E603–E613 (2009).

596. Pénzes, L. & Boross, M. Intestinal absorption of some heterocyclic and aromatic amino acids from the ageing gut. *Experimental Gerontology* **9**, 253–258 (1974).

597. Dickinson, J. M., Drummond, M. J., Coben, J. R., Volpi, E. & Rasmussen, B. B. Aging differentially affects human skeletal muscle amino acid transporter expression when essential amino acids are ingested after exercise. *Clinical Nutrition* **32**, 273–280 (2013).

598. Wendowski, O., Redshaw, Z. & Mutungi, G. Dihydrotestosterone treatment rescues the decline in protein synthesis as a result of sarcopenia in isolated mouse skeletal muscle fibres. *Journal of Cachexia, Sarcopenia and Muscle* **8**, 48–56 (2017).

599. Crocco, P. *et al.* Physical decline and survival in the elderly are affected by the genetic variability of amino acid transporter genes. *Aging* **10**, 658–673 (2018).

600. Reeds, P. J., Burrin, D. G., Stoll, B. & Jahoor, F. Intestinal Glutamate Metabolism. *The Journal of Nutrition* **130**, 978S-982S (2000).

601. Newsholme, P., Procopio, J., Lima, M. M. R., Pithon-Curi, T. C. & Curi, R. Glutamine and glutamate—their central role in cell metabolism and function. *Cell Biochemistry and Function* **21**, 1–9 (2003).

602. Zhou, Y. & Danbolt, N. C. Glutamate as a neurotransmitter in the healthy brain. *J Neural Transm (Vienna)* **121**, 799–817 (2014).

603. Weidong Xiao *et al.* Glutamate prevents intestinal atrophy via luminal nutrient sensing in a mouse model of total parenteral nutrition. *The FASEB Journal* **28**, 2073–2087 (2014).

604. Yan, D. Protection of the glutamate pool concentration in enteric bacteria. *Proc Natl Acad Sci U S A* **104**, 9475–9480 (2007).

605. Mc, D. *et al.* The Gap1 general amino acid permease acts as an amino acid sensor for activation of protein kinase A targets in the yeast Saccharomyces cerevisiae. *Molecular microbiology* **50**, (2003).

606. Van Zeebroeck, G., Bonini, B. M., Versele, M. & Thevelein, J. M. Transport and signaling via the amino acid binding site of the yeast Gap1 amino acid transceptor. *Nat Chem Biol* **5**, 45–52 (2009).

607. Van Nuland, A. *et al.* Ammonium permease-based sensing mechanism for rapid ammonium activation of the protein kinase A pathway in yeast. *Molecular Microbiology* **59**, 1485–1505 (2006).

608. Pan, X., Harashima, T. & Heitman, J. Signal transduction cascades regulating pseudohyphal differentiation of Saccharomyces cerevisiae. *Current Opinion in Microbiology* **3**, 567–572 (2000).

609. Brito, A. S., Neuhäuser, B., Wintjens, R., Marini, A. M. & Boeckstaens, M. Yeast filamentation signaling is connected to a specific substrate translocation mechanism of the Mep2 transceptor. *PLOS Genetics* **16**, e1008634 (2020).

610. Smith, D. G., Garcia-Pedrajas, M. D., Gold, S. E. & Perlin, M. H. Isolation and characterization from pathogenic fungi of genes encoding ammonium permeases and their roles in dimorphism. *Molecular Microbiology* **50**, 259–275 (2003).

611. Biswas, K. & Morschhäuser, J. The Mep2p ammonium permease controls nitrogen starvation-induced filamentous growth in Candida albicans. *Molecular Microbiology* **56**, 649–669 (2005).

612. Giots, F., Donaton, M. C. V. & Thevelein, J. M. Inorganic phosphate is sensed by specific phosphate carriers and acts in concert with glucose as a nutrient signal for activation of the protein kinase A pathway in the yeast Saccharomyces cerevisiae. *Mol Microbiol* **47**, 1163–1181 (2003).

613. Popova, Y., Thayumanavan, P., Lonati, E., Agrochão, M. & Thevelein, J. M. Transport and signaling through the phosphate-binding site of the yeast Pho84 phosphate transceptor. *Proceedings of the National Academy of Sciences* **107**, 2890–2895 (2010).

614. Samyn, D. R. *et al.* Mutational analysis of putative phosphate- and proton-binding sites in the Saccharomyces cerevisiae Pho84 phosphate:H(+) transceptor and its effect on signalling to the PKA and PHO pathways. *Biochem J* **445**, 413–422 (2012).

615. Kankipati, H. N., Rubio-Texeira, M., Castermans, D., Diallinas, G. & Thevelein, J. M. Sul1 and Sul2 sulfate transceptors signal to protein kinase A upon exit of sulfur starvation. *J Biol Chem* **290**, 10430–10446 (2015).

616. Walch-Liu, P. & Forde, B. G. Nitrate signalling mediated by the NRT1.1 nitrate transporter antagonises l-glutamate-induced changes in root architecture. *The Plant Journal* **54**, 820–828 (2008).

617. Tollefson, J. Carbon emissions hit new high: warning from COP27. *Nature* (2022) doi:10.1038/d41586-022-03657-w.

618. Heublein, S. *et al.* Proton-assisted amino-acid transporters are conserved regulators of proliferation and amino-acid-dependent mTORC1 activation. *Oncogene* **29**, 4068–4079 (2010).

619. Fan, S.-J. *et al.* PAT4 levels control amino-acid sensitivity of rapamycin-resistant mTORC1 from the Golgi and affect clinical outcome in colorectal cancer. *Oncogene* **35**, 3004–3015 (2016).

620. Pinilla, J., Barber, A. & Lostao, M. P. Active transport of alanine by the neutral amino-acid exchanger ASCT1. *Can J Physiol Pharmacol* **79**, 1023–1029 (2001).

621. Boudko, D. Y. *et al.* Substrate specificity and transport mechanism of amino-acid transceptor Slimfast from Aedes aegypti. *Nat Commun* **6**, 8546 (2015).

622. Abe, K. & Saito, H. Possible linkage between glutamate transporter and mitogen-activated protein kinase cascade in cultured rat cortical astrocytes. *J Neurochem* **76**, 217–223 (2001).

623. Hennig, K. M., Colombani, J. & Neufeld, T. P. TOR coordinates bulk and targeted endocytosis in the Drosophila melanogaster fat body to regulate cell growth. *Journal of Cell Biology* **173**, 963–974 (2006).

624. Nowak, K., Seisenbacher, G., Hafen, E. & Stocker, H. Nutrient restriction enhances the proliferative potential of cells lacking the tumor suppressor PTEN in mitotic tissues. *eLife* **2**, e00380 (2013).

625. Arquier, N. *et al.* Drosophila ALS Regulates Growth and Metabolism through Functional Interaction with Insulin-Like Peptides. *Cell Metabolism* **7**, 333–338 (2008).

626. Walker, D. K. *et al.* Insulin increases mRNA abundance of the amino acid transporter SLC7A5/LAT1 via an mTORC1-dependent mechanism in skeletal muscle cells. *Physiological Reports* **2**, e00238 (2014).

627. Boisclair, Y. R., Rhoads, R. P., Ueki, I., Wang, J. & Ooi, G. T. The acid-labile subunit (ALS) of the 150 kDa IGF-binding protein complex: an important but forgotten component of the circulating IGF system. *J Endocrinol* **170**, 63–70 (2001).

628. Bjordal, M., Arquier, N., Kniazeff, J., Pin, J. P. & Léopold, P. Sensing of Amino Acids in a Dopaminergic Circuitry Promotes Rejection of an Incomplete Diet in Drosophila. *Cell* **156**, 510–521 (2014).

629. Sun, J. *et al.* Drosophila FIT is a protein-specific satiety hormone essential for feeding control. *Nat Commun* **8**, 14161 (2017).

630. Huang, Y. *et al.* The Cationic Amino Acid Transporters CAT1 and CAT3 Mediate NMDA Receptor Activation-Dependent Changes in Elaboration of Neuronal Processes via the Mammalian Target of Rapamycin mTOR Pathway. *J Neurosci* **27**, 449–458 (2007).

631. Kimball, S. R. & Jefferson, L. S. Amino acids as regulators of gene expression. *Nutr Metab (Lond)* **1**, 3 (2004).

632. Fernandez, J., Yaman, I., Sarnow, P., Snider, M. D. & Hatzoglou, M. Regulation of internal ribosomal entry site-mediated translation by phosphorylation of the translation initiation factor eIF2alpha. *J Biol Chem* **277**, 19198–19205 (2002).

633. Fernandez, J. *et al.* Transcriptional control of the arginine/lysine transporter, cat-1, by physiological stress. *J Biol Chem* **278**, 50000–50009 (2003).

634. Lopez, A. B. *et al.* A feedback transcriptional mechanism controls the level of the arginine/lysine transporter cat-1 during amino acid starvation. *Biochem J* **402**, 163–173 (2007).

635. Hyatt, S., Aulak, K., Malandro, M., Kilberg, M. & Hatzoglou, M. Adaptive regulation of the cationic amino acid transporter-1 (Cat-1) in Fao cells. *The Journal of biological chemistry* **272**, (1997).

636. Werner, A. *et al.* Induced arginine transport via cationic amino acid transporter-1 is necessary for human T-cell proliferation. *Eur J Immunol* **46**, 92–103 (2016).

637. Yeramian, A. *et al.* Arginine transport via cationic amino acid transporter 2 plays a critical regulatory role in classical or alternative activation of macrophages. *J Immunol* **176**, 5918–5924 (2006).

638. Lu, Y. *et al.* Cationic amino acid transporter-1 (CAT-1) promotes fibroblast-like synoviocyte proliferation and cytokine secretion by taking up L-arginine in rheumatoid arthritis. *Arthritis Research & Therapy* **24**, 234 (2022).

639. Chauhan, K., Jandu, J. S., Goyal, A. & Al-Dhahir, M. A. Rheumatoid Arthritis. in *StatPearls* (StatPearls Publishing, 2022).

640. Gong, W., Chen, Y. & Zhang, Y. Prognostic and clinical significance of Solute Carrier Family 7 Member 1 in ovarian cancer. *Translational Cancer Research* **10**, (2021).

641. Lu, Y. *et al.* Overexpression of Arginine Transporter CAT-1 Is Associated with Accumulation of L-Arginine and Cell Growth in Human Colorectal Cancer Tissue. *PLOS ONE* **8**, e73866 (2013).

642. Okita, K. *et al.* Antitumor effects of novel mAbs against cationic amino acid transporter 1 (CAT1) on human CRC with amplified CAT1 gene. *Cancer Science* **112**, 563–574 (2021).

643. Ikeda, A. *et al.* Colorectal Cancer–Derived CAT1-Positive Extracellular Vesicles Alter Nitric Oxide Metabolism in Endothelial Cells and Promote Angiogenesis. *Molecular Cancer Research* **19**, 834–846 (2021).

644. He, W. *et al.* S119N Mutation of the E3 Ubiquitin Ligase SPOP Suppresses SLC7A1 Degradation to Regulate Hepatoblastoma Progression. *Mol Ther Oncolytics* **19**, 149–162 (2020).

645. Chang, J. *et al.* miR-122, a Mammalian Liver-Specific microRNA, is Processed from hcr mRNA and May Downregulate the High Affinity Cationic Amino Acid Transporter CAT-1. *RNA Biology* **1**, 106–113 (2004).

646. Dai, R. *et al.* Hepatitis B virus X protein-induced upregulation of CAT-1 stimulates proliferation and inhibits apoptosis in hepatocellular carcinoma cells. *Oncotarget* **8**, 60962–60974 (2017).

647. Abdelmagid, S. A., Rickard, J. A., McDonald, W. J., Thomas, L. N. & Too, C. K. L. CAT-1-mediated arginine uptake and regulation of nitric oxide synthases for the survival of human breast cancer cell lines. *J Cell Biochem* **112**, 1084–1092 (2011).

648. Latif, S. & Kang, Y.-S. Change in Cationic Amino Acid Transport System and Effect of Lysine Pretreatment on Inflammatory State in Amyotrophic Lateral Sclerosis Cell Model. *Biomolecules & therapeutics* **29**, (2021).

649. Bronte, V. & Zanovello, P. Regulation of immune responses by L-arginine metabolism. *Nat Rev Immunol* **5**, 641–654 (2005).

650. Wu, G. *et al.* Arginine metabolism and nutrition in growth, health and disease. *Amino Acids* **37**, 153–168 (2009).

651. Gad, M. Z. Anti-aging effects of l-arginine. *Journal of Advanced Research* **1**, 169–177 (2010).

652. Sax, H. C. Arginine stimulates wound healing and immune function in elderly human beings. *JPEN J Parenter Enteral Nutr* **18**, 559–560 (1994).

653. Barbul, A., Lazarou, S. A., Efron, D. T., Wasserkrug, H. L. & Efron, G. Arginine enhances wound healing and lymphocyte immune responses in humans. *Surgery* **108**, 331–6; discussion 336-7 (1990).

654. Wu, M., Xiao, H., Shao, F., Tan, B. & Hu, S. Arginine accelerates intestinal health through cytokines and intestinal microbiota. *International Immunopharmacology* **81**, 106029 (2020).

655. Singh, K. *et al.* Dietary Arginine Regulates Severity of Experimental Colitis and Affects the Colonic Microbiome. *Front Cell Infect Microbiol* **9**, 66 (2019).

656. Nüse, B. & Mattner, J. L-arginine as a novel target for clinical intervention in inflammatory bowel disease. *Explor Immunol.* **1**, 80–89 (2021).

657. Kim, Y. J. *et al.* Arginine-mediated gut microbiome remodeling promotes host pulmonary immune defense against nontuberculous mycobacterial infection. *Gut Microbes* **14**, 2073132 (2022).

658. Tokarz, J. *et al.* Common Muscle Metabolic Signatures Highlight Arginine and Lysine Metabolism as Potential Therapeutic Targets to Combat Unhealthy Aging. *International Journal of Molecular Sciences* **22**, 7958 (2021).

659. Ma, S. *et al.* Cell culture-based profiling across mammals reveals DNA repair and metabolism as determinants of species longevity. *eLife* **5**, e19130 (2016).

660. Edwards, C. *et al.* Mechanisms of amino acid-mediated lifespan extension in Caenorhabditis elegans. *BMC Genetics* **16**, 8 (2015).

661. Tsugawa, Y., Handa, H. & Imai, T. Arginine induces IGF-1 secretion from the endoplasmic reticulum. *Biochemical and Biophysical Research Communications* **514**, 1128–1132 (2019).

662. Alba-Roth, J., Müller, O., Schopohl, J. & von Werder, K. Arginine stimulates growth hormone secretion by suppressing endogenous somatostatin secretion. *The Journal of clinical endocrinology and metabolism* **67**, (1988).

663. Holzenberger, M. *et al.* IGF-1 receptor regulates lifespan and resistance to oxidative stress in mice. *Nature* **421**, 182–187 (2003).

664. Aguiar-Oliveira, M. H. & Bartke, A. Growth Hormone Deficiency: Health and Longevity. *Endocrine Reviews* **40**, 575–601 (2019).

665. Canfield, C.-A. & Bradshaw, P. C. Amino acids in the regulation of aging and aging-related diseases. *Translational Medicine of Aging* **3**, 70–89 (2019).

666. Carroll, B. *et al.* Control of TSC2-Rheb signaling axis by arginine regulates mTORC1 activity. *eLife* **5**, e11058 (2016).

667. Hoffman, J. M. *et al.* Effects of age, sex, and genotype on high-sensitivity metabolomic profiles in the fruit fly, Drosophila melanogaster. *Aging Cell* **13**, 596–604 (2014).

668. Bayliak, M. M. *et al.* Dietary l-arginine accelerates pupation and promotes high protein levels but induces oxidative stress and reduces fecundity and life span in Drosophila melanogaster. *J Comp Physiol B* **188**, 37–55 (2018).

669. Katayama, S. & Mine, Y. Antioxidative Activity of Amino Acids on Tissue Oxidative Stress in Human Intestinal Epithelial Cell Model. *J. Agric. Food Chem.* **55**, 8458–8464 (2007).

670. Cheng, S. *et al.* Distinct metabolomic signatures are associated with longevity in humans. *Nat Commun* **6**, 6791 (2015).

671. Li, X. & Snyder, M. P. Yeast longevity promoted by reversing aging-associated decline in heavy isotope content. *npj Aging Mech Dis* **2**, 1–10 (2016).

672. Wan, Q.-L. *et al.* Metabolomic signature associated with reproduction-regulated aging in Caenorhabditis elegans. *Aging (Albany NY)* **9**, 447–463 (2017).

673. Hastings, J. *et al.* Multi-Omics and Genome-Scale Modeling Reveal a Metabolic Shift During C. elegans Aging. *Frontiers in Molecular Biosciences* **6**, (2019).

674. Pontoizeau, C. *et al.* Metabolomics Analysis Uncovers That Dietary Restriction Buffers Metabolic Changes Associated with Aging in Caenorhabditis elegans. *J. Proteome Res.* **13**, 2910–2919 (2014).

675. Gebeyew, K., Yang, C., He, Z. & Tan, Z. Low-protein diets supplemented with methionine and lysine alter the gut microbiota composition and improve the immune status of growing lambs. *Appl Microbiol Biotechnol* **105**, 8393–8410 (2021).

676. Yin, J. *et al.* Lysine Restriction Affects Feed Intake and Amino Acid Metabolism via Gut Microbiome in Piglets. *Cell Physiol Biochem* **44**, 1749–1761 (2017).

677. Hoffman, J. M., Dudeck, S. K., Patterson, H. K. & Austad, S. N. Sex, mating and repeatability of Drosophila melanogaster longevity. *Royal Society Open Science* **8**, 210273 (2021).

678. Yin, J. *et al.* Long-term effects of lysine concentration on growth performance, intestinal microbiome, and metabolic profiles in a pig model. *Food Funct* **9**, 4153–4163 (2018).

679. Hall, D. J., Grewal, S. S., de la Cruz, A. F. A. & Edgar, B. A. Rheb-TOR signaling promotes protein synthesis, but not glucose or amino acid import, in Drosophila. *BMC Biol* **5**, 10 (2007).

680. Ghosh, A., Rideout, E. J. & Grewal, S. S. TIF-IA-Dependent Regulation of Ribosome Synthesis in Drosophila Muscle Is Required to Maintain Systemic Insulin Signaling and Larval Growth. *PLOS Genetics* **10**, e1004750 (2014).

681. Rajan, A. & Perrimon, N. Drosophila cytokine unpaired 2 regulates physiological homeostasis by remotely controlling insulin secretion. *Cell* **151**, 123–137 (2012).

682. Tomé, D. The Roles of Dietary Glutamate in the Intestine. *Ann Nutr Metab* **73 Suppl 5**, 15–20 (2018).

683. Janeczko, M. J., Stoll, B., Chang, X., Guan, X. & Burrin, D. G. Extensive Gut Metabolism Limits the Intestinal Absorption of Excessive Supplemental Dietary Glutamate Loads in Infant Pigs. *The Journal of Nutrition* **137**, 2384–2390 (2007).

684. Haÿs, S. P., Ordonez, J. M., Burrin, D. G. & Sunehag, A. L. Dietary Glutamate Is Almost Entirely Removed in Its First Pass Through the Splanchnic Bed in Premature Infants. *Pediatr Res* **62**, 353–356 (2007).

685. Lin, M. *et al.* L-Glutamate supplementation improves small intestinal architecture and enhances the expressions of jejunal mucosa amino acid receptors and transporters in weaning piglets. *PLOS ONE* **9**, (2014).

686. Conway, M. E. Alzheimer's disease: targeting the glutamatergic system. *Biogerontology* **21**, 257–274 (2020).

687. Bukke, V. N. *et al.* The Dual Role of Glutamatergic Neurotransmission in Alzheimer's Disease: From Pathophysiology to Pharmacotherapy. *International Journal of Molecular Sciences* **21**, 7452 (2020).

688. Choi, D. W. Excitotoxic cell death. *J Neurobiol* **23**, 1261–1276 (1992).

689. Hague, S. M., Klaffke, S. & Bandmann, O. Neurodegenerative disorders: Parkinson's disease and Huntington's disease. *J Neurol Neurosurg Psychiatry* **76**, 1058–1063 (2005).

690. Wang, R. & Reddy, P. H. Role of glutamate and NMDA receptors in Alzheimer's disease. *J Alzheimers Dis* **57**, 1041–1048 (2017).

691. Hynd, M. R., Scott, H. L. & Dodd, P. R. Glutamate-mediated excitotoxicity and neurodegeneration in Alzheimer's disease. *Neurochem Int* **45**, 583–595 (2004).

692. Iovino, L., Tremblay, M. E. & Civiero, L. Glutamate-induced excitotoxicity in Parkinson's disease: The role of glial cells. *J Pharmacol Sci* **144**, 151–164 (2020).

693. Kaiser, L. G., Schuff, N., Cashdollar, N. & Weiner, M. W. Age-related glutamate and glutamine concentration changes in normal human brain: 1H MR spectroscopy study at 4 T. *Neurobiol Aging* **26**, 665–672 (2005).

694. Hädel, S., Wirth, C., Rapp, M., Gallinat, J. & Schubert, F. Effects of age and sex on the concentrations of glutamate and glutamine in the human brain. *Journal of Magnetic Resonance Imaging* **38**, 1480–1487 (2013).

695. Marsman, A. *et al.* Glutamate changes in healthy young adulthood. *European Neuropsychopharmacology* **23**, 1484–1490 (2013).

696. Eisenberg, D., Gill, H. S., Pfluegl, G. M. & Rotstein, S. H. Structure-function relationships of glutamine synthetases. *Biochim Biophys Acta* **1477**, 122–145 (2000).

697. Márquez, J., de la Oliva, A. R. L., Matés, J. M., Segura, J. A. & Alonso, F. J. Glutaminase: a multifaceted protein not only involved in generating glutamate. *Neurochem Int* **48**, 465–471 (2006).

698. Li, Q., Tao, Q., Teixeira, J. S., Shu-Wei Su, M. & Gänzle, M. G. Contribution of glutaminases to glutamine metabolism and acid resistance in Lactobacillus reuteri and other vertebrate host adapted lactobacilli. *Food Microbiol* **86**, 103343 (2020).

699. Tan, C. *et al.* The role of gut microbiota and amino metabolism in the effects of improvement of islet β-cell function after modified jejunoileal bypass. *Sci Rep* **11**, 4809 (2021).

700. Yu, Y. *et al.* Changes to gut amino acid transporters and microbiome associated with increased E/I ratio in Chd8+/− mouse model of ASD-like behavior. *Nat Commun* **13**, 1151 (2022).

701. Beaufrère, A. M. *et al.* Long-term intermittent glutamine supplementation repairs intestinal damage (structure and functional mass) with advanced age: assessment with plasma citrulline in a rodent model. *J Nutr Health Aging* **18**, 814–819 (2014).

702. Hayashi, M. K. & Yasui, M. The transmembrane transporter domain of glutamate transporters is a process tip localizer. *Sci Rep* **5**, 9032 (2015).

703. Lunetti, P. *et al.* Mitochondrial glutamate carriers from Drosophila melanogaster: Biochemical, evolutionary and modeling studies. *Biochimica et Biophysica Acta (BBA) - Bioenergetics* **1827**, 1245–1255 (2013).

704. Lunetti, P. *et al.* The mitochondrial aspartate/glutamate carrier (AGC or Aralar1) isoforms in D. melanogaster: biochemical characterization, gene structure, and evolutionary analysis. *Biochim Biophys Acta Gen Subj* **1865**, 129854 (2021).

705. Daniels, R. W. *et al.* Increased Expression of the Drosophila Vesicular Glutamate Transporter Leads to Excess Glutamate Release and a Compensatory Decrease in Quantal Content. *J. Neurosci.* **24**, 10466–10474 (2004).

706. Besson, M. T., Soustelle, L. & Birman, S. Selective high-affinity transport of aspartate by a Drosophila homologue of the excitatory amino-acid transporters. *Curr Biol* **10**, 207–210 (2000).

707. Jutabha, P. *et al.* Human Sodium Phosphate Transporter 4 (hNPT4/SLC17A3) as a Common Renal Secretory Pathway for Drugs and Urate. *J Biol Chem* **285**, 35123–35132 (2010).

708. Shim, M. S. *et al.* A novel type of dietary and metabolic glutamate transporter (dmGLUT) plays a crucial role in megamitochondrial formation in Drosophila. *The FASEB Journal* **26**, lb140–lb140 (2012).

709. Spradling, A. C. *et al.* The Berkeley Drosophila Genome Project gene disruption project: Single P-element insertions mutating 25% of vital Drosophila genes. *Genetics* **153**, 135–177 (1999).

710. Gegelashvili, G. & Schousboe, A. Cellular distribution and kinetic properties of high-affinity glutamate transporters. *Brain Res Bull* **45**, 233–238 (1998).

711. Seal, R. P., Daniels, G. M., Wolfgang, W. J., Forte, M. A. & Amara, S. G. Identification and characterization of a cDNA encoding a neuronal glutamate transporter from Drosophila melanogaster. *Recept Channels* **6**, 51–64 (1998).

712. Storck, T., Schulte, S., Hofmann, K. & Stoffel, W. Structure, expression, and functional analysis of a Na(+)-dependent glutamate/aspartate transporter from rat brain. *Proceedings of the National Academy of Sciences* **89**, 10955–10959 (1992).

713. Tanaka, K. Expression cloning of a rat glutamate transporter. *Neuroscience Research* **16**, 149–153 (1993).

714. Pines, G. *et al.* Cloning and expression of a rat brain L-glutamate transporter. *Nature* **360**, 464–467 (1992).

715. Kanai, Y. & Hediger, M. A. Primary structure and functional characterization of a high-affinity glutamate transporter. *Nature* **360**, 467–471 (1992).

716. Fairman, W. A., Vandenberg, R. J., Arriza, J. L., Kavanaught, M. P. & Amara, S. G. An excitatory amino-acid transporter with properties of a ligand-gated chloride channel. *Nature* **375**, 599–603 (1995).

717. Arriza, J. L., Eliasof, S., Kavanaugh, M. P. & Amara, S. G. Excitatory amino acid transporter 5, a retinal glutamate transporter coupled to a chloride conductance. *Proceedings of the National Academy of Sciences* **94**, 4155–4160 (1997).

718. Boudker, O., Ryan, R. M., Yernool, D., Shimamoto, K. & Gouaux, E. Coupling substrate and ion binding to extracellular gate of a sodium-dependent aspartate transporter. *Nature* **445**, 387–393 (2007).

719. Reyes, N., Ginter, C. & Boudker, O. Transport mechanism of a bacterial homologue of glutamate transporters. *Nature* **462**, 880–885 (2009).

720. Guskov, A., Jensen, S., Faustino, I., Marrink, S. J. & Slotboom, D. J. Coupled binding mechanism of three sodium ions and aspartate in the glutamate transporter homologue GltTk. *Nat Commun* **7**, 13420 (2016).

721. Canul-Tec, J. C. *et al.* Structure and allosteric inhibition of excitatory amino acid transporter 1. *Nature* **544**, 446–451 (2017).

722. Kato, T. *et al.* Structural insights into inhibitory mechanism of human excitatory amino acid transporter EAAT2. *Nat Commun* **13**, 4714 (2022).

723. Setiadi, J., Heinzelmann, G. & Kuyucak, S. Computational Studies of Glutamate Transporters. *Biomolecules* **5**, 3067–3086 (2015).

724. Qiu, B., Matthies, D., Fortea, E., Yu, Z. & Boudker, O. Cryo-EM structures of excitatory amino acid transporter 3 visualize coupled substrate, sodium, and proton binding and transport. *Science Advances* **7**, eabf5814 (2021).

725. Owe, S. G., Marcaggi, P. & Attwell, D. The ionic stoichiometry of the GLAST glutamate transporter in salamander retinal glia. *The Journal of Physiology* **577**, 591–599 (2006).

726. Zerangue, N. & Kavanaugh, M. P. Flux coupling in a neuronal glutamate transporter. *Nature* **383**, 634–637 (1996).

727. Levy, L. M., Warr, O. & Attwell, D. Stoichiometry of the Glial Glutamate Transporter GLT-1 Expressed Inducibly in a Chinese Hamster Ovary Cell Line Selected for Low Endogenous Na+-Dependent Glutamate Uptake. *J. Neurosci.* **18**, 9620–9628 (1998).

728. Vandenberg, R. J. & Ryan, R. M. Mechanisms of Glutamate Transport. *Physiological Reviews* **93**, 1621–1657 (2013).

729. Arriza, J. L. *et al.* Cloning and expression of a human neutral amino acid transporter with structural similarity to the glutamate transporter gene family. *J Biol Chem* **268**, 15329–15332 (1993).

730. Shafqat, S. *et al.* Cloning and expression of a novel Na(+)-dependent neutral amino acid transporter structurally related to mammalian Na+/glutamate cotransporters. *Journal of Biological Chemistry* **268**, 15351–15355 (1993).

731. Hofmann, K., Düker, M., Fink, T., Lichter, P. & Stoffel, W. Human neutral amino acid transporter ASCT1: structure of the gene (SLC1A4) and localization to chromosome 2p13-p15. *Genomics* **24**, 20–26 (1994).

732. Utsunomiya-Tate, N., Endou, H. & Kanai, Y. Cloning and Functional Characterization of a System ASC-like Na+-dependent Neutral Amino Acid Transporter *. *Journal of Biological Chemistry* **271**, 14883–14890 (1996).

733. Yernool, D., Boudker, O., Jin, Y. & Gouaux, E. Structure of a glutamate transporter homologue from Pyrococcus horikoshii. *Nature* **431**, 811–818 (2004).

734. Nothmann, D. *et al.* Hetero-oligomerization of neuronal glutamate transporters. *J Biol Chem* **286**, 3935–3943 (2011).

735. Marie, H. *et al.* The Amino Terminus of the Glial Glutamate Transporter GLT-1 Interacts with the LIM Protein Ajuba. *Molecular and Cellular Neuroscience* **19**, 152–164 (2002).

736. Sullivan, S. M. *et al.* Cytoskeletal Anchoring of GLAST Determines Susceptibility to Brain Damage: an Identified role for GFAP. *Journal of Biological Chemistry* **282**, 29414–29423 (2007).

737. Sheean, R. K., Lau, C. L., Shin, Y. S., O'Shea, R. D. & Beart, P. M. Links between L-glutamate transporters, Na+/K+-ATPase and cytoskeleton in astrocytes: evidence following inhibition with rottlerin. *Neuroscience* **254**, 335–346 (2013).

738. Lehre, K. P. & Danbolt, N. C. The number of glutamate transporter subtype molecules at glutamatergic synapses: chemical and stereological quantification in young adult rat brain. *J Neurosci* **18**, 8751–8757 (1998).

739. Danbolt, N. C. Glutamate uptake. *Progress in Neurobiology* **65**, 1–105 (2001).

740. Nakayama, T., Kawakami, H., Tanaka, K. & Nakamura, S. Expression of three glutamate transporter subtype mRNAs in human brain regions and peripheral tissues. *Molecular Brain Research* **36**, 189–192 (1996).

741. Matthews, J. C. *et al.* Activity and protein localization of multiple glutamate transporters in gestation day 14 vs. day 20 rat placenta. *American Journal of Physiology-Cell Physiology* **274**, C603–C614 (1998).

742. Huggett, J., Vaughan-Thomas, A. & Mason, D. The open reading frame of the Na+-dependent glutamate transporter GLAST-1 is expressed in bone and a splice variant of this molecule is expressed in bone and brain. *FEBS Letters* **485**, 13–18 (2000).

743. Martínez-López, I., García, C., Barber, T., Viña, J. R. & Miralles, V. J. The L-glutamate transporters GLAST (EAAT1) and GLT-1 (EAAT2): Expression and regulation in rat lactating mammary gland. *Molecular Membrane Biology* **15**, 237–242 (1998).

744. Rothstein, J. D. *et al.* Localization of neuronal and glial glutamate transporters. *Neuron* **13**, 713–725 (1994).

745. Kugler, P. & Schmitt, A. Glutamate transporter EAAC1 is expressed in neurons and glial cells in the rat nervous system. *Glia* **27**, 129–142 (1999).

746. Conti, F., DeBiasi, S., Minelli, A., Rothstein, J. D. & Melone, M. EAAC1, a high-affinity glutamate tranporter, is localized to astrocytes and gabaergic neurons besides pyramidal cells in the rat cerebral cortex. *Cerebral Cortex* **8**, 108–116 (1998).

747. Haugeto, Ø. *et al.* Brain Glutamate Transporter Proteins Form Homomultimers *. *Journal of Biological Chemistry* **271**, 27715–27722 (1996).

748. Holmseth, S. *et al.* The Density of EAAC1 (EAAT3) Glutamate Transporters Expressed by Neurons in the Mammalian CNS. *J. Neurosci.* **32**, 6000–6013 (2012).

749. Bailey, C. G. *et al.* Loss-of-function mutations in the glutamate transporter SLC1A1 cause human dicarboxylic aminoaciduria. *J Clin Invest* **121**, 446–453 (2011).

750. Peghini, P., Janzen, J. & Stoffel, W. Glutamate transporter EAAC-1-deficient mice develop dicarboxylic aminoaciduria and behavioral abnormalities but no neurodegeneration. *The EMBO Journal* **16**, 3822–3832 (1997).

751. Liu, M.-T., Rothstein, J. D., Gershon, M. D. & Kirchgessner, A. L. Glutamatergic Enteric Neurons. *J. Neurosci.* **17**, 4764–4784 (1997).

752. Dehnes, Y. *et al.* The Glutamate Transporter EAAT4 in Rat Cerebellar Purkinje Cells: A Glutamate-Gated Chloride Channel Concentrated near the Synapse in Parts of the Dendritic Membrane Facing Astroglia. *J. Neurosci.* **18**, 3606–3619 (1998).

753. Rival, T. *et al.* Physiological requirement for the glutamate transporter dEAAT1 at the adult Drosophila neuromuscular junction. *Journal of Neurobiology* **66**, 1061–1074 (2006).

754. Stacey, S. M. *et al.* Drosophila Glial Glutamate Transporter Eaat1 Is Regulated by Fringe-Mediated Notch Signaling and Is Essential for Larval Locomotion. *J Neurosci* **30**, 14446–14457 (2010).

755. Chung, V. Y. & Turney, B. W. A Drosophila genetic model of nephrolithiasis: transcriptional changes in response to diet induced stone formation. *BMC Urology* **17**, 109 (2017).

756. Hu, W., MacDonald, M. L., Elswick, D. E. & Sweet, R. A. The glutamate hypothesis of schizophrenia: evidence from human brain tissue studies. *Ann N Y Acad Sci* **1338**, 38–57 (2015).

757. Karlsson, R.-M., Tanaka, K., Heilig, M. & Holmes, A. Loss of glial glutamate and aspartate transporter (excitatory amino acid transporter 1) causes locomotor hyperactivity and exaggerated responses to psychotomimetics: rescue by haloperidol and metabotropic glutamate 2/3 agonist. *Biol Psychiatry* **64**, 810–814 (2008).

758. Bauer, D., Gupta, D., Harotunian, V., Meador-Woodruff, J. H. & McCullumsmith, R. E. Abnormal expression of glutamate transporter and transporter interacting molecules in prefrontal cortex in elderly patients with schizophrenia. *Schizophr Res* **104**, 108–120 (2008).

759. Bauer, D., Haroutunian, V., Meador-Woodruff, J. H. & McCullumsmith, R. E. Abnormal glycosylation of EAAT1 and EAAT2 in prefrontal cortex of elderly patients with schizophrenia. *Schizophr Res* **117**, 92–98 (2010).

760. Shan, D. *et al.* Abnormal expression of glutamate transporters in temporal lobe areas in elderly patients with schizophrenia. *Schizophrenia Research* **144**, 1–8 (2013).

761. Rothstein, J. D., Martin, L. J. & Kuncl, R. W. Decreased glutamate transport by the brain and spinal cord in amyotrophic lateral sclerosis. *N Engl J Med* **326**, 1464–1468 (1992).

762. Ferrarese, C. *et al.* Decreased platelet glutamate uptake in patients with amyotrophic lateral sclerosis. *Neurology* **56**, 270–272 (2001).

763. Lin, C. L. *et al.* Aberrant RNA processing in a neurodegenerative disease: the cause for absent EAAT2, a glutamate transporter, in amyotrophic lateral sclerosis. *Neuron* **20**, 589–602 (1998).

764. Foran, E. & Trotti, D. Glutamate Transporters and the Excitotoxic Path to Motor Neuron Degeneration in Amyotrophic Lateral Sclerosis. *Antioxid Redox Signal* **11**, 1587–1602 (2009).

765. Wood, O. W. G., Yeung, J. H. Y., Faull, R. L. M. & Kwakowsky, A. EAAT2 as a therapeutic research target in Alzheimer's disease: A systematic review. *Frontiers in Neuroscience* **16**, (2022).

766. Pereira, A. C. *et al.* Age and Alzheimer's disease gene expression profiles reversed by the glutamate modulator riluzole. *Mol Psychiatry* **22**, 296–305 (2017).

767. Brothers, H. M. *et al.* Riluzole partially rescues age-associated, but not LPS-induced, loss of glutamate transporters and spatial memory. *J Neuroimmune Pharmacol* **8**, 1098–1105 (2013).

768. Potier, B. *et al.* Reduction in glutamate uptake is associated with extrasynaptic NMDA and metabotropic glutamate receptor activation at the hippocampal CA1 synapse of aged rats. *Aging Cell* **9**, 722–735 (2010).

769. Todd, A. C. & Hardingham, G. E. The Regulation of Astrocytic Glutamate Transporters in Health and Neurodegenerative Diseases. *Int J Mol Sci* **21**, 9607 (2020).

770. Pedraz-Cuesta, E. *et al.* The glutamate transport inhibitor DL-Threo-β-Benzyloxyaspartic acid (DL-TBOA) differentially affects SN38- and oxaliplatin-induced death of drug-resistant colorectal cancer cells. *BMC Cancer* **15**, 411 (2015).

771. M. Ribeiro, F., Paquet, M., P. Cregan, S. & S. G. Ferguson, S. Group I Metabotropic Glutamate Receptor Signalling and its Implication in Neurological Disease. *CNS & Neurological Disorders - Drug Targets- CNS & Neurological Disorders)* **9**, 574–595 (2010).

772. Willard, S. S. & Koochekpour, S. Glutamate, Glutamate Receptors, and Downstream Signaling Pathways. *Int J Biol Sci* **9**, 948–959 (2013).

773. Yu, L. J., Wall, B. A., Wangari-Talbot, J. & Chen, S. Metabotropic Glutamate Receptors in Cancer. *Neuropharmacology* **115**, 193–202 (2017).

774. de Groot, J. F., Liu, T. J., Fuller, G. & Yung, W. K. A. The excitatory amino acid transporter-2 induces apoptosis and decreases glioma growth in vitro and in vivo. *Cancer Res* **65**, 1934–1940 (2005).

775. Xiong, J. *et al.* SLC1A1 mediated glutamine addiction and contributed to natural killer T-cell lymphoma progression with immunotherapeutic potential. *EBioMedicine* **72**, 103614 (2021).

776. Lyons, S. A., Chung, W. J., Weaver, A. K., Ogunrinu, T. & Sontheimer, H. Autocrine glutamate signaling promotes glioma cell invasion. *Cancer Res* **67**, 9463–9471 (2007).

777. Ungard, R. G., Seidlitz, E. P. & Singh, G. Inhibition of breast cancer-cell glutamate release with sulfasalazine limits cancer-induced bone pain. *PAIN®* **155**, 28–36 (2014).

778. Zhu, Y. F. *et al.* Bone cancer-induced pain is associated with glutamate signalling in peripheral sensory neurons. *Mol Pain* **16**, 1744806920911536 (2020).

779. Seidlitz, E. P., Sharma, M. K., Saikali, Z., Ghert, M. & Singh, G. Cancer cell lines release glutamate into the extracellular environment. *Clin Exp Metastasis* **26**, 781 (2009).

780. Garber, K. Cancer anabolic metabolism inhibitors move into clinic. *Nat Biotechnol* **34**, 794–795 (2016).

781. Gross, M. I. *et al.* Antitumor Activity of the Glutaminase Inhibitor CB-839 in Triple-Negative Breast Cancer. *Molecular Cancer Therapeutics* **13**, 890–901 (2014).

782. Robinson, M. M. *et al.* Novel mechanism of inhibition of rat kidney-type glutaminase by bis-2-(5-phenylacetamido-1,2,4-thiadiazol-2-yl)ethyl sulfide (BPTES). *Biochem J* **406**, 407–414 (2007).

783. Parlati, F. *et al.* Antitumor Activity Of The Glutaminase Inhibitor CB-839 In Hematological Malignances. *Blood* **122**, 4226 (2013).

784. Matés, J. M., Campos-Sandoval, J. A., Santos-Jiménez, J. de los & Márquez, J. Dysregulation of glutaminase and glutamine synthetase in cancer. *Cancer Letters* **467**, 29–39 (2019).

785. Niswender, C. M. & Conn, P. J. Metabotropic Glutamate Receptors: Physiology, Pharmacology, and Disease. *Annu Rev Pharmacol Toxicol* **50**, 295–322 (2010).

786. Mitri, C., Parmentier, M.-L., Pin, J.-P., Bockaert, J. & Grau, Y. Divergent Evolution in Metabotropic Glutamate Receptors: A New Receptor Activated by an Endogenous Ligand Different from Glutamate in Insects. *Journal of Biological Chemistry* **279**, 9313–9320 (2004).

787. Bogdanik, L. *et al.* The Drosophila Metabotropic Glutamate Receptor DmGluRA Regulates Activity-Dependent Synaptic Facilitation and Fine Synaptic Morphology. *J Neurosci* **24**, 9105–9116 (2004).

788. Parmentier, M.-L., Pin, J.-P., Bockaert, J. & Grau, Y. Cloning and Functional Expression of a DrosophilaMetabotropic Glutamate Receptor Expressed in the Embryonic CNS. *The Journal of Neuroscience* **16**, 6687 (1996).

789. Choi, C. H. *et al.* Multiple Drug Treatments That Increase cAMP Signaling Restore Long-Term Memory and Aberrant Signaling in Fragile X Syndrome Models. *Frontiers in Behavioral Neuroscience* **10**, (2016).

790. Shin, S.-S., Martino, J. J. & Chen, S. Metabotropic glutamate receptors (mGluRs) and cellular transformation. *Neuropharmacology* **55**, 396–402 (2008).

791. Morimoto, R. *et al.* Secretion of L-glutamate from osteoclasts through transcytosis. *EMBO J* **25**, 4175–4186 (2006).

792. Frati, C. *et al.* Expression of functional mGlu5 metabotropic glutamate receptors in human melanocytes. *J Cell Physiol* **183**, 364–372 (2000).

793. Genever, P. G. *et al.* Evidence for a novel glutamate-mediated signaling pathway in keratinocytes. *J Invest Dermatol* **112**, 337–342 (1999).

794. Storto, M. *et al.* Insulin secretion is controlled by mGlu5 metabotropic glutamate receptors. *Mol Pharmacol* **69**, 1234–1241 (2006).

795. Tong, Q., Ouedraogo, R. & Kirchgessner, A. L. Localization and function of group III metabotropic glutamate receptors in rat pancreatic islets. *Am J Physiol Endocrinol Metab* **282**, E1324-1333 (2002).

796. Storto, M. *et al.* Selective blockade of mGlu5 metabotropic glutamate receptors protects rat hepatocytes against hypoxic damage. *Hepatology* **31**, 649–655 (2000).

797. Gill, S. S., Pulido, O. M., Mueller, R. W. & McGuire, P. F. Immunochemical localization of the metabotropic glutamate receptors in the rat heart. *Brain Res Bull* **48**, 143–146 (1999).

798. Storto, M. *et al.* Expression of metabotropic glutamate receptors in murine thymocytes and thymic stromal cells. *J Neuroimmunol* **109**, 112–120 (2000).

799. Hu, H. Z. *et al.* Functional group I metabotropic glutamate receptors in submucous plexus of guinea-pig ileum. *Br J Pharmacol* **128**, 1631–1635 (1999).

800. Ferrigno, A. *et al.* Localization and role of metabotropic glutamate receptors subtype 5 in the gastrointestinal tract. *World J Gastroenterol* **23**, 4500–4507 (2017).

801. Melchiorri, D. *et al.* Metabotropic glutamate receptors in stem/progenitor cells. *Neuropharmacology* **53**, 473–480 (2007).

802. Morikawa, H., Khodakhah, K. & Williams, J. T. Two intracellular pathways mediate metabotropic glutamate receptor-induced Ca2+ mobilization in dopamine neurons. *J Neurosci* **23**, 149–157 (2003).

803. Hagenston, A. M., Fitzpatrick, J. S. & Yeckel, M. F. MGluR-mediated calcium waves that invade the soma regulate firing in layer V medial prefrontal cortical pyramidal neurons. *Cereb Cortex* **18**, 407–423 (2008).

804. Flint, A. C., Dammerman, R. S. & Kriegstein, A. R. Endogenous activation of metabotropic glutamate receptors in neocortical development causes neuronal calcium oscillations. *Proceedings of the National Academy of Sciences* **96**, 12144–12149 (1999).

805. Hartmann, J., Henning, H. A. & Konnerth, A. mGluR1/TRPC3-mediated Synaptic Transmission and Calcium Signaling in Mammalian Central Neurons. *Cold Spring Harb Perspect Biol* **3**, a006726 (2011).

806. Neyer, C. *et al.* mGluR-mediated calcium signalling in the thalamic reticular nucleus. *Cell Calcium* **59**, 312–323 (2016).

807. Kellner, V. *et al.* Dual metabotropic glutamate receptor signaling enables coordination of astrocyte and neuron activity in developing sensory domains. *Neuron* **109**, 2545-2555.e7 (2021).

808. Sun, W. *et al.* Glutamate-Dependent Neuroglial Calcium Signaling Differs Between Young and Adult Brain. *Science* **339**, 197–200 (2013).

809. Wang, X., Takano, T. & Nedergaard, M. Astrocytic Calcium Signaling: Mechanism and Implications for Functional Brain Imaging. *Methods Mol Biol* **489**, 93–109 (2009).

810. Nakahara, K., Okada, M. & Nakanishi, S. The Metabotropic Glutamate Receptor mGluR5 Induces Calcium Oscillations in Cultured Astrocytes via Protein Kinase C Phosphorylation. *Journal of Neurochemistry* **69**, 1467–1475 (1997).

811. Gu, Y. & Publicover, S. J. Expression of Functional Metabotropic Glutamate Receptors in Primary Cultured Rat Osteoblasts: Cross-Talk with N-Methyl-d-Astartate Receptors. *Journal of Biological Chemistry* **275**, 34252–34259 (2000).

812. Zhu, D.-Y. *et al.* Involvement of metabotropic glutamate receptor 5 in cardiomyocyte differentiation from mouse embryonic stem cells. *Stem Cells Dev* **21**, 2130–2141 (2012).

813. Luyt, K., Varadi, A. & Molnar, E. Functional metabotropic glutamate receptors are expressed in oligodendrocyte progenitor cells. *Journal of neurochemistry* **84**, (2003).

814. Purgert, C. A. *et al.* Intracellular mGluR5 Can Mediate Synaptic Plasticity in the Hippocampus. *J. Neurosci.* **34**, 4589–4598 (2014).

815. Aronica, E. *et al.* Expression and functional role of mGluR3 and mGluR5 in human astrocytes and glioma cells: opposite regulation of glutamate transporter proteins. *European Journal of Neuroscience* **17**, 2106–2118 (2003).

816. Vermeiren, C. *et al.* Acute up-regulation of glutamate uptake mediated by mGluR5a in reactive astrocytes. *Journal of Neurochemistry* **94**, 405–416 (2005).

817. Peterson, A. R. & Binder, D. K. Astrocyte Glutamate Uptake and Signaling as Novel Targets for Antiepileptogenic Therapy. *Frontiers in Neurology* **11**, (2020).

818. Filer, D. *et al.* RNA polymerase III limits longevity downstream of TORC1. *Nature* **552**, 263–267 (2017).

819. Hu, Q. X. *et al.* Expression of Glutamate Transporters in Mouse Liver, Kidney, and Intestine. *J Histochem Cytochem* **66**, 189–202 (2018).

820. Roberts, R. C., Roche, J. K. & McCullumsmith, R. E. Localization of excitatory amino acid transporters EAAT1 and EAAT2 in human postmortem cortex: a light and electron microscopic study. *Neuroscience* **277**, 522–540 (2014).

821. Genda, E. N. *et al.* Co-compartmentalization of the Astroglial Glutamate Transporter, GLT-1, with Glycolytic Enzymes and Mitochondria. *J. Neurosci.* **31**, 18275–18288 (2011).

822. Bauer, D. E. *et al.* The glutamate transporter, GLAST, participates in a macromolecular complex that supports glutamate metabolism. *Neurochem Int* **61**, 566–574 (2012).

823. Magi, S. *et al.* Physical and Functional Interaction of NCX1 and EAAC1 Transporters Leading to Glutamate-Enhanced ATP Production in Brain Mitochondria. *PLoS One* **7**, e34015 (2012).

824. Bhutia, Y. D., Babu, E., Ramachandran, S. & Ganapathy, V. Amino Acid Transporters in Cancer and Their Relevance to “Glutamine Addiction”: Novel Targets for the Design of a New Class of Anticancer Drugs. *Cancer Research* **75**, 1782–1788 (2015).

825. Stepulak, A., Rola, R., Polberg, K. & Ikonomidou, C. Glutamate and its receptors in cancer. *J Neural Transm* **121**, 933–944 (2014).

826. Clapham, D. E. Calcium Signaling. *Cell* **131**, 1047–1058 (2007).

827. Dupont, G., Combettes, L., Bird, G. S. & Putney, J. W. Calcium Oscillations. *Cold Spring Harb Perspect Biol* **3**, a004226 (2011).

828. Brini, M. & Carafoli, E. Calcium Pumps in Health and Disease. *Physiological Reviews* **89**, 1341–1378 (2009).

829. Magi, S. *et al.* Glutamate-Induced ATP Synthesis: Relationship between Plasma Membrane Na+/Ca2+ Exchanger and Excitatory Amino Acid Transporters in Brain and Heart Cell Models. *Mol Pharmacol* **84**, 603–614 (2013).

830. Blaustein, M. P. & Lederer, W. J. Sodium/Calcium Exchange: Its Physiological Implications. *Physiological Reviews* **79**, 763–854 (1999).

831. Philipson, K. D. & Nicoll, D. A. Sodium-calcium exchange: a molecular perspective. *Annu Rev Physiol* **62**, 111–133 (2000).

832. Annunziato, L., Pignataro, G. & Renzo, G. F. D. Pharmacology of Brain Na+/Ca2+ Exchanger: From Molecular Biology to Therapeutic Perspectives. *Pharmacol Rev* **56**, 633–654 (2004).

833. Zhong, X., You, N., Wang, Q., Li, L. & Huang, C. Reverse mode of sodium/calcium exchanger subtype 1 contributes to detrusor overactivity in rats with partial bladder outflow obstruction. *Am J Transl Res* **10**, 806–815 (2018).

834. Smets, I. *et al.* Ca2+ uptake in mitochondria occurs via the reverse action of the Na+/Ca2+ exchanger in metabolically inhibited MDCK cells. *American Journal of Physiology-Renal Physiology* **286**, F784–F794 (2004).

835. Castaldo, P. *et al.* Role of the mitochondrial sodium/calcium exchanger in neuronal physiology and in the pathogenesis of neurological diseases. *Progress in Neurobiology* **87**, 58–79 (2009).

836. Magi, S., Piccirillo, S., Amoroso, S. & Lariccia, V. Excitatory Amino Acid Transporters (EAATs): Glutamate Transport and Beyond. *Int J Mol Sci* **20**, 5674 (2019).

837. Lai, T. K. Y. *et al.* The receptor-receptor interaction between mGluR1 receptor and NMDA receptor: a potential therapeutic target for protection against ischemic stroke. *FASEB J* **33**, 14423–14439 (2019).

838. Rolfe, D. F. & Brown, G. C. Cellular energy utilization and molecular origin of standard metabolic rate in mammals. *Physiol Rev* **77**, 731–758 (1997).

839. Baskin, K. K., Winders, B. R. & Olson, E. N. Muscle as a "Mediator" of Systemic Metabolism. *Cell Metab* **21**, 237–248 (2015).

840. Xu, Y. *et al.* Altered Fecal Microbiota Composition in Older Adults With Frailty. *Frontiers in Cellular and Infection Microbiology* **11**, (2021).

841. Wang, P.-X., Deng, X.-R., Zhang, C.-H. & Yuan, H.-J. Gut microbiota and metabolic syndrome. *Chin Med J (Engl)* **133**, 808–816 (2020).

842. Heneghan, A. F., Pierre, J. F. & Kudsk, K. A. JAK-STAT and intestinal mucosal immunology. *JAKSTAT* **2**, e25530 (2013).

843. Zhang, L., Sui, C., Yang, W. & Luo, Q. Amino acid transporters: Emerging roles in drug delivery for tumor-targeting therapy. *Asian Journal of Pharmaceutical Sciences* **15**, 192 (2020).